

**TOTAL SYNTHESIS OF BIOLOGICALLY ACTIVE FUNGAL NATURAL
PRODUCTS DALDIQUINONE AND BULGAREIN, AND
INTRAMOLECULAR DIELS-ALDER REACTIONS FOR FLUORANTHENE
SYNTHESIS.**

A THESIS SUBMITTED TO
THE GRADUATE SCHOOL OF ENGINEERING AND SCIENCE
OF BILKENT UNIVERSITY
IN PARTIAL FULFILLMENT OF THE REQUIREMENTS FOR
THE DEGREE OF
MASTER OF SCIENCE
IN
CHEMISTRY

By
Dilgam AHMADLI

June 2021

TOTAL SYNTHESIS OF BIOLOGICALLY ACTIVE FUNGAL NATURAL PRODUCTS
DALDIQUINONE AND BULGAREIN, AND INTRAMOLECULAR DIELS-ALDER REACTIONS FOR
FLUORANTHENE SYNTHESIS

By Dilgam AHMADLI

June 2021

We certify that we have read this thesis and that in our opinion it is fully
adequate, in scope and in quality, as a thesis for the degree of Master of Science.

Yunus Emre TÜRKMEN (Advisor)

Bilge BAYTEKİN

Ferdı KARADAŞ

Hamdullah KILIÇ

Görkem GÜNBAŞ

Approved for the Graduate School of Engineering and Science:

Ezhan KARAŞAN

Director of the Graduate School

ABSTRACT

TOTAL SYNTHESIS OF BIOLOGICALLY ACTIVE FUNGAL NATURAL PRODUCTS DALDIQUINONE AND BULGAREIN, AND INTRAMOLECULAR DIELS-ALDER REACTIONS FOR FLUORANTHENE SYNTHESIS.

Dilgam AHMADLI

MSc. in Chemistry

Advisor: Asst. Prof. Dr. Yunus Emre Türkmen

June 2021

Natural products continue to play a significant role in drug discovery and be a substantial source for novel pharmaceutical drugs. Total synthesis of biologically active natural products is critical for deciphering how natural products regulate cellular and other biological processes and, structure determination. In addition, the total synthesis of natural products has also been a stimulus for the discovery of new methodologies and reactions.

The fungal natural product daldiquinone (**15**), which possesses a highly oxidized binaphthyl skeleton, was isolated in 2018 from *Daldinia concéntrica*, and was shown to have antiangiogenesis activity against HUVECs with an IC₅₀ value of 7.5 µM. Another fungal natural product bulgarein (**1**) was first isolated in 1976 from the fungus *Bulgaria inquinans*, and was shown to induce topoisomerase I-mediated DNA cleavage. However, as in the case of daldiquinone (**15**), total synthesis of bulgarein (**1**) has yet to be reported. In this work, we report the first total syntheses of daldiquinone (**15**) and bulgarein (**1**) starting from the commercially available 1,8-DHN (1,8-dihydroxynaphthalene, 1,8-naphthalenediol) via a concise route. Pd-catalyzed Suzuki coupling and

C-H arylation reactions between functionalized naphthalenes and hypervalent iodine-mediated double oxidation of phenol to *o*-quinone were employed as key steps.

Thanks to their thermal stability and electronic properties, fluoranthene derivatives have widespread medicinal chemistry and organic optoelectronics applications. A significant number of fluoranthene-based natural products are known, including bulgarein (**1**). Although many procedures have been developed to synthesize fluoranthenes, practical and modular strategy for synthesizing many substituted unsymmetrical fluoranthenes is still desirable. In this work, we report a novel approach to achieve modular syntheses of fluoranthene derivatives based on intramolecular Diels-Alder reaction.

Keywords: Natural Products, Total Synthesis, Daldiquinone, Bulgarein, Fluoranthene, Diels-Alder reactions.

ÖZET

BİYOLOJİK AKTİVİTEYE SAHİP DALDİKİNON VE BULGAREİN MANTAR DOĞAL ÜRÜNLERİNİN TOTAL SENTEZİ VE İNTRAMOLEKÜLER DİELS-ALDER TEPKİMELERİ KULLANARAK FLORANTEN TÜREVLERİNİN SENTEZİ.

Dilgam AHMADLI

Kimya Bölümü, Yüksek Lisans

Tez Danışmanı: Dr. Öğr. Üyesi Yunus Emre Türkmen

Haziran 2021

Doğal ürünler ilaç keşfinde önemli bir rol oynamaya ve yeni farmasötik ilaçların kaynağı olmaya devam etmektedir. Biyolojik aktiviteye sahip doğal ürünlerin total sentezi, hem doğal ürünlerin hücrel ve biyolojik sistemlerde nasıl davrandığının anlaşılması hem de yapı tayini açısından kritik öneme sahiptir. Aynı zamanda, doğal ürünlerin total sentezi yeni tepkimelerin ve yöntemlerin bulunmasına neden olmaktadır.

Yüksek oranda oksitlenmiş bir binaftil iskeletine sahip mantar doğal ürünü daldikinon (**15**), 2018'de *Daldinia concéntrica*'dan izole edildi ve 7.5 μ M IC₅₀ değeri ile HUVEC'lere karşı antianjiyogenez aktivitesine sahip olduğu gösterildi. Başka bir mantar doğal ürünü olan bulgarein (**1**) ilk olarak 1976'da *Bulgaristan inquinans* mantarından izole edildi ve topoizomerez I aracılı DNA bölünmesini indüklediği gösterildi. Günümüze kadar, her iki doğal ürün için de total sentez geliştirilmemiştir. Bu çalışmada, satın alınabilen 1,8-DHN'den (1,8-dihidroksinaftalin, 1,8-

naftalindiol) başlayarak kısa bir yoldan daldikinon (**15**) ve bulgareinin (**1**)'in ilk total sentezlerini sunuyoruz. Fonksiyonelleştirilmiş naftalinler arasındaki Pd katalizörlüğünde Suzuki kenetlenmesi ve elde edilen fenol türevlerinin o-kinona yükseltgenmesi anahtar adımlar olarak kullanılmıştır.

Termal kararlılıkları ve elektronik özellikleri sayesinde floranten türevleri, tıbbi kimya ve organik optoelektronik alanlarında yaygın olarak kullanılmaktadır. Bulgarein (**1**) de dahil olmakla önemli sayıda floranten bazlı doğal ürün bilinmektedir. Floranten türevlerinin sentezi için birçok stratejiler geliştirilmiş olmasına rağmen, çoklu süstitüentlere sahip, simetrik olmayan floranten türevlerini sentezlemek için pratik ve modüler strateji geliştirilememiştir. Bu çalışmada, intramoleküler Diels-Alder tepkimelerini kullanarak floranten türevlerinin modüler sentezlerine yönelik yeni bir yöntem sunuyoruz.

Anahtar kelimeler: Doğal ürünler, total sentez, Daldikinon, Bulgarein, Floranten, intramoleküler Diels-Alder tepkimeleri.

ACKNOWLEDGEMENT

I am particularly grateful to Dr. Yunus Emre Türkmen for his trust, help, support and guidance during these years. He did not only teach me the basics of organic chemistry but also helped me to convert my dreams into life objectives and supported me when I was going through hard times. I cannot express in words how significant influence he has made in my life. It has been a great pleasure to work under his supervision and learn from his experience. He is not only a great chemist but also a very kind and supportive person.

I want to thank my thesis committee members Asst. Prof. Dr. Bilge Baytekin, Asst. Prof. Dr. Ferdi Karadaş, Prof. Dr. Hamdullah Kılıç and Assoc. Prof. Dr. Görkem Günbaş for taking their time to examine my thesis and for their valuable feedbacks.

I would like to thank to Türkmen Research Group members-Selin Ezgi Dönmez, Merve Yence, Flora Mammadova, Aqşin Qarayev, Yeşim Şahin, Bilge Banu Yağcı for their help and the great time we spent together.

I would like to especially thank Yeşim Şahin, who helped me along the way not only as a labmate but also as a kind and honest friend. We have a lot of unforgettable memories which will always be a part of my life. She always listened to my complaints, tolerated my mistakes, encouraged me and made me a better person than I was before.

I want to express my deep gratitude to my family for everything they have done to give me a bright future. I will always be grateful to my father, İlham Ehmedov, my mother Almaz Ehmedova, my brother Tebriz and my sisters İlhame and Ülviyye, for their support and trust. I could have never reached my goals without the sacrifices they have made.

I am also very lucky to have the greatest group of friends anyone ever had. I want to thank Ferid Musayev, Nureddin Kazımov, Tahir Nadirov and Eli Babayev for their incredible friendship and for all the delightful conversations we had together.

We thank TÜBİTAK (The Scientific and Technological Research Council of Turkey) for financial support (Project No: 119Z534)

Dedicated to my lovely family...

LIST OF ABBREVIATIONS

AcCl	Acetyl chloride
APCI	Atmospheric-pressure chemical ionization
BnBr	Benzyl bromide
Bpin	Pinacolato boronic ester
B₂pin₂	Bis(pinacolato)diboron
CAN	Ceric ammonium nitrate
DBU	1,8-Diazabicyclo[5.4.0]undec-7-ene
DCM	Dichloromethane
DDQ	2,3-Dichloro-5,6-dicyano-1,4-benzoquinone
DMF	Dimethylformamide
DMSO	Dimethyl sulfoxide
DPEPhos	Bis[(2-diphenylphosphino)phenyl] ether
dppf	1,1'-Bis(diphenylphosphino)ferrocene
dppm	1,1-Bis(diphenylphosphino)methane
DSSC	Dye-sensitized solar cell
EtOAc	Ethyl acetate
HRMS	High Resolution Mass Spectrometry
IBX	2-Iodoxy benzoic acid
KHMDS	Potassium bis(trimethylsilyl)amide
KOAc	Potassium acetate
MeOH	Methanol
MOM	Methoxymethyl

<i>m</i>-CPBA	<i>meta</i> -Chloroperoxybenzoic acid
m.p.	Melting point
NBS	N-Bromosuccinimide
NIS	N-Iodosuccinimide
NMR	Nuclear Magnetic Resonance
OLED	Organic Light Emitting Diode
PCC	Pyridinium chlorochromate
PIDA	(Diacetoxyiodo)benzene
PIFA	Phenyl iodine bis(trifluoroacetate)
Pyr	Pyridine
TBAC	Tetrabutylammounium chloride
TBAF	Tetrabutylammounium fluoride
TBHP	<i>tert</i> -Butyl hydroperoxide
TFA	Trifluoroacetic acid
THF	Tetrahydrofuran
TIPS	Triisopropylsilyl
TLC	Thin-Layer Chromatography
TMS	Trimethylsilyl
UV	Ultraviolet

TABLE OF CONTENTS

CHAPTER 1: TOTAL SYNTHESIS OF BIOACTIVE FUNGAL NATURAL PRODUCTS DALDIQUINONE AND BULGAREIN	1
1.1. INTRODUCTION.....	1
1.1.1. Fluoranthene-based Natural Products.....	1
1.1.2. Biosynthesis of benzo[<i>j</i>]fluoranthene metabolites.....	5
1.1.3. Total Synthesis of Fluoranthene-based Natural Products	6
1.1.4. <i>ortho</i> -Naphthoquinone-based Natural Products	8
1.1.5. Aim of This Work.....	10
1.2. RESULTS AND DISCUSSION.....	11
1.2.1. Retrosynthetic analysis	11
1.2.2 Total Synthesis of Daldiquinone	13
1.2.3. Total Synthesis of Bulgarein	18
1.2.4. Semisynthesis of Daldiquinone from Daldinol	24
1.3. CONCLUSION.....	25
CHAPTER 2: INTRAMOLECULAR DIELS-ALDER REACTIONS FOR THE SYNTHESSES OF FLUORANTHENE DERIVATIVES	27
2.1. INTRODUCTION.....	27
2.1.1. General applications of Fluoranthene derivatives	27
2.1.2. Reported strategies for synthesis of fluoranthene derivatives	30
2.1.2.1. Diels Alder reactions.....	30
2.1.2.2. Transition metal-catalyzed processes.....	32
2.1.3. Aim of this work.....	35

2.2. RESULTS AND DISCUSSION	37
2.3. CONCLUSION	42
CHAPTER 3: EXPERIMENTAL SECTION	43
3.1 GENERAL INFORMATION	43
3.2. CHAPTER 1: Total Synthesis of Daldinol, Daldiquinone and Bulgarein	44
3.3. Diels-Alder reactions for Fluoranthene synthesis.	78
3.3.1. General Procedure A for the synthesis of alkynes 43a-43d	78
3.3.2. General Procedure B for the Sonogashira reaction between alkynes and 1,8-diiodonaphthalene	83
3.3.3. General Procedure C for the oxidation of propargyl alcohols with PCC... ..	87
3.3.4. General Procedure D for the syntheses of Fluoranthenes.....	92
¹ H and ¹³ C spectra.....	98
BIBLIOGRAPHY	170

LIST OF FIGURES

Figure 1. Structures of fluoranthene and benzo[<i>j</i>]fluoranthene.	1
Figure 2. Selected examples of fluoranthene-based natural products.	3
Figure 3. Chemical constituents of <i>Bulgaria inquinans</i>	4
Figure 4. Unnamed benzo[<i>j</i>]fluoranthene metabolites.	5
Figure 5. Selected examples of 1,2-naphthaquinone based natural products.	9
Figure 6. Selected fluoranthene derivatives.	28
Figure 7. ¹ H-NMR spectrum of 22 in CDCl ₃	98
Figure 8. ¹³ C-NMR spectrum of 22 in CDCl ₃	99
Figure 9. ¹ H-NMR spectrum of 24 in CDCl ₃	100
Figure 10. ¹³ C-NMR spectrum of 24 in CDCl ₃	101
Figure 11. ¹ H-NMR spectrum of 25 in CDCl ₃	102
Figure 12. ¹³ C-NMR spectrum of 25 in CDCl ₃	103
Figure 13. ¹ H-NMR spectrum of 33 in CDCl ₃	104
Figure 14. ¹³ C-NMR spectrum of 33 in CDCl ₃	105
Figure 15. ¹ H-NMR spectrum of 34 in CDCl ₃	106
Figure 16. ¹³ C-NMR spectrum of 34 in CDCl ₃	107
Figure 17. ¹ H-NMR spectrum of 35 in CDCl ₃	108
Figure 18. ¹³ C-NMR spectrum of 35 in CDCl ₃	109
Figure 19. ¹ H-NMR spectrum of 27 in CDCl ₃	110
Figure 20. ¹³ C-NMR spectrum of 27 in CDCl ₃	111
Figure 21. ¹ H-NMR spectrum of 29 in CDCl ₃	112
Figure 22. ¹³ C-NMR spectrum of 29 in CDCl ₃	113
Figure 23. ¹ H-NMR spectrum of daldiquinone (15) in CDCl ₃	114

Figure 24. ^{13}C -NMR spectrum of daldiquinone (15) in CDCl_3 .	115
Figure 25. ^1H -NMR spectrum of 26 in CDCl_3 .	116
Figure 26. ^{13}C -NMR spectrum of 26 in CDCl_3 .	117
Figure 27. ^1H -NMR spectrum of daldinol (28) in CDCl_3 .	118
Figure 28. ^{13}C -NMR spectrum of daldinol (28) in CDCl_3 .	119
Figure 29. ^1H -NMR spectrum of 38 in CDCl_3 .	120
Figure 30. ^{13}C -NMR spectrum of 38 in CDCl_3 .	121
Figure 31. ^1H -NMR spectrum of 39 in CDCl_3 .	122
Figure 32. ^{13}C -NMR spectrum of 39 in CDCl_3 .	123
Figure 33. ^1H -NMR spectrum of 40 in CDCl_3 .	124
Figure 34. ^{13}C -NMR spectrum of 40 in CDCl_3 .	125
Figure 35. ^1H -NMR spectrum of 41 in CDCl_3 .	126
Figure 36. ^{13}C -NMR spectrum of 41 in CDCl_3 .	127
Figure 37. ^1H -NMR spectrum of 42 in CDCl_3 .	128
Figure 38. ^1H -NMR spectrum of 36 in CDCl_3 .	129
Figure 39. ^{13}C -NMR spectrum of 36 in CDCl_3 .	130
Figure 40. ^1H -NMR spectrum of 37 in CDCl_3 .	131
Figure 41. ^{13}C -NMR spectrum of 37 in CDCl_3 .	132
Figure 42. ^1H -NMR spectrum of 30 in CDCl_3 .	133
Figure 43. ^1H -NMR spectrum of 31 in CDCl_3 .	134
Figure 44. ^1H -NMR spectrum of 32 in CDCl_3 .	135
Figure 45. ^1H -NMR spectrum of 43a in CDCl_3 .	136
Figure 46. ^{13}C -NMR spectrum of 43a in CDCl_3 .	137
Figure 47. ^1H -NMR spectrum of 43b in CDCl_3 .	138

Figure 48. ^{13}C -NMR spectrum of 43b in CDCl_3 .	139
Figure 49. ^1H -NMR spectrum of 43c in CDCl_3 .	140
Figure 50. ^{13}C -NMR spectrum of 43c in CDCl_3 .	141
Figure 51. ^1H -NMR spectrum of 43d in CDCl_3 .	142
Figure 52. ^{13}C -NMR spectrum of 43d in CDCl_3 .	143
Figure 53. ^1H -NMR spectrum of 46a in CDCl_3 .	144
Figure 54. ^{13}C -NMR spectrum of 46a in CDCl_3 .	145
Figure 55. ^1H -NMR spectrum of 46b in CDCl_3 .	146
Figure 56. ^{13}C -NMR spectrum of 46b in CDCl_3 .	147
Figure 57. ^1H -NMR spectrum of 46c in CDCl_3 .	148
Figure 58. ^{13}C -NMR spectrum of 46c in CDCl_3 .	149
Figure 59. ^1H -NMR spectrum of 46d in CDCl_3 .	150
Figure 60. ^{13}C -NMR spectrum of 46d in CDCl_3 .	151
Figure 61. ^1H -NMR spectrum of 47a in CDCl_3 .	152
Figure 62. ^{13}C -NMR spectrum of 47a in CDCl_3 .	153
Figure 63. ^1H -NMR spectrum of 47b in CDCl_3 .	154
Figure 64. ^{13}C -NMR spectrum of 47b in CDCl_3 .	155
Figure 65. ^1H -NMR spectrum of 47c in CDCl_3 .	156
Figure 66. ^{13}C -NMR spectrum of 47c in CDCl_3 .	157
Figure 67. ^1H -NMR spectrum of 47d in CDCl_3 .	158
Figure 68. ^{13}C -NMR spectrum of 47d in CDCl_3 .	159
Figure 69. ^1H -NMR spectrum of 48a in CDCl_3 .	160
Figure 70. ^{13}C -NMR spectrum of 48a in CDCl_3 .	161
Figure 71. ^1H -NMR spectrum of 48b in CDCl_3 .	162

Figure 72. ^{13}C -NMR spectrum of 48b in CDCl_3 .	163
Figure 73. ^1H -NMR spectrum of 48c in CDCl_3 .	164
Figure 74. ^{13}C -NMR spectrum of 48c in CDCl_3 .	165
Figure 75. ^1H -NMR spectrum of 48d in CDCl_3 .	166
Figure 76. ^{13}C -NMR spectrum of 48d in CDCl_3 .	167
Figure 77. ^1H -NMR spectrum of 45 in CDCl_3 .	168
Figure 78. ^{13}C -NMR spectrum of 45 in CDCl_3 .	169

LIST OF TABLES

Table 1. Screening of reaction conditions for Miyaura borylation of 25 .	15
Table 2. Screening of reaction conditions for Suzuki cross-coupling between 25 and 31 .	17
Table 3. Screening of conditions to activate enone double bond in 29 .	19
Table 4. Screening of reaction conditions for the oxidation of 41 to 42 .	23
Table 5. Screening of oxidants for semisynthesis of daldiquinone (15) from daldinol (28).	25

LIST OF SCHEMES

Scheme 1. Proposed biogenetic pathway for benzo[j]fluoranthene-based natural products.....	6
Scheme 2. Dalavalle's total synthesis of benzo[j]fluoranthene-4,9-diol (2).	7
Scheme 3. Hosokawa's total synthesis of XR774 (14).....	8
Scheme 4. Proposed synthetic route for the synthesis of daldiquinone (15) and bulgarein (1).....	11
Scheme 5. Retrosynthetic analysis of daldiquinone (15) and bulgarein (1).	12
Scheme 6. Proposed cyclization of 18	13
Scheme 7. Synthesis of 25 from 1,8-naphthalenediol.	14
Scheme 8. Dimerization of 25 under Miyaura borylation conditions.	14
Scheme 9. Synthesis of daldinol (28) via one-pot Suzuki-Miyaura coupling reaction ...	15
Scheme 10. Synthesis of daldiquinone (15) from 27	16
Scheme 11. Synthesis of unsymmetrical binaphthalene 32	17
Scheme 12. Total synthesis of daldiquinone (15).	18
Scheme 13. Proposed formation of fluoranthene skeleton via cyclization.	19
Scheme 14. Attempt to construct fluoranthene core by using 34 and 37	21
Scheme 15. Total Synthesis of bulgarein (1).....	22
Scheme 16. Semisynthesis of daldiquinone (15) from daldinol (28).....	25
Scheme 17. Fluoranthene derivative as a reporter molecule.	29
Scheme 18. Selected Diels-Alder reactions to synthesize fluoranthene derivatives.	30
Scheme 19. Diels-Alder reaction between acenaphthylene and isobenzofuran.	31
Scheme 20. Reported synthesis of substituted fluoranthene.	31

Scheme 21. Selected Pd catalyzed processes to assemble fluoranthene core.	33
Scheme 22. Au(I) catalyzed Friedel-Crafts-type alkenylation of arenes for the synthesis of 3-substituted fluoranthenes.	34
Scheme 23. Rh(I)-catalyzed [(2+2)+2] cycloaddition between norbornadiene and 1,8-naphthalene.	34
Scheme 24. KHMDS-promoted cascade cyclization strategy for fluoranthene synthesis.	35
Scheme 25. Proposed strategy to synthesize substituted hydroxyfluoranthenes.	36
Scheme 26. Synthesis of alkynes 43a-d	37
Scheme 27. Synthesis of 1,8-diiodonaphthalene.	38
Scheme 28. Mono-Sonogashira reaction of alkynes with 1,8-diiodonaphthalene.	39
Scheme 29. Oxidation of alkyne-ols to ketones.	40
Scheme 30. One-pot three steps synthesis of fluoranthene derivatives	41
Scheme 31. Representation for one-pot three steps formation of hydroxyfluoranthenes.	41

CHAPTER 1: TOTAL SYNTHESIS OF BIOACTIVE FUNGAL NATURAL PRODUCTS DALDIQUINONE AND BULGAREIN

1.1. INTRODUCTION

1.1.1. Fluoranthene-based Natural Products

Fluoranthene is a cyclopenta-fused polycyclic aromatic hydrocarbon (PAH) (Figure 1). A significant number of fluoranthene and benzo[*j*]fluoranthene-based secondary metabolites are isolated from nature, many of which exhibit promising biological activities (Figure 2).¹

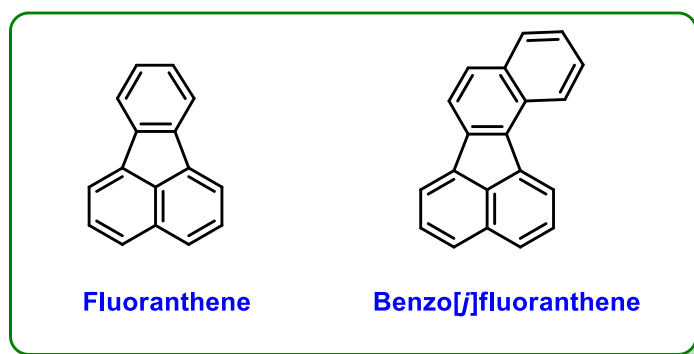


Figure 1. Structures of fluoranthene and benzo[*j*]fluoranthene.

Fungal natural products, truncatone A, C and D were isolated from the extracts of *Annulohyphoxylon* species.² Upon biological tests, benzo[*j*]fluoranthene derivatives showed moderate cytotoxicity to the mouse fibroblast cell line L929.² Among the chemical constituents of mushroom *Hyphoxylon truncatum*, hyphoxylon D and E exhibited antiproliferative activity against human umbilical vein endothelial cells (HUVECs) and human umbilical artery endothelial cells (HUAECs) with low IC₅₀ values (4.1-7.4 μM).³ Another group of benzo[*j*]fluoranthene-based metabolites isolated from

Annulohypoxyton species is daldinones A-D.⁴ Screenings for biological activity revealed cytotoxicity of daldinone C and daldinone D against SW1116 cell line with the IC₅₀ values of 49.5 and 41.0 μM. Later, daldinone D was found to be strongly cytotoxic to Jurkat J16 and Ramos (human leukemia and lymphoma) cell lines with low IC₅₀ values.⁴

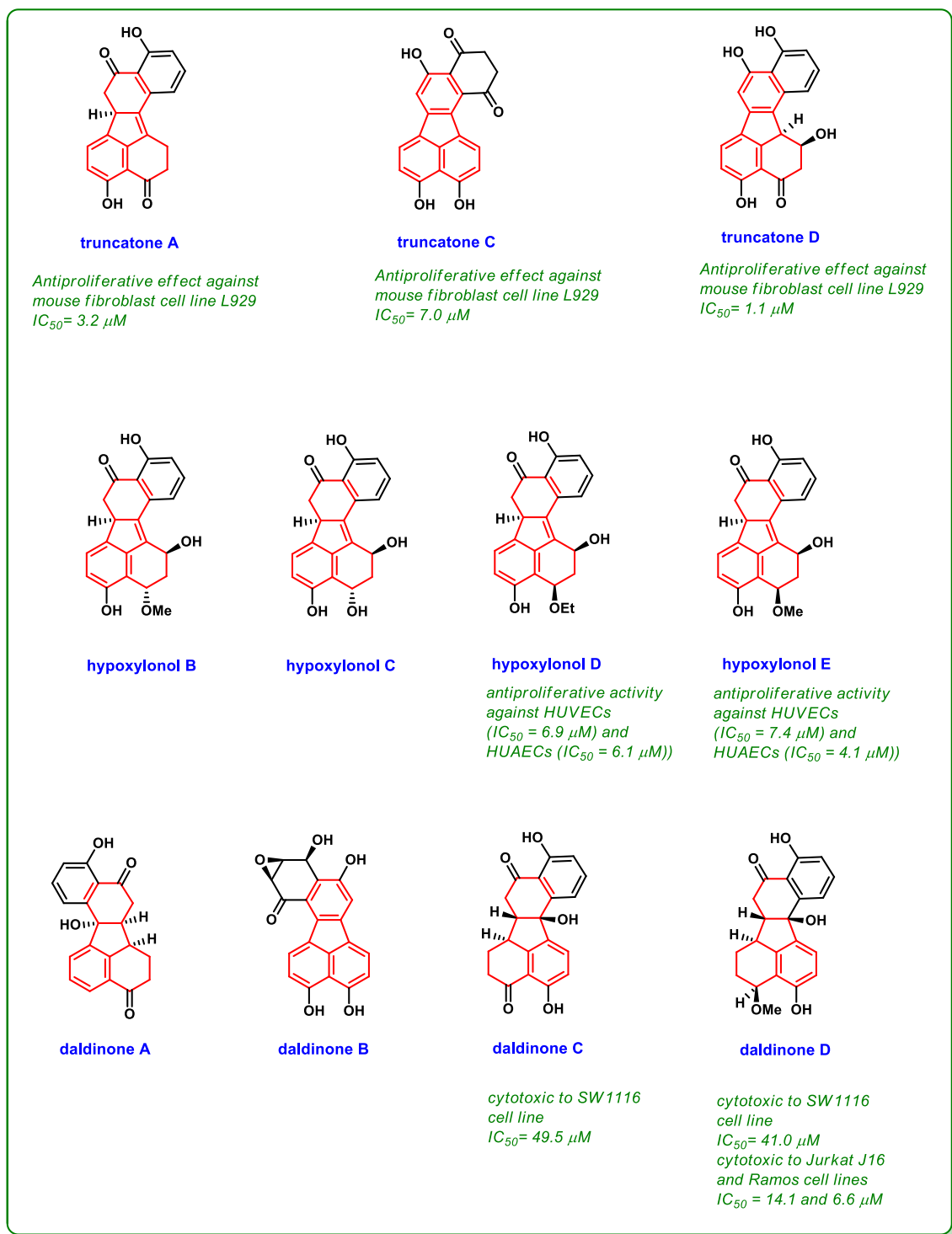


Figure 2. Selected examples of fluoranthene-based natural products.

In 1976, R. L. Edwards and H. J. Lockett examined the extracts from fungus *Bulgaria inquinans* and reported two new secondary benzo[*j*]fluoranthene metabolites, bulgarein (**1**) and bulgarhodin (Figure 3).⁵ Later studies revealed promising bioactivity of the fungal natural product bulgarein to induce topoisomerase I-mediated DNA cleavage.⁶

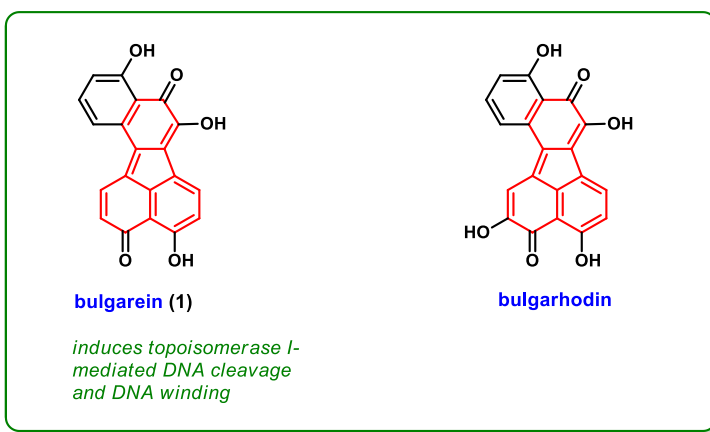


Figure 3. Chemical constituents of *Bulgaria inquinans*.

There are also unnamed fluoranthene derivatives with attractive bioactivity profiles (Figure 4). A fungal natural product with reduced benzo[*j*]fluoranthene-3-one skeleton is a potent inhibitor of anti-CD28-induced IL-2 production ($IC_{50} = 400$ nM) and Abl tyrosine kinase ($IC_{50} = 60$ nM).⁷ Another natural product, benzo[*j*]fluoranthene-4,9 diol (**2**), was isolated from fungus *Daldinia eschscholzii* and exhibited immunosuppressive activity.⁸

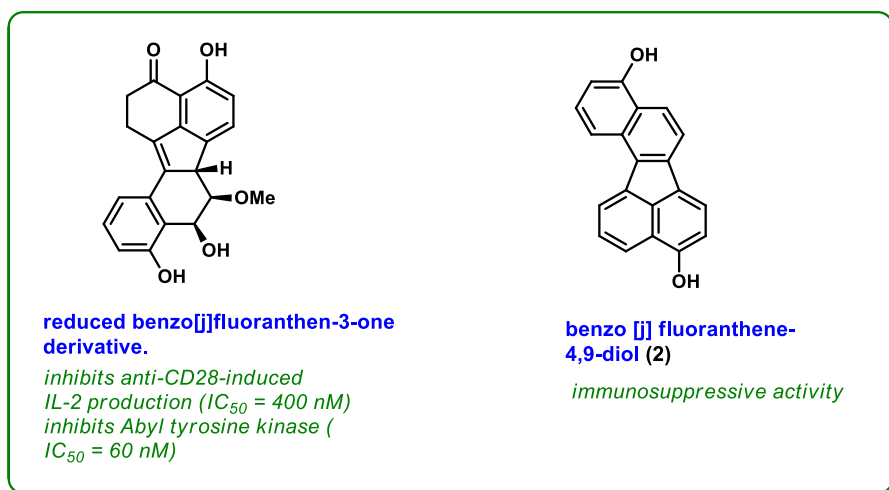
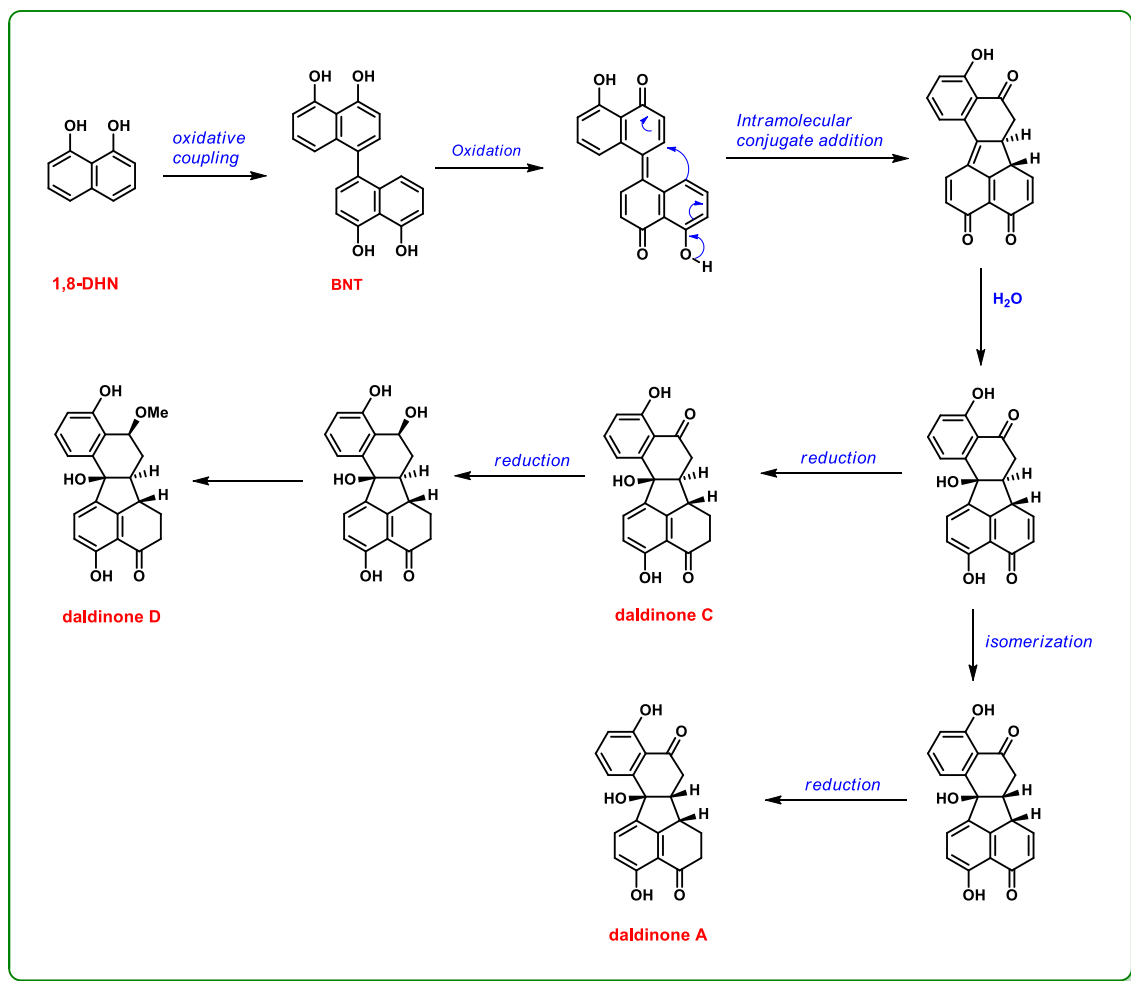


Figure 4. Unnamed benzo[j]fluoranthene metabolites.

1.1.2. Biosynthesis of benzo[j]fluoranthene metabolites

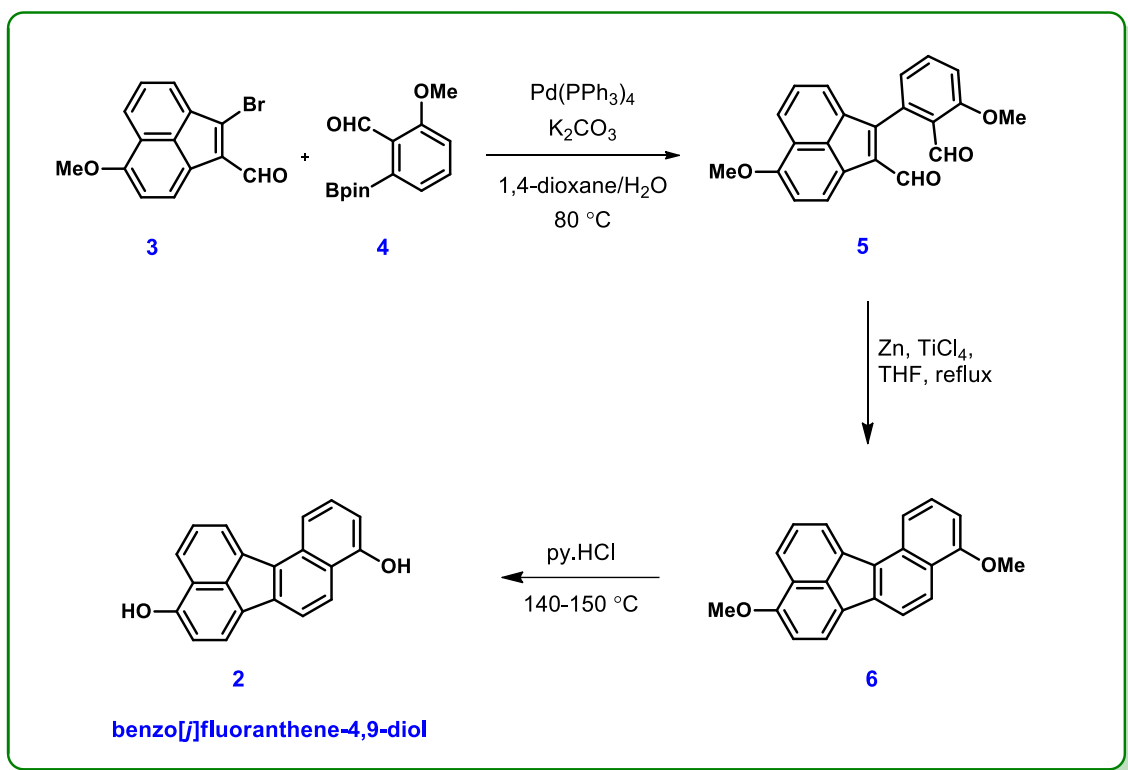
In a previously reported study^{4d}, biosynthesis of benzo[j]fluoranthene-based natural products was proposed to start with the conversion of 1,8-DHN (1,8-dihydroxynaphthalene) to BNT ([1,1'-binaphthalene]-4,4',5,5'-tetrol) via oxidative para coupling. According to the proposed biogenetic pathway, BNT then experiences the sequence of events described in Scheme 1 to generate benzo[j]fluoranthene derivatives, daldinones A, C and D.



Scheme 1. Proposed biogenetic pathway for benzo[*j*]fluoranthene-based natural products.

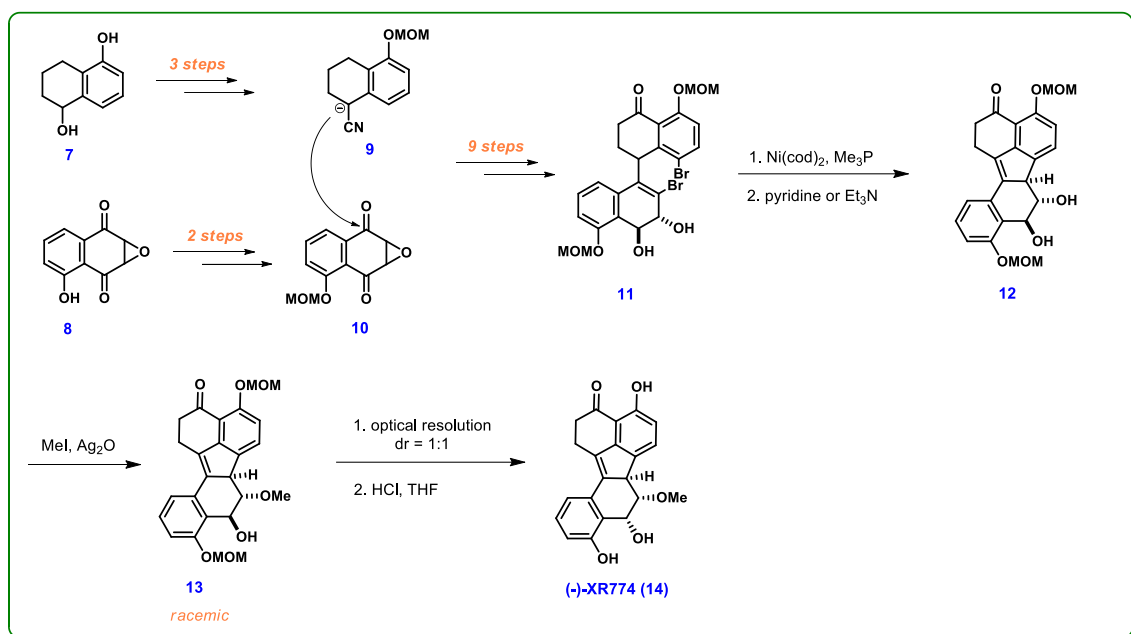
1.1.3. Total Synthesis of Fluoranthene-based Natural Products

To date, only two total syntheses have been reported for the fluoranthene-based natural products. In 2013, Dalavalle and co-workers reported a 7-steps total synthesis (LLS) of pentacyclic natural product benzo[*j*]fluoranthene-4,9-diol (**2**).⁹ Suzuki coupling reaction between boronate (**4**) and bromoaldehyde (**3**), and Mc-Murry coupling of resulting dialdehyde (**5**) were employed as key steps (Scheme 2). Final demethylation of **6** afforded benzo[*j*]fluoranthene-4,9-diol (**2**).



Scheme 2. Dalavalle's total synthesis of benzo[*j*]fluoranthene-4,9-diol (**2**).

In 2018, Hosokawa and co-workers reported the first total synthesis and structural determination of tyrosine kinase inhibitor XR774 (**14**).¹⁰ The long synthetic route was marked by series of challenging chemical transformations including regioselective 1,2-addition of lithiated tetraline **9** to **10**, dibromination of tetracyclic core and Ni-mediated cyclization to assemble benzo[*j*]fluoranthene skeleton (Scheme 3). Racemic **13** was finally converted to optically active (-)-XR774 (**14**) by optical resolution (dr = 1:1) followed by treatment with HCl.



Scheme 3. Hosokawa's total synthesis of XR774 (**14**).

1.1.4. *ortho*-Naphthoquinone-based Natural Products

A number of naturally occurring *ortho*-naphthoquinone derivatives are known. β -Lapachone was isolated from lapacho tree by Paterno in 1882.¹¹ A broad spectrum of biological activities reported for β -lapachone, including antifungal, antibacterial, antitrypanocidal and antitumor activities.^{12,13} Several routes have been reported for the synthesis of β -lapachone.¹¹ Mansonone E and F were isolated from a tree called *Ulmus pumila* L. whose extracts have been used in traditional Chinese medicine.¹⁴ Tests for antiproliferative activities revealed cytotoxicity of mansonone E and mansonone F against various human tumor cells with IC₅₀ values of 0.9-7.9 μ M and 3.0-29.4 μ M, respectively. Constitutional isomer of β -lapachone, rhinacanthone is another naturally occurring 1,2-naphthoquinone metabolite with antitumor and antifungal (ED₅₀ = μ g/ml) activities.¹⁵ In 2016, triphyoquinone A was isolated as one of the chemical constituents of *Triphophyllum peltatum* and showed axial chirality phenomenon.¹⁶ Recently,

Koyama and co-workers separated fungal natural product daldiquinone (**15**) from the chemical constituents of *Daldinia concentrica*, which showed antiangiogenesis activity against HUVECs with an IC₅₀ value of 7.5 μM.¹⁷

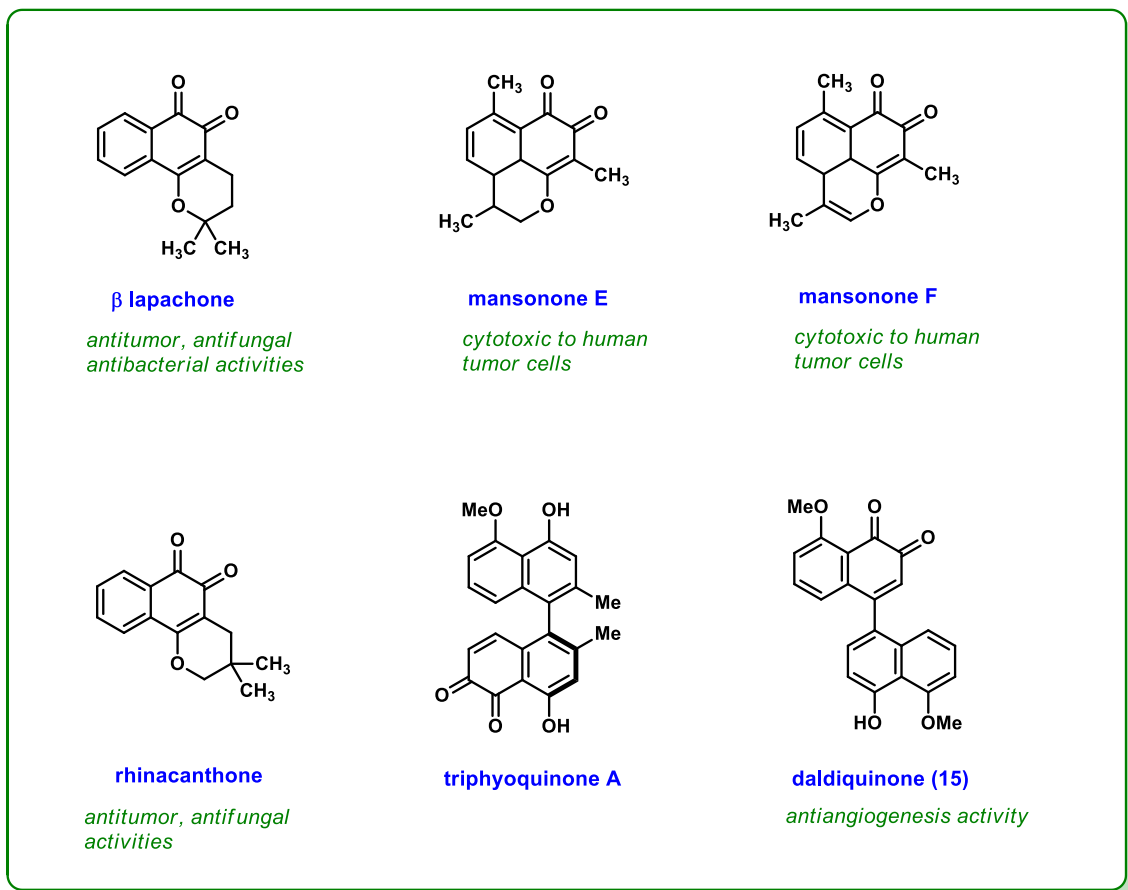
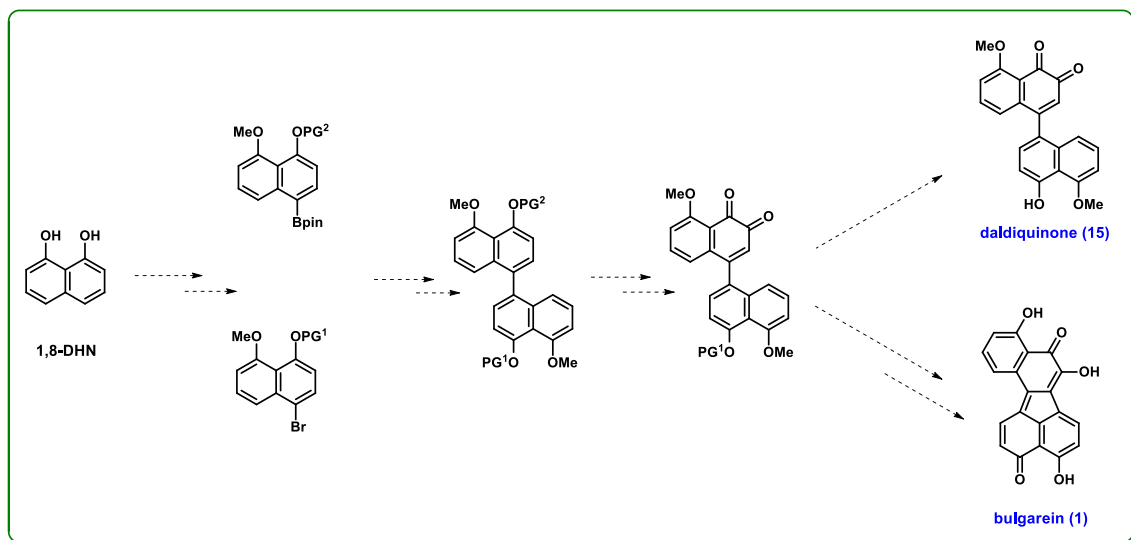


Figure 5. Selected examples of 1,2-naphthaquinone based natural products.

1.1.5. Aim of This Work

Biologically active natural product bulgarein (**1**), which possesses a highly oxygenated pentacyclic benzo[*j*]fluoranthene skeleton, was first isolated in 1976 from the extracts of Fungus *Bulgaria inquinans* and exhibited topoisomerase I inhibition.⁵ In 2018, another fungal natural product daldiquinone (**15**) was isolated from *Daldinia concentrica* and showed antiangiogenesis activity against HUVECs with a low IC₅₀ value (7.5 μM).¹⁷ Despite attractive biological activities and grown interest in the chemistry of fluoranthene and naphthoquinone metabolites, total syntheses for both natural products have yet to be reported. This work aims to achieve total syntheses of bulgarein (**1**) and daldiquinone (**15**) starting from commercially available 1,8-naphthalenediol via a concise route. Suzuki coupling reaction between functionalized naphthalene derivatives followed by selective deprotection and double oxidation to *o*-quinone will generate protected 1,2-naphthoquinone derivative, which is proposed to be a common precursor for both natural products (Scheme 4). The findings of the study may also shed light on the biogenetic pathway of natural products.



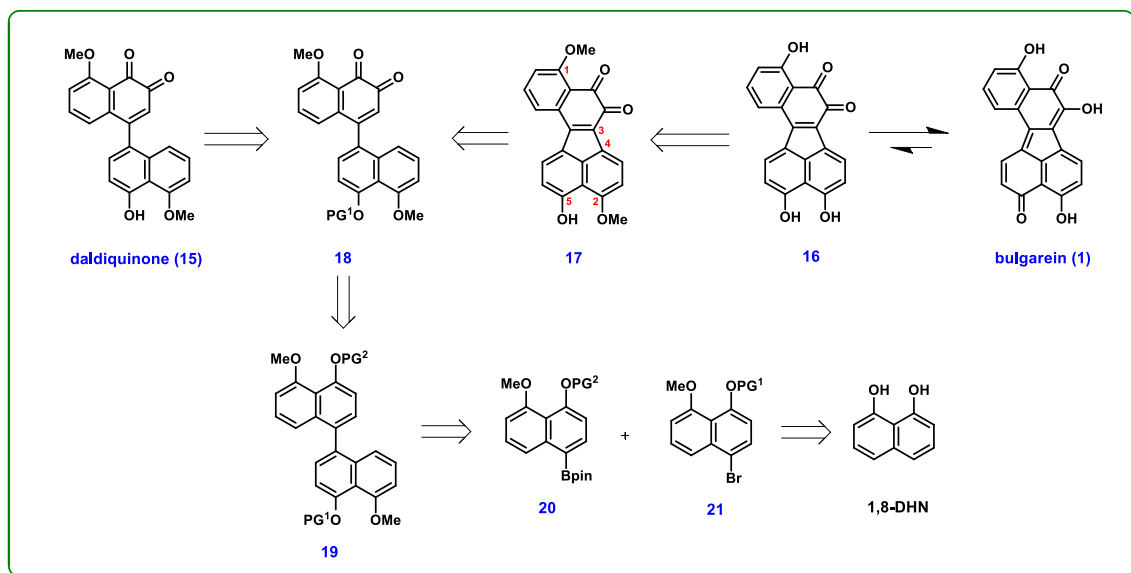
Scheme 4. Proposed synthetic route for the synthesis of daldiquinone (**15**) and bulgarein (**1**).

1.2. RESULTS AND DISCUSSION

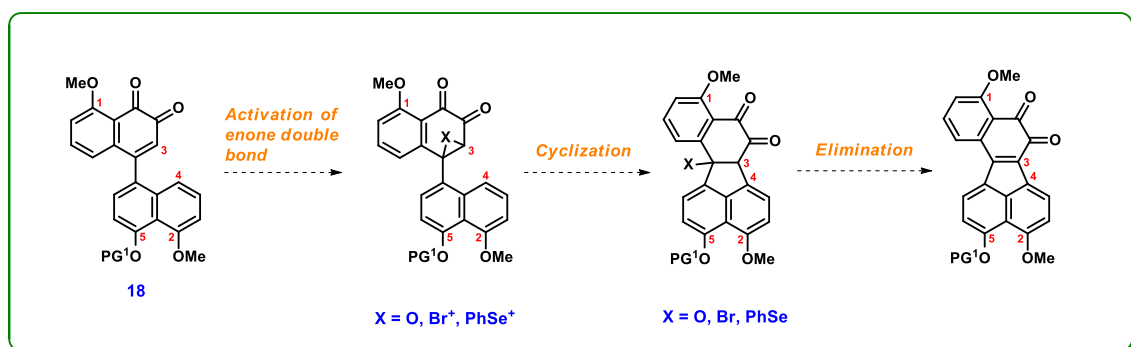
1.2.1. Retrosynthetic analysis

From a retrosynthetic perspective, we started with structural analysis of daldiquinone (**15**) and bulgarein (**1**), which revealed significant similarities between the two natural products. In terms of the core skeleton, both natural products contain two naphthalene rings and have the same number of oxygen atoms. Structural similarity between daldiquinone and bulgarein became even more apparent when we considered the tautomeric form of bulgarein **16** (Scheme 5). The energy difference between these tautomeric forms presumably arises from intramolecular hydrogen bonding. This suggests, if hydroxyl groups on C1 and C2 are protected as methyl ether, then **17** will be the major tautomeric form since six-membered intramolecular hydrogen bonding will be preferred over a five-membered one. A reasonable strategy to make the carbon-carbon

bond between C3 and C4 can be executed by activating the enone double bond followed by an electrophilic aromatic attack to sp^3 hybridized α -carbon (C3) from anisole ring (C4). Finally, regeneration of the enone double bond via elimination can complete the transformation. (Scheme 6). However, intramolecular hydrogen bonding makes the phenol ring more electron-rich than the anisole ring. As a result, electron push from phenol ring to activated alkene will be more likely, which can be prevented if hydroxyl group on C5 is also protected. With that in mind, we envisioned naphthoquinone **18** as a common precursor for both daldiquinone (**15**) and bulgarein (**1**). Compound **18** can be derived from unsymmetrical binaphthalene **19** by selective deprotection and subsequent oxidation. Suzuki-Miyaura coupling between functionalized naphthalene derivatives **20** and **21** can be used to deliver **19**. Both **20** and **21** can be traced back to commercially available 1,8-naphthalenediol (**1,8-DHN**).



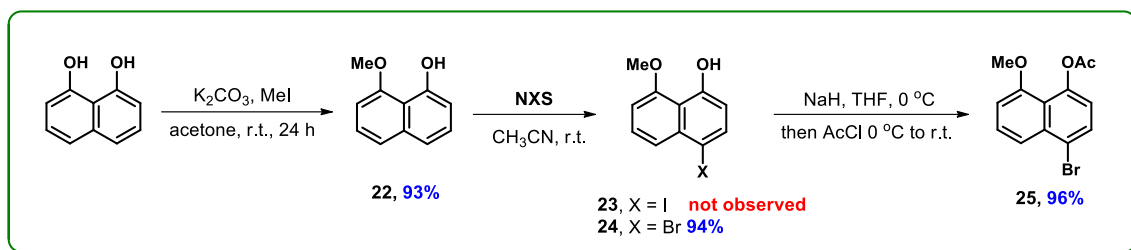
Scheme 5. Retrosynthetic analysis of daldiquinone (**15**) and bulgarein (**1**).



Scheme 6. Proposed cyclization of **18**.

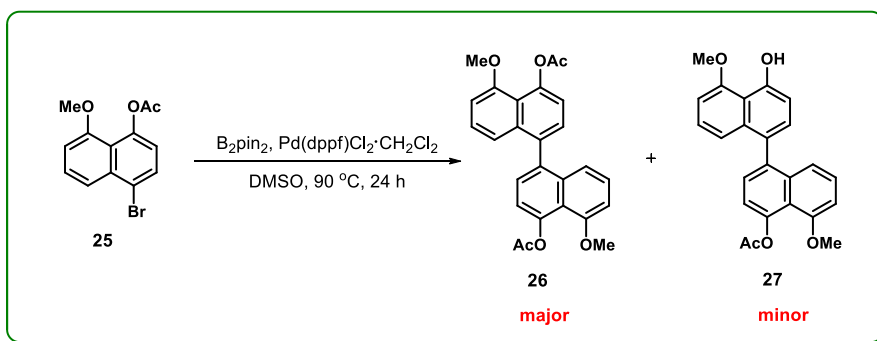
1.2.2 Total Synthesis of Daldiquinone

At the outset, synthetic sequence commenced with monomethylation of commercially available 1,8-naphthalenediol by using iodomethane as an electrophilic methyl source to give **22** in 93% yield.¹⁸ In addition to the para selectivity of naphthalene ring due to the relative stability of Wheland intermediate in electrophilic aromatic substitution reactions, compound **22** also has intramolecular hydrogen bonding,¹⁹ which provides further regioselectivity between phenol and anisole rings by making phenol ring more electron-rich. Although all efforts for electrophilic aromatic iodination of **22** by using NIS or I₂ failed to give desired product **23**, electrophilic aromatic bromination product **24** was synthesized using NBS in 94% yield.¹⁸ Notably, using anhydrous CH₃CN and recrystallization of NBS from H₂O depleted the formation of side products and increased the yield of the reaction. Acetylation of **24** using AcCl and NaH proceeded smoothly to furnish **25** in 96% yield (Scheme 7).



Scheme 7. Synthesis of **25** from 1,8-naphthalenediol.

The next step was the Miyaura borylation reaction of **25** which resulted in the unexpected formation of symmetrical dimeric naphthalene derivative **26** and the partially hydrolyzed side product **27**, possibly due to the rapid Suzuki coupling reaction between formed boronic ester and starting material compared to the Miyaura borylation (Scheme 8). Screening the reaction temperature, catalyst loading and the amount of B_2pin_2 did not provide an improvement (Table 1).



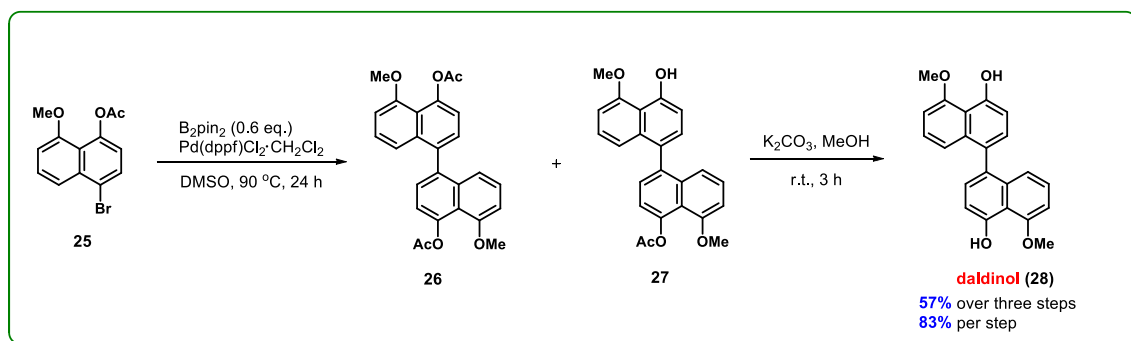
Scheme 8. Dimerization of **25** under Miyaura borylation conditions.

Table 1. Screening of reaction conditions for Miyaura borylation of **25**.

Entry	Pd(dppf)Cl ₂ ·CH ₂ Cl ₂ (equiv.)	B ₂ pin ₂ (equiv.)	Temperature (°C)	Ar-Bpin formation
1	0.1	1.05	90	Not observed
2	0.05	1.05	80	Not observed
3	0.03	2.0	80	Not observed
4	0.05	1.0	70	Not observed

Reaction conditions: Mixture of **25**, B₂pin₂, Pd(dppf)Cl₂·CH₂Cl₂ and KOAc (3 equiv.) in DMSO (purged with N₂ for 10-15 minutes) in a round-bottomed flask sealed with a glass stopper and heated to specified temperature.

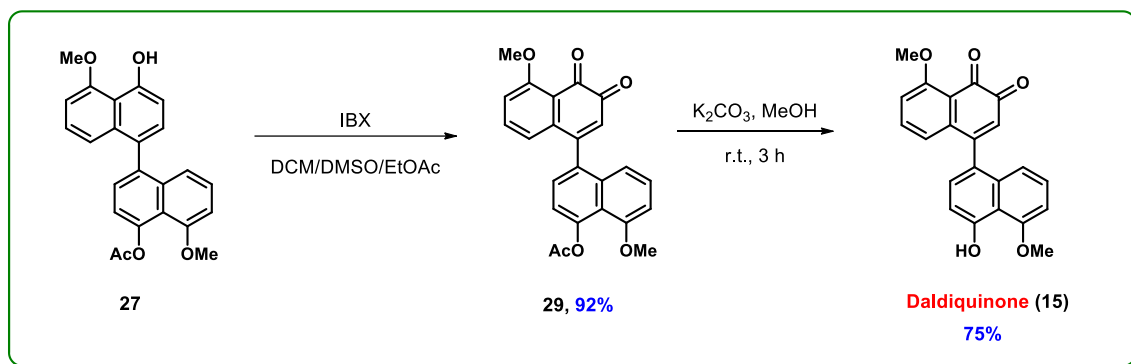
Basic hydrolysis of the reaction mixture obtained from the one-pot Suzuki-Miyaura coupling reaction of **25** by using 0.6 equivalents of B₂pin₂, furnished natural product daldinol (**28**) in 57% yield over three steps (Scheme 9).^{20,21}



Scheme 9. Synthesis of daldinol (**28**) via one-pot Suzuki-Miyaura coupling reaction

At this stage, partially hydrolyzed side product **27** was purified by column chromatography and oxidized by using IBX²² to give naphthoquinone **29** in high yield (92%). This double oxidation of phenol to *o*-quinone proceeds via sigmatropic oxygen

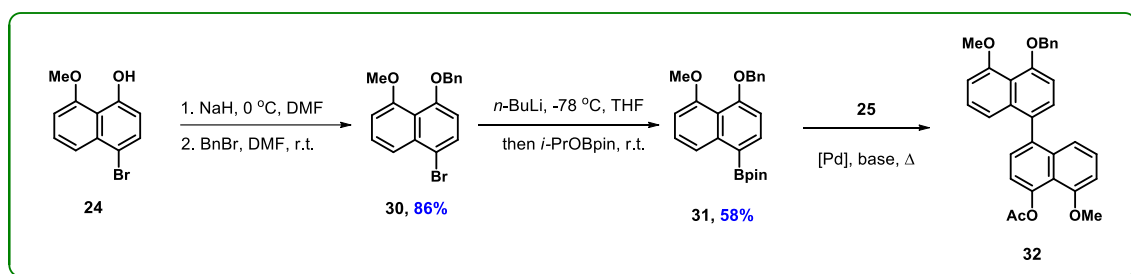
transfer from iodanyl complex formed after condensation of IBX and phenol.^{22b} Both commercially available S-IBX²³ and the one prepared from IBA following the literature procedure²⁴ were effective and led to similar results. Final deprotection of acetyl group of **29** by using K₂CO₃ in MeOH afforded daldiquinone (**15**) in 75% yield (Scheme 10).



Scheme 10. Synthesis of daldiquinone (**15**) from **27**.

Inspired by these results, the optimized synthesis of binaphthyl **27** was targeted. An unsymmetrical binaphthalene containing an orthogonal protecting group to acetate was required. Since the benzyl group can be deprotected with palladium-catalyzed hydrogenolysis²⁵ it can be selectively removed in the presence of acetate group in the later stage of the sequence to give **27**. To prepare a boronic ester partner for Suzuki cross-coupling reaction, benzyl-protected naphthalene derivative **30** was synthesized in 86% yield from **24** by using BnBr and NaH. Compound **30** was then converted to boronic ester **31** in 58% yield by using lithium-bromide exchange reaction followed by addition of *i*-PrOBpin. With boronic ester in hand, the stage was set for a seemingly straightforward Suzuki coupling reaction (Scheme 11). Unfortunately, the coupling reaction between boronic ester **31** and acetoxynaphthalene **25** turned out to be

remarkably difficult and proceeded in meager yields to give **32** under typical Suzuki coupling conditions (Table 2).



Scheme 11. Synthesis of unsymmetrical binaphthalene **32**.

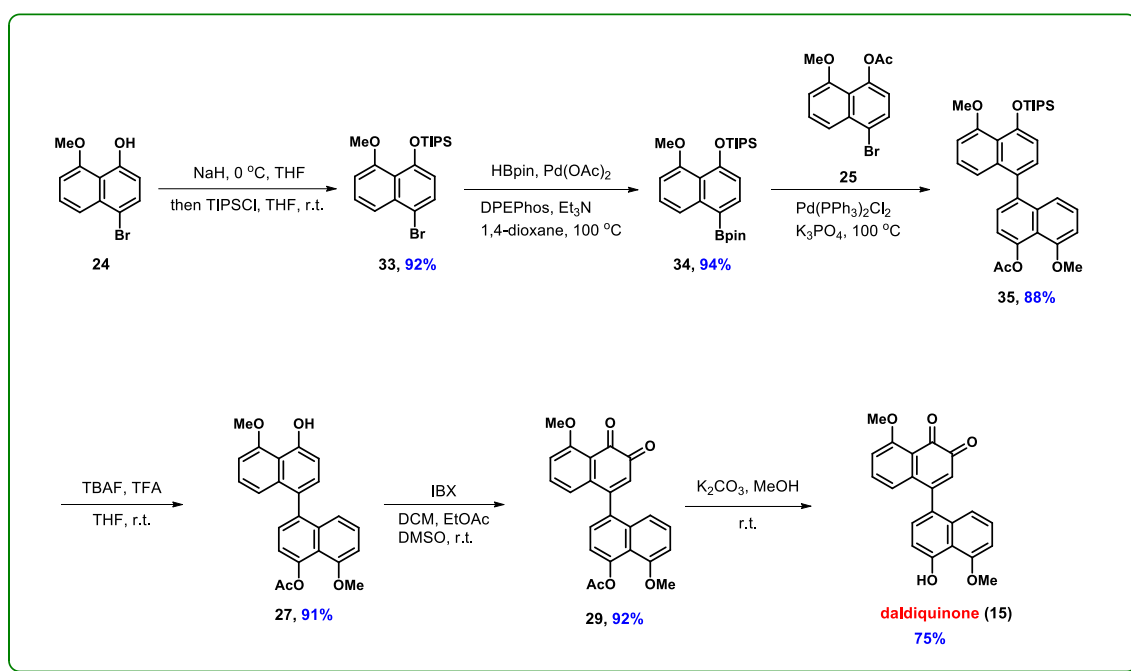
Table 2. Screening of reaction conditions for Suzuki cross-coupling between **25** and **31**.

Entry	Base	Catalyst	Solvent, temperature, time	Formation of 32
1	K ₃ PO ₄	Pd(PPh ₃) ₄	DMF, 80 °C, 5 h	10 %
2	K ₃ PO ₄	Pd(PPh ₃) ₄	DMF, 80 °C, 6.5 h	24%
3^a	KOAc	Pd(dppf)Cl ₂ ·CH ₂ Cl ₂	DMSO, 80 °C, 4 h	21%
4	KOAc	Pd(dppf)Cl ₂ ·CH ₂ Cl ₂	DMSO, 80 °C, 5 h	32%
5^b	Ba(OH) ₂ ·8H ₂ O	Pd(PPh ₃) ₄	DME/H ₂ O	33%

Reaction conditions: A mixture of **25**, **31**, Pd catalyst, and base in given solvent(s) heated to 80 °C. Stirred at 80 °C until TLC indicated the full consumption of **25** or **31**. ^a1.2 equiv. boronic ester **31** used. ^bNMR conversion. 1.1 equiv boronic ester used.

In the light of previous results where acetoxynaphthalene **25** readily dimerized under Miyaura borylation conditions, low yields of Suzuki coupling were associated with the benzyl-protected boronic ester **31**. As a viable alternative to the benzyl protecting group, silyl ether protection was employed. TIPS-protected naphthalene derivative **33** was prepared from **24** in 92% yield. Siloxynaphthalene **33** was then converted to the corresponding boronic ester **34** by using HBpin²⁶ in 94% yield, which

set the stage for the coupling reaction. Suzuki cross-coupling reaction between acetoxynaphthalene **25** and boronic ester **34** afforded desired unsymmetrical binaphthalene **35** in high yield (88%). TIPS ether was selectively deprotected to give **27** in 91% yield using TBAF as a fluoride source. TFA was used to protonate the formed oxyanion, which otherwise leads to side products by attacking the acetate group of starting material **35** or product **27**. Finally, oxidation of **27** by using IBX followed by hydrolysis of acetate group concluded the first optimized total synthesis of bioactive fungal natural product daldiquinone (**15**) (Scheme 12).

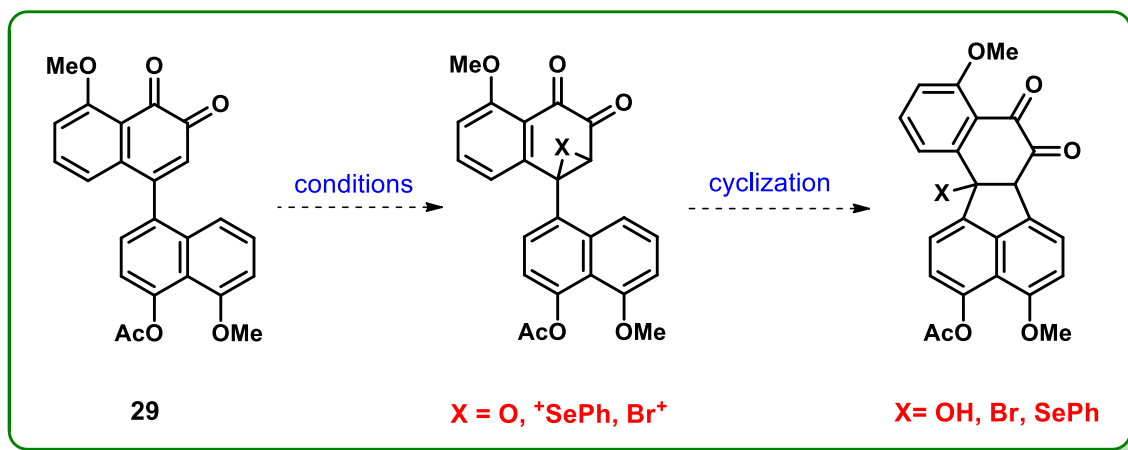


Scheme 12. Total synthesis of daldiquinone (**15**).

1.2.3. Total Synthesis of Bulgarein

Having completed the total synthesis of daldiquinone we turned our attention to test our hypothesis by examining the possible synthesis of bulgarein (**1**) from **29**. To activate electron-deficient enone double bond and trigger cyclization (Scheme 13),

various sets of conditions were tested (Table 3). Much to our chagrin, none of the conditions delivered the desired transformation.



Scheme 13. Proposed formation of fluoranthene skeleton via cyclization.

Table 3. Screening of conditions to activate enone double bond in **29**.

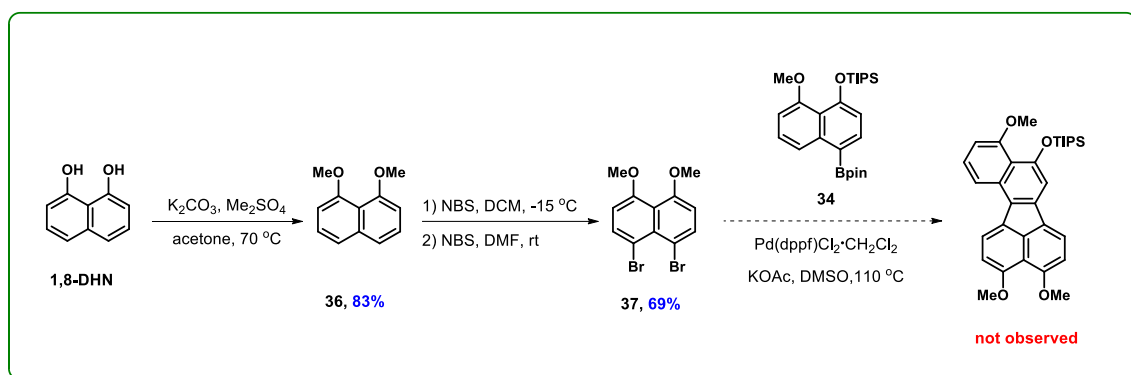
Entry	Conditions	Result
1	H ₂ O ₂ , NaOH, EtOH/DCM, r.t.	Complex mixture
2	H ₂ O ₂ , K ₂ CO ₃ , EtOH/DCM, r.t.	Complex mixture
3	H ₂ O ₂ , TBAF, DCM/DMSO	Daldiquinone formation
4	TBHP, NaH, DCM/DMSO	No reaction
5	m-CPBA, DCM, r.t.	Probably Bayer-Villiger oxidation
6	PhSeBr, CH ₃ CN, r.t. then 45 °C	No reaction
7	NaClO, 1,4-dioxane, 0 °C	Decomposition
8	Br ₂	Slow reaction. Formation of multiple products
9	NBS	Slow reaction. Formation of multiple products

Reaction Conditions: A mixture of **29** and reagents in given solvent(s) stirred at specified temperature until TLC indicated the full consumption of **29**.

The labile acetate group in **29** reacted with nucleophilic oxidizing agents well-suited for the epoxidation of electron-deficient olefins. It resulted in either decomposition (Table 3, entries 1,2) or formation of daldiquinone (entry 3). To obviate acetate hydrolysis, the use of sterically bulky TBHP alongside non-nucleophilic base NaH not resulted in any detectable product formation (entry 4). Halohydrin epoxidation by using hypochlorite bleach solution led to decomposition of **29** (entry 7). Attempts to activate electron-deficient alkene by common electrophilic epoxidizing agent *m*-CPBA resulted in a product we believe obtained from Baeyer-Villiger oxidation of diketone (entry 5). Unfortunately, the exact position of oxygen insertion could not be determined from the ¹H-NMR spectrum. The idea of activating double bond using PhSeBr, and regenerating enone double bond via pyrolytic syn-elimination was also fruitless since alkene was not reactive enough to attack PhSeBr (entry 6). The electrophilic bromination of the alkene by using Br₂ and NBS failed primarily due to the competing electrophilic aromatic substitution of electron-rich benzene rings (entries 8, 9).

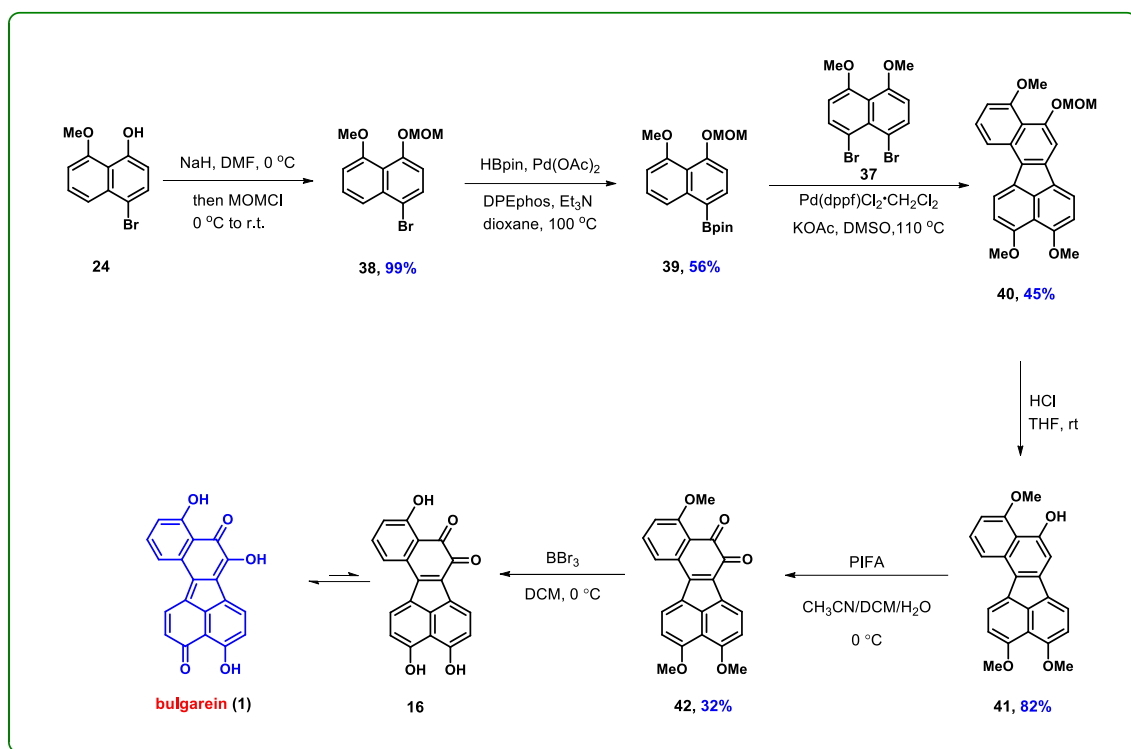
At this point, we modified our retrosynthetic plan for the total synthesis of bulgarein (**1**), and to construct the highly unsaturated pentacyclic fluoranthene core we decided to utilize a method developed by our group which is based on Suzuki coupling reaction between 1,8-dihalonaphthalene and aryl boronic ester followed by intramolecular C-H arylation.¹ To this end, 1,8-dibromo-4,5-dimethoxynaphthalene (**37**) was prepared from 1,8-naphthalenediol according to previously reported procedures.^{19,27} When TIPS-protected boronic ester **34** and 1,8-dibromo-4,5-dimethoxynaphthalene (**37**) were subjected to reaction conditions, no product formation was observed (Scheme 14). Detailed examination of the crude reaction mixture by ¹H-NMR revealed decomposition

of boronic ester **34**. This result was attributed to the presence of TIPS ether on aryl boronic ester **34**, which presumably does not tolerate harsh reaction conditions.



Scheme 14. Attempt to construct fluoranthene core by using **34** and **37**.

To circumvent this undesirable decomposition, the synthesis of aryl boronic ester with a more inert protecting group was planned. With this in mind, MOM-protected naphthalene derivative **38** was prepared from **24** in quantitative yield (99%) and then converted to corresponding boronic ester **39**. Gratifyingly, coupling of MOM-protected boronic ester **39** and 1,8-dibromo-4,5-dimethoxynaphthalene (**37**) furnished highly functionalized fluoranthene core in 45% yield. The endgame of synthesis consisted of three steps and started with demethoxymethylation of **40** upon exposure to HCl in THF to afford **41** in 82% yield (Scheme 15).²⁵



Scheme 15. Total Synthesis of bulgarein (**1**).

By contrast to the double oxidation of **27** with IBX in daldiquinone (**15**) synthetic sequence, similar oxidation of **41** to *o*-quinone turned out to be exceedingly challenging. Up to this point, various sets of reaction conditions were tested, and the best result was obtained by PIFA oxidation^{22b} (32% yield) where the solution of PIFA was added slowly for 20-minutes to the solution of **41** at 0 °C (Table 4, entry 2). The low solubility of **41** did not allow conducting oxidation by using PIFA at lower temperatures than 0 °C. Oxidation by using IBX afforded desired product **42** in a slightly lower yield (30%). Since IBX is poorly soluble in common organic solvents²⁸ except for DMSO (m.p. = 18 °C), oxidation could not be carried out at lower temperatures. When the oxidation with IBX was carried out in other organic solvents in which IBX is slightly soluble, the formation of the desired *o*-quinone was not observed (entries 8,9,10). Further

investigation and modifications of reaction conditions are required to increase the yield of this oxidation step. When compared to oxidation of **27**, lower yields obtained for the oxidation of fluoranthene **41** are likely to be the result of the planar structure of **41**. Unlike **27**, π electrons of all four benzene rings are delocalized in **41** resulting in highly functionalized electron-rich polycyclic aromatic hydrocarbon which may react with oxidants in many different undesirable and unpredictable pathways including SET (single electron transfer), oxidative coupling, cationic polymerization, radicalic polymerization, etc.

Table 4. Screening of reaction conditions for the oxidation of **41** to **42**.

Entry	Oxidant	Equiv.	Solvent, additive	Temperature	Formation of 42
1^a	PIFA	2.2	CH ₃ CN/H ₂ O/DCM (4:2:1)	0 °C then 23 °C	23% yield
2^b	PIFA^b	2.2	CH₃CN/H₂O/DCM (2:1:1)	0 °C	32% yield
3²⁹	PIDA	2.2	CH ₃ CN/DCM/ H ₂ O (2:2:1)	0 °C	Not observed
4^{c e}	S-IBX	4.5	DMSO/DCM (3:2)	23 °C	30% yield
5^f	S-IBX	4.0	DCM/DMSO (1:1)	23 °C	19% yield
6^e	S-IBX	2.0	DCM/DMSO(1:1)	23 °C	16% yield
7	S-IBX	1.5	DMSO	23 °C	6% yield
8^e	S-IBX^e	1.2	DMF	23 °C	Not observed
9	S-IBX	1.1	THF	23 °C	Not observed
10	S-IBX	1.1	EtOAc	23 °C	Not observed
11³⁰	S-IBX^{ref 14}	1.5	DCM/H ₂ O (1:1), TBAB	23 °C	Not observed
12	CAN	4.0	DCM/H ₂ O (2:1)	23 °C	Not observed
13^{d,31}	m-CPBA	1.5	DCM	23 °C	Not observed
14³²	O₂(air)	-	EtOH, CuCl ₂ (0.3 equiv), DMAP (0.3 equiv)	23 °C	Not observed

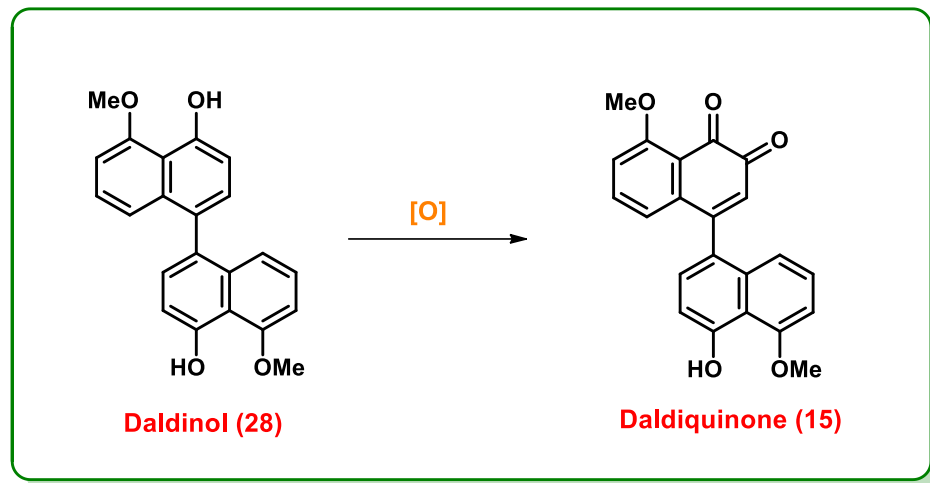
^aDilute solution (0.025) of oxidant in H₂O/DCM (2:1) added dropwise during 10 minutes. ^bDilute solution (0.0067M) of oxidant in CH₃CN/H₂O/DCM (3:1.5:1) added dropwise during 20 minutes. ^cSolid S-IBX was added in four different portions during 3 hours. ^dm-CPBA was added in portions during 30 minutes. ^eReaction was carried out in dark. ^fAdditional 4.0 equiv. oxidant was added after 75 minutes

The last step of the sequence was global demethylation of **42** which was first tested with heating **42** in excess of molten pyridine hydrochloride (m.p. = 144 °C).³³ Although high temperature (180 °C) resulted in the decomposition of **42**, a product formed at 147 °C (monitored by TLC). However, the formed product could not be characterized by analytical tools due to the large excess of pyridine, which could not be removed despite all efforts.

Gratifyingly, complete demethylation of **42** was accomplished using BBr₃ in DCM³⁴ to furnish bulgarein (**1**) (Scheme 15). Although full characterization was difficult due to the poor solubility and small amount of bulgarein, we obtained satisfactory analytical data for bulgarein (**1**). In addition to HRMS data, UV-Vis absorption and color of the final product in concentrated and dilute ethanolic solutions are in complete agreement with literature.⁵

1.2.4. Semisynthesis of Daldiquinone from Daldinol

Possible semisynthesis of daldiquinone (**15**) from daldinol (**28**) was also investigated (Scheme 16). Among the oxidants tested (Table 5), successful oxidation was only possible with S-IBX in low yield (10%). Further optimization of reaction conditions may increase the yield of oxidation with S-IBX. These results prove the importance of synthesis of unsymmetrical binaphthalene **35** and justifies the synthetic strategy followed in this work.



Scheme 16. Semisynthesis of daldiquinone (**15**) from daldinol (**28**).

Table 5. Screening of oxidants for semisynthesis of daldiquinone (**15**) from daldinol (**28**).

Entry	Oxidant (equiv.)	Solvent	Result
1	PIFA (2.0)	Acetone/H ₂ O (3:1)	Complex mixture
2	PIDA (2.0)	Acetone/H ₂ O (4:1)	Complex mixture
3	CAN (4.0)	CH ₃ CN/DCM/H ₂ O (1.2:1:1)	Complex mixture
4	DDQ (1.0)	DCM	Complex mixture
5	S-IBX (2.5)	DCM/DMSO (2:1.5)	10% yield

1.3. CONCLUSION

In summary, we have achieved the first total synthesis of bioactive fungal natural product daldiquinone (**15**) in 8 steps starting from commercially available 1,8-naphthalenediol. Our synthesis is marked by Suzuki coupling reaction between functionalized naphthalene derivatives and facile oxidation of phenol moiety to *o*-quinone by hypervalent iodine reagent IBX.

Total synthesis of highly oxygenated bioactive fungal natural product bulgarein (**1**) was accomplished via a concise route consisting of 8 steps. Suzuki coupling reaction

between MOM-protected naphthalene boronic ester **39** and 1,8-dibromo-4,5-dimethoxynaphthalene (**37**) followed by intramolecular C-H arylation was proven to be effective to assemble highly functionalized fluoranthene skeleton. Subsequent deprotection, oxidation and deprotection sequence set the stage for synthesis completion.

In this study, another natural product daldinol (**28**) was also synthesized from **25** in 57% yield over three steps by employing a one-pot Suzuki-Miyaura coupling reaction.

CHAPTER 2: INTRAMOLECULAR DIELS-ALDER REACTIONS FOR THE SYNTHESSES OF FLUORANTHENE DERIVATIVES

2.1. INTRODUCTION

2.1.1. General applications of Fluoranthene derivatives

Owing to their unique photophysical, thermal and electrochemical properties, fluoranthenes and derivatives have been explored extensively and found a broad range of applications in material science, organic electronics and medicinal chemistry.³⁵ Fluoranthenes generally exhibit better thermal and electrochemical stability together with high photoluminescence quantum yield and do not suffer from oxygen quenching. A wide band gap of fluoranthene derivatives results in blue light emission, which is one of the critical colors to achieve full-color display in white OLEDs.³⁵ With their deep blue light emitting properties fluoranthene derivatives DPBF and TPF were suggested for utilization in OLEDs.³⁶ In 2008, Cao and co-workers developed sulfur-hetero benzo[*k*]fluoranthene derivatives as organic semiconductors.³⁷ Hua and coworkers reported fluoranthene-based dyes for potential application in solar cells.³⁸ Triphenylamine-containing fluoranthene derivatives were prepared by group of Jianhua as sensitizers and suggested for utilization in optoelectronic materials.³⁹ Another exciting property of fluoranthene is the tunability of its optical and photophysical properties by installing donor-acceptor functionalities. FLUN 550, which contains electron donor and acceptor groups on fluoranthene ring, exhibited a large Stokes shift (220 nm) and was used as a probe in selective staining of lipid droplets (LDs) (Figure 6).⁴⁰

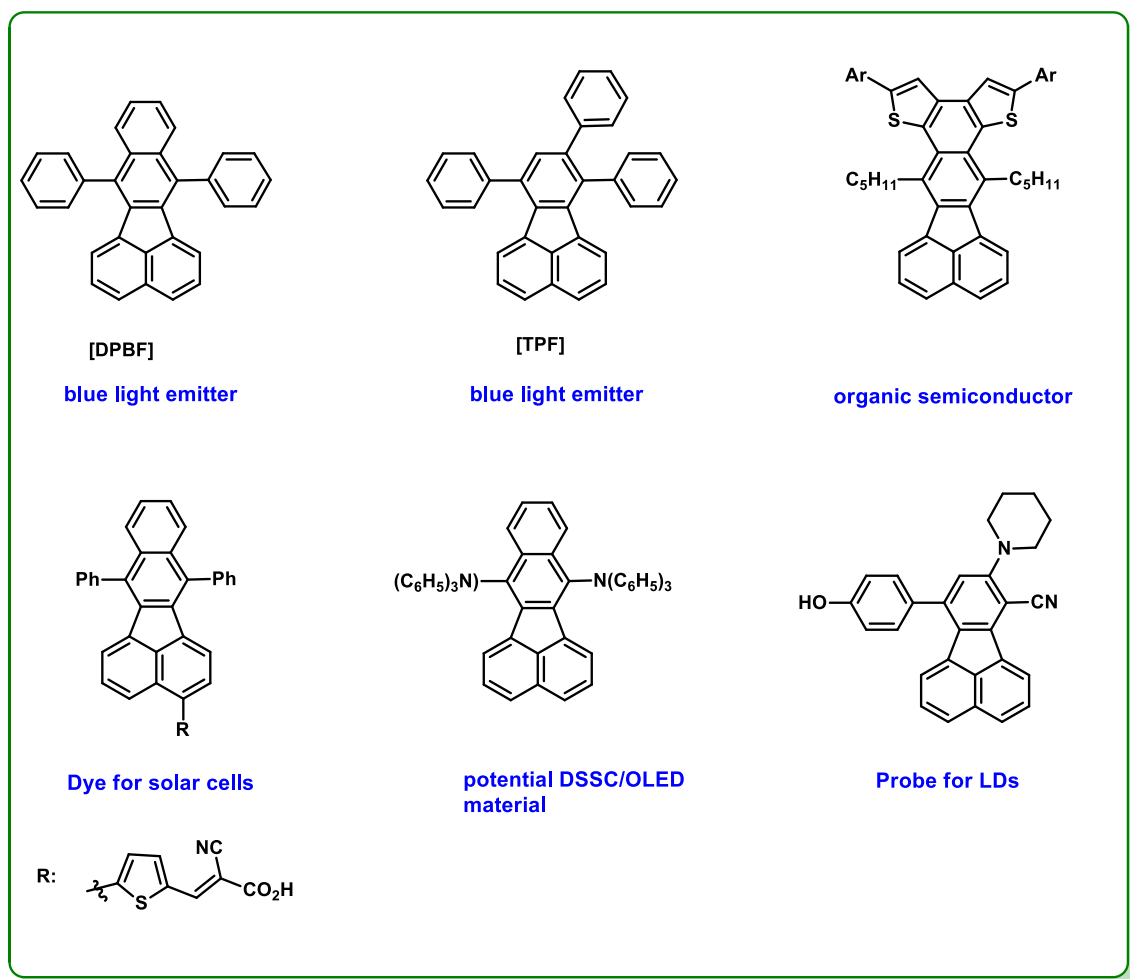
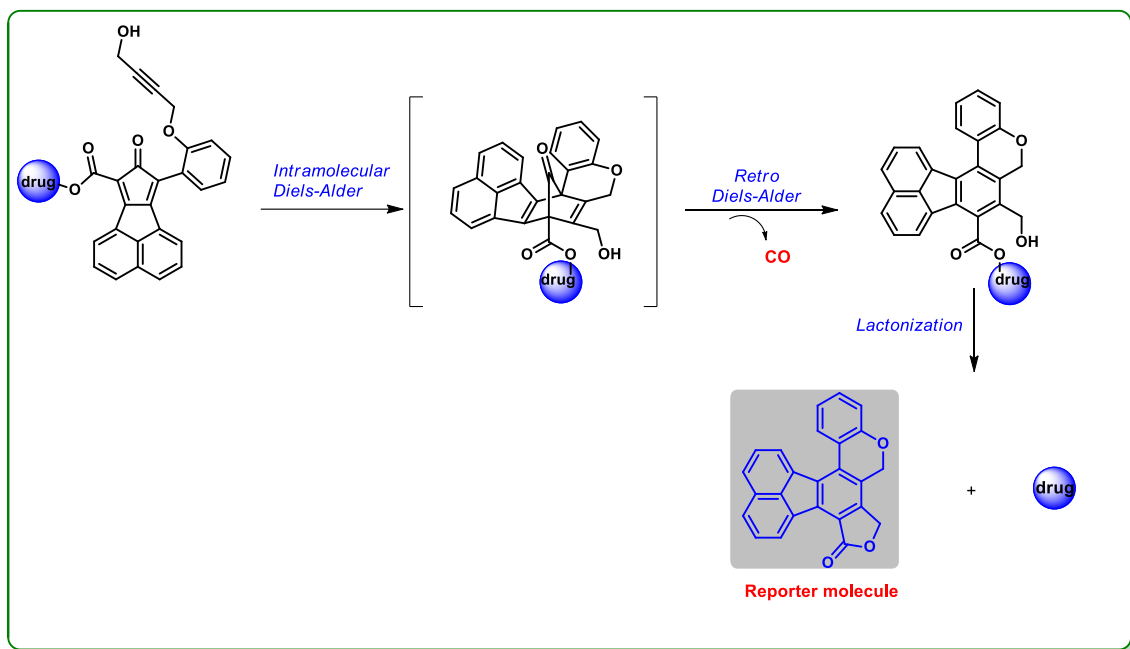


Figure 6. Selected fluoranthene derivatives.

An elegant use of fluoranthene in medicinal chemistry is reported by Wang and co-workers in 2018.⁴¹ As a part of a click-release-fluoresce strategy, a fluoranthene-based fluorescent side product was generated, which allowed easy monitoring of CO delivery. Cascade strategy developed, starts with intramolecular inverse-electron demand Diels-Alder reaction followed by the release of CO via fast retro Diels-Alder reaction of norbornenone intermediate and final lactonization of benzyl alcohol to produce fluorescent side product (Scheme 7).

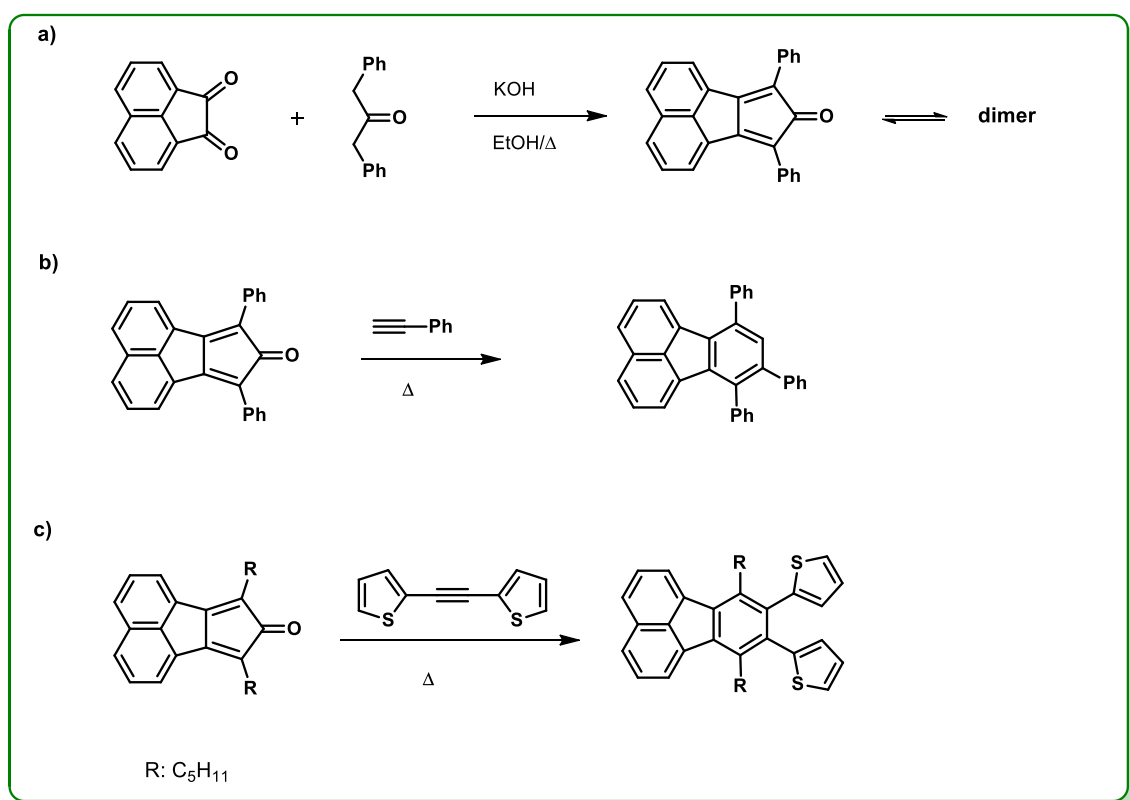


Scheme 17. Fluoranthene derivative as a reporter molecule.

2.1.2. Reported strategies for synthesis of fluoranthene derivatives

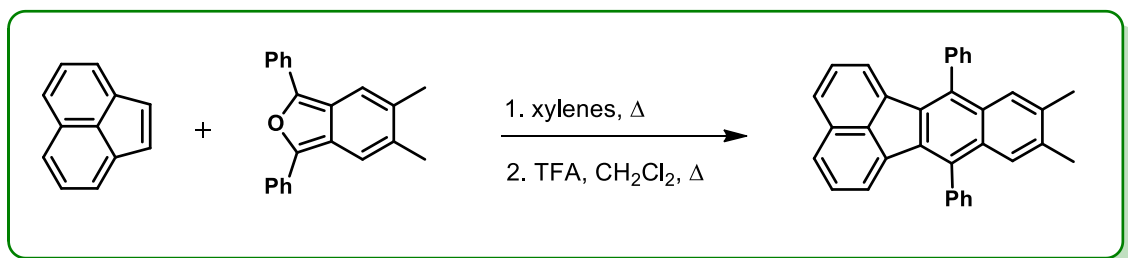
2.1.2.1. Diels Alder reactions

In 1952, Allen et al. reported Knoevenagel condensation of acenaphthenequinone with a variety of alkyl ketones.⁴² It was also shown that condensation product dimerizes at room temperature via Diels-Alder cycloaddition and found in equilibrium with its dimer, which showed the ability of the condensation product to act as a diene. Later, Diels-Alder reaction between cyclopentadienone and suitable dienophiles followed by decarbonylation of cycloaddition product was utilized to construct the fluoranthene core (Scheme 18).^{37,43}



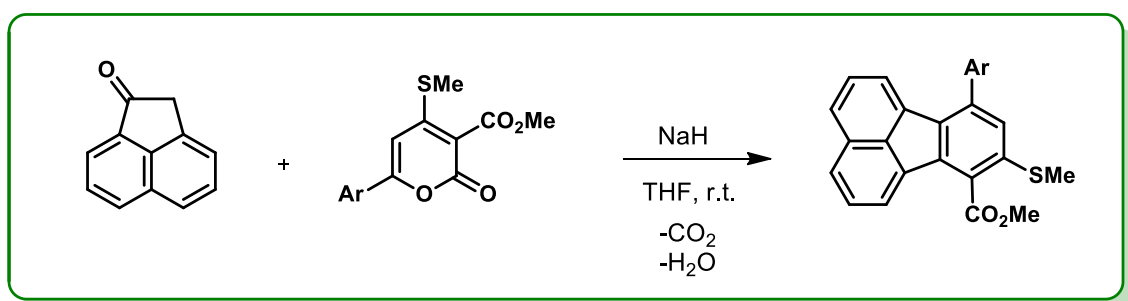
Scheme 18. Selected Diels-Alder reactions to synthesize fluoranthene derivatives.

In another study, Diels-Alder cycloaddition between acenaphthylene and substituted isobenzofuran was employed to construct benzo[*k*]fluoranthene skeleton (Scheme 19).⁴⁴



Scheme 19. Diels-Alder reaction between acenaphthylene and isobenzofuran.

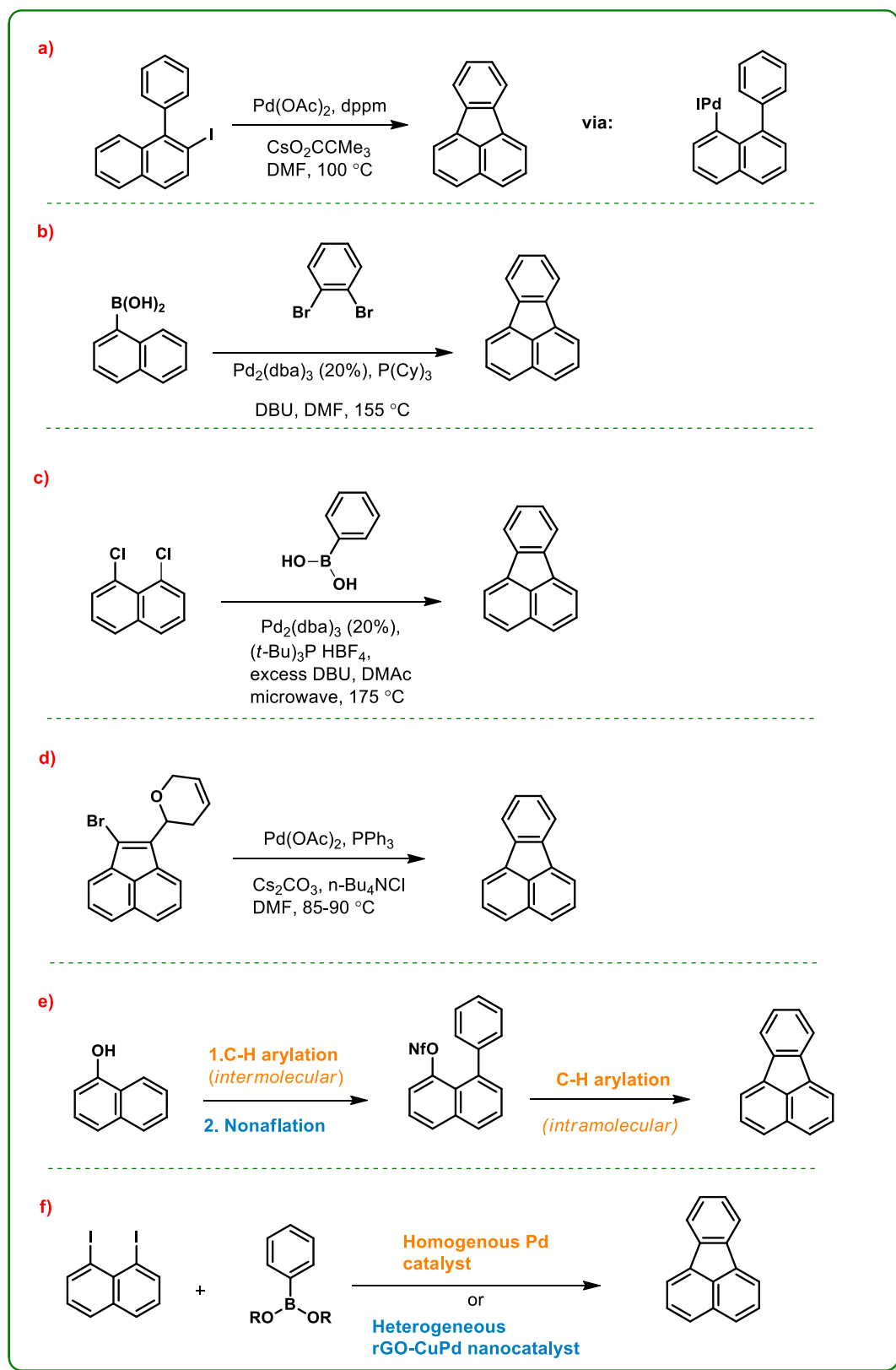
Treatment of 2H-acenaphthylen-1-one and 2H-pyran-3-carboxylic acid methyl esters with NaH in THF gave access to substituted fluoranthenes after the loss of CO_2 and H_2O (Scheme 20).⁴⁵ It should be noted that initial ring formation can also proceed via 1,6-addition followed by cyclization. The main drawback of using Diels-Alder strategies is the formation of a mixture of regioisomers with unsymmetrical dienes/dieneophiles.



Scheme 20. Reported synthesis of substituted fluoranthene.

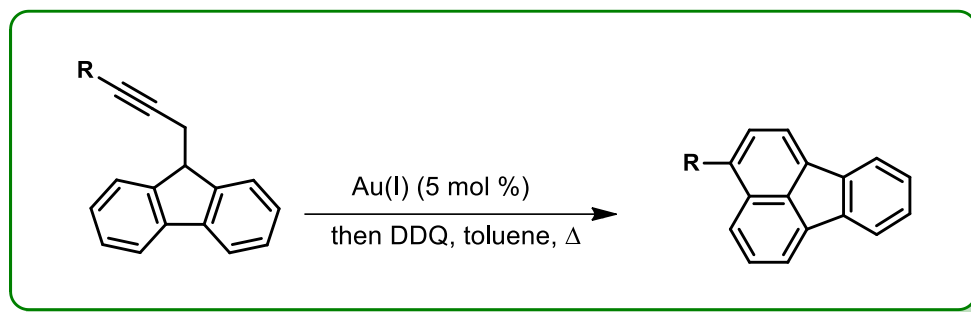
2.1.2.2. Transition metal-catalyzed processes

Over the years, transition metal-catalyzed transformations are shown to be extremely useful for the synthesis of fluoranthene derivatives. Among them, palladium-catalyzed processes have emerged as a powerful tool. In an elegant work reported by Campo et al. 1,4 palladium migration followed by CH arylation was employed to assemble fluoranthene skeleton.⁴⁶ Suzuki-Heck-type coupling cascade between mono-functionalized naphthalene and *ortho*-difunctionalized benzene or *peri*-difunctionalized naphthalene and mono-functionalized benzene is shown to be an effective strategy.^{47, 48} In 2008, Ray and co-workers reported Pd-assisted electrocyclic process by using Pd(OAc)₂ (10 mol%), PPh₃ (5 mol%) and TBAC.⁴⁹ In 2016, a 3-step synthetic sequence was developed by Yamaguchi et al. to access fluoranthene derivatives starting from various 1-naphthols.⁵⁰ Following year, our group, in collaborative work with Metin group, developed an effective strategy to synthesize fluoranthene derivatives by using both homogeneous Pd catalyst and heterogeneous rGO-CuPd nanoparticles (Scheme 21).¹ All of these methodologies have the same common limitation of modularity since all of them construct fluoranthene core from at most two building blocks. As a result, those methods are not well-suited for the modular synthesis of polysubstituted fluoranthene derivatives.



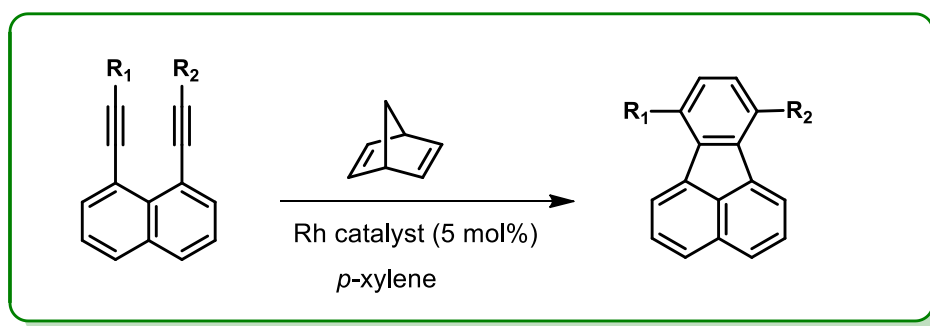
Scheme 21. Selected Pd catalyzed processes to assemble fluorene core.

In addition to the Pd-catalyzed processes, Au(I)-catalyzed Friedel-Crafts-type alkenylation of arenes was developed by the group of Echavarren for the synthesis of 3-substituted fluoranthenes (Scheme 22).⁵¹



Scheme 22. Au(I) catalyzed Friedel-Crafts-type alkenylation of arenes for the synthesis of 3-substituted fluoranthenes.

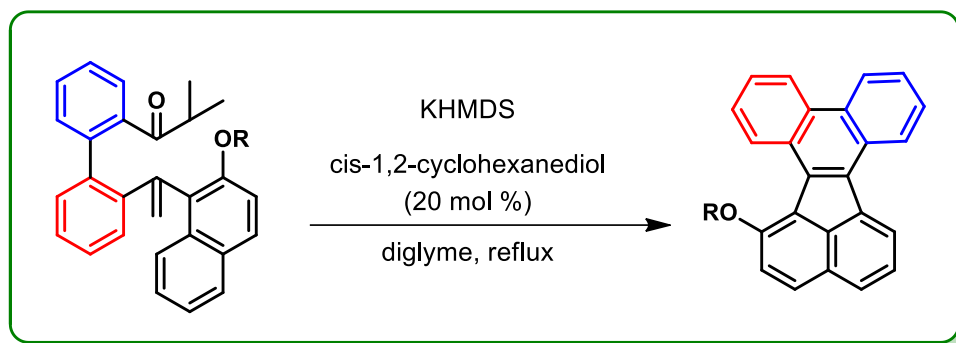
An elegant entry to fluoranthene synthesis methodologies by using transition metal catalysis was reported by Wu et al. where Rh(I)-catalyzed [(2+2)+2] cycloaddition between norbornadiene and 1,8-naphthalene diyne was employed (Scheme 23).⁵²



Scheme 23. Rh(I)-catalyzed [(2+2)+2] cycloaddition between norbornadiene and 1,8-naphthalene.

In 2017, Takasu and co-workers developed KHMDS-promoted cascade cyclization of biaryl compounds bearing acyl and naphthylalkenyl functionalities for the synthesis of 9-hydroxydibenzo[*j,l*]fluoranthenes (Scheme 24).⁵³ One main disadvantage

of this methodology is that transformation proceeds from highly specialized starting material in terms of both structure and functional group pattern.

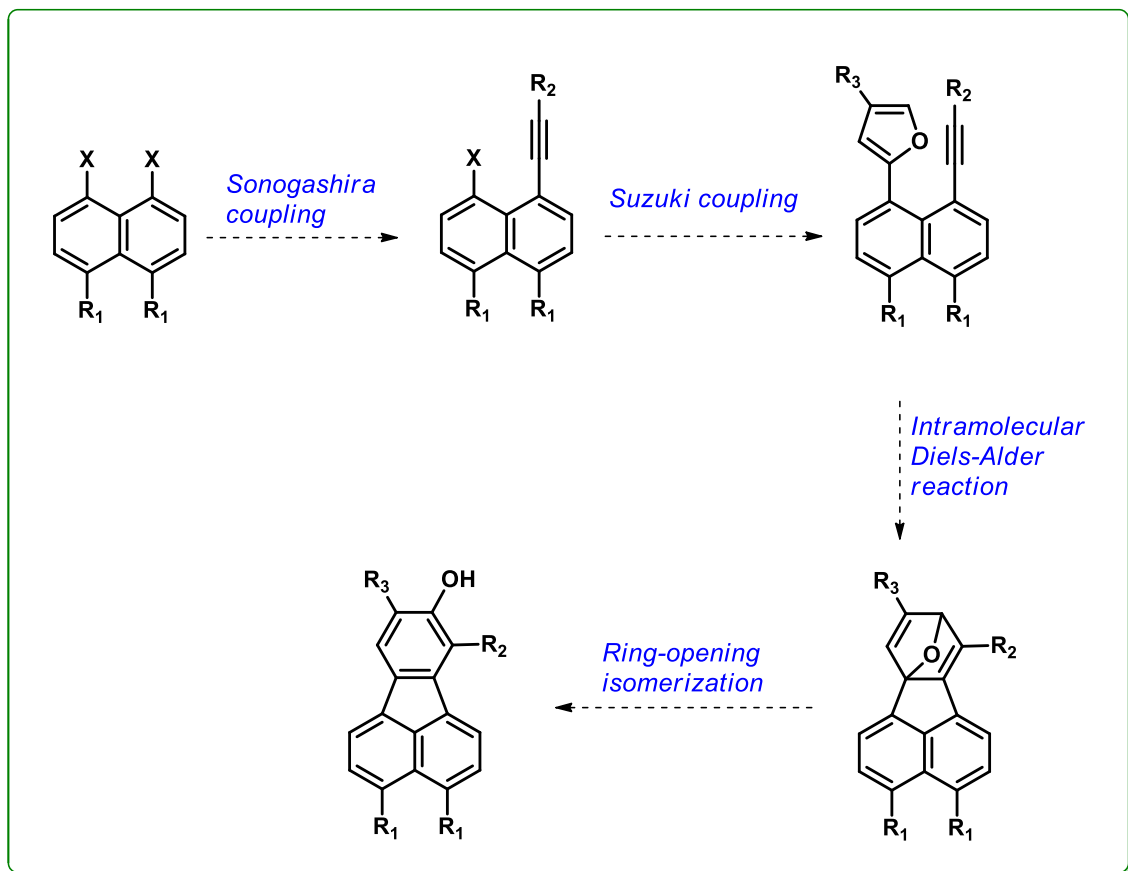


Scheme 24. KHMDS-promoted cascade cyclization strategy for fluoranthene synthesis.

2.1.3. Aim of this work

Most of the methods developed for the synthesis of fluoranthene derivatives suffer from the lack of modularity, harsh reaction conditions or high catalyst loading. Procedures based on Diels-Alder reactions mainly give access to only symmetrical fluoranthenes. In addition, fluoranthene derivatives generated by reported strategies rarely bear functional groups for further functionalization of fluoranthenes which is extremely useful to adjust the electronic properties. KHMDS-promoted anionic-radical reaction cascade developed by Takasu and co-workers allows the synthesis of hydroxyfluoranthenes. Upon transformation of hydroxyl group into triflate, three different fluoranthene derivatives were readily prepared.⁵³ Although this work shows the ability of hydroxyfluoranthenes for further modifications, the method requires complicated starting materials. Hydroxylation of arenes is a challenging transformation, and reported methods usually require pre-functionilization.⁵⁴ Starting with hydroxyl-containing aryls usually is a disadvantage as it requires protection/deprotection steps for successful coupling reactions. To this end, a flexible and facile strategy to synthesize

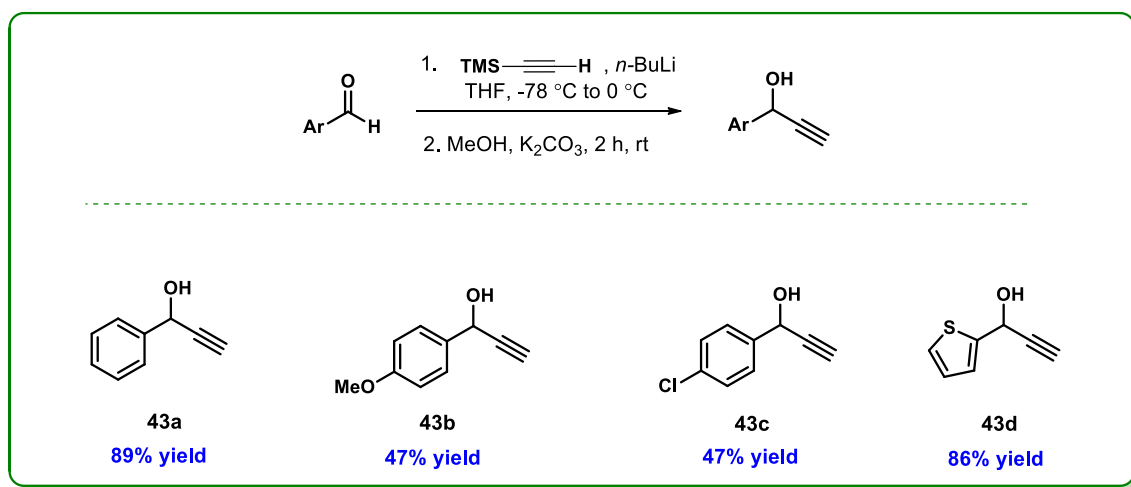
unsymmetrical hydroxyfluoranthene derivatives from easily accessible starting materials is desirable. This work aims to develop a novel, modular approach based on the intramolecular Diels-Alder reaction of furan (IMDAF). As described in Scheme 25, synthesis of *peri*-disubstituted naphthalene derivatives from 1,8-dihalonaphthalenes will be achieved via successive Sonogashira coupling with terminal alkynes and Suzuki coupling with 2-furanylboronic acid. Then, the obtained product will undergo an intramolecular Diels-Alder reaction followed by ring-opening isomerization to furnish hydroxyfluoranthenes. Since all three components (alkyne, furan and naphthalene) may bear different substituents, the strategy is modular and will allow the synthesis of many substituted hydroxyfluoranthenes.



Scheme 25. Proposed strategy to synthesize substituted hydroxyfluoranthenes.

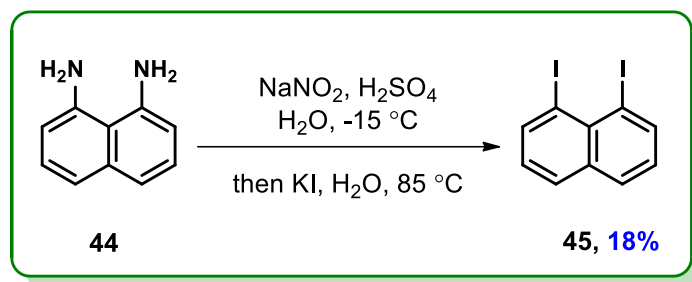
2.2. RESULTS AND DISCUSSION

To test our synthetic design and optimize reaction conditions our work was first started with the syntheses of alkynes. Commercially available trimethylsilylacetylene was deprotonated with *n*-BuLi, and 1,2-addition of generated lithium alkynide to benzaldehyde at -78 °C followed by removal of TMS group by methanolysis gave 1-phenylpropargyl alcohol **43a** in 89% yield. Under similar reaction conditions, alkynes with electron-rich anisole ring **43b**, electron-deficient *p*-chlorobenzene ring **43c** and heterocyclic thiophene ring **43d** were prepared in moderate to high yields (Scheme 26).



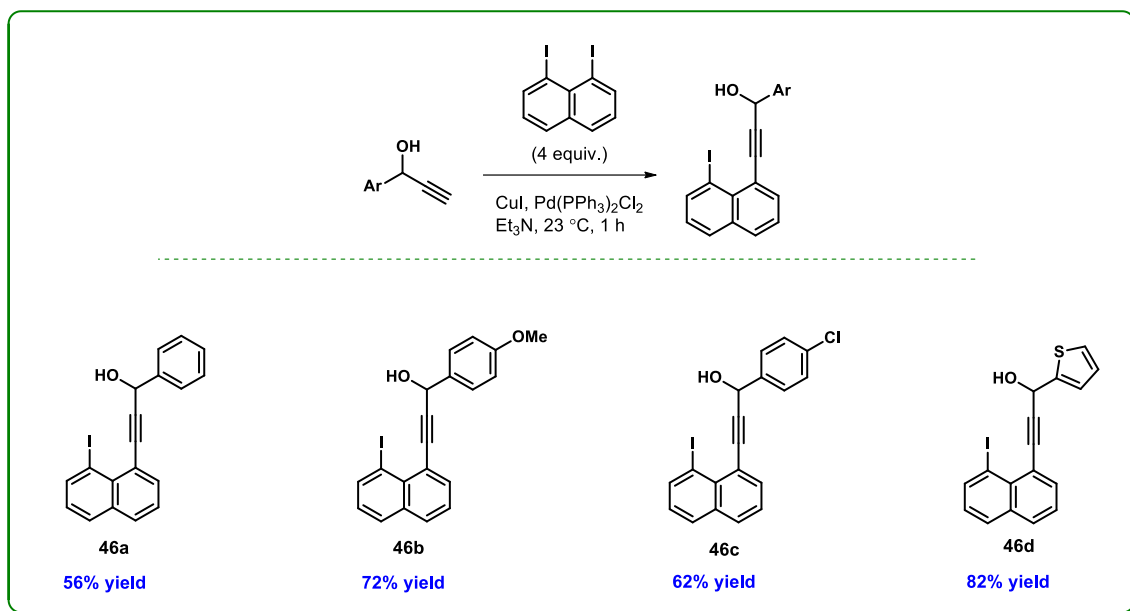
Scheme 26. Synthesis of alkynes **43a-d**.

1,8-diiodonaphthalene(**45**) was prepared from commercially available 1,8-diaminonaphthalene (**44**) by Sandmeyer reaction following reported literature procedure (Scheme 27).⁵⁵



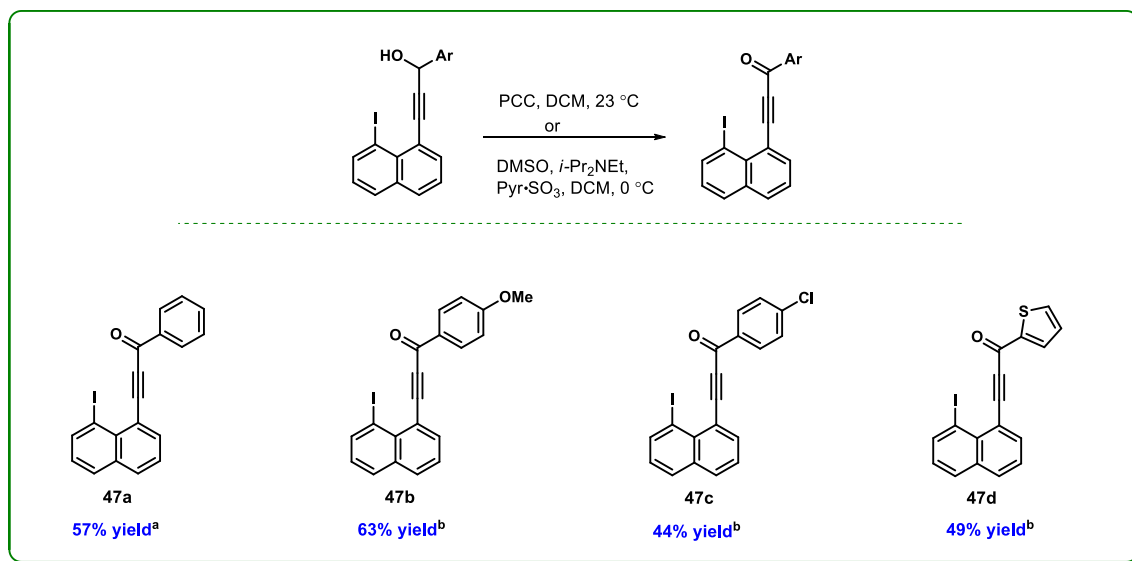
Scheme 27. Synthesis of 1,8-diiodonaphthalene.

As we expected, the mono-Sonogashira coupling reaction between alkynes and 1,8-diiodonaphthalene was challenging due to two competing reactions (di-Sonogashira and Glaser coupling). When an excess of alkyne **43a** was used⁵⁶ to compensate material loss resulting from oxidative coupling, obtained product **46a** could not be purified from starting alkyne and unknown side product (product: alkyne **43a** ratio = 1:1; calculated from the recorded ¹H-NMR spectrum). To eliminate problems often encountered with homo-coupling of the alkyne **43a**, the reaction was conducted under copper-free Sonogashira coupling conditions⁵⁷ which gave the desired mono-Sonogashira product **46a** only in 26% yield. When an excess of 1,8-diiodonaphthalene (4 equiv.) was used, and the reaction was carried out at 23 °C in Et₃N, competing side reactions were suppressed and mono-Sonogashira product **46a** was synthesized in 53% yield. Notably, unreacted 1,8-diiodonaphthalene was easily recovered at the end of the reaction by column chromatography (See Experimental section). Similarly, reactions of **43b**, **43c** and **43d** with 1,8-diiodonaphthalene were conducted, and mono-Sonogashira products **46b-46d** were obtained in high yields (Scheme 28).



Scheme 28. Mono-Sonogashira reaction of alkynes with 1,8-diiodonaphthalene.

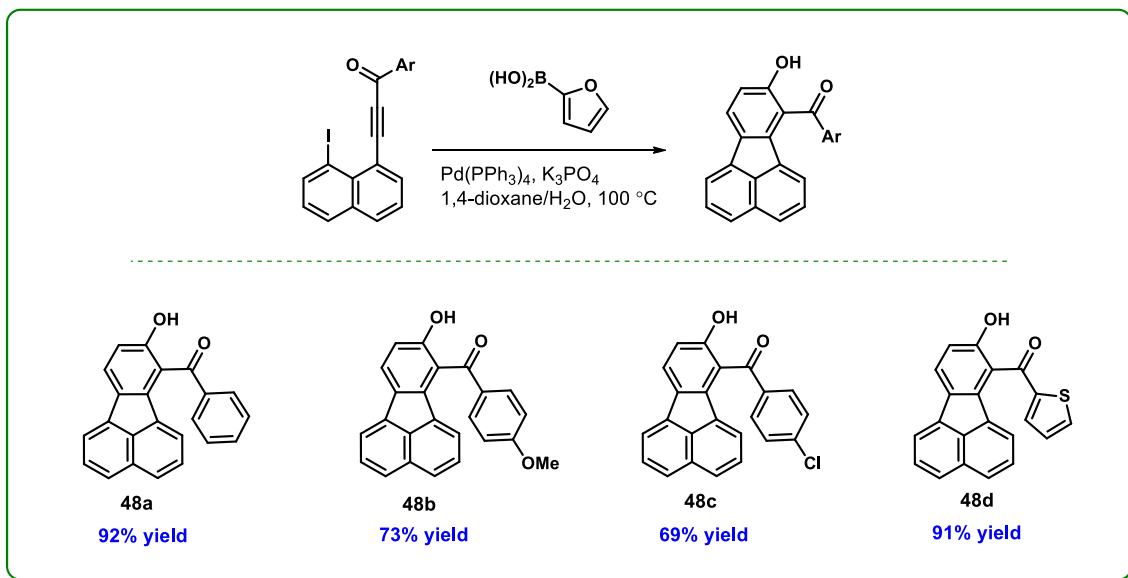
Oxidation of alkyne-ols (**46a-46d**) was achieved by either Parikh-Doering modification⁵⁸ of Swern oxidation or conventional Corey-Suggs reagent⁵⁹ (PCC) and ketones **47a-47d** were prepared in moderate yields. (Scheme 29). Since the oxidation product can act as a Michael acceptor, non-nucleophilic Hünig's base was utilized instead of Et₃N to avoid any side reaction between trialkylamine base and α,β -unsaturated ketone in Parikh-Doering oxidation. For PCC oxidation, adding molecular sieves (4 Å) and/or celite to the reaction mixture at the beginning or at the end of the reaction did not improve the yields. When alkyne-ol **43d** was used as a model, the yield of the oxidation (50%) with IBX was found to be similar to those obtained by PCC.



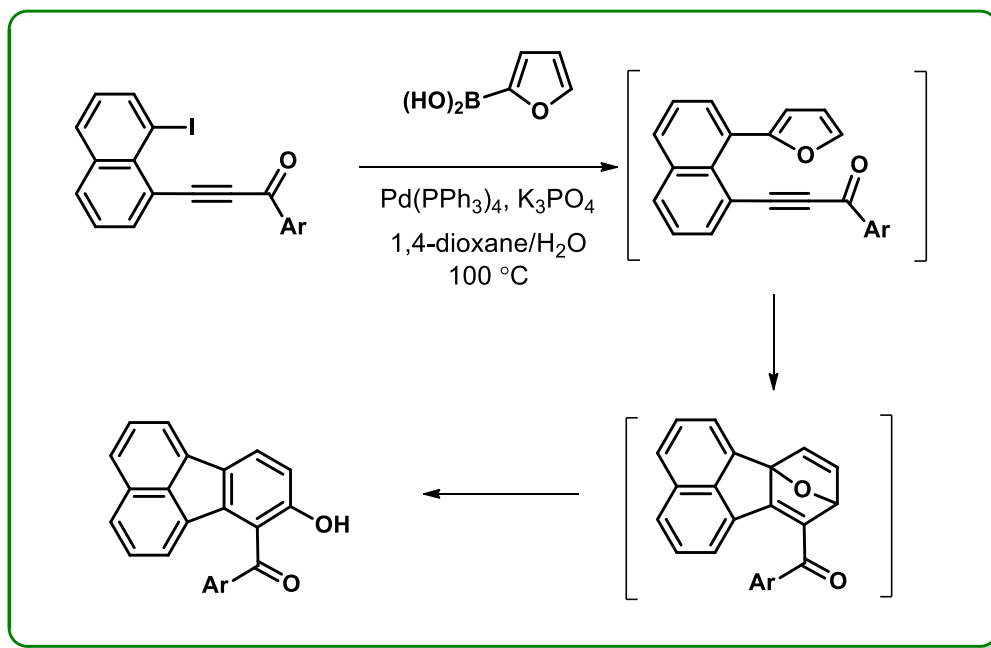
Scheme 29. Oxidation of alkyne-ols to ketones.

a: Parikh-Doering oxidation, b: PCC oxidation

With ketones in hand, the stage was set for Suzuki coupling reaction with 2-furanylboronic acid. To our delight, when ketone **47a** and 2-furanylboronic acid were subjected to Suzuki coupling conditions, one-pot Suzuki coupling reaction followed by intramolecular Diels-Alder cycloaddition and final isomerization of cycloaddition product by ring-opening (Scheme 31) furnished fluoranthene **48a** in 92% yield. By using the same reaction conditions, fluoranthenes **48b-48d** were prepared in high yields (Scheme 30).



Scheme 30. One-pot three steps synthesis of fluoranthene derivatives



Scheme 31. Representation for one-pot three steps formation of hydroxyfluoranthenes.

2.3. CONCLUSION

In summary, we have developed a novel modular strategy to prepare hydroxyfluoranthenes starting from 1,8-dihalonaphthalenes through intramolecular Diels-Alder reaction of furan. The last three steps of sequence (Suzuki coupling, Diels-Alder cycloaddition, and ring-opening isomerization) proceeds in the same pot. So far, we have achieved the synthesis of four different ketone-containing hydroxyfluoranthenes (**48a-d**) in high yields. Based on current results, we believe our method will be effective for the concise modular synthesis of functionalized fluoranthene derivatives.

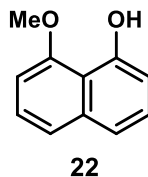
CHAPTER 3: EXPERIMENTAL SECTION

3.1 GENERAL INFORMATION

All reaction were conducted under an inert atmosphere of nitrogen and using flame- or oven-dried glassware. The progress of reactions were monitored by thin-layer chromatography (TLC) using aluminum-backed plates pre-coated with silica gel (Merck, Silica Gel 60 F₂₅₄). For TLC visualization UV light and/or KMnO₄ solutions were used. Purification were done by flash column chromatography on Silicycle 40-63 μm (230-400 mesh) flash silica gel. NMR spectra were recorded on a Bruker spectrometer at 400 MHz for ¹H-NMR spectra and 100 MHz for ¹³C-NMR spectra and calibrated from internal standard (TMS, 0 ppm) or residual solvent signals (chloroform at 7.26 ppm for ¹H spectra, and at 77.16 ppm and for ¹³C spectra). ¹H-NMR data are reported as follows: chemical shift (parts per million, ppm), integration, multiplicity (s = singlet, d = doublet, t = triplet, dd = doublet of doublets, ddd = doublet of doublet of doublets, m = multiplet, br = broad, app = apparent), coupling constant (Hz). Infrared (FTIR) spectra were measured on a Bruker Alpha-Platinum-ATR spectrometer with only selected peaks were reported. Mass spectral analyses were performed at UNAM-National Nanotechnology Research Center and Institute of Materials Science and Nanotechnology, Bilkent University and DAYTAM-East Anatolia High Technology Application and Research Center, Atatürk University

Materials: Anhydrous CH₃CN was obtained by distillation over P₂O₅ under an inert atmosphere of nitrogen. *N*-Bromosuccinimide (NBS) was recrystallized from H₂O, dried thoroughly, and stored in refrigerator. Anhydrous CH₂Cl₂ and DME were purchased from Acros Organics (AcroSeal®) and used as received. All other commercially available reagents were used as received unless stated otherwise.

3.2. CHAPTER 1: Total Synthesis of Daldinol, Daldiquinone and Bulgarein

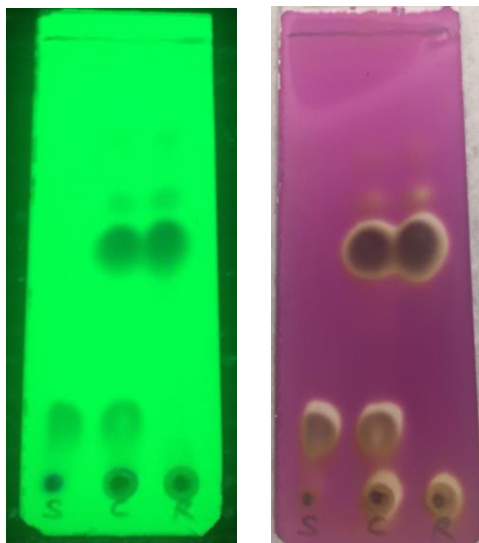


1,8-Dihydroxynaphthalene (4.00 g, 25.0 mmol) was dissolved in 100 mL of acetone in a 250-mL round-bottomed flask. K_2CO_3 (4.15 g, 30.0 mmol) and CH_3I (2.33 mL, 37.5 mmol) were added sequentially, and the resulting heterogeneous mixture was stirred at 23 °C for 24 h. TLC analysis indicated full consumption of 1,8-DHN. The reaction mixture was treated with H_2O (30 mL) and saturated aqueous solution of NH_4Cl (30 mL). The aqueous phase was extracted with EtOAc (3×50 mL). The combined organic phase was washed with brine (100 mL) and dried over anhydrous Na_2SO_4 . After filtration, the clear solution was concentrated under reduced pressure to give a brown solid. The crude product was purified by flash column chromatography (SiO_2 ; EtOAc:hexanes = 1:19 → 1:9) to afford pure **22** (4.04 g, 93% yield) as white solid.

Note:

- This procedure was observed to work successfully on various reaction scales. 8-Methoxy-1-naphthol (**22**) was isolated in 92% and 96% yields, when the reaction was conducted starting from 2.00 g (12.5 mmol) and 200 mg (1.25 mmol) of 1,8-DHN, respectively.

TLC Images:



Left image: TLC under UV light (254 nm)

Right image: TLC stained with KMnO_4 solution

Spots from left to right:

S: Starting material (**1,8-DHN**);

C: Co-spot of 1,8-DHN and reaction mixture;

R: Reaction mixture.

Mobile phase: EtOAc:hexanes = 1:9

M.P. 57-59 °C (EtOAc, hexanes); 57-58 °C (recrystallized from heptane).

$R_f = 0.51$ (EtOAc:hexanes = 1:9)

TLC Visualization: UV active; stains with KMnO_4 solution.

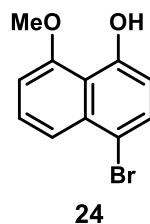
^1H NMR (400 MHz; CDCl_3) δ : 9.34 (1H, s), 7.43 (1H, dd, $J = 8.2, 0.9$ Hz), 7.39-7.29 (3H, m), 6.91 (1H, dd, $J = 7.5, 1.4$ Hz), 6.77 (1H, dd, $J = 7.7, 0.8$ Hz), 4.04 (3H, s).

^{13}C NMR (100 MHz; CDCl_3) δ : 156.3, 154.6, 136.9, 127.8, 125.7, 122.0, 119.0, 115.2, 110.5, 104.0, 56.2.

FTIR ν_{max} (ATR, solid)/ cm^{-1} 3352, 3051, 2951, 2844, 1629, 1609, 1580, 1513, 1451, 1397.

HRMS (+APCI) Calcd for $\text{C}_{11}\text{H}_{11}\text{O}_2$ $[\text{M}+\text{H}]^+$: 175.0754; found: 175.0759.

Elemental (Combustion) analysis: Anal. calcd for $\text{C}_{11}\text{H}_{10}\text{O}_2$: C, 75.84; H, 5.79; found: C, 75.61; H, 5.44.

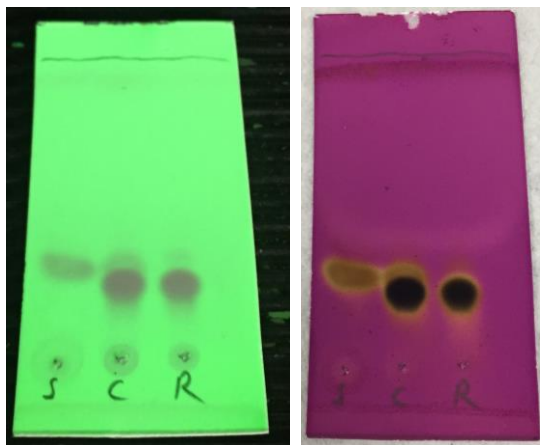


An oven-dried, 100-mL, round-bottomed flask was cooled under vacuum and refilled with nitrogen. It was charged with 8-methoxy-1-naphthol (**22**) (3.00 g, 17.2 mmol), and then evacuated and refilled with nitrogen. Anhydrous CH₃CN (40 mL) was added via syringe forming a colorless, clear solution. Afterwards, NBS (3.07 g, 17.2 mmol) was added in one portion at 23 °C. The flask was covered with Al foil, and the resulting pale yellow solution was stirred at 23 °C under nitrogen for 1 hr. TLC analysis indicated that the reaction was over at this point. All volatiles were removed under reduced pressure. Purification by flash column chromatography (SiO₂; EtOAc:hexanes = 1:19 → 1:9) afforded bromonaphthol product **24** (4.085 g, 94%) as white solid.

Notes:

- This procedure was observed to work successfully on various reaction scales. Reaction product **24** was isolated in 85% and 92% yields, when the reaction was conducted starting from 1.00 g (5.74 mmol) and 100 mg (0.57 mmol) of 8-methoxy-1-naphthol (**22**), respectively.

TLC Images:



Left image: TLC under UV light

(254 nm)

Right image: TLC stained with KMnO_4 solution

Spots from left to right:

S: Starting material (**22**);

C: Co-spot of **22** and reaction mixture;

R: Reaction mixture.

Mobile phase: EtOAc:hexanes = 1:19

M.P. 110-111 °C (EtOAc, hexanes)

R_f = 0.49 (EtOAc:hexanes = 1:9); 0.22 (EtOAc:hexanes = 1:19).

TLC Visualization: UV active; stains with KMnO_4 solution.

^1H NMR (400 MHz; CDCl_3) δ : 9.45 (1H, s), 7.82 (1H, dd, J = 8.6, 0.7 Hz), 7.64 (1H, d, J = 8.3 Hz), 7.41 (1H, t, 8.03 Hz), 6.82 (1H, d, J = 7.7 Hz), 6.76 (1H, d, J = 8.3 Hz), 4.04 (3H, s).

^{13}C NMR (100 MHz; CDCl_3) δ : 156.3, 154.7, 134.3, 131.7, 127.1, 121.3, 116.3, 111.4, 111.2, 105.0, 56.5.

FTIR ν_{max} (ATR, solid)/ cm^{-1} 3323, 2944, 2842, 1607, 1570, 1454, 1424, 1390, 1360, 1249, 1234.

HRMS (+APCI) Calcd for $\text{C}_{11}\text{H}_{10}^{79}\text{BrO}_2$ $[\text{M}+\text{H}]^+$ 252.9859; found: 252.9870; Calcd for $\text{C}_{11}\text{H}_{10}^{81}\text{BrO}_2$ $[\text{M}+\text{H}]^+$ 254.9839; found: 254.9853.

Elemental (Combustion) analysis: Anal. calcd for C₁₁H₉BrO₂: C, 52.20; H, 3.58; found: C, 52.53; H, 3.58.



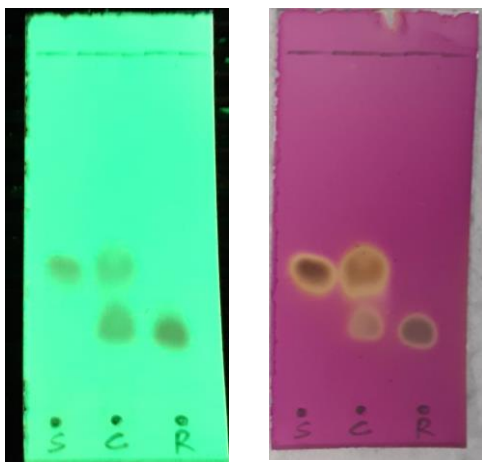
A solution of bromonaphthol **24** (1.50 g, 5.93 mmol) in 15 mL of anhydrous THF was cooled to 0 °C under an inert atmosphere of nitrogen. After 10 min, NaH (284 mg, 7.11 mmol, 60% dispersion in mineral oil) was added carefully in portions. Vigorous gas evolution was observed. After 15 min, acetyl chloride (550 μL, 7.70 mmol) was added slowly via syringe. The resulting mixture was stirred for 10 min at 0 °C and afterwards for 90 min at 23 °C. TLC analysis indicated full consumption of bromonaphthol **24** at this point. The reaction mixture was quenched with H₂O (30 mL), and the aqueous phase was extracted with EtOAc (3×20 mL). The combined organic phase was dried over anhydrous Na₂SO₄, filtered and concentrated under reduced pressure. Purification by column chromatography (SiO₂; EtOAc:hexanes = 1:9 → only EtOAc) gave pure **25** (1.68 g, 96% yield) as white solid.

Note:

- This procedure was observed to work successfully on various reaction scales. Reaction product **25** was isolated in 87% and 80% yields, when the reaction was conducted starting from 750 mg (2.97 mmol) and 300 mg (1.19 mmol) of naphthol (**24**), respectively.

- For the recrystallization of product **25**, dissolving it in a minimum amount of heptane by heating and then cooling back to room temperature was found to be an effective method.

TLC Images:



Left image: TLC under UV light (254 nm)

Right image: TLC stained with KMnO_4 solution

Spots from left to right:

S: Starting material (**24**);

C: Co-spot of **24** and reaction mixture;

R: Reaction mixture.

Mobile phase: EtOAc:hexanes = 1:9

M.P. 90-92 °C (recrystallized from heptane).

$R_f = 0.27$ (EtOAc:hexanes = 1:9)

TLC Visualization: UV active; stains with KMnO_4 solution.

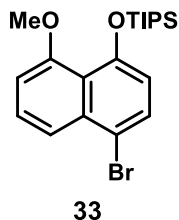
^1H NMR (400 MHz; CDCl_3) δ : 7.89 (1H, dd, $J = 8.6, 0.8$ Hz), 7.76 (1H, d, $J = 8.0$ Hz), 7.50 (1H, dd, $J = 8.4, 8.0$ Hz), 6.95-6.91 (2H, m), 3.94 (3H, s), 2.38 (3H, s).

^{13}C NMR (100 MHz; CDCl_3) δ : 170.1, 155.5, 146.5, 134.9, 130.3, 128.0, 120.6, 120.4, 120.3, 119.8, 107.1, 56.5, 21.1

FTIR ν_{max} (ATR, solid)/ cm^{-1} 3001, 2967, 2938, 1749, 1594, 1569, 1500, 1462, 1397, 1360, 1265, 1210.

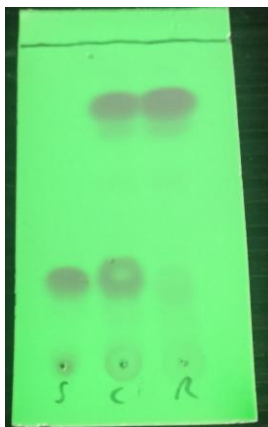
HRMS (+APCI) Calcd for $C_{13}H_{12}^{79}BrO_3$ $[M+H]^+$ 294.9965; found: 294.9980; Calcd for $C_{13}H_{12}^{81}BrO_3$ $[M+H]^+$ 296.9944; found: 296.9963.

Elemental (Combustion) analysis: Anal. calcd for $C_{13}H_{11}BrO_3$: C, 52.91; H, 3.76; found: C, 52.70; H, 3.79.



An oven-dried, 100-mL, two-neck, round-bottomed flask was fitted with a septum on one neck and connected to the Schlenk line via an adapter on the second neck. It was cooled under vacuum and refilled with nitrogen. It was then charged with bromonaphthol **24** (700 mg, 2.77 mmol). Anhydrous THF (15 mL) was added via syringe, and the resulting clear, colorless solution was cooled to 0 °C in an ice bath. Sodium hydride (NaH, 133 mg, 3.32 mmol, 60% dispersion in mineral oil) was added carefully resulting in a vigorous gas evolution. After the mixture was stirred at 0 °C for 15 min, TIPSCl was added dropwise via syringe. After 30 min, the ice bath was removed, and the yellowish-gray, cloudy reaction mixture was stirred at 23 °C for 23 h. Afterwards, the mixture was quenched with a saturated aqueous NH_4Cl solution (15 mL). The aqueous phase was extracted with CH_2Cl_2 (3×15 mL). The combined organic phase was dried over anhydrous Na_2SO_4 , filtered and concentrated under reduced pressure. Purification by flash column chromatography (SiO_2 ; only hexanes → 1% EtOAc in hexanes → 2% EtOAc in hexanes) gave pure **33** (1.043 g, 92%) as pale yellow oil.

TLC Images-I:



Left image: TLC under UV light (254 nm)

Right image: TLC stained with KMnO₄ solution

Spots from left to right:

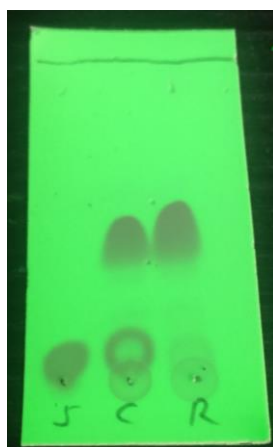
S: Starting material (**24**);

C: Co-spot of **24** and reaction mixture;

R: Reaction mixture.

Mobile phase: EtOAc:hexanes = 1:19

TLC Images-II:



Left image: TLC under UV light (254 nm)

Right image: TLC stained with KMnO₄ solution

Spots from left to right:

S: Starting material (**24**);

C: Co-spot of **24** and reaction

mixture;

R: Reaction mixture.

Mobile phase: only hexanes

$R_f = 0.40$ (only hexanes)

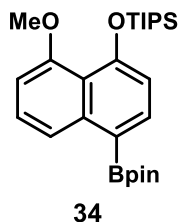
TLC Visualization: UV active; stains with KMnO_4 solution.

^1H NMR (400 MHz; CDCl_3) δ : 7.78 (1H, dd, $J = 8.6, 0.8$ Hz), 7.56 (1H, d, $J = 8.2$ Hz), 7.43 (1H, t, $J = 8.2$ Hz), 6.85 (1H, d, $J = 7.7$ Hz), 6.67 (1H, d, $J = 8.2$ Hz), 3.90 (3H, s), 1.36 (3H, app quint, $J = 7.7$ Hz), 1.13 (18H, d, $J = 7.5$ Hz).

^{13}C NMR (100 MHz; CDCl_3) δ : 157.7, 153.5, 135.2, 130.5, 127.5, 120.8, 119.9, 114.9, 113.5, 105.8, 55.5, 18.1, 13.5

FTIR ν_{max} (ATR, film)/ cm^{-1} 2943, 2865, 1575, 1459, 1399, 1372, 1311, 1275.

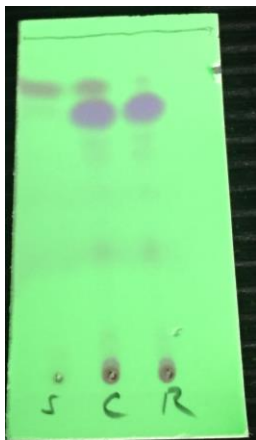
Elemental (Combustion) analysis: Anal. calcd for $\text{C}_{20}\text{H}_{29}\text{BrO}_2\text{Si}$: C, 58.67; H, 7.14; found: C, 58.53; H, 7.10.



To a solution of **33** (200 mg, 0.49 mmol) in 2.0 ml dioxane, Et_3N (272 μL , 1.95 mmol), $\text{Pd}(\text{OAc})_2$ (5.4 mg, 0.025 mmol), DPEphos (27 mg, 0.05 mmol) and HBpin (213 μL , 1.47 mmol) were added sequentially. Reaction mixture heated to 100 $^\circ\text{C}$ and stirred

for 2 hours. TLC indicated the full consumption of **33**. Purification by flash column chromatography (SiO₂; only hexanes) gave pure **34** (210 mg, 94%) as pale yellow oil.

TLC Images:



Left image: TLC under UV light
(254 nm)

Right image: TLC stained with
KMnO₄ solution

Spots from left to right:

S: Starting material (**33**);

C: Co-spot of **33** and reaction
mixture;

R: Reaction mixture.

Mobile phase: EtOAc:hexanes =
1:9

$R_f = 0.35$ (2% EtOAc in hexanes)

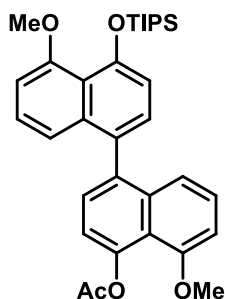
TLC Visualization: UV active under 366 nm and 254 nm; stains to yellow with KMnO₄ solution.

¹H NMR (400 MHz; CDCl₃) δ : 8.49 (1H, d, $J = 8.0$ Hz), 8.05 (1H, d, $J = 7.7$ Hz), 7.47 (1H, t, $J = 8.1$ Hz), 6.91 (1H, d, $J = 7.8$ Hz), 6.84 (1H, d, $J = 7.6$ Hz), 3.94 (3H, s), 1.53-1.41 (3H, m), 1.46 (12H, s), 1.24 (18H, d, $J = 7.5$ Hz).

¹³C NMR (100 MHz; CDCl₃) δ : 157.7, 156.6, 141.8, 137.1, 126.6, 121.0, 119.4, 114.2, 104.9, 83.5, 55.3, 25.1, 18.2, 13.5

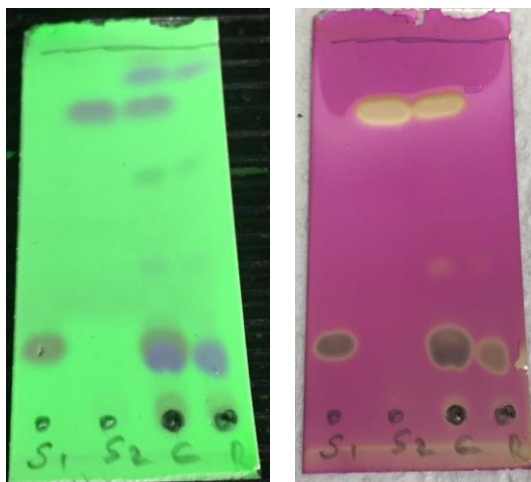
FTIR ν_{\max} (ATR, film)/ cm^{-1} 2944, 2866, 1578, 1462, 1324, 1289, 1270.

HRMS (+APCI) Calcd for $\text{C}_{26}\text{H}_{42}^{10}\text{BO}_4\text{Si}$ $[\text{M}+\text{H}]^+$ 456.2977; found: 456.2969; Calcd for $\text{C}_{26}\text{H}_{42}^{11}\text{BO}_4\text{Si}$ $[\text{M}+\text{H}]^+$ 457.2940; found: 457.2964.



Arylboronic ester **34** (1.47 g, 3.22 mmol) and acetoxybromonaphthalene **25** (634 mg, 2.15 mmol) were dissolved in THF (8 mL) and H_2O (8 mL). Afterwards, $\text{Pd}(\text{PPh}_3)_2\text{Cl}_2$ (151 mg, 0.22 mmol) and K_3PO_4 (2.74 g, 12.9 mmol) were added sequentially, and the resulting mixture was heated to 100 °C. The reaction mixture was stirred at this temperature for 4.5 h. It was then cooled to ambient temperature and quenched with H_2O . The aqueous phase was extracted three times with EtOAc. The combined organic phase was dried over anhydrous Na_2SO_4 , filtered and concentrated under reduced pressure. Purification by column chromatography (SiO_2 ; EtOAc:hexanes = 1:9 \rightarrow 1:4) gave pure **35** (1.027 g, 88% yield) as pale yellow solid.

TLC Images:



Left image: TLC under UV light

(254 nm)

Right image: TLC stained with KMnO_4 solution

Spots from left to right:

S1: Starting material 1 (**25**);

S2: Starting material 2 (**34**);

C: Co-spot of **25**, **34** and reaction mixture;

R: Reaction mixture.

Mobile phase: EtOAc:hexanes = 1:9

Note: The product (**35**) exhibits weak fluorescence, and therefore it can be distinguished on the TLC plate from the starting material **25**.

M.P. 152-154 °C (heptane).

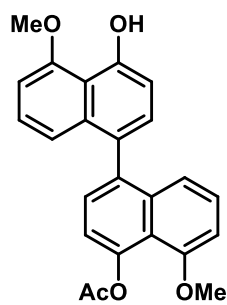
$R_f = 0.47$ (EtOAc:hexanes = 1:3)

TLC Visualization: UV active; stains with KMnO_4 solution.

^1H NMR (400 MHz; CDCl_3) δ : 7.40 (1H, d, $J = 7.6$ Hz), 7.22 (1H, d, $J = 8.0$ Hz), 7.18-7.09 (3H, m), 6.94 (1H, d, $J = 8.0$ Hz), 6.90 (1H, d, $J = 8.0$ Hz), 6.84-6.81 (2H, m), 6.76 (1H, d, $J = 8.0$ Hz), 3.96 (3H, s), 3.92 (3H, s), 2.42 (3H, s), 1.44 (3H, sept, $J = 7.4$ Hz), 1.19 (18H, d, $J = 7.6$ Hz).

¹³C NMR (100 MHz; CDCl₃) δ: 170.5, 157.7, 155.5, 153.3, 146.1, 137.7, 136.9, 136.7, 130.70, 130.68, 128.6, 128.5, 126.3, 126.1, 120.3, 119.44, 119.35, 119.0, 114.2, 106.2, 104.9, 56.3, 55.4, 21.3, 18.3, 13.6.

FTIR ν_{\max} (ATR, film)/cm⁻¹ 2944, 2866, 1764, 1581, 1462, 1402, 1374.

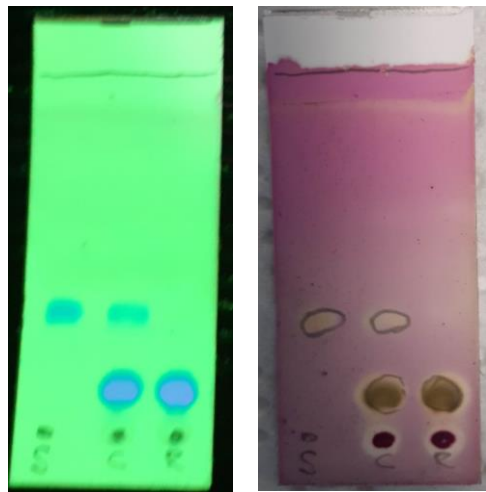


27

Binaphthalene **35** (200 mg, 0.37 mmol) was dissolved in 5.0 mL of anhydrous THF to give a clear, colorless solution. Tetrabutylammonium fluoride (TBAF, 1.0 M solution in THF; 0.55 mL, 0.55 mmol) was added at 23 °C, and the color of the solution turned yellow. After 1 min, trifluoroacetic acid (TFA; 28 μ L, 0.37 mmol) was added. TLC analysis of the resulting green solution indicated full consumption of binaphthalene **35**. The reaction mixture was quenched with 5 mL of saturated aqueous NH₄Cl solution. The aqueous phase was extracted with EtOAc (3 \times 10 mL). The combined organic phase was dried over anhydrous Na₂SO₄, filtered and concentrated under reduced pressure. Purification by column chromatography (SiO₂; EtOAc:hexanes = 1:4 \rightarrow 1:2 \rightarrow only EtOAc) gave pure **27** (126 mg, 89% yield) as pale yellow solid.

Note: In another experiment reaction product **27** was isolated in 91% yield when the reaction was conducted starting from 100 mg (0.184 mmol) **35**.

TLC Images:



Left image: TLC under UV light (254 nm)

Right image: TLC stained with KMnO_4 solution

Spots from left to right:

S: Starting material (**35**);

C: Co-spot of **35** and reaction mixture;

R: Reaction mixture.

Mobile phase: EtOAc:hexanes = 1:5

M.P. 238-240 °C (CHCl_3).

$R_f = 0.39$ (EtOAc:hexanes = 1:2)

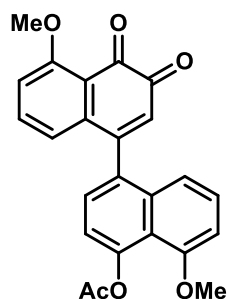
TLC Visualization: UV active; stains with KMnO_4 solution.

^1H NMR (400 MHz; CDCl_3) δ : 9.54 (1H, s), 7.39 (1H, d, $J = 7.6$ Hz), 7.34 (1H, d, $J = 7.8$ Hz), 7.19-7.10 (3H, m), 6.99-6.91 (3H, m), 6.83 (1H, d, $J = 7.7$ Hz), 6.79 (1H, d, $J = 7.7$ Hz), 4.10 (3H, s), 3.96 (3H, s), 2.43 (3H, s).

^{13}C NMR (100 MHz; CDCl_3) δ : 170.5, 156.5, 155.5, 154.6, 146.2, 137.2, 136.7, 135.9, 130.1, 129.3, 128.6, 126.4, 125.9, 121.0, 120.1, 119.4, 119.0, 115.1, 110.2, 106.2, 104.2, 56.4, 56.3, 21.2.

FTIR ν_{\max} (ATR, film)/ cm^{-1} 3390, 1759, 1609, 1598, 1583, 1466, 1400, 1379, 1365, 1267.

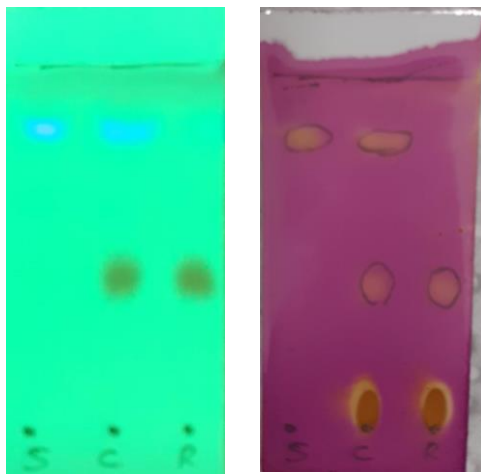
HRMS (+APCI) Calcd for $\text{C}_{24}\text{H}_{21}\text{O}_5$ $[\text{M}+\text{H}]^+$ 389.1384; found: 389.1379.



29

Binaphthalene **27** (335 mg, 0.86 mmol) was dissolved in EtOAc/DCM (20 ml/14 ml) with the aid of heating and vigorous stirring. Then IBX (605 mg, 2.16 mmol) and DMSO (14 ml) were added at 23 °C. Initially formed white suspension first became yellow then orange and finally a red solution. Stirred at 23 °C for 7 hours. TLC indicated the full consumption of **27**. The reaction mixture was quenched with saturated aqueous Na_2CO_3 solution (30 ml). The aqueous phase was extracted with DCM (3×20 ml). The combined organic phase was dried over anhydrous Na_2SO_4 , filtered and concentrated under reduced pressure. Purification by column chromatography (SiO_2 ; only DCM → 1% MeOH in DCM) gave pure **29** (318 mg, 92% yield) as red solid.

TLC Images after Aqueous Work-up:



Left image: TLC under UV light (254 nm)

Right image: TLC stained with KMnO_4 solution

Spots from left to right:

S: Starting material (**27**);

C: Co-spot of **27** and reaction mixture;

R: Reaction mixture.

Mobile phase: EtOAc:hexanes = 1:1

M.P. °C 268.3-269.6 °C (CH_2Cl_2).

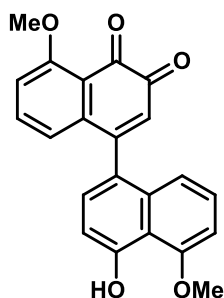
$R_f = 0.67$ (only EtOAc)

TLC Visualization: UV active; stains with KMnO_4 solution.

^1H NMR (400 MHz; CDCl_3) δ : 7.40 (1H, d, $J = 7.7$ Hz), 7.36-7.31 (2H, m), 7.27-7.25 (1H, m), 7.16 (1H, d, $J = 7.6$ Hz), 7.08 (1H, d, $J = 8.6$ Hz), 6.89 (1H, d, $J = 7.7$ Hz), 6.51 (1H, s), 6.42 (1H, d, $J = 7.7$ Hz), 4.02 (3H, s), 3.97 (3H, s), 2.42 (3H, s).

^{13}C NMR (100 MHz; CDCl_3) δ : 181.0, 178.7, 170.2, 163.2, 156.4, 155.8, 147.7, 138.0, 136.7, 134.6, 133.0, 129.3, 127.6, 126.6, 123.3, 119.6, 119.5, 119.1, 118.9, 115.6, 106.9, 56.6, 56.4, 21.1.

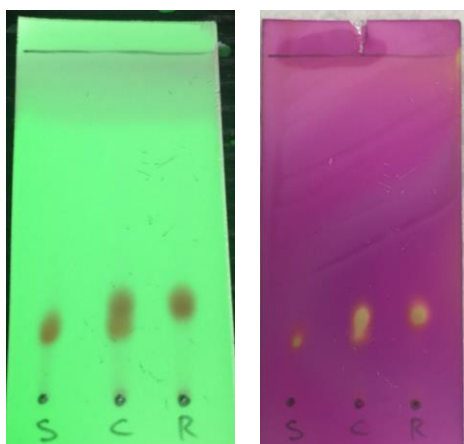
FTIR ν_{max} (ATR, film)/ cm^{-1} 3011, 2942, 2840, 1760, 1666, 1583, 1468.



Daldiquinone (15)

Naphthaquinone **29** (17.6 mg, 0.044 mmol) was dissolved in MeOH/DCM (3ml/3ml) in a vial by vigorous stirring. To the resulting clear red solution, K_2CO_3 (9.07 mg, 0.066 mmol) was added in one portion. The reaction mixture was stirred at 23 °C. Rxn became black at the end of the first 15 minutes. TLC indicated the full consumption of **29** after 2 hours. The black reaction mixture was then quenched with saturated aqueous NH_4Cl solution (10 ml). The aqueous phase was extracted with DCM (3×15 ml). The combined organic phase was dried over anhydrous Na_2SO_4 , filtered and concentrated under reduced pressure. Purification by column chromatography (SiO_2 ; EtOAc:hexanes = 1:2 → 1:1) gave pure Daldiquinone (**15**) (11.9 mg, 75% yield) as red solid.

TLC Images after Aqueous Work-up:



Left image: TLC under UV light (254 nm)

Right image: TLC stained with $KMnO_4$ solution

Spots from left to right:

S: Starting material (**29**);

C: Co-spot of **29** and reaction mixture;

R: Reaction mixture.

Mobile phase: EtOAc:hexanes = 1:1

$R_f = 0.68$ (only EtOAc); 0.23 (EtOAc:hexanes = 1:1)

M.P. °C 268.7-268.9 °C (CHCl₃).

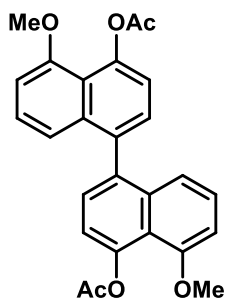
TLC Visualization: UV active; stains to yellow with KMnO₄ solution upon heating.

¹H NMR (400 MHz; CDCl₃) δ: 9.63 (1H, s), 7.34 (1H, t, $J = 8.2$ Hz), 7.32 (1H, d, $J = 7.9$ Hz), 7.25 (2H, m), 7.07 (1H, d, $J = 8.6$ Hz), 6.96 (1H, d, $J = 7.9$ Hz), 6.85 (1H, dd, $J = 7.1, 0.9$ Hz), 6.48 (1H, s), 6.47 (1H, d, $J = 7.9$ Hz), 4.12 (1H, s), 4.02 (1H, s).

¹³C NMR (100 MHz; CDCl₃) δ: 181.2, 179, 163.1, 157.1, 156.6, 156.0, 138.5, 136.5, 134.4, 129.4, 128.6, 126.8, 125.6, 123.2, 120, 119.6, 115.4, 115.3, 110.3, 104.8, 56.6, 56.5.

FTIR ν_{\max} (ATR, film)/cm⁻¹ 3379 (br), 3011, 2944, 2842, 1663, 1608, 1585, 1470, 1410, 1339.

HRMS (+APCI) Calcd for C₂₂H₁₇O₅ [M+H]⁺ 361.1071, found: 361.1075.



26

Appearance: Dark orange solid

$R_f = 0.35$ (EtOAc:hexanes = 1:2)

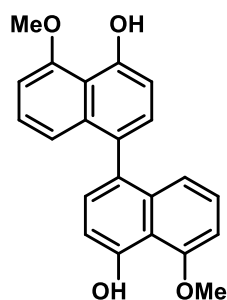
TLC Visualization: UV active; stains with KMnO_4 solution upon heating.

^1H NMR (400 MHz; CDCl_3) δ : 7.41 (2H, d, $J = 7.6$ Hz), 7.18 (2H, t, $J = 8.2$ Hz), 7.16 (2H, d, $J = 7.6$ Hz), 6.93 (2H, d, $J = 8.5$ Hz), 6.84 (2H, d, $J = 7.7$ Hz), 3.96 (6H, s), 2.43 (6H, s).

^{13}C NMR (100 MHz; CDCl_3) δ : 170.5, 155.5, 146.5, 136.7, 136.3, 128.4, 126.6, 120.1, 119.3, 119.0, 106.3, 56.4, 21.2

FTIR ν_{max} (ATR, film)/ cm^{-1} 1762, 1594, 1462, 1402, 1367, 1266, 1209, 1083, 1032.

HRMS (+APCI) Calcd for $\text{C}_{26}\text{H}_{23}\text{O}_6$ $[\text{M}+\text{H}]^+$ 431.1490, found: 431.1508.



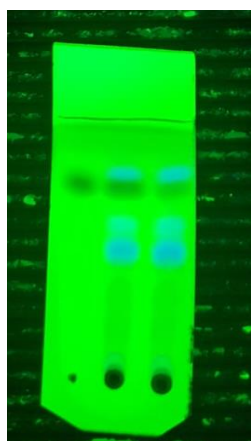
Daldinol (28)

An oven-dried, 50-mL, round-bottomed flask was cooled under vacuum and refilled with nitrogen. It was then charged with 20 mL of DMSO, which was deoxygenated by purging with nitrogen gas for 15 min. Afterwards, acetoxynaphthalene **25** (350 mg, 1.19 mmol), B_2pin_2 (166 mg, 0.65 mmol), $\text{Pd}(\text{dppf})\text{Cl}_2 \cdot \text{CH}_2\text{Cl}_2$ (97 mg, 0.12 mmol) and potassium acetate (349 mg, 3.56 mmol) were added sequentially. The flask was then sealed with a glass stopper, and the reaction mixture was stirred at 90°C for 24 h. TLC analysis indicated full consumption of the starting material (**25**). The mixture

was then cooled to ambient temperature and quenched with 20 mL of H₂O. The aqueous phase was extracted with EtOAc (3×15 mL). The combined organic phase was dried over anhydrous Na₂SO₄, filtered and concentrated under reduced pressure. The crude mixture was purified by flash column chromatography (SiO₂; EtOAc:hexanes = 1:4 → 1:2 → 1:1) to afford a mixture of **26** and partially hydrolyzed product **27**.

The mixture of **26** and **27** was dissolved in 15 mL of MeOH and 5 mL of CH₂Cl₂ in a 50-mL, round-bottomed flask. To the orange solution was added K₂CO₃ (165 mg, 1.19 mmol), and the resulting heterogeneous mixture was stirred at 23 °C for 3 h. It was then quenched with a saturated aqueous solution of NH₄Cl. The aqueous phase was extracted three times with EtOAc and twice with CH₂Cl₂. The combined organic phase was dried over anhydrous Na₂SO₄, filtered and concentrated under reduced pressure. Purification by flash column chromatography (SiO₂; EtOAc:hexanes = 1:4 → 1:2 → 1:1) gave pure daldinol (**28**) (117 mg, 57% over 3 steps) as a yellow solid.

TLC images for the formation of mixture of 26 and 27 after Aqueous Work-up:



Left image: TLC under UV light (254 nm)

Right image: TLC stained with KMnO₄ solution

Spots from left to right:

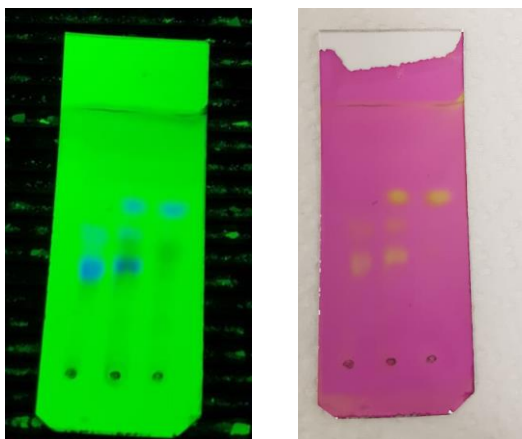
Left spot: starting material (**25**);

Middle spot : Co-spot of **25** and reaction mixture;

Right spot: Reaction mixture.

Mobile phase: EtOAc:hexanes = 1:2

TLC Images for the hydrolysis of the mixture of 26 and 27 to give Daldinol (28):



Left image: TLC under UV light (254 nm)

Right image: TLC stained with KMnO₄ solution

Spots from left to right:

Left spot: mixture of **26** and **27**;

Middle spot : Co-spot of mixture (**26** and **27**) and reaction mixture;

Right spot: Reaction mixture.

Mobile phase: EtOAc:hexanes = 1:2

M.P. 269-270 °C (CH₂Cl₂);

$R_f = 0.39$ (EtOAc:hexanes = 1:4)

TLC Visualization: UV active; stains with KMnO₄ solution.

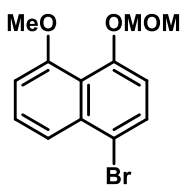
¹H NMR (400 MHz; CDCl₃) δ : 9.52 (2H, s), 7.31 (2H, d, $J = 7.8$ Hz), 7.11 (2H, t, $J = 8.1$ Hz), 6.97 (2H, d, $J = 7.8$ Hz), 6.94 (2H, d, $J = 8.6$ Hz), 6.78 (2H, d, $J = 7.6$ Hz), 4.10 (6H, s).

¹³C NMR (100 MHz; CDCl₃) δ : 156.5, 154.3, 136.2, 130.3, 129.7, 125.7, 121.0, 115.2, 110.3, 104.1, 56.4

FTIR ν_{\max} (ATR, solid)/cm⁻¹ 3388, 2924, 2854, 1609, 1584, 1399, 1258.

HRMS (+APCI) Calcd for C₂₂H₁₉O₄ [M+H]⁺ 347.1278; found: 347.1276.

Elemental (Combustion) analysis: Anal. calcd for C₂₂H₁₈O₄: C, 76.29; H, 5.24; found: C, 75.90; H, 5.41.

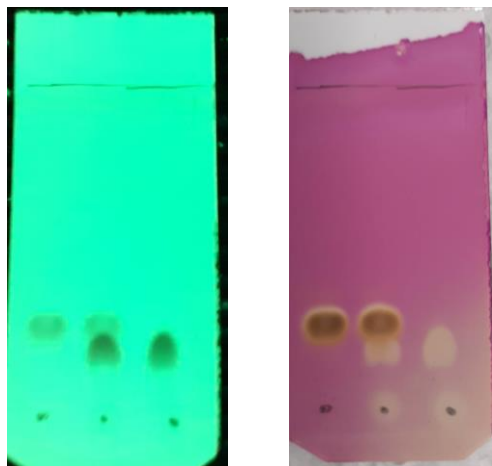


38

An oven-dried 100-ml round-bottomed flask cooled under vacuum and refilled with N₂(×3). Naphthalene derivative **24** (2.38 gram, 5.93 mmol) was added and dissolved in 15 ml anhydrous DMF under N₂ at 23 °C. The resulting clear pale yellow solution was cooled down to 0 °C in an ice bath for 10 min. Sodium hydride (NaH, 285 mg, 7.13 mmol, 60% dispersion in mineral oil) was slowly added resulted in gas evolution. After 10 minutes of stirring at 0 °C, MOMCl (675 μL) was added resulted in vapor evolution. Ice bath removed after 5 minutes and reaction mixture stirred at 23 °C. TLC indicated the full consumption of **24** after 90 minutes. The reaction mixture was quenched with saturated aqueous NH₄Cl solution (20 ml). The aqueous phase was extracted with EtOAc (3×20ml). The combined organic phase was dried over anhydrous Na₂SO₄, filtered and concentrated under reduced pressure. Purification by column chromatography (SiO₂; EtOAc:hexanes = 1:9 → 1:5) gave pure **38** (2.67 g, 96% yield) as white solid.

Note: In another experiment reaction product **38** was isolated in 99% yield when the reaction was conducted starting from 1.5 g (5.93 mmol) **24**.

TLC Images after Aqueous Work-up:



Left image: TLC under UV light (254 nm)

Right image: TLC stained with KMnO_4 solution

Spots from left to right:

Left spot: Starting material (**24**);

Middle spot: Co-spot of **24** and reaction mixture;

Right spot: Reaction mixture.

Mobile phase: EtOAc:hexanes = 1:19
(developed twice)

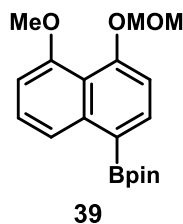
$R_f = 0.50$ (EtOAc:hexanes = 1:4)

TLC Visualization: UV active; stains with KMnO_4 solution to yellow upon heating.

^1H NMR (400 MHz; CDCl_3) δ : 7.85 (1H, d, $J = 8.6$ Hz), 7.67 (1H, d, $J = 8.3$ Hz), 7.48 (1H, t, $J = 8.2$ Hz), 6.94 (2H, t, $J = 7.7$ Hz), 5.25 (2 H, s), 3.97 (3H, s), 3.59 (3H, s)

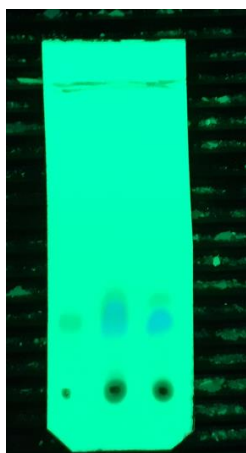
^{13}C NMR (100 MHz; CDCl_3) δ : 157.1, 154.1, 135.1, 130.5, 127.8, 120.4, 120.0, 116.0, 113.8, 107.3, 97.0, 56.7, 56.6

FTIR ν_{max} (ATR, film)/ cm^{-1} 1613, 1588, 1575, 1460, 1397, 1375, 1266, 1233, 1150, 1095, 994, 948, 815, 751.



To a pale yellow solution of **38** (500 mg, 1.68 mmol) in 3 ml dioxane, Et₃N (0.94 mL, 6.72 mmol), Pd(OAc)₂ (37.72 mg, 0.168 mmol) and DPEphos (183 mg, 0.34 mmol) were added sequentially. To the resulting brown solution HBpin (730 μL, 5.04 mmol) was added dropwise resulted in a color change to dark brown and gas evolution Reaction mixture was then heated to 100 °C and stirred for 2 hours. Reaction stopped and cooled to 23 °C. Purification by flash column chromatography (SiO₂; only hexanes) gave pure **39** (324 mg, 56%) as green oil.

TLC Images after Aqueous Work-up:



Left image: TLC under UV light (254 nm)

Right image: TLC stained with KMnO₄ solution

Spots from left to right:

Left spot: starting material (**38**);

Middle spot : Co-spot of **38** and reaction mixture;

Right spot: Reaction mixture.

Mobile phase: EtOAc:hexanes = 1:19

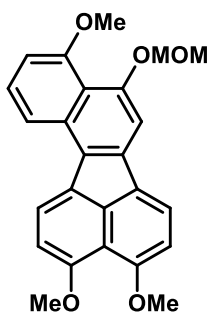
$R_f = 0.39$ (10% EtOAc in hexanes)

TLC Visualization: UV active; stains to dark yellow with KMnO_4 solution.

^1H NMR (400 MHz; CDCl_3) δ : 8.41 (1H, d, $J = 8.5$ Hz), 8.00 (1H, d, $J = 7.8$ Hz), 7.43 (1H, t, $J = 8.0$ Hz), 7.04 (1H, d, $J = 7.8$ Hz), 6.88 (1H, d, $J = 7.7$ Hz), 5.31 (2H, s), 3.96 (3H, s), 3.59 (3H, s), 1.40 (12H, s).

^{13}C NMR (100 MHz; CDCl_3) δ : 157.1, 157.0, 141.4, 137.1, 126.8, 121.5, 118.4, 111.4, 106.5, 96.3, 83.6, 56.55, 56.54, 25.0

FTIR ν_{max} (ATR, film)/ cm^{-1} 1613, 1578, 1515, 1464, 1326, 1326, 1262, 1142, 1099.

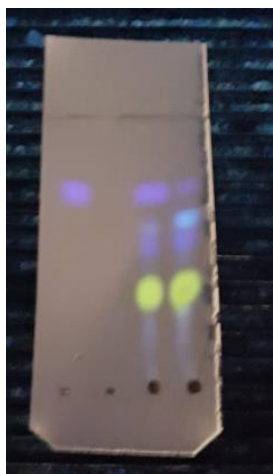
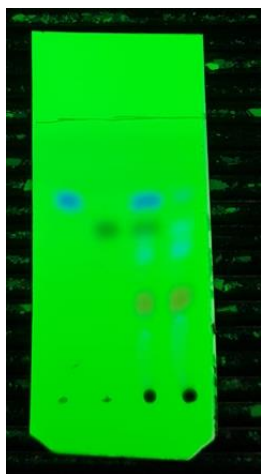


40

To a green solution of boronic ester **29** (400 mg, 1.16 mmol) in DMSO (7 ml, purged with N_2 for 15 minutes) was added **37** (365 mg, 1.06 mmol). To this light brown suspension $\text{Pd}(\text{ddpf})\text{Cl}_2 \cdot \text{CH}_2\text{Cl}_2$ (130 mg, 0.16 mmol) was added and resulted in a color change to red. KOAc (417 mg, 4.24 mmol) was added flask was closed with a glass

stopper and heated to 110 °C. TLC indicated the full consumption of **37** after 24 hours. Reaction stopped and cooled to 23 °C. The reaction mixture was quenched with H₂O. The aqueous phase was extracted with EtOAc (several times). The combined organic phase was dried over anhydrous Na₂SO₄, filtered and concentrated under reduced pressure. Purification by column chromatography (SiO₂; EtOAc:hexanes = 1:5 → 1:3 → 1:2 → 1:1 → EtOAc only) gave pure **40** (192 mg, 45% yield) as goldish yellow solid.

TLC Images:



Left image: TLC under UV light (254 nm)

Right image: TLC under UV light (366nm)

Spots from left to right:

1st spot: Naphthalene boronic ester **39**;

2nd spot: Dibromonaphthalene **37**

3rd spot: Co-spot of **37**, **39** and reaction mixture;

4th spot: Reaction mixture.

Mobile phase: EtOAc:hexanes = 1:2

M.P. 215.2-216.4 °C (CHCl₃).

R_f = 0.37 (EtOAc:hexanes = 1:2)

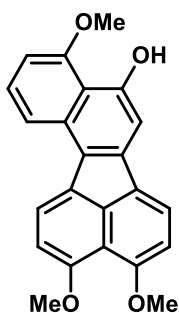
TLC Visualization: UV active; yellow under 366 nm, doesn't stain with KMnO₄ solution.

¹H NMR (400 MHz; CDCl₃) δ: 8.27 (2H, m), 7.93 (1H, d, *J* = 7.8 Hz), 7.63 (1H,s), 7.49 (1H, t, *J* = 8.1 Hz), 6.95 (2H, t, *J* = 8.0 Hz), 6.86 (1H, d, *J* = 7.7 Hz), 5.36 (2H, s), 4.08 (6H, s), 4.01 (3H, s), 3.68 (3H, s).

¹³C NMR (100 MHz; CDCl₃) δ: 158.9, 157.9, 157.4, 153.7, 137.5, 135.6, 133.6, 130.2, 129.1, 128.1, 127.3, 124.8, 122.6, 118.0, 117.3, 114.4, 108.2, 106.9, 106.7, 105.7, 97.7, 56.7, 56.61, 56.6, 56.5.

FTIR ν_{\max} (ATR, solid)/cm⁻¹ 1585, 1458, 1425, 1395, 1283, 1251, 1154, 1124, 1093, 1050.

HRMS (ESI+) Calcd for C₂₅H₂₂O₅Na [M+Na]⁺: 425.1360, found: 425.1362.

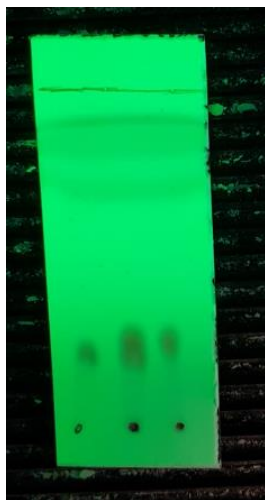


41

Fluoranthene derivative **40** (100 mg, 0.25 mmol) was dissolved in 10 ml anhydrous THF with the aid of heating by a heat gun. To this yellowish-orange solution, concentrated HCl solution (0.83 ml, 10 mmol, 12 M) was added dropwise at 23 °C resulted in a color change to green and the formation of black insoluble particles. Stirred at this temperature for 1 hour. TLC indicated the full consumption of **40** after 1 hour. The reaction mixture was then treated with H₂O (20 ml). The aqueous phase was extracted with EtOAc(3×20 ml). The combined organic phase was dried over anhydrous Na₂SO₄, filtered and concentrated under reduced pressure. Purification by column

chromatography (SiO₂; EtOAc:hexanes = 1:6 → 1:4 → 1:1 → EtOAc only) gave pure **41** (72.6 mg, 82% yield) as yellowish orange solid.

TLC Images:



Left image: TLC under UV light (254 nm)

Right image: TLC stained with KMnO₄ solution

Spots from left to right:

Left spot: Starting material (**40**);

Middle spot: Co-spot of **40** and reaction mixture;

Right spot: reaction mixture

M.P. 228.1-229.2 °C (CHCl₃).

$R_f = 0.25$ (EtOAc:hexanes = 1:5).

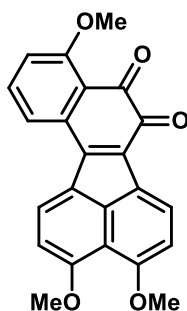
TLC Visualization: UV active; yellow under 366 nm, stains to yellow with KMnO₄ solution.

¹H NMR (400 MHz; CDCl₃) δ: 9.64 (1H, s), 8.23 (1H, d, $J = 8.6$ Hz), 8.18 (1H, d, $J = 7.9$ Hz), 7.90 (1H, d, $J = 7.7$ Hz), 7.45 (1H, d, $J = 7.9$ Hz), 7.42 (1H, s), 6.95 (2H, d, $J = 7.9$ Hz), 6.78 (1H, d, $J = 7.7$ Hz), 4.10 (3H, s), 4.08 (6H, s).

¹³C NMR (100 MHz; CDCl₃) δ: 158.9, 157.3, 156.9, 154.5, 139.2, 135.6, 132.8, 130.5, 129.2, 126.8, 124.8, 123.6, 122.6, 118.4, 114.5, 114.2, 106.9, 106.8, 104.6, 103.4, 56.62, 56.59, 56.3.

FTIR ν_{\max} (ATR, solid)/cm⁻¹ 3393, 1595, 1458, 1424, 1399, 1380, 1273, 1243, 1158, 1116, 1088, 811.

HRMS (ESI+) Calcd for C₂₃H₁₈NaO₄ [M+Na]⁺: 381.1098, found: 381.1108.



42

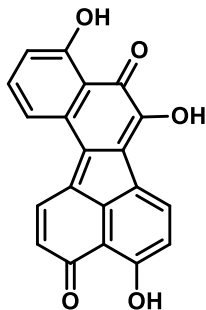
A 100 ml round-bottomed flask was charged with **41** (30 mg, 0.084 mmol) and dissolved in 10 ml CH₃CN and 5 ml DCM. To this solution 5 ml H₂O was added. The orange biphasic reaction mixture was cooled down to 0 °C. PIFA (80 mg, 0.184 mmol) was dissolved in a mixture of CH₃CN (15 ml), DCM (5 ml) and H₂O (7.5 ml), and added dropwise to the reaction mixture for 20-minutes at 0 °C. The reaction mixture gradually became dark-red and TLC indicated the full consumption of **41** after 30 minutes. The reaction mixture was treated with brine. The aqueous phase was extracted with EtOAc. The combined organic phase was dried over anhydrous Na₂SO₄, filtered and concentrated under reduced pressure. Purification by column chromatography (SiO₂; EtOAc only) gave pure **42** (10.0 mg, 32% yield).

$R_f = 0.63$ (MeOH:CH₂Cl₂ = 1:9).

¹H NMR (400 MHz; CDCl₃) δ : 8.41 (1H, d, $J = 8.2$ Hz), 8.18 (1H, d, $J = 8.2$ Hz), 7.81 (1H, d, 6.8 Hz), 7.57 (1H, t, $J = 8.0$ Hz), 7.02 (2H, d, $J = 8.4$ Hz), 6.95 (1H, d, $J = 8.3$ Hz), 4.10 (3H, s), 4.08 (6H, s), 4.01 (3H, s).

FTIR ν_{\max} (ATR, solid)/cm⁻¹ 1640, 1601, 1586, 1502, 1461, 1422, 1364, 1343, 1277, 1256, 1230, 1135, 1120, 1099.

HRMS (ESI+) Calcd for C₂₃H₁₆NaO₅ [M+Na]⁺: 395.0890, found: 395.0897.

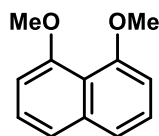


Bulgarein (1)

Compound **42** (4.0 mg, 0.011 mmol) was dissolved in DCM (1 ml). Obtained solution transferred to an oven-dried Schlenk tube under N₂. To obtained dark-red solution, 0.3 ml BBr₃ (1M in DCM) was added along the walls at 0 °C. Stirred at 0 °C for 2 hours. Then stirred at 23 °C for 22 hours. After that reaction mixture was cooled down to 0 °C and quenched with an excess of water. Stirred at 0 °C for 10 minutes. The aqueous phase was extracted with EtOAc. The combined organic phase was dried over anhydrous Na₂SO₄, filtered and concentrated under reduced pressure. Purified by Prep. TLC (10% MeOH in DCM) to give bulgarein (**1**).

UV-Vis Spectrum: : λ_{max} (nm) (EtOH, blue solution): 370 (sh), 400 (sh), 630 (sh).

HRMS (ESI-) Calcd for C₂₀H₉O₅ [M-H]⁻: 329.0455, found: 329.0535.



36

A 250-ml round-bottom flask was charged with 1,8-dihydroxynaphthalene (2.0 gram, 12.5 mmol). 100 ml acetone was added at 23 °C to give a brown solution. K_2CO_3 (17.3 gram, 125 mmol) and Me_2SO_4 were added sequentially at 23 °C. The resulting suspension was heated to 70 °C and vigorously stirred under reflux at 70-80 °C for 64 hours at the end of which TLC indicated the full consumption of 1,8-dihydroxynaphthalene. The reaction mixture was then cooled down to 23 °C and acetone was removed under reduced pressure. To the solution of the remaining solid in CH_2Cl_2 , 100 ml 4M aqueous NaOH solution was added at 23 °C and stirred at this temperature for 2 hours. Layers were separated and the aqueous phase was washed with CH_2Cl_2 ($\times 3$). The combined organic phase was dried over anhydrous Na_2SO_4 , filtered and concentrated under reduced pressure. Purification by column chromatography (SiO_2 ; EtOAc:hexanes = 1:19 \rightarrow 1:9 \rightarrow 1:5 \rightarrow 1:1) gave pure **36** (1.96 g, 83% yield) as brownish-yellow solid.

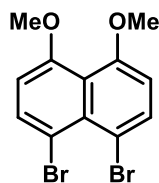
$R_f = 0.46$ (EtOAc:hexanes = 1:9).

1H NMR (400 MHz; $CDCl_3$) δ : 7.43-7.33 (4H, m), 6.86 (2H, dd, $J = 7.2, 1.5$ Hz), 3.98 (6H, s).

^{13}C NMR (100 MHz; $CDCl_3$) δ : 157.2, 137.5, 126.5, 121.0, 119.0, 106.4, 56.6.

FTIR ν_{max} (ATR, solid)/ cm^{-1} 1580, 1510, 1460, 1427, 1386, 1348, 1273, 1237, 1180.

HRMS (+APCI) Calcd for $C_{12}H_{13}O_2$ $[M+H]^+$ 189.0911; found: 189.0917.



37

To a 50-ml round-bottom flask, **36** (1.0 gram, 5.31 mmol) was added and dissolved in 17 ml anhydrous CH_2Cl_2 . To the resulting yellow solution, NBS (945 mg, 5.31 mmol) was slowly added at 23 °C. The dark-gray reaction mixture was stirred at 23 °C for 40 minutes. CH_2Cl_2 was removed under reduced pressure. The remaining solid was dissolved in 17 ml anhydrous DMF. To this solution, NBS (993 mg, 5.58 mmol) was slowly added at 23 °C. The resulting reddish-gray reaction mixture was stirred at 23 °C for 40 minutes and then quenched with saturated aqueous $\text{Na}_2\text{S}_2\text{O}_3$ solution (20 ml). The aqueous phase was extracted with EtOAc (3×20 mL). The combined organic phase was dried over anhydrous Na_2SO_4 , filtered and concentrated under reduced pressure. Purification by flash column chromatography (SiO_2 ; EtOAc:hexanes = 1:19 → 1:9 → 1:5 → 1:2 → 1:1) gave pure **37** (1.27 gram, 69% yield) as goldish yellow solid.

^1H NMR (400 MHz; CDCl_3) δ : 7.82 (2H, d, $J = 8.5$ Hz), 6.72 (2H, d, $J = 8.5$ Hz), 3.93 (6H, s).

^{13}C NMR (100 MHz; CDCl_3) δ : 157.8, 135.9, 131.6, 121.7, 110.3, 107.8, 56.9

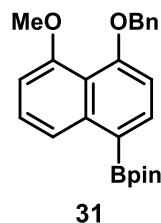
FTIR ν_{max} (ATR, solid)/ cm^{-1} 3010, 2965, 2916, 2837, 1583, 1508, 1462, 1448, 1369, 1351, 1293, 1231.

HRMS (APCI+) calculated: $\text{C}_{12}\text{H}_{11}^{79}\text{Br}_2\text{O}_2$ $[\text{M}+\text{H}]^+$: 344.9121, found: 344.9122.



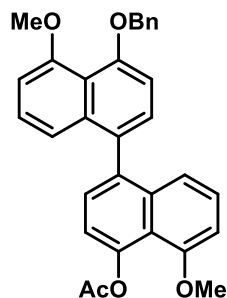
An oven-dried 50-ml round-bottomed flask was cooled under vacuum and refilled with N₂(×3). Naphthalene derivative **24** (984 mg, 3.89 mmol) was added and dissolved in 20 ml anhydrous DMF under N₂ at 23 °C. The resulting solution was cooled down to 0 °C in an ice bath for 10 min. Sodium hydride (NaH, 185 mg, 4.67 mmol, 60% dispersion in mineral oil) was added slowly resulted in gas evolution. After 10 minutes of stirring at 0 °C, BnBr (600 μL, 863 mg, 5.06 mmol) was added. Ice bath removed after 5 minutes and reaction mixture stirred at 23 °C. TLC indicated the full consumption of **24** after 2 hours. The reaction mixture was quenched with H₂O (20 ml). The aqueous phase was extracted with EtOAc (3×20ml). The combined organic phase was dried over anhydrous Na₂SO₄, filtered and concentrated under reduced pressure. Purification by column chromatography (SiO₂; EtOAc:hexanes = 1:19 → 1:9) gave pure **30** (1.15 g, 86% yield).

¹H NMR (400 MHz; CDCl₃) δ: 7.84 (1H, d, *J* = 8.5), 7.66 (1H, dd, *J* = 8.3, 1.4 Hz), 7.58 (2H, d, *J* = 7.6 Hz), 7.50 (1H, td, *J* = 8.4, 1.4 Hz), 7.42 (2H, t, *J* = 7.4 Hz), 7.33 (1H, t, *J* = 7.2 Hz), 6.94 (1H, d, *J* = 7.8 Hz), 6.80 (1H, d, *J* = 8.4 Hz), 5.19 (2H, s), 3.96 (3H, s).



A flame-dried Schlenk tube was cooled under vacuum and refilled with N₂(×3). Naphthalene bromide derivative **30** (100 mg, 0.291 mmol) was added and dissolved in 4 ml anhydrous THF under N₂ at 23 °C. Then reaction mixture cooled to -78 °C and *n*-BuLi (218.5 μL, 0.350 mmol, 1.6 M in Hexane) was added dropwise at -78 °C. After 15 minutes of stirring at -78 °C *i*-PrOBpin (77.2 μL, 70.4 mg, 0.38 mmol) was added. The reaction mixture gradually allowed to heat to 23 °C. Reaction stopped after 16 hours, and the reaction mixture was quenched with H₂O. The aqueous phase was extracted with EtOAc. The organic phase was dried over anhydrous Na₂SO₄, filtered and concentrated under reduced pressure. Purification by column chromatography (SiO₂; EtOAc:hexanes = 1:19) gave pure **31** (64.5 mg, 58% yield).

¹H NMR (400 MHz; CDCl₃) δ: 8.46 (1H, d, *J* = 8.5), 8.05 (1H, d, *J* = 7.9 Hz), 7.66 (2H, d, *J* = 7.7 Hz), 7.47 (3H, m), 7.42 (2H, t, *J* = 7.4 Hz), 7.37 (1H, t, *J* = 7.4 Hz), 6.97 (1H, d, *J* = 7.9 Hz), 6.93 (1H, d, *J* = 7.8 Hz), 5.29 (2H, s), 3.99 (3H, s), 1.45 (12H, s).



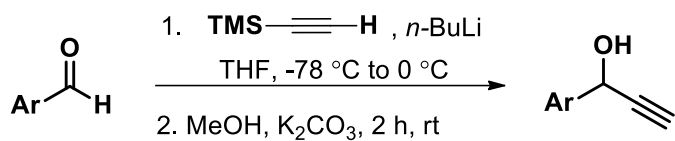
32

To a 25-ml round-bottomed flask, 3 ml DMSO was added and purged with N₂ for 10 minutes. Boronic ester **31** (50 mg, 0.128 mmol), acetoxynaphthalene **25** (37.7 mg, 0.128 mmol) and KOAc (25.12 mg, 0.256 mmol) were added at 23 °C. After 15 minutes stirring at 23 °C under N₂, Pd(dppf)Cl₂·CH₂Cl₂ (10.45 mg, 0.0128 mmol) was added. Flask sealed with glass stopper and heated to 80 °C. Stirred for 5 hours at this temperature. After that reaction was stopped and cooled to 23 °C. Quenched with H₂O. The aqueous phase was extracted with EtOAc. The organic phase was dried over anhydrous Na₂SO₄, filtered and concentrated under reduced pressure. Purification by column chromatography (SiO₂; EtOAc:hexanes = 1:9) gave pure **32** (20.0 mg, 32% yield).

¹H NMR (400 MHz; CDCl₃) δ: 7.67 (2H, d, *J* = 7.2 Hz), 7.48-7.39 (3H, m), 7.38-7.32 (2H, m), 7.20-7.14 (3H, m), 7.04 (1H, d, *J* = 8.0 Hz), 6.96 (1H, d, *J* = 8.5 Hz), 6.90 (1H, d, *J* = 8.5 Hz), 6.86 (1H, d, *J* = 7.8 Hz), 6.83 (1H, d, *J* = 7.6 Hz), 5.30 (2H, s), 3.99 (3H, s), 3.96 (3H, s), 2.43 (3H, s).

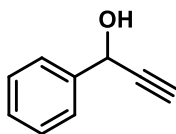
3.3. Diels-Alder reactions for Fluoranthene synthesis.

3.3.1. General Procedure A for the synthesis of alkynes 43a-43d.



Compounds **43a-43d** were synthesized according to reported literature procedure.⁶⁰

An oven-dried 2-neck round-bottomed flask was cooled under vacuum and refilled with N₂(×3). Trimethylsilylacetylene (1.1 equiv.) was added and dissolved in 10 ml anhydrous THF under N₂. The resulting solution was then cooled to -78 °C and stirred for 10 minutes. After that *n*-BuLi (1.6 M in hexane, 1.06 equiv.) was added dropwise at -78 °C, and the reaction flask was transferred to 0 °C after 10 minutes. After 20 minutes of stirring at 0 °C, the reaction mixture was cooled back to -78 °C. After 10 minutes of stirring at this temperature, a solution of aryl aldehyde (1 equiv.) in 3 ml anhydrous THF was added dropwise at -78 °C. The reaction mixture heated to 0 °C after 10 minutes and gradually allowed to heat to 23 °C. After 2 hours of stirring, MeOH (10 ml) and K₂CO₃ (196 mg, 1.42 mmol) were added at 23 °C. The resulting reaction mixture was stirred for 2 h at 23 °C and quenched with saturated aqueous NH₄Cl. The aqueous phase was extracted with CH₂Cl₂ (3×15 mL), and the combined organic phase was dried over anhydrous Na₂SO₄, and concentrated under reduced pressure. The residue was purified by column chromatography.



43a

Alkyne **43a** was prepared from benzaldehyde (500 mg, 479 μL , 4.71 mmol), trimethylsilylacetylene (513 mg, 724 μL , 5.22 mmol), *n*-BuLi (1.6 M in hexane, 3.12 ml, 4.99 mmol) and THF (13 ml) according to General Procedure A. The crude product was purified by flash column chromatography (SiO_2 ; EtOAc:hexanes = 1:9 \rightarrow 1:8 \rightarrow 1:5) to afford pure **43a** (556 mg, 89% yield) as a colorless oil.

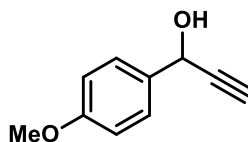
R_f = 0.31 (EtOAc:hexanes = 1:5)

TLC Visualization: UV active; stains with KMnO_4 solution.

^1H NMR (400 MHz; CDCl_3) δ : 7.57-7.55 (2H, m) 7.42-7.33 (3H, m), 5.47 (1H, dd, J = 6.2, 2.2 Hz), 2.68 (1H, d, J = 2.3 Hz), 2.44 (1H, br d, J = 4.7 Hz), 2.29 (1H, t, J = 6.3 Hz).

^{13}C NMR (100 MHz; CDCl_3) δ : 140.2, 128.8, 128.7, 126.7, 83.6, 75.0, 64.5.

FTIR ν_{max} (ATR, solid)/ cm^{-1} 3290, 1493, 1453, 2349, 1493, 1453, 1262, 1191, 1019, 946, 723.



43b

Alkyne **43b** was prepared from *p*-anisaldehyde (504 mg, 450 μL , 3.70 mmol), trimethylsilylacetylene (403 mg, 569 μL , 4.11 mmol), *n*-BuLi (1.6 M in hexane, 2.45 ml, 3.92 mmol) and THF (11 ml) according to General Procedure A. The crude product was

purified by flash column chromatography (SiO₂; EtOAc:hexanes = 1:9 → 1:5) to afford pure **43b** (312 mg, 47% yield) as a yellow oil.

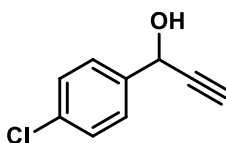
$R_f = 0.43$ (EtOAc:hexanes = 1:3)

TLC Visualization: UV active; stains with KMnO₄ solution.

¹H NMR (400 MHz; CDCl₃) δ : 7.46 (2H, app d, $J = 8.4$ Hz), 6.90 (2H, app d, $J = 8.8$ Hz), 5.40 (1H, d, $J = 2.2$ Hz), 3.80 (3H, s), 2.66 (1H, d, $J = 2.2$ Hz), 2.56 (1H, br s).

¹³C NMR (100 MHz; CDCl₃) δ : 159.9, 132.5, 128.2, 114.1, 83.9, 74.7, 64.1, 55.5.

FTIR ν_{\max} (ATR, film)/cm⁻¹ 3394 (br), 3285, 1610, 1510, 1304, 1243, 1172, 1025, 947, 831, 810.



43c

Alkyne **43c** was prepared from *p*-chlorobenzaldehyde (250 mg, 1.78 mmol), trimethylsilylacetylene (199 mg, 280 μ L, 2.02 mmol), *n*-BuLi (1.6 M in hexane, 1.20 ml, 1.92 mmol) and THF (7 ml) according to General Procedure A. The crude product was purified by flash column chromatography (SiO₂; EtOAc:hexanes = 1:19 → 1:9 → 1:5) to afford pure **43c** (138 mg, 47% yield) as a yellow oil.

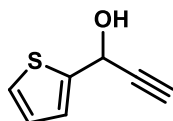
$R_f = 0.52$ (EtOAc:hexanes = 1:4)

TLC Visualization: UV active; stains with KMnO₄ solution.

¹H NMR (400 MHz; CDCl₃) δ: 7.44 (2H, d, *J* = 8.5 Hz), 7.33 (2H, d, *J* = 8.4 Hz), 5.39 (1H, br s), 3.11 (1H, app d, *J* = 4.4 Hz), 2.67 (1H, dd, *J* = 2.2, 0.6 Hz).

¹³C NMR (100 MHz; CDCl₃) δ: 138.5, 134.4, 128.9, 128.1, 83.2, 75.3, 63.7.

FTIR ν_{max} (ATR, film)/cm⁻¹ 3294, 2886, 2120, 1597, 1490, 1405, 1261, 1191, 1090, 1013, 944.



43d

Alkyne **43d** was prepared from thiophene-2-carboxaldehyde (500 mg, 416 μ L, 4.46 mmol), trimethylsilylacetylene (486 mg, 686 μ L, 4.95 mmol), *n*-BuLi (1.6 M in hexane, 2.96 ml, 4.73 mmol) and THF (13 ml) according to General Procedure A. The crude product was purified by flash column chromatography (SiO₂; EtOAc:hexanes = 1:19 \rightarrow 1:5 \rightarrow 1:2) to afford pure **43d** (527 mg, 86% yield) as orange oil.

R_f = 0.32 (EtOAc:hexanes = 1:5)

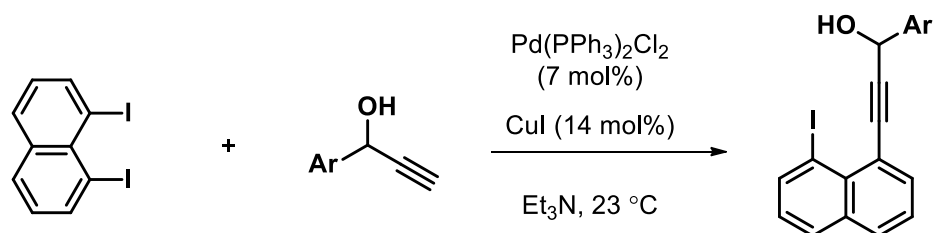
TLC Visualization: UV active; stains with KMnO₄ solution.

¹H NMR (400 MHz; CDCl₃) δ: 7.31-7.30 (1H, m), 7.18 (1H, app d, *J* = 3.5 Hz), 6.98 (1H, dd, *J* = 5.1, 3.5 Hz), 5.63 (1H, dd, *J* = 6.5, 1.8 Hz), 3.05 (1H, br s), 2.68 (1H, d, *J* = 2.2 Hz).

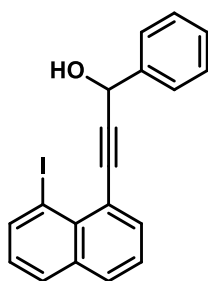
¹³C NMR (100 MHz; CDCl₃) δ: 143.9, 126.8, 126.3, 125.9, 82.9, 74.4, 60.0.

FTIR ν_{max} (ATR, film)/cm⁻¹ 3286, 1261, 1229, 1009, 917.

3.3.2. General Procedure B for the Sonogashira reaction between alkynes and 1,8-diiodonaphthalene



To a solution of alkyne (1.0 equiv.) and 1,8-diiodonaphthalene (4 equiv.) in Et₃N (0.03 M), Pd(PPh₃)₂Cl₂ (0.07 equiv.) and CuI (0.14 equiv.) were added at 23 °C under N₂. The resulting reaction mixture stirred at 23 °C until TLC showed full consumption of alkyne. Usually, a color change from yellow to orange was observed. Et₃N was removed under reduced pressure. The remaining residue was dissolved in a sufficient amount of EtOAc or CH₂Cl₂ and washed once with H₂O. The organic phase was dried over anhydrous Na₂SO₄, and concentrated under reduced pressure. The residue was purified by column chromatography



46a

Sonogashira coupling product **46a** prepared from 1,8-diiodonaphthalene (350 mg, 0.92 mmol), alkyne **43a** (30.5 mg, 0.23 mmol), Pd(PPh₃)₂Cl₂ (11.2 mg, 0.016

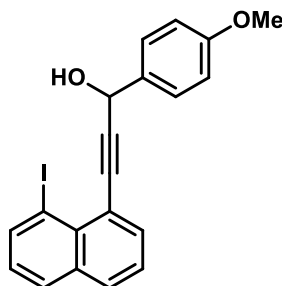
mmol), CuI (6.2 mg, 0.032 mmol) and Et₃N (6 mL) according to General Procedure B. The crude product was purified by flash column chromatography (SiO₂; EtOAc:hexanes = 1:5) to afford pure **46a** (50 mg, 56% yield) as orange oil. After column chromatography unreacted 1,8-diiodonaphthalene (287 mg, 82%) was recovered.

TLC Visualization: UV active; stains with KMnO₄ solution.

¹H NMR (400 MHz; CDCl₃) δ: 8.26 (1H, dd, *J* = 7.4, 1.3 Hz), 7.86 (1H, dd, *J* = 7.2, 1.4 Hz), 7.82 (1H, dd, *J* = 4.3, 1.2 Hz), 7.80 (1H, dd, *J* = 4.5, 1.3 Hz), 7.70-7.66 (2H, m), 7.45-7.33 (4H, m), 7.09 (1H, dd, *J* = 8.0, 7.5 Hz), 5.81 (1H, d, *J* = 5.3 Hz), 2.46 (1H, d, *J* = 5.8 Hz).

¹³C NMR (100 MHz; CDCl₃) δ: 142.9, 140.2, 136.5, 135.0, 132.1, 130.9, 130.3, 128.8, 128.5, 127.3, 127.2, 125.5, 122.0, 100.0, 92.9, 86.4, 66.1.

FTIR ν_{max} (ATR, film)/cm⁻¹ 3371, 2918, 2850, 1553, 1493, 1453, 1362, 1196, 1047, 1036, 1002, 947, 817, 758, 717, 698.



46b

Sonogashira coupling product **46b** prepared from 1,8-diiodonaphthalene (291 mg, 0.76 mmol), alkyne **43b** (31 mg, 0.19 mmol), Pd(PPh₃)₂Cl₂ (9.4 mg, 0.013 mmol), CuI (5.1 mg, 0.026 mmol) and Et₃N (6 mL) according to General Procedure B. The crude product was purified by flash column chromatography (SiO₂; EtOAc:hexanes =

1:9 → 1:5) to afford pure **46b** (57 mg, 72% yield) as reddish orange oil. After column chromatography unreacted 1,8-diiodonaphthalene (209 mg, 72%) was recovered.

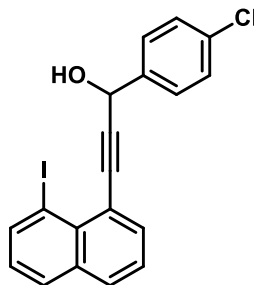
$R_f = 0.40$ (EtOAc:hexanes = 1:3)

TLC Visualization: UV active; stains with KMnO_4 solution.

^1H NMR (400 MHz; CDCl_3) δ : 8.24 (1H, dd, $J = 7.4, 1.2$ Hz), 7.84 (1H, dd, $J = 7.3, 1.4$ Hz), 7.82-7.75 (2H, m), 7.60 (2H, app d, $J = 8.6$ Hz), 7.38 (1H, dd, $J = 8.2, 7.3$ Hz), 7.07 (1H, dd, $J = 8.0, 7.5$ Hz), 5.76 (1H, s), 3.81 (3H, s), 2.65 (1H, br s).

^{13}C NMR (100 MHz; CDCl_3) δ : 159.8, 142.8, 136.4, 134.9, 132.6, 130.8, 130.2, 128.6, 128.4, 127.2, 125.4, 122.1, 114.1, 100.3, 92.9, 86.04, 65.6, 55.5.

FTIR ν_{max} (ATR, film)/ cm^{-1} 3399 (br), 1610, 1510, 1362, 1303, 1248, 1172, 1034.



46c

Sonogashira coupling product **46c** prepared from 1,8-diiodonaphthalene (328 mg, 0.86 mmol), alkyne **43c** (36 mg, 0.22 mmol), $\text{Pd}(\text{PPh}_3)_2\text{Cl}_2$ (10.5 mg, 0.015 mmol), CuI (5.7 mg, 0.030 mmol) and Et_3N (6 mL) according to General Procedure B. The crude product was purified by flash column chromatography (SiO_2 ; EtOAc:hexanes = 1:9 → 1:7 → 1:6 → 1:5) to afford pure **46c** (56 mg, 62% yield) as reddish orange oil.

After column chromatography unreacted 1,8-diiodonaphthalene (240 mg, 73%) was recovered.

M.P. 109.3-109.6 °C (CHCl₃)

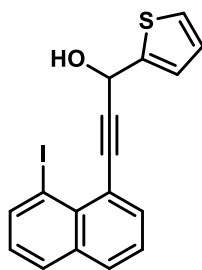
R_f = 0.42 (EtOAc:hexanes = 1:4)

TLC Visualization: UV active; stains with KMnO₄ solution.

¹H NMR (400 MHz; CDCl₃) δ: 8.25 (1H, dd, *J* = 7.4, 1.2 Hz), 7.84-7.78 (3H, m), 7.61-7.58 (2H, m), 7.41-7.35 (3H, m), 7.08 (1H, t, *J* = 7.8 Hz), 5.78 (1H, s), 2.72 (1H, br s).

¹³C NMR (100 MHz; CDCl₃) δ: 142.9, 138.7, 136.5, 134.9, 134.2, 132.0, 131.1, 130.3, 128.8, 128.5, 127.3, 125.5, 121.7, 99.5, 92.8, 86.6, 65.3.

FTIR ν_{max} (ATR, film)/cm⁻¹ 3365 (br), 1553, 1489, 1405, 1362, 1197, 1089, 1048, 1036, 1014.



46d

Sonogashira coupling product **46d** prepared from 1,8-diiodonaphthalene (308 mg, 0.81 mmol), alkyne **43d** (28 mg, 0.20 mmol), Pd(PPh₃)₂Cl₂ (10.0 mg, 0.014 mmol), CuI (5.4 mg, 0.028 mmol) and Et₃N (6 mL) according to General Procedure B. The crude product was purified by flash column chromatography (SiO₂; EtOAc:hexanes =

1:9 → 1:5) to afford pure **46d** (64.5 mg, 82% yield) as reddish orange oil. After column chromatography unreacted 1,8-diiodonaphthalene (223 mg, 72%) was recovered.

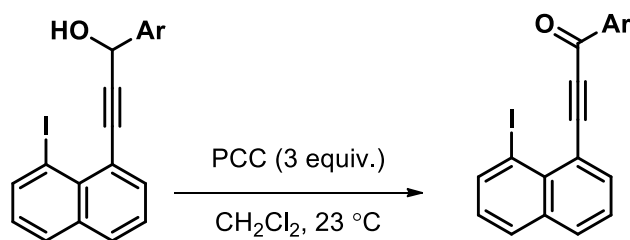
$R_f = 0.44$ (EtOAc:hexanes = 1:5)

TLC Visualization: UV active; stains with KMnO_4 solution.

^1H NMR (400 MHz; CDCl_3) δ : 8.25 (1H, dd, $J = 7.4, 1.3$ Hz), 7.87 (1H, dd, 7.2, 1.4 Hz), 7.81-7.79 (2H, m), 7.40 (1H, dd, $J = 8.1, 7.3$ Hz), 7.33 (1H, dd, $J = 5.1, 1.3$ Hz), 7.31 (1H, dt, $J = 3.5, 1.0$ Hz), 7.08 (1H, t, $J = 7.8$ Hz), 7.01 (1H, dd, $J = 5.0, 3.6$ Hz), 6.02 (1H, d, $J = 6.5$ Hz), 2.77 (1H, d, $J = 6.5$ Hz).

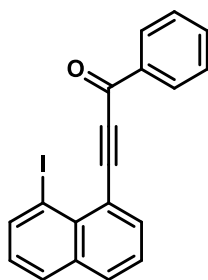
^{13}C NMR (100 MHz; CDCl_3) δ : 144.3, 142.8, 136.6, 134.9, 132.1, 131.1, 130.3, 127.3, 126.9, 126.1, 125.9, 125.5, 121.7, 99.3, 92.9, 85.8, 61.8.

FTIR ν_{max} (ATR, film)/ cm^{-1} 3367, 1553, 1363, 1227, 1199, 1047, 1034, 997, 939.



3.3.3. General Procedure C for the oxidation of propargyl alcohols with PCC

To a solution of propargyl alcohol in CH_2Cl_2 (0.01 M), PCC (3 equiv.) was added at 23 °C to give a dark red reaction mixture. The progress of the reaction was monitored by TLC which indicated full consumption of alcohol in 2-3 hours. Reaction mixture diluted with CH_2Cl_2 and filtered. SiO_2 was added to the resulting solution and the solvent was removed under reduced pressure and obtained solid loaded directly to the column. Purification by column chromatography on SiO_2 gave pure desired ketone.



47a

Propargyl alcohol **46a** (25 mg, 0.065 mmol) was dissolved in 2.0 ml anhydrous CH_2Cl_2 at 23 °C. To this solution *i*-Pr₂Net (63 mg, 85 μL , 0.49 mmol) and DMSO (0.10 mL, 1.4 mmol) were added. The resulting reaction mixture was cooled down to 0 °C in an ice bath and stirred for 10 minutes. After that $\text{SO}_3 \cdot \text{pyridine}$ (41.4 mg, 0.26 mmol) was added. After 10 minutes of stirring at 0 °C, a saturated aqueous solution of NaHCO_3 (5 ml) was added and stirred for 5 minutes. The reaction mixture was then diluted with H_2O and EtOAc. The aqueous phase was extracted with EtOAc. The combined organic phase was dried over anhydrous Na_2SO_4 . After filtration, the clear solution was concentrated under reduced pressure. The crude product was purified by flash column chromatography (SiO_2 ; EtOAc:hexanes = 1:19) to afford pure **47a** (14.2 mg, 57% yield) as yellow oil.

$R_f = 0.23$ (EtOAc:hexanes = 1:19)

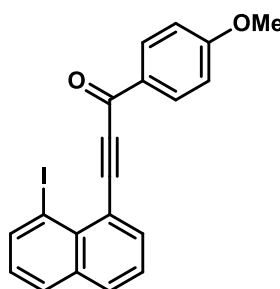
TLC Visualization: UV active; stains with KMnO_4 solution.

^1H NMR (400 MHz; CDCl_3) δ : 8.32 (3H, app d, $J = 7.4$ Hz), 8.10 (1H, dd, $J = 7.2, 1.3$ Hz), 7.94 (1H, dd, $J = 8.2, 0.9$ Hz), 7.89 (1H, dd, $J = 8.1, 0.8$ Hz), 7.64 (1H, tt, $J = 7.4, 1.3$ Hz), 7.57-7.48 (3H, m), 7.18 (1H, dd, $J = 8.0, 7.5$ Hz)

^{13}C NMR (100 MHz; CDCl_3) δ : 178.1, 143.3, 138.6, 137.1, 135.1, 134.2, 133.0, 132.8, 130.4, 130.0, 128.8, 127.8, 125.6, 120.3, 99.2, 93.1, 92.5.

FTIR ν_{max} (ATR, film)/ cm^{-1} 2174, 1632, 1597, 1578, 1449, 1363, 1339, 1313, 1286, 1226, 1170, 1046, 979, 817, 756, 698.

HRMS (ESI+) Calcd for $\text{C}_{19}\text{H}_{12}\text{IO}$ $[\text{M}+\text{H}]^+$: 382.9927, found: 382.9927.



47b

Compound **47b** was obtained from alcohol **46b** (55 mg, 0.13 mmol), PCC (75 mg, 0.35 mmol) and CH_2Cl_2 (3 mL) according to General Procedure C. The crude product was purified by flash column chromatography (SiO_2 ; EtOAc:hexanes = 1:5 \rightarrow 1:3) to afford pure **47b** (34.3 mg, 63% yield) as orange oil.

R_f = 0.53 (EtOAc:hexanes = 1:3)

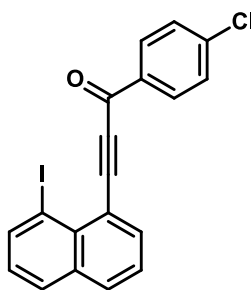
TLC Visualization: UV active; stains with KMnO_4 solution.

^1H NMR (400 MHz; CDCl_3) δ : 8.31-8.27 (3H, m), 8.06 (1H, dd, J = 7.3, 1.4 Hz), 7.91 (1H, dd, J = 8.2, 1.1 Hz), 7.86 (1H, dd, J = 8.2, 1.2 Hz), 7.48 (1H, dd, J = 8.1, 7.3 Hz), 7.15 (1H, dd, J = 8.1, 7.4 Hz), 6.99 (2H, app d, J = 9.0 Hz), 3.90 (3H, s).

¹³C NMR (100 MHz; CDCl₃) δ: 176.6, 164.5, 143.0, 138.3, 134.9, 132.6, 132.5, 132.2, 130.4, 130.2, 127.6, 125.4, 120.3, 113.9, 99.1, 93.0, 91.6, 55.6.

FTIR ν_{\max} (ATR, film)/cm⁻¹ 2174, 1627, 1596, 1572, 1508, 1290, 1258, 1235, 1162, 1028.

HRMS (ESI+) Calcd for C₂₀H₁₄IO₂ [M+H]⁺: 413.0033, found: 413.0041.



47c

Compound **47c** was obtained from alcohol **46c** (53 mg, 0.13 mmol), PCC (82 mg, 0.38 mmol) and CH₂Cl₂ (8 mL) according to General Procedure C. The crude product was purified by flash column chromatography (SiO₂; EtOAc:hexanes = 1:9 → 1:4) to afford pure **47c** (23 mg, 44% yield) as bright orange solid.

R_f = 0.36 (EtOAc:hexanes = 1:9)

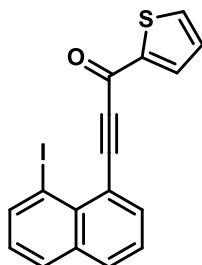
TLC Visualization: UV active; stains with KMnO₄ solution.

¹H NMR (400 MHz; CDCl₃) δ: 8.31 (1H, dd, J = 7.4, 1.2 Hz), 8.27-8.23 (2H, m), 8.08 (1H, dd, J = 7.2, 1.4 Hz), 7.95 (1H, dd, J = 8.2, 1.3 Hz), 7.88 (1H, dd, J = 8.2, 1.1 Hz), 7.52-7.48 (3H, m), 7.18 (1H, t, J = 7.8 Hz).

¹³C NMR (100 MHz; CDCl₃) δ: 176.7, 143.3, 141.8, 140.8, 138.7, 135.5, 135.1, 133.2, 131.3, 130.4, 129.2, 127.8, 125.6, 120.0, 98.8, 93.03, 93.01.

FTIR ν_{\max} (ATR, film)/ cm^{-1} 2175, 1634, 1586, 1363, 1339, 1287, 1224, 1167, 1090, 981.

HRMS (ESI+) Calcd for $\text{C}_{19}\text{H}_{10}^{35}\text{ClNaO}$ $[\text{M}+\text{Na}]^+$: 438.9357, found: 438.9357.



47d

Compound **47d** was obtained from alcohol **46d** (60 mg, 0.15 mmol), PCC (99 mg, 0.46 mmol) and CH_2Cl_2 (10 mL) according to General Procedure C. The crude product was purified by flash column chromatography (SiO_2 ; EtOAc:hexanes = 1:9 \rightarrow 1:5) to afford pure **47d** (29.1 mg, 49% yield) as a bright orangish-yellow oil.

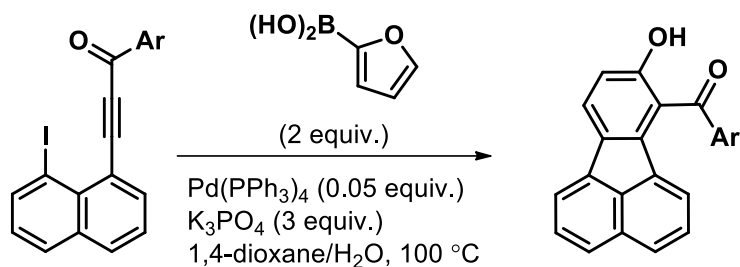
R_f = 0.41 (EtOAc:hexanes = 1:7)

TLC Visualization: UV active; stains with KMnO_4 solution.

^1H NMR (400 MHz; CDCl_3) δ : 8.30 (1H, d, J = 7.3 Hz), 8.16 (1H, dd, J = 3.8, 1.2 Hz), 8.05 (1H, dd, J = 7.2, 0.9 Hz), 7.92 (1H, dd, J = 8.2, 1.3 Hz), 7.87 (1H, dd, J = 8.1, 1.1 Hz), 7.73 (1H, dd, J = 5.0, 1.2 Hz), 7.48 (1H, t, J = 7.7 Hz), 7.21-7.14 (2H, m).

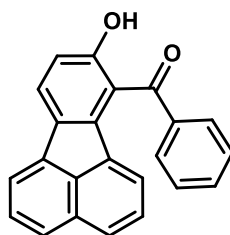
^{13}C NMR (100 MHz; CDCl_3) δ : 169.9, 145.1, 143.2, 138.7, 135.5, 135.2, 135.0, 133.0, 132.7, 130.4, 128.5, 127.8, 125.6, 120.0, 98.6, 93.1, 91.1

FTIR ν_{\max} (ATR, film)/ cm^{-1} 2178, 1610, 1514, 1410, 1363, 1301, 1231, 1051, 949.



3.3.4. General Procedure D for the syntheses of Fluoranthenes.

To a 25 ml, round-bottomed flask alkyne **47** (1.0 equiv.) was added and dissolved in 1.0 ml 1,4-dioxane at 23 °C under N₂. To this solution 2-furanylboronic acid (2.0 equiv.), K₃PO₄ (3.0 equiv.) and Pd(PPh₃)₄ (0.05 equiv) were added. After that 1.0 ml 1,4-dioxane and 1.0 ml H₂O were added along the walls. The resulting reaction mixture was heated to 100 °C under stirred under reflux for 3-6 hours. The reaction mixture was cooled to 23 °C and before the addition of H₂O (5 ml). The aqueous phase was extracted with EtOAc (3×10 mL). The combined organic phase was dried over anhydrous Na₂SO₄, filtered and concentrated under reduced pressure. The residue was purified by column chromatography on SiO₂.



48a

Fluoranthene derivative **48a** was synthesized from alkyne **47a** (18.5 mg, 0.048 mmol), 2-furanylboronic acid (10.8 mg, 0.096 mmol), K₃PO₄ (30.8 mg, 0.145 mmol) and Pd(PPh₃)₄ (2.8 mg, 0.0024 mmol) according to General Procedure D. The crude product

was purified by flash column chromatography (SiO₂; EtOAc:hexanes = 1:9 → 1:9 → 1:4) to afford pure **48a** (14.4 mg, 92% yield) as greenish yellow amorphous solid.

$R_f = 0.52$ (EtOAc:hexanes = 1:2)

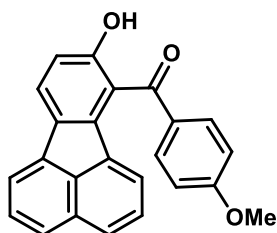
TLC Visualization: UV active under 254 ve 366 nm; stains with KMnO₄ solution.

¹H NMR (400 MHz; CDCl₃) δ : 8.83 (1H, s), 7.98 (3 H, app t, $J = 7.0$ Hz), 7.88 (1H, d, $J = 7.0$ Hz), 7.76 (1H, d, $J = 8.2$ Hz), 7.69 (1H, d, $J = 8.1$ Hz), 7.63-7.54 (2H, m), 7.39 (2H, t, $J = 7.8$ Hz), 7.17 (1H, t, $J = 7.7$ Hz), 7.09 (1H, d, $J = 8.6$ Hz), 6.78 (1H, d, $J = 7.2$ Hz).

¹³C NMR (100 MHz; CDCl₃) δ : 199.3, 158.0, 139.4, 138.3, 135.9, 135.7, 134.1, 132.54, 132.52, 130.7, 129.9, 129.0, 128.0, 127.7, 127.5, 126.4, 126.3, 126.1, 125.7, 119.5, 116.5.

FTIR ν_{\max} (ATR, film)/cm⁻¹ 3359, 1653, 1581, 1449, 1440, 1395, 1316, 1286, 1226, 815, 773.

HRMS (ESI-) Calcd for C₂₃H₁₃O₂ [M-H]⁻: 321.0921, found: 321.0918.



48b

Fluoranthene derivative **48b** was synthesized from alkyne **47b** (28.5 mg, 0.070 mmol), 2-furanylboronic acid (15.5 mg, 0.14 mmol), K₃PO₄ (44 mg, 0.21 mmol) and Pd(PPh₃)₄ (4.0 mg, 0.0035 mmol) according to General Procedure D. The crude product

was purified by flash column chromatography (SiO₂; EtOAc:hexanes = 1:9 → 1:1) to afford pure **48b** (17.8 mg, 73% yield) as brown oil.

R_f = 0.37 (EtOAc:hexanes = 1:2); 0.71 (EtOAc:hexanes = 1:1).

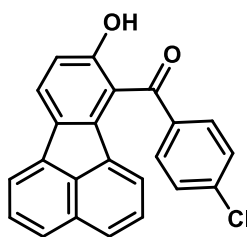
TLC Visualization: UV active under 254 ve 366 nm; stains with KMnO₄ solution.

¹H NMR (400 MHz; CDCl₃) δ: 8.47 (1H, s), 7.97-7.93 (3H, m), 7.87 (1H, d, J = 6.9 Hz), 7.75 (1H, d, J = 8.2 Hz), 7.70 (1H, d, J = 8.1 Hz), 7.60 (1H, dd, J = 8.0, 7.0 Hz), 7.24 (1H, t, J = 7.7 Hz), 7.06 (1H, d, J = 8.2 Hz), 6.92 (1H, d, J = 7.2 Hz), 6.85 (2H, d, J = 8.9 Hz), 3.83 (3H, s).

¹³C NMR (100 MHz; CDCl₃) δ: 197.3, 164.6, 157.3, 139.1, 136.0, 135.7, 133.1, 132.6, 132.4, 130.9, 128.0, 127.8, 127.3, 126.2, 125.9, 125.7, 120.1, 119.4, 116.3, 114.3, 114.1, 55.7.

FTIR ν_{\max} (ATR, film)/cm⁻¹ 3317 (br), 1643, 1594, 1439, 1262, 1159.

HRMS (ESI-) Calcd for C₂₄H₁₅O₃ [M-H]⁻: 351.1027, found: 351.1028.



48c

Fluoranthene derivative **48c** was synthesized from alkyne **47c** (20 mg, 0.048 mmol), 2-furanylboronic acid (10.7 mg, 0.096 mmol), K₃PO₄ (30.6 mg, 0.144 mmol) and Pd(PPh₃)₄ (2.8 mg, 0.0024 mmol) according to General Procedure D. The crude product

was purified by flash column chromatography (SiO₂; EtOAc:hexanes = 1:9 → 1:5) to afford pure **48c** (11.8 mg, 69% yield) as a brown oil.

$R_f = 0.53$ (EtOAc:hexanes = 1:2)

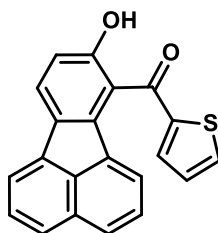
TLC Visualization: UV active under 254 ve 366 nm; stains with KMnO₄ solution.

¹H NMR (400 MHz; CDCl₃) δ : 8.53 (1H, s), 7.97 (1H, d, $J = 8.3$ Hz), 7.92-7.87 (3H, m), 7.77 (1H, d, $J = 8.2$ Hz), 7.73 (1H, d, $J = 8.1$ Hz), 7.61 (1H, dd, $J = 8.2, 6.9$ Hz), 7.38-7.35 (2H, m), 7.25 (1H, dd, $J = 8.1, 7.2$ Hz), 7.07 (1H, d, $J = 8.3$ Hz), 6.86 (1H, d, $J = 7.2$ Hz).

¹³C NMR (100 MHz; CDCl₃) δ : 197.7, 157.6, 140.6, 139.2, 136.5, 135.8, 135.4, 132.64, 132.55, 132.0, 131.9, 129.9, 129.4, 128.1, 127.73, 127.67, 126.5, 126.3, 125.9, 119.7, 116.5.

FTIR ν_{\max} (ATR, film)/cm⁻¹ 3361 (br), 1654, 1584, 1439, 1398, 1310, 1286, 1226, 1091.

HRMS (ESI-) Calcd for C₂₃H₁₂³⁵ClO₂ [M-H]⁻: 355.0531, found: 355.0532; Calcd for C₂₃H₁₂³⁷ClO₂ [M-H]⁻: 357.0502, found 357.0502.



48d

Fluoranthene derivative **48d** was synthesized from alkyne **47d** (17.0 mg, 0.044 mmol), 2-furanylboronicacid (9.9 mg, 0.088 mmol), K₃PO₄ (28 mg, 0.13 mmol) and Pd(PPh₃)₄ (2.5 mg, 0.0022 mmol) according to General Procedure D. The crude product

was purified by flash column chromatography (SiO₂; EtOAc:hexanes = 1:5 → 1:3) to afford pure **48d** (13.1 mg, 91% yield) as dark yellow solid.

$R_f = 0.48$ (EtOAc:hexanes = 1:2)

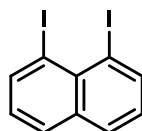
TLC Visualization: UV active under 254 ve 366 nm; stains with KMnO₄ solution.

¹H NMR (400 MHz; CDCl₃) δ : 7.99 (1H, br s), 7.94 (1H, d, $J = 8.1$ Hz), 7.87 (1H, d, $J = 6.9$ Hz), 7.76 (3H, m), 7.61 (2H, m), 7.32 (1H, dd, $J = 8.1, 7.2$ Hz), 7.14 (1H, d, $J = 7.1$ Hz), 7.05 (1H, d, $J = 8.1$ Hz), 6.95 (1H, dd, $J = 4.8, 3.9$ Hz).

¹³C NMR (100 MHz; CDCl₃) δ : 190.1, 156.4, 144.0, 138.9, 137.4, 136.0, 135.9, 135.7, 132.8, 132.6, 130.0, 128.7, 128.1, 127.8, 127.5, 126.4, 125.8, 125.5, 120.4, 119.6, 116.2.

FTIR ν_{\max} (ATR, film)/cm⁻¹ 3332 (br), 1625, 1582, 1509, 1453, 1439, 1408, 1396, 1379, 1354, 1309, 1288, 1228, 1210, 1055, 1039, 904.

HRMS (ESI-) Calcd for C₂₁H₁₁O₂S [M-H]⁻: 327.0485, found: 327.0486.



1,8-Diodonaphthalene (**45**). A 250 mL 3-neck round-bottomed flask was charged with 1,8-diaminonaphthalene (**44**) (1.00 g, 6.32 mmol) and cooled down to -15 °C in an ice/NaCl bath. Then it was dissolved in 11.6 mL 6.9 M H₂SO₄(aq). To this solution, NaNO₂ (1.308 g, 18.96 mmol, dissolved in 5 mL H₂O) was added dropwise resulting in the formation of a brown gas. Then, KI (6.029 g, 37.92 mmol, dissolved in 5 mL H₂O) was added dropwise at -15 °C. The resulting reaction mixture was heated quickly to 85 °C and stirred at this temperature for 45 minutes. Cooled to 23 °C and

neutralized with NaOH pellets. The resulting solid filtered off with suction and then extracted with DCM in a Soxhlet apparatus for 10 hours. The resulting extract was sequentially washed with 10 % HCl solution, saturated aqueous Na₂S₂O₃ solution and 1M NaOH solution. Then, the organic phase was dried over anhydrous Na₂SO₄, filtered and concentrated under reduced pressure. Purification by column chromatography (SiO₂; hexanes only) gave pure 1,8-diiodonaphthalene **45** (430 mg, 18% yield) as yellow solid.

$R_f = 0.41$ (Only hexanes)

TLC Visualization: UV active; stains with KMnO₄ solution.

¹H NMR (400 MHz; CDCl₃) δ : 8.39 (2H, d, $J = 7.3$ Hz), 7.79 (2H, d, $J = 8.0$ Hz), 7.03 (2H, t, $J = 7.7$ Hz).

¹³C NMR (100 MHz; CDCl₃) δ : 144.1, 135.8, 132.1, 131.1, 127.0, 96.2.

IR ν_{maks} (ATR, solid)/cm⁻¹: 3051, 2923, 2853, 1532, 1488, 1417.

HRMS (APCI+) Calcd for C₁₀H₆I₂ [M]⁺: 379.8554; found: 379.8562.

¹H and ¹³C spectra

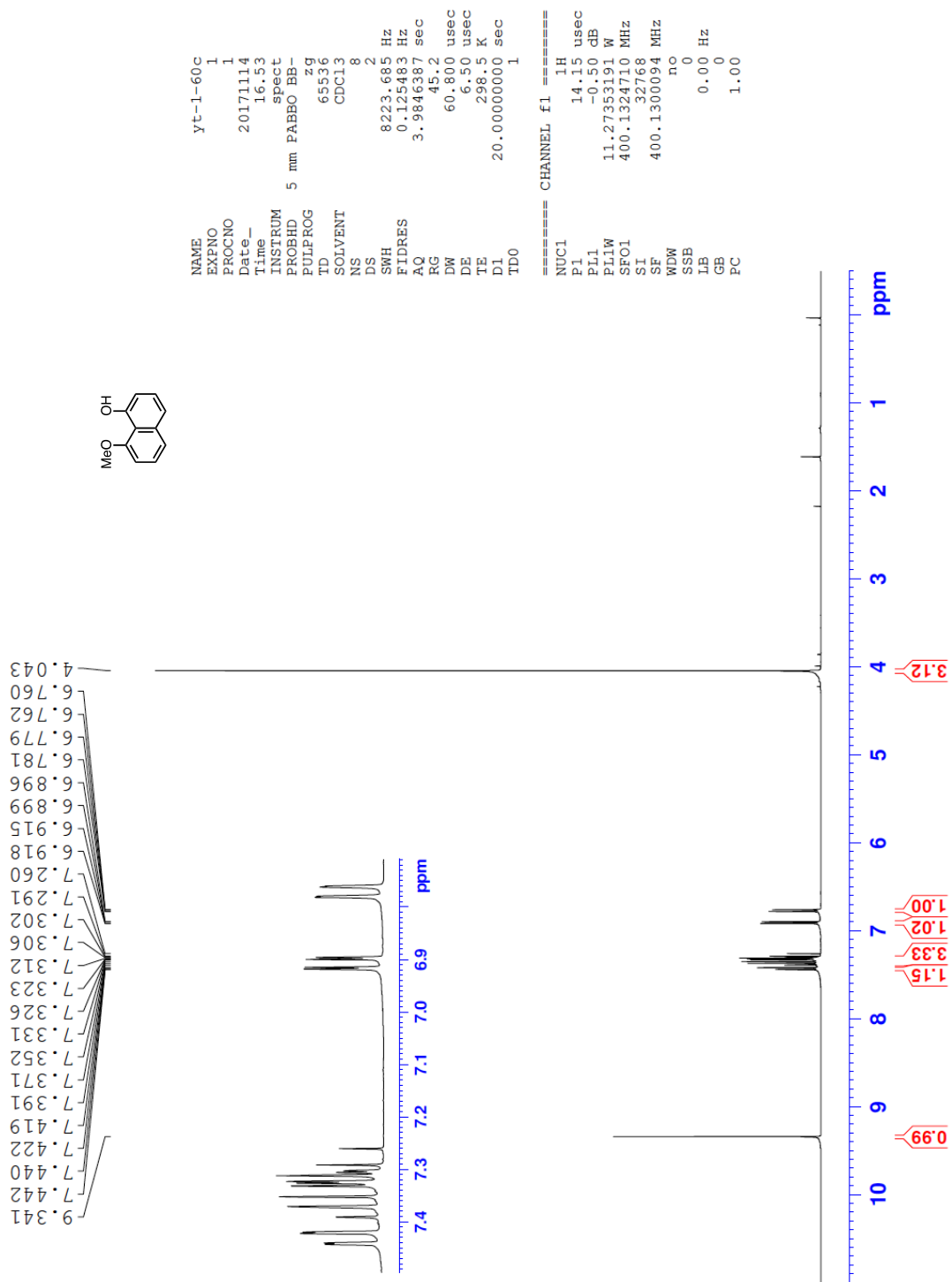


Figure 7. ¹H-NMR spectrum of **22** in CDCl₃.

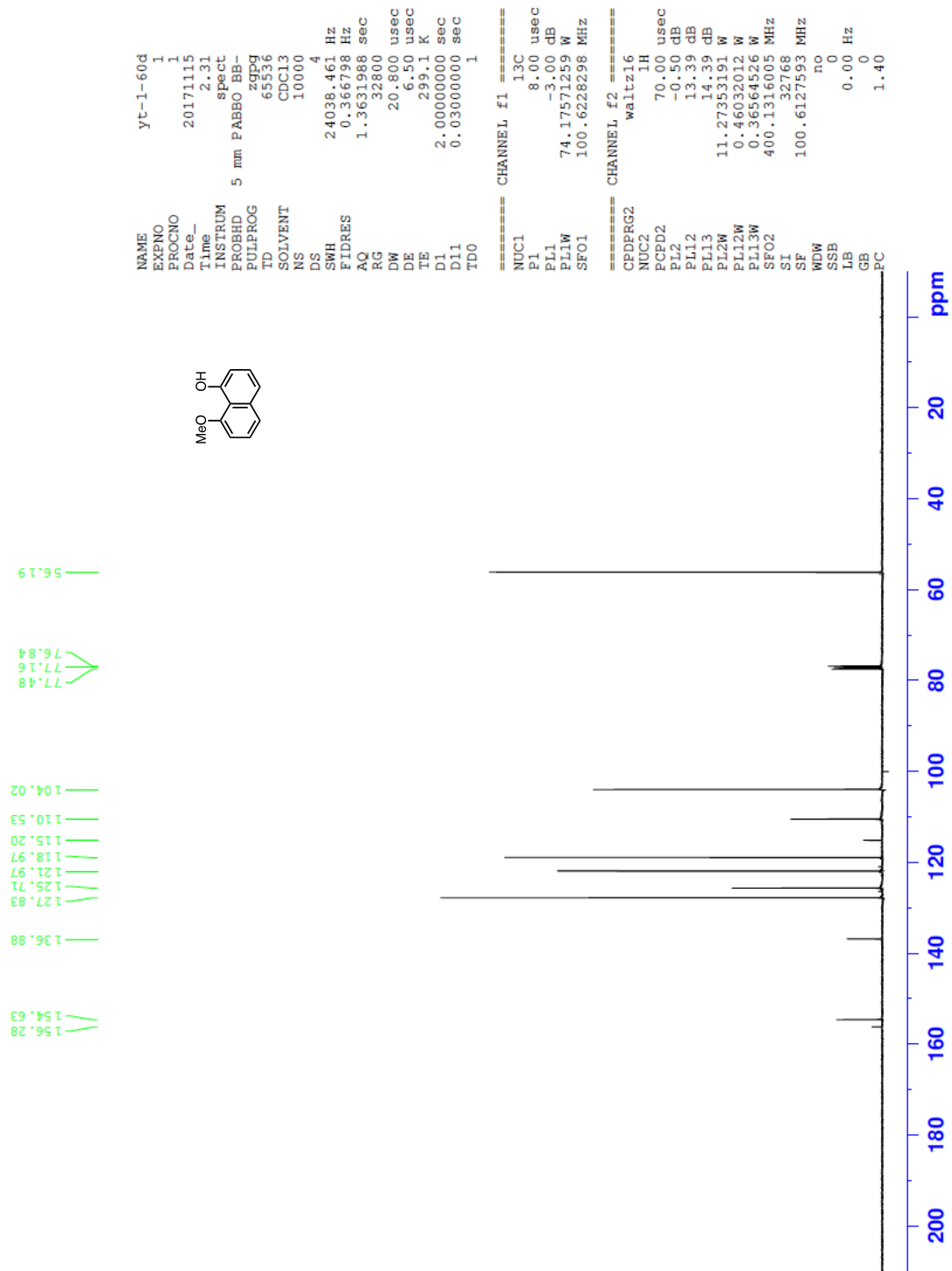


Figure 8. ^{13}C -NMR spectrum of **22** in CDCl_3 .

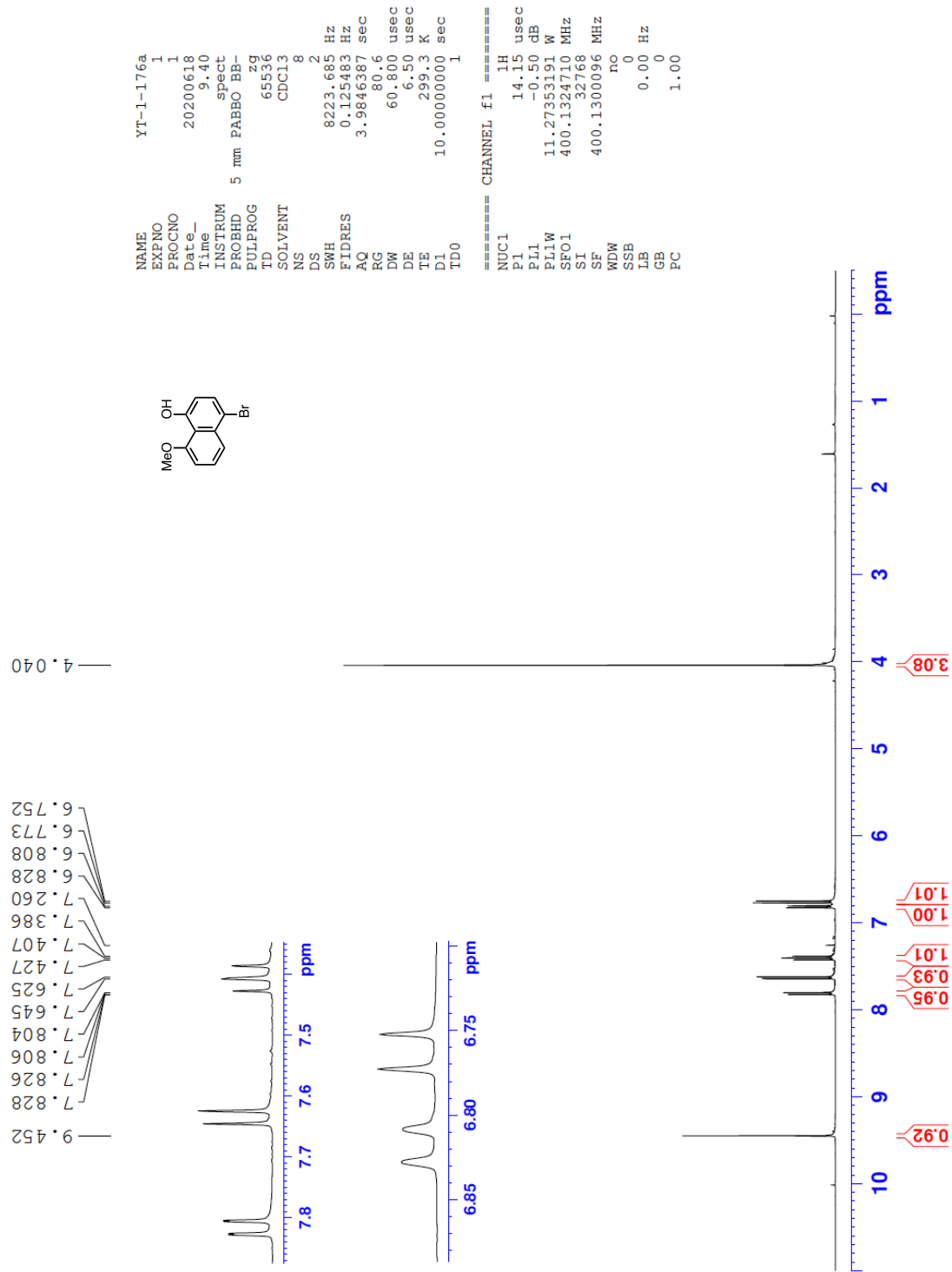


Figure 9. $^1\text{H-NMR}$ spectrum of **24** in CDCl_3 .

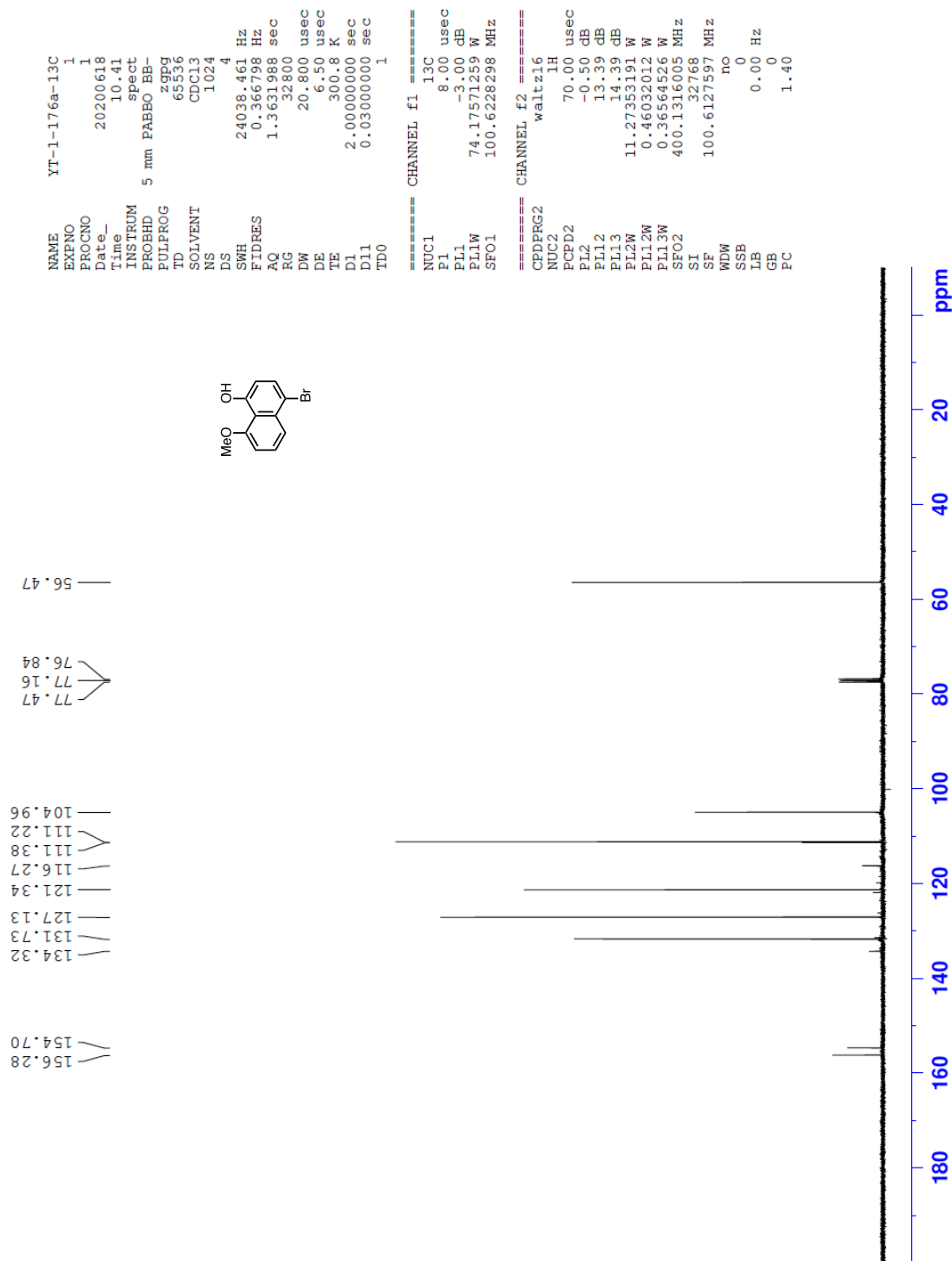


Figure 10. ^{13}C -NMR spectrum of **24** in CDCl_3 .

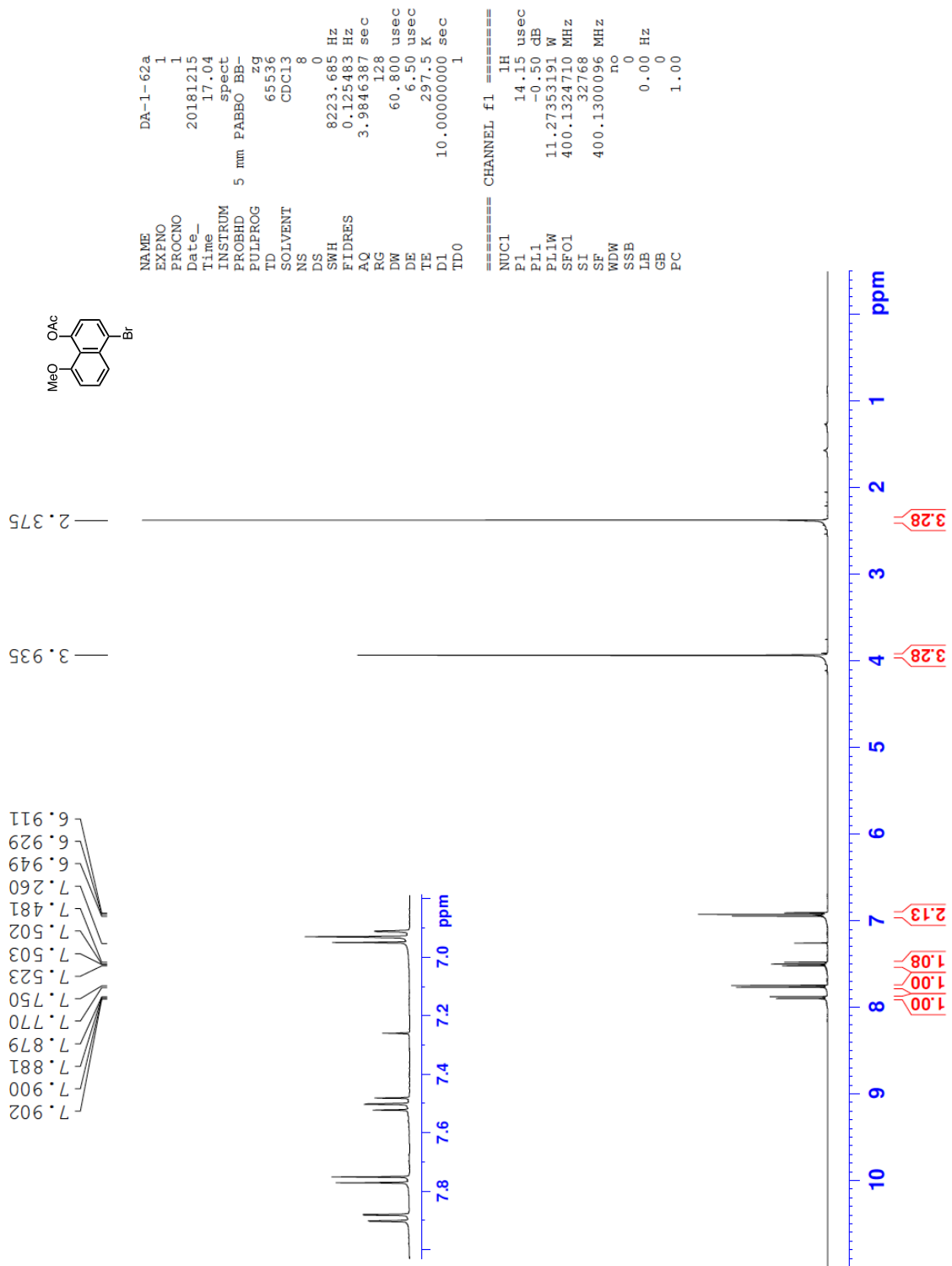


Figure 11. $^1\text{H-NMR}$ spectrum of **25** in CDCl_3 .

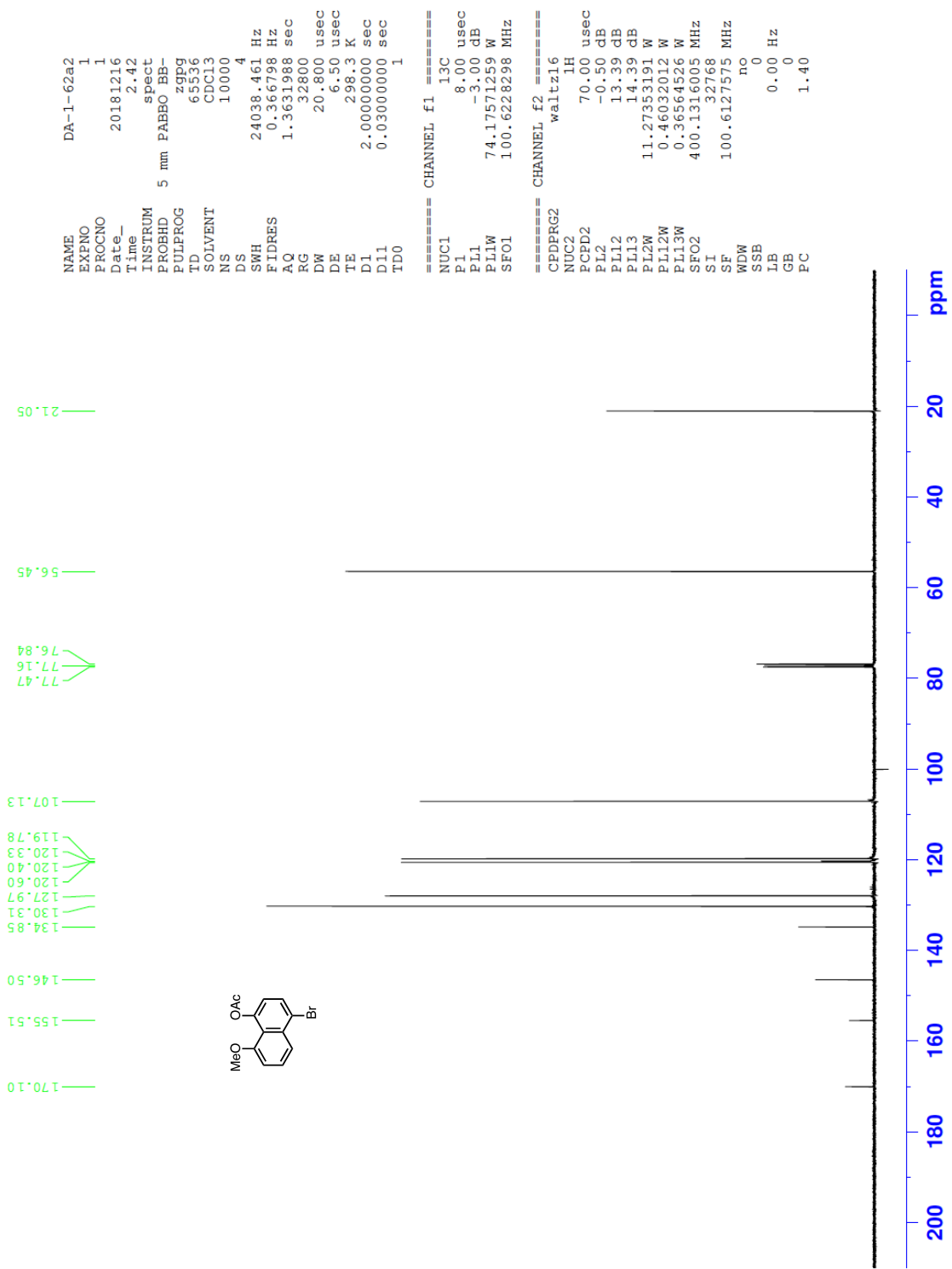


Figure 12. ^{13}C -NMR spectrum of **25** in CDCl_3 .

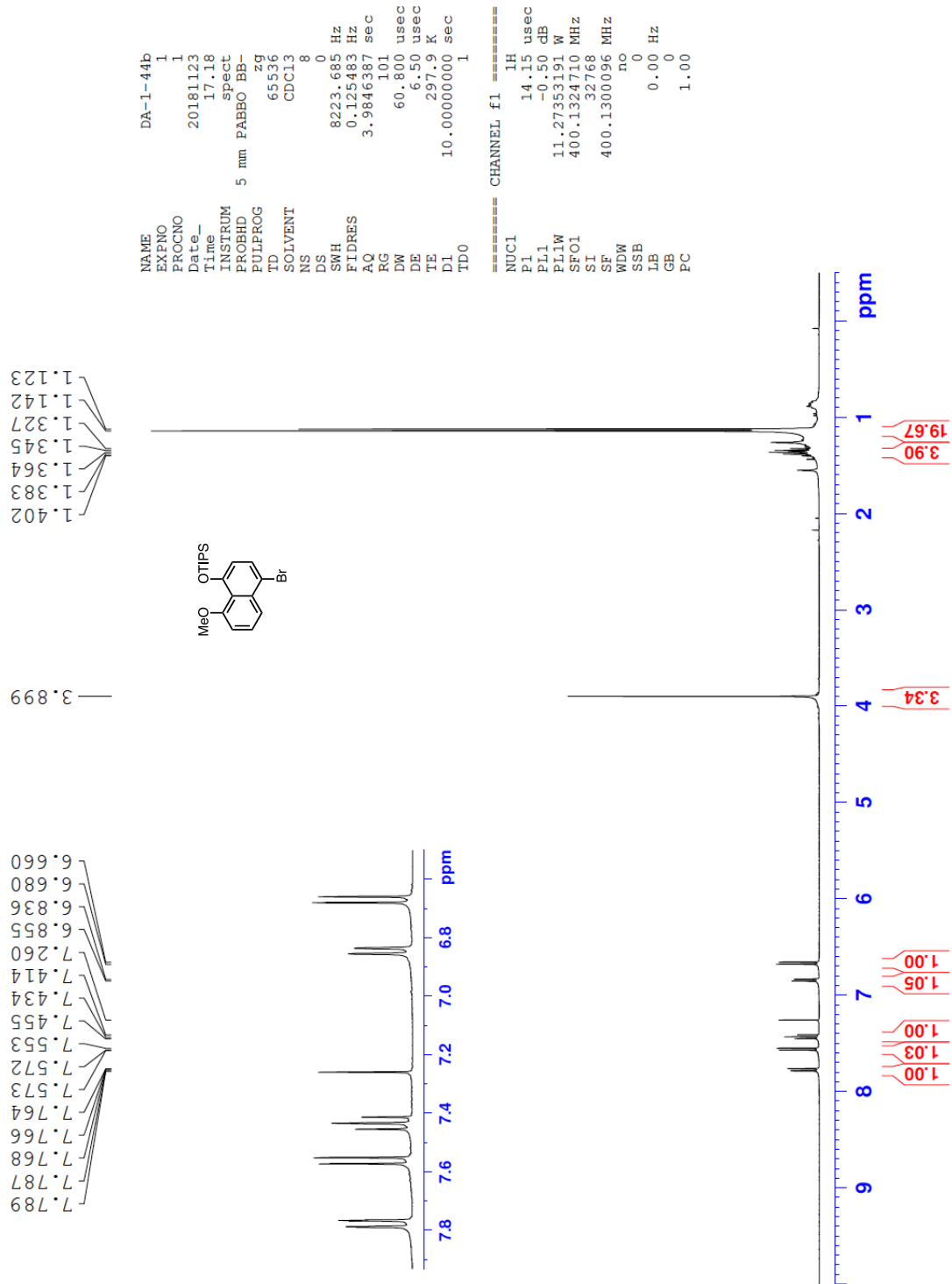


Figure 13. ¹H-NMR spectrum of **33** in CDCl₃.

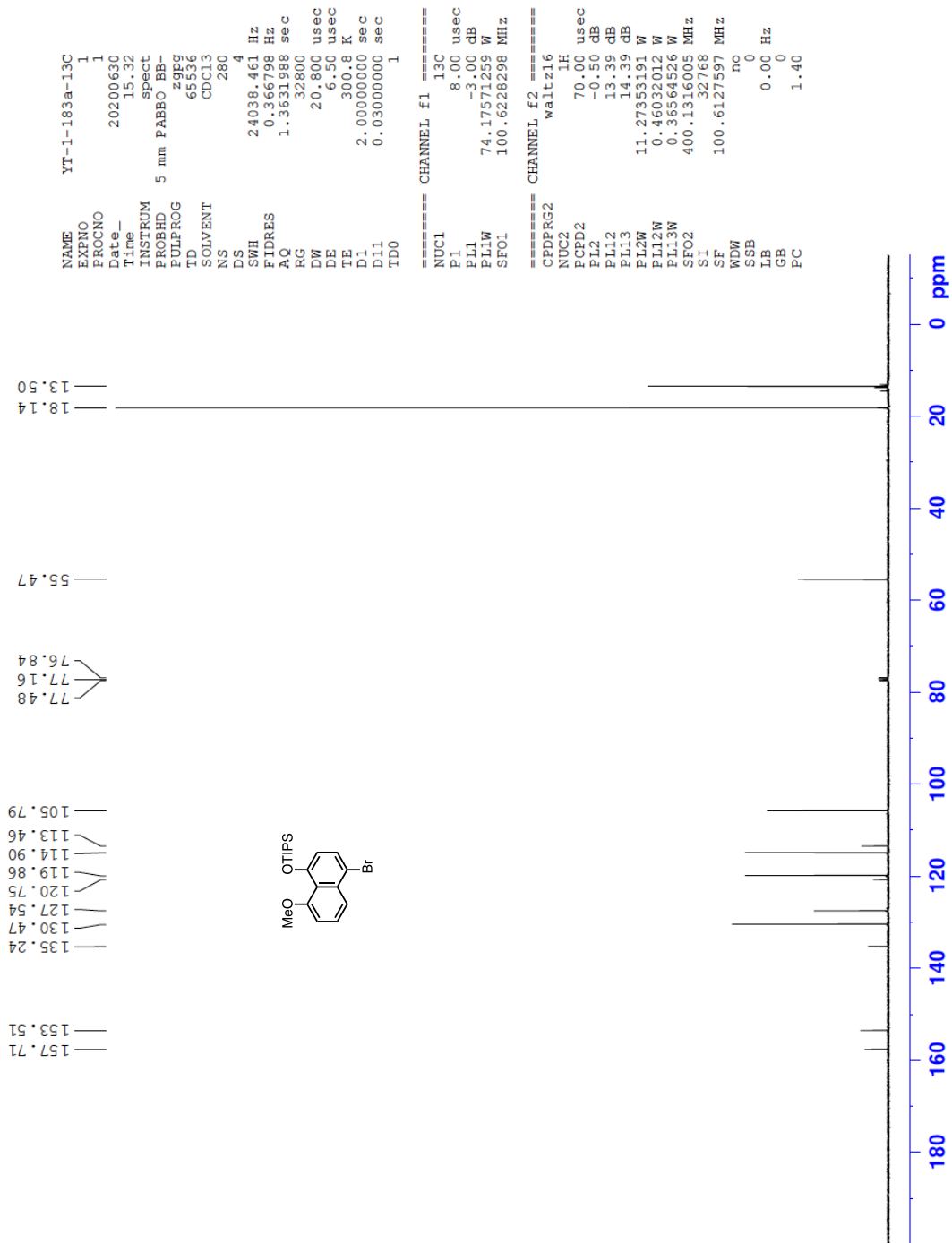


Figure 14. ^{13}C -NMR spectrum of **33** in CDCl_3 .

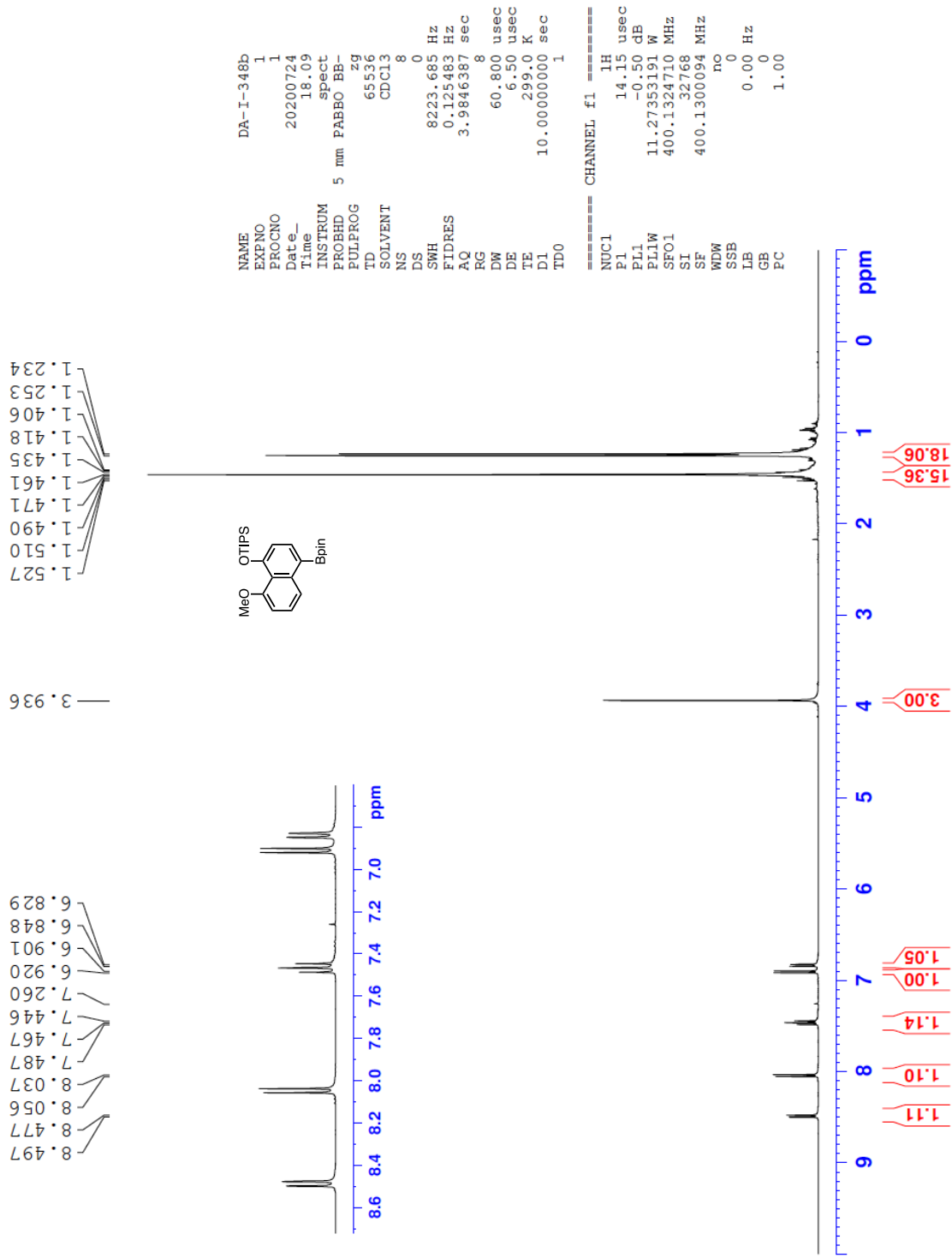


Figure 15. ¹H-NMR spectrum of **34** in CDCl₃.

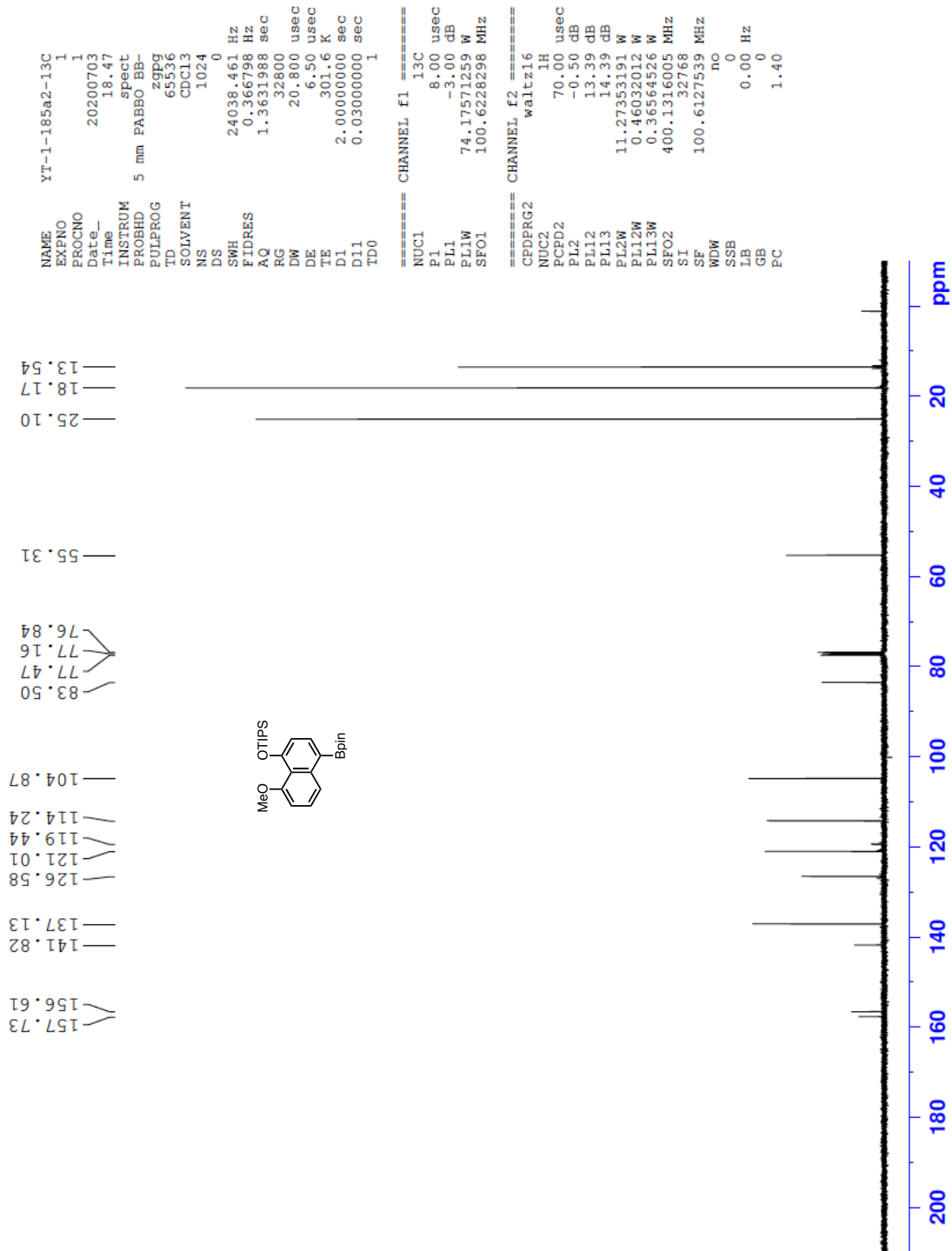


Figure 16. ^{13}C -NMR spectrum of **34** in CDCl_3 .

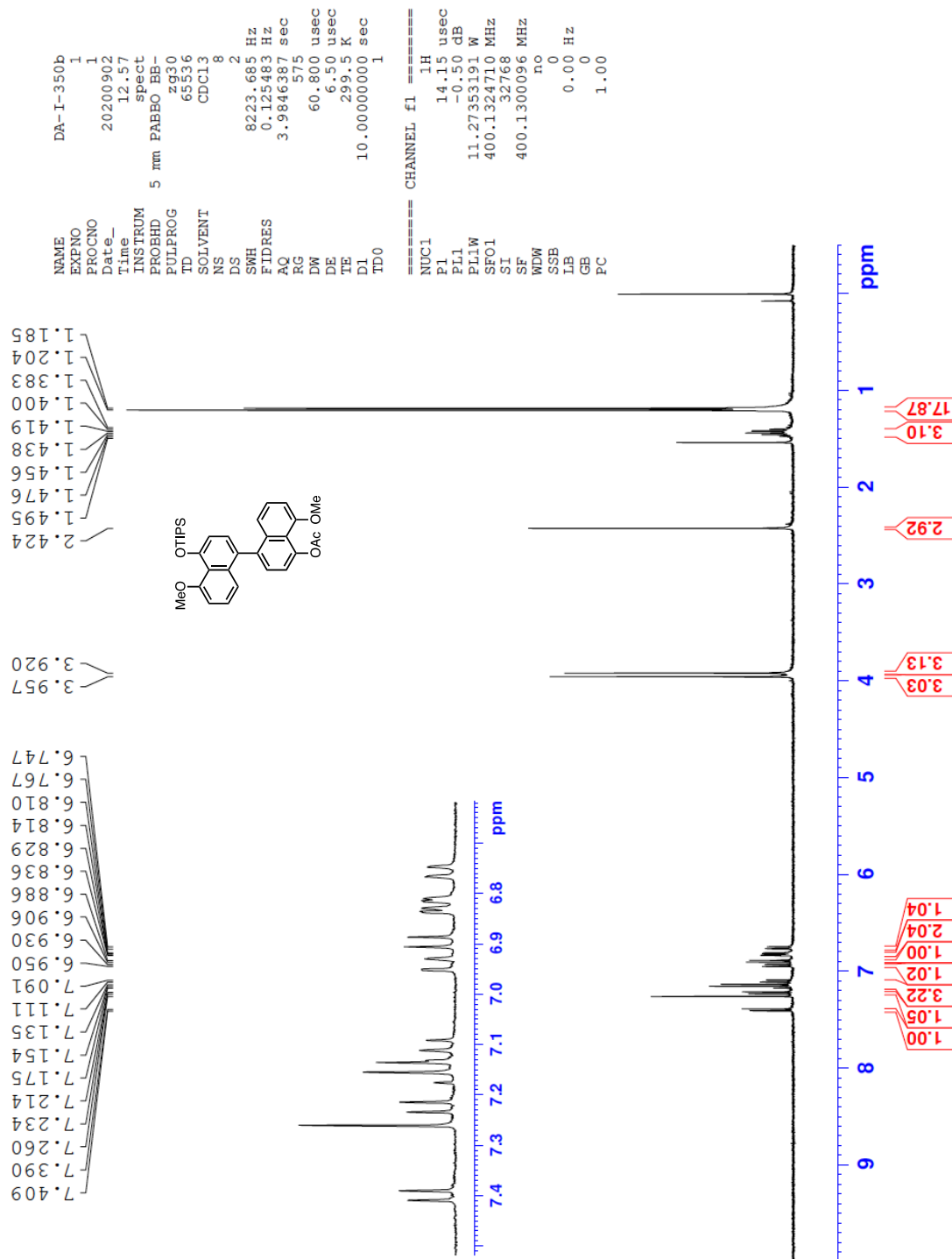


Figure 17. $^1\text{H-NMR}$ spectrum of **35** in CDCl_3 .

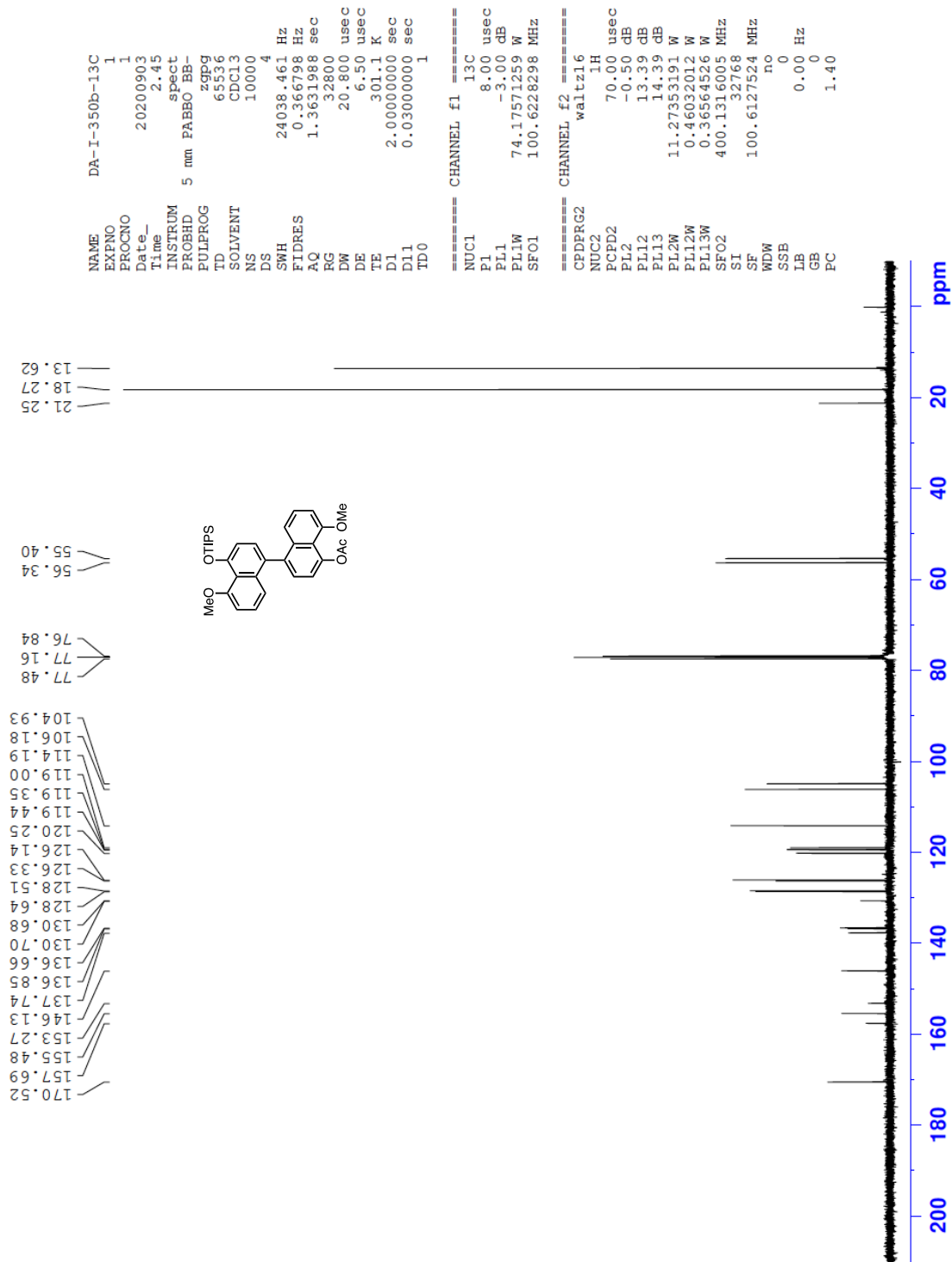


Figure 18. ^{13}C -NMR spectrum of **35** in CDCl_3 .

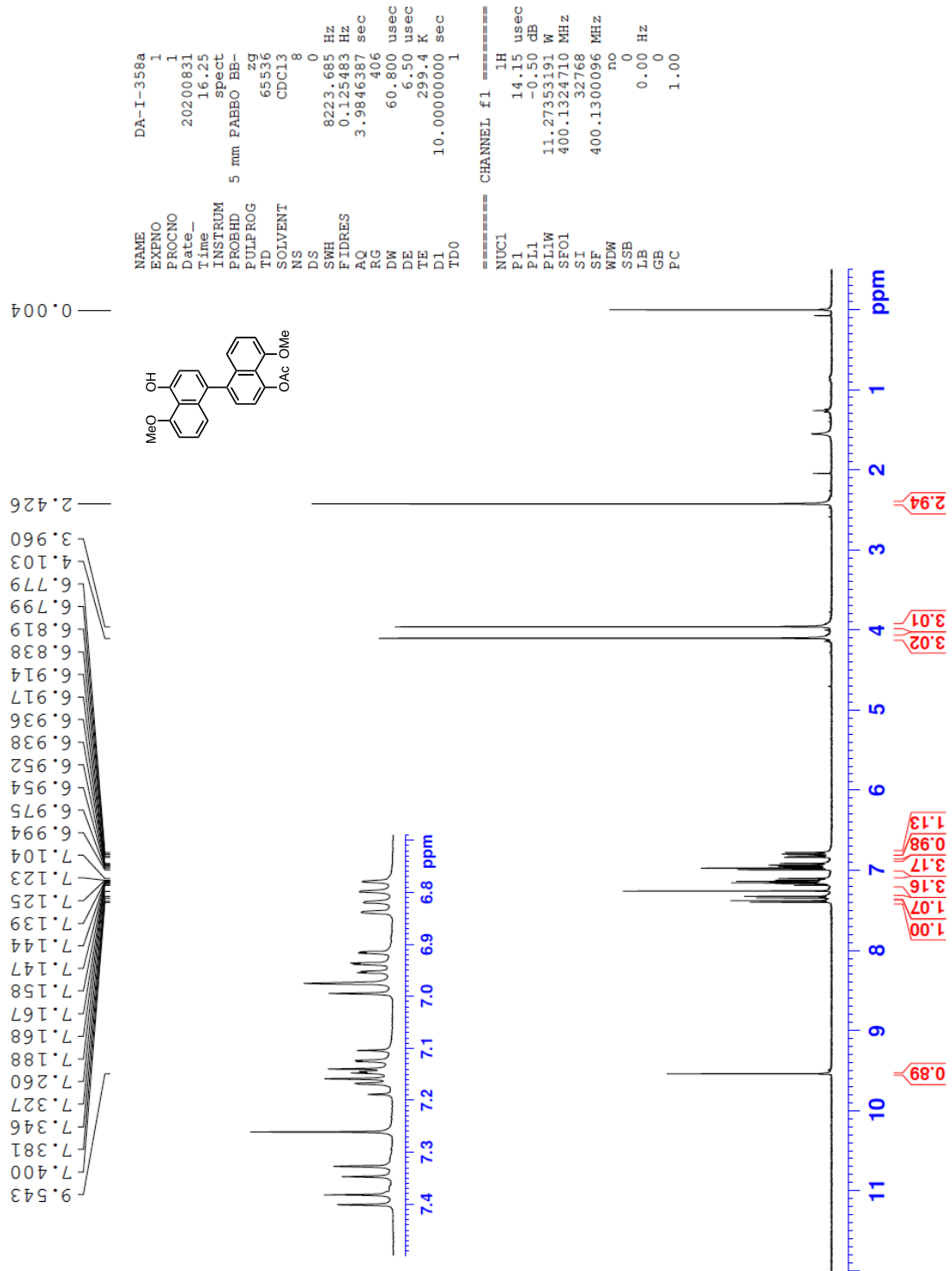


Figure 19. ¹H-NMR spectrum of **27** in CDCl₃.

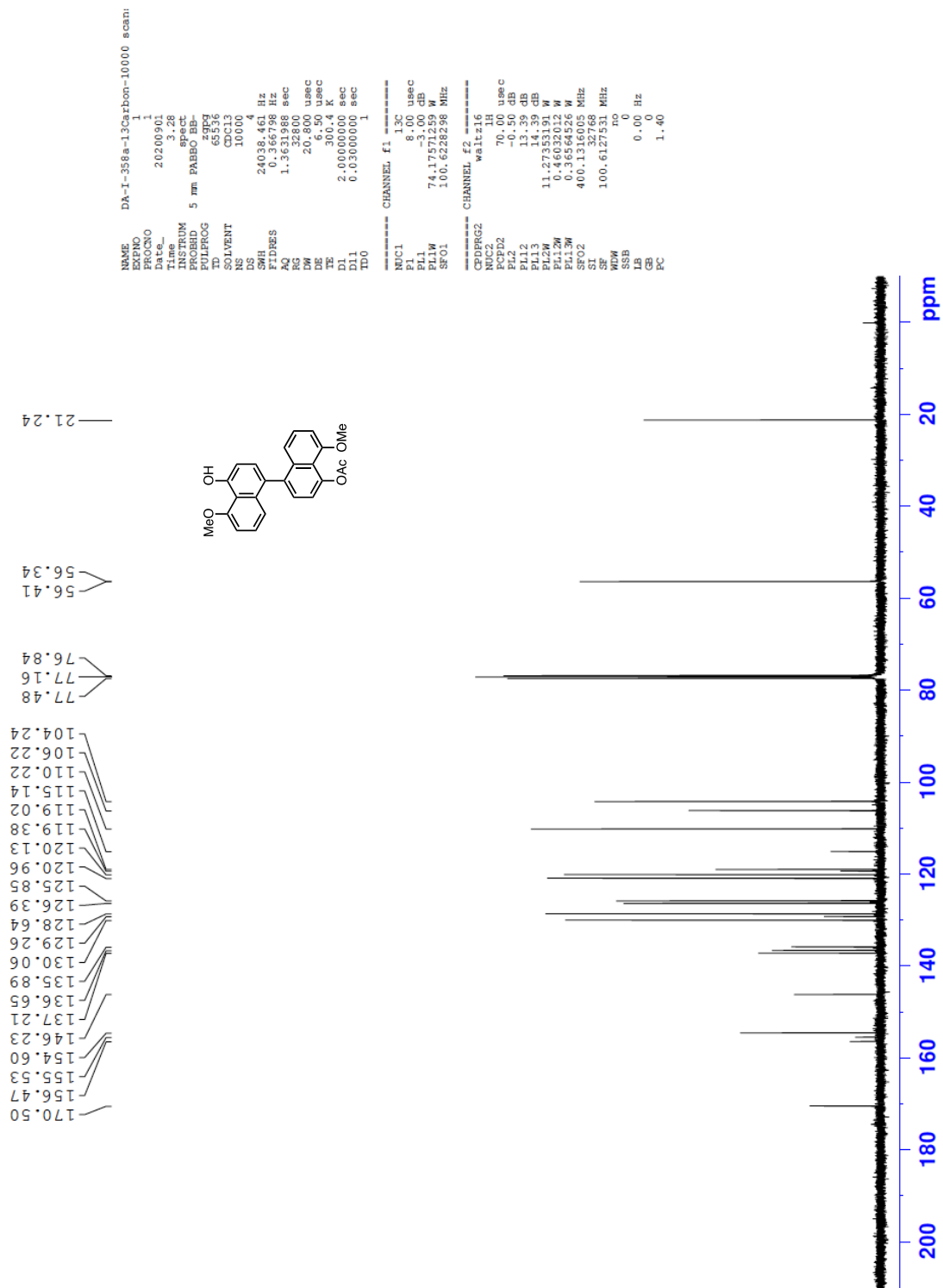


Figure 20. ^{13}C -NMR spectrum of **27** in CDCl_3 .

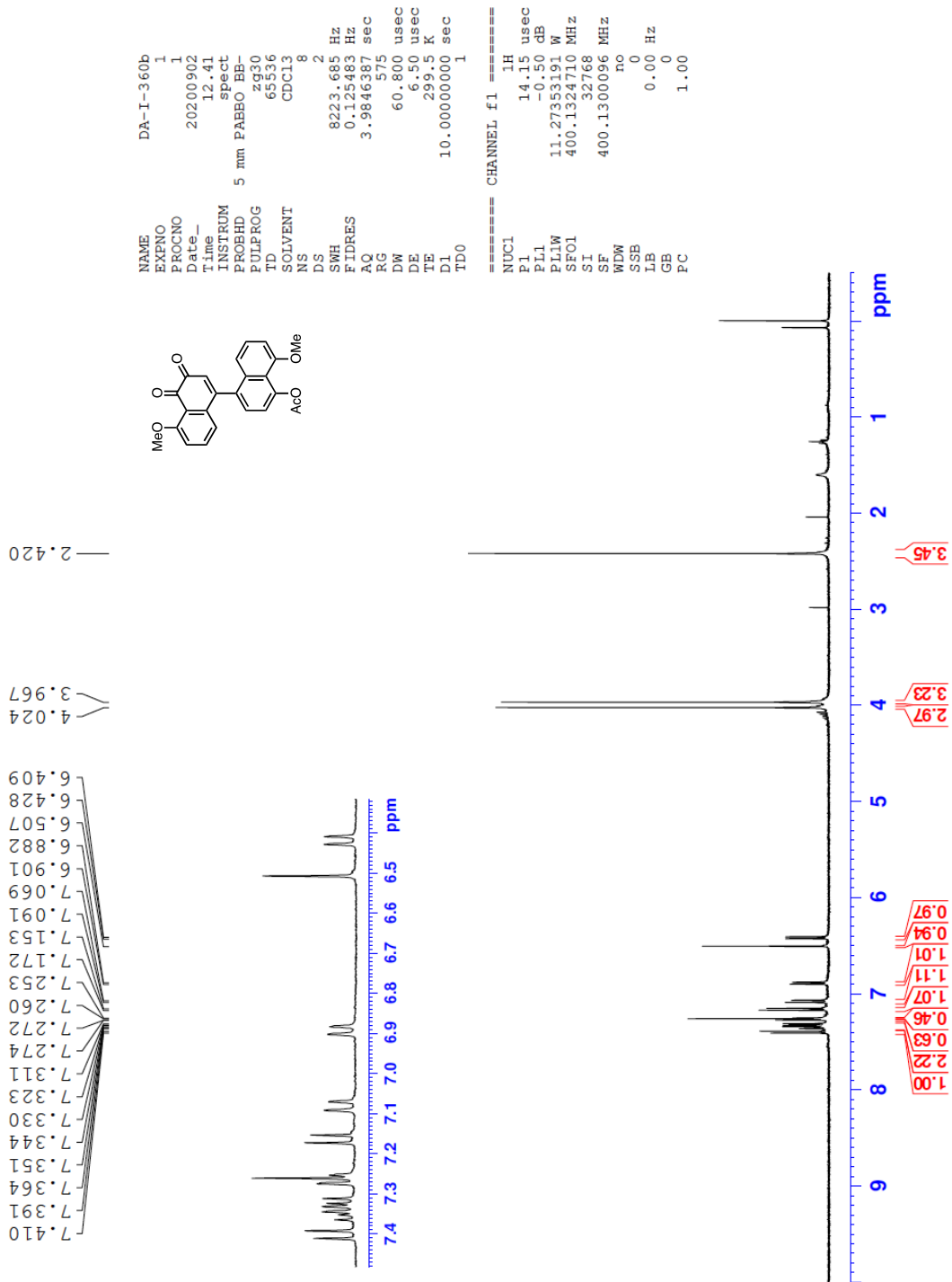


Figure 21. ¹H-NMR spectrum of **29** in CDCl₃.

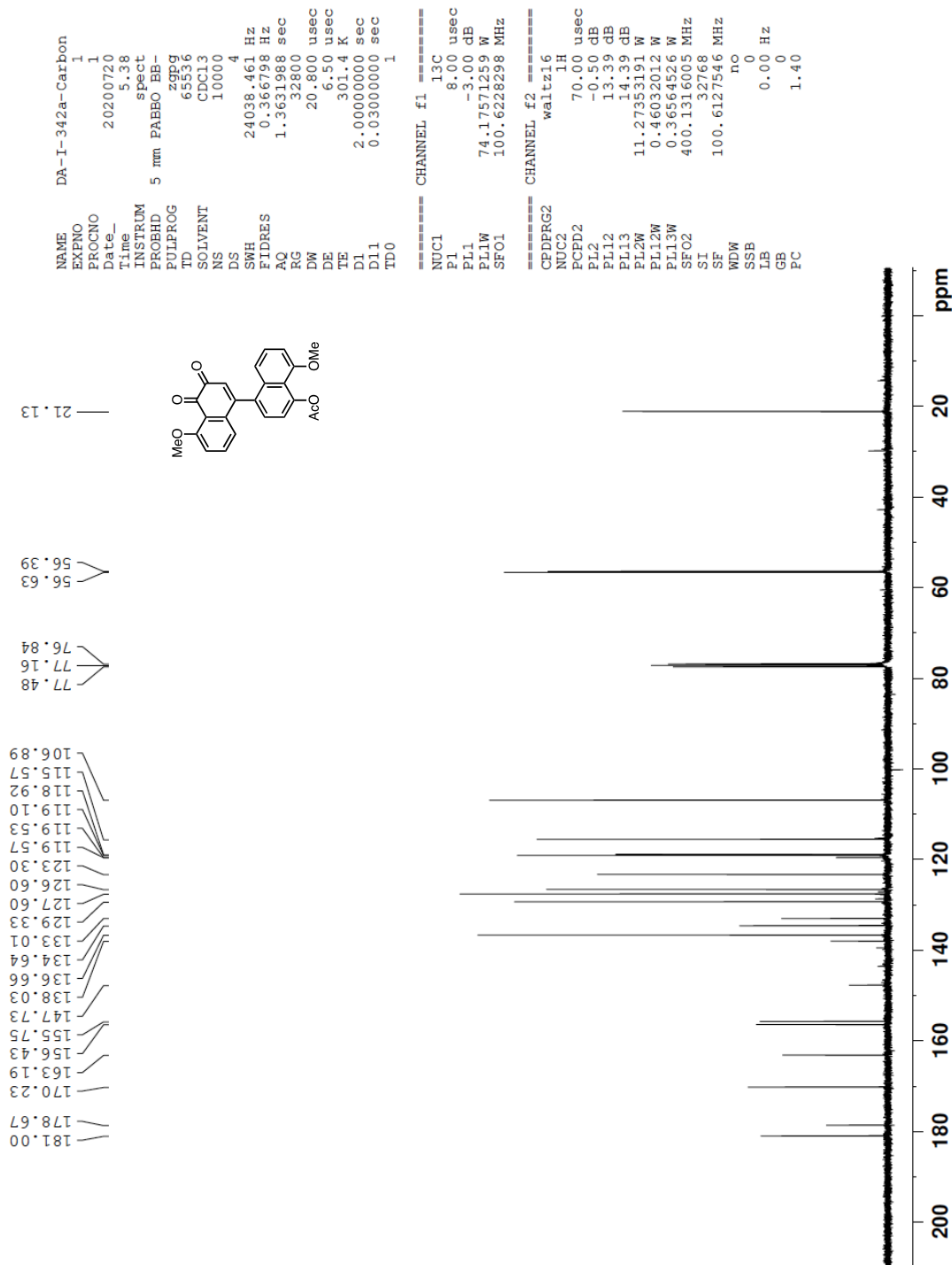


Figure 22. ^{13}C -NMR spectrum of **29** in CDCl_3 .

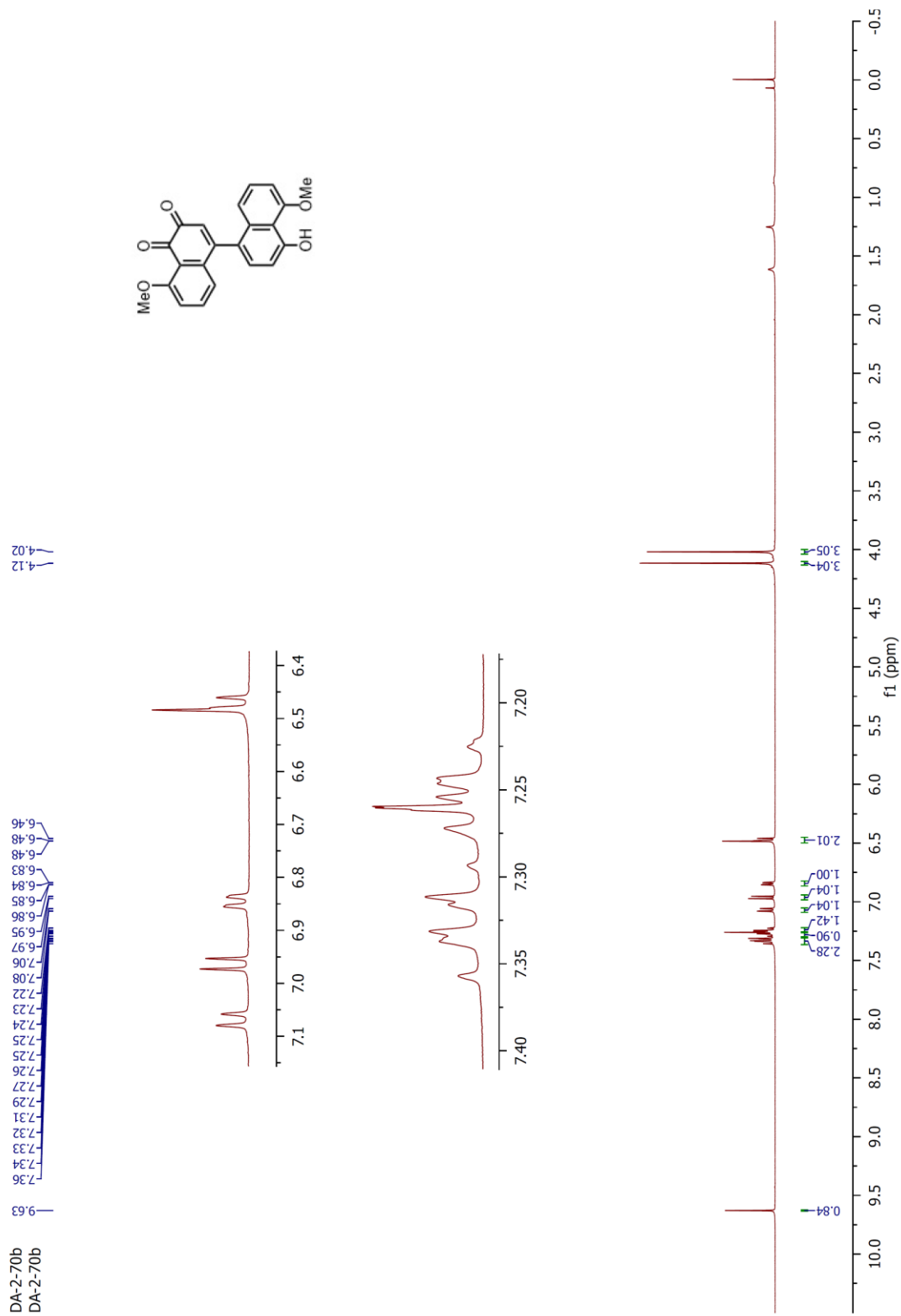


Figure 23. ¹H-NMR spectrum of daldiquinone (**15**) in CDCl₃.

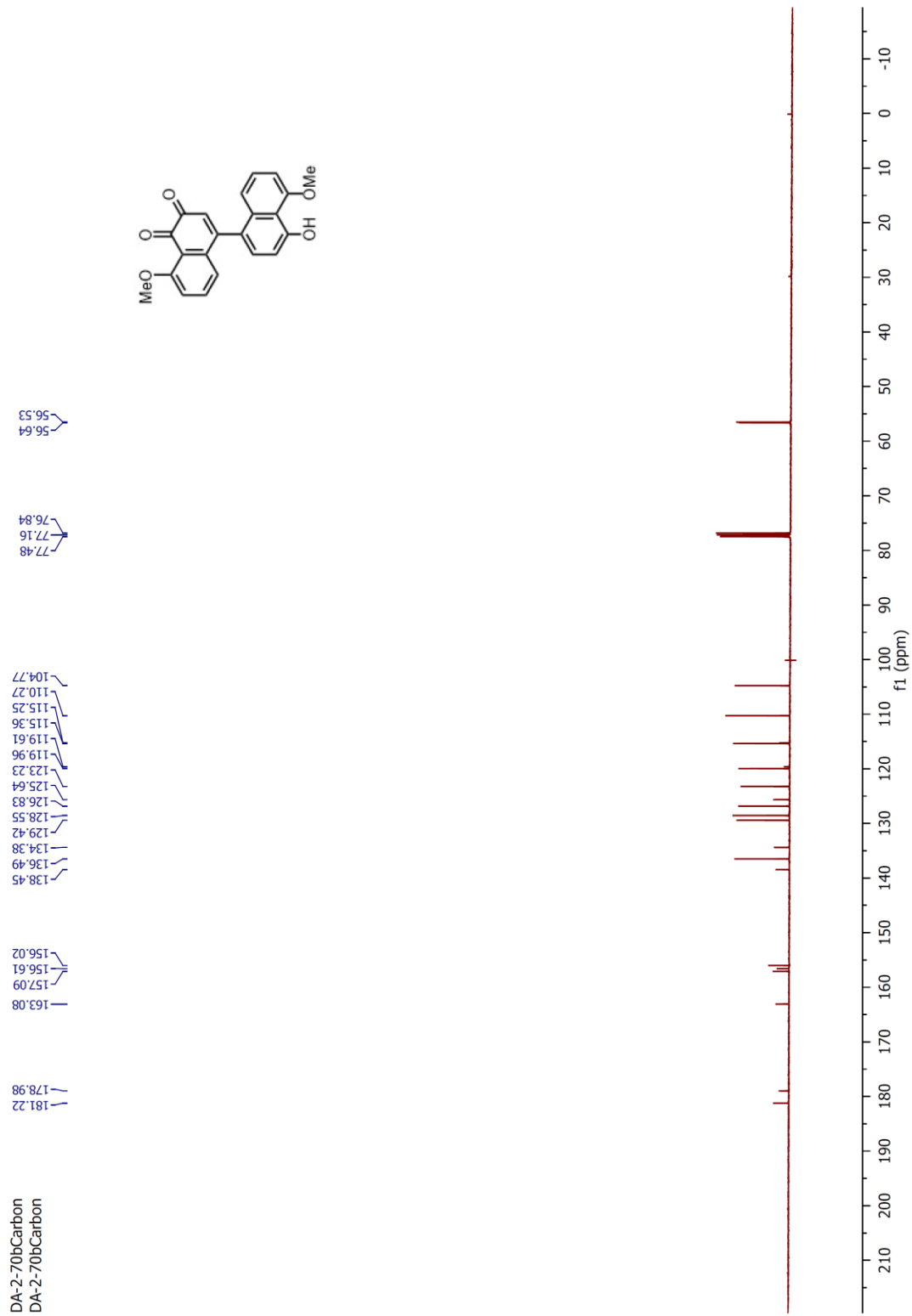


Figure 24. ^{13}C -NMR spectrum of daldiquinone (**15**) in CDCl_3 .

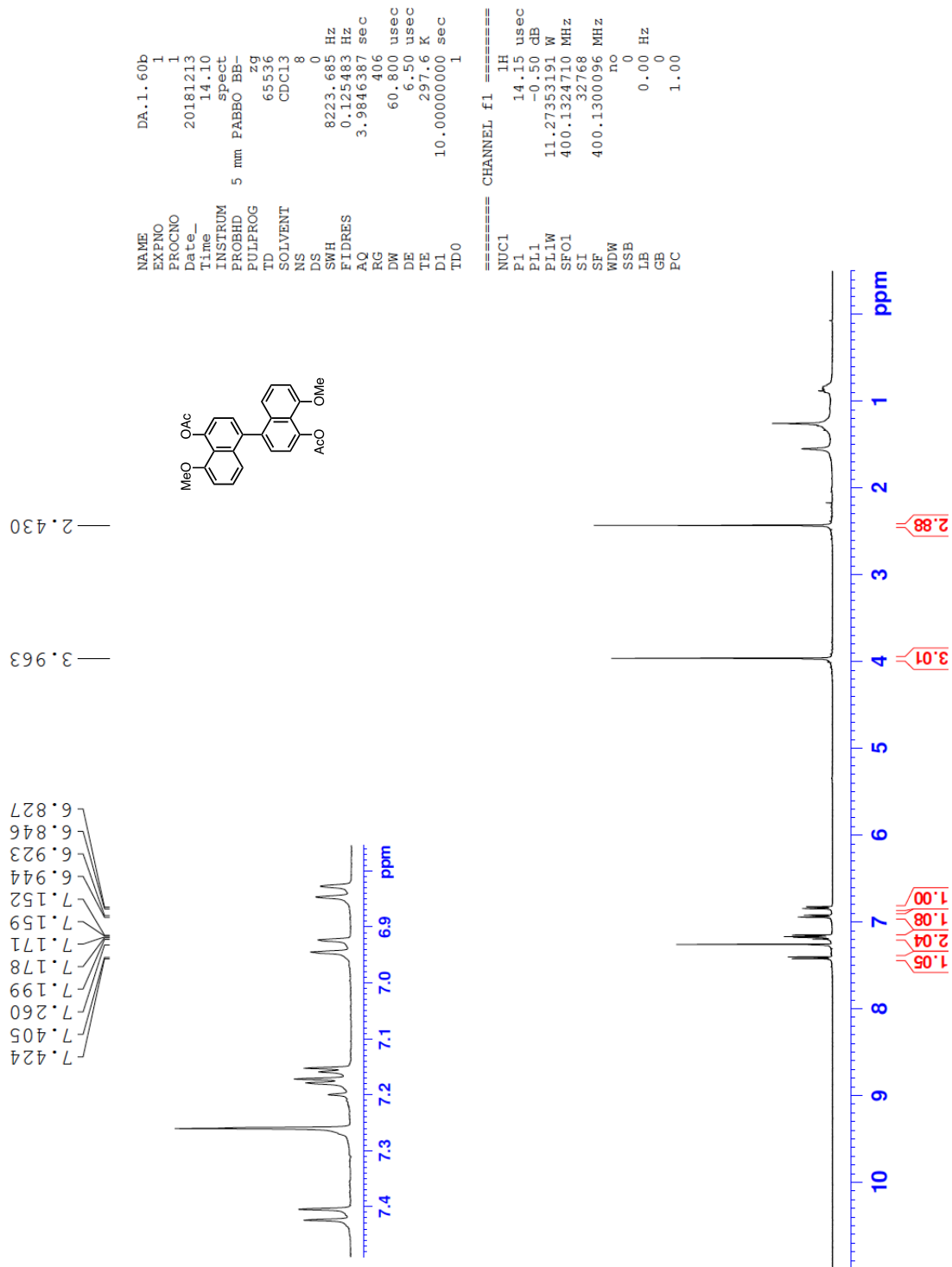


Figure 25. ¹H-NMR spectrum of **26** in CDCl₃.

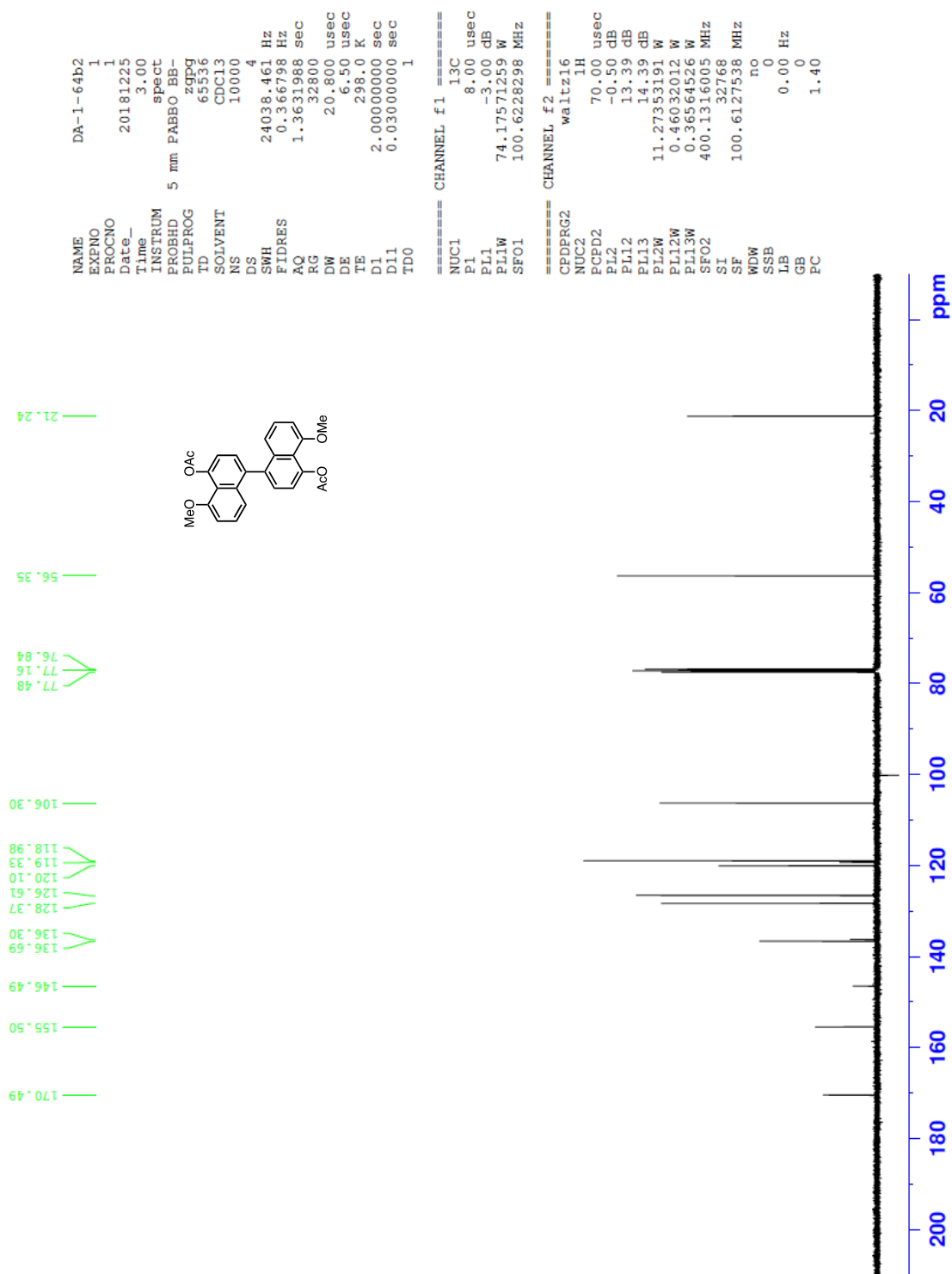


Figure 26. ^{13}C -NMR spectrum of **26** in CDCl_3 .

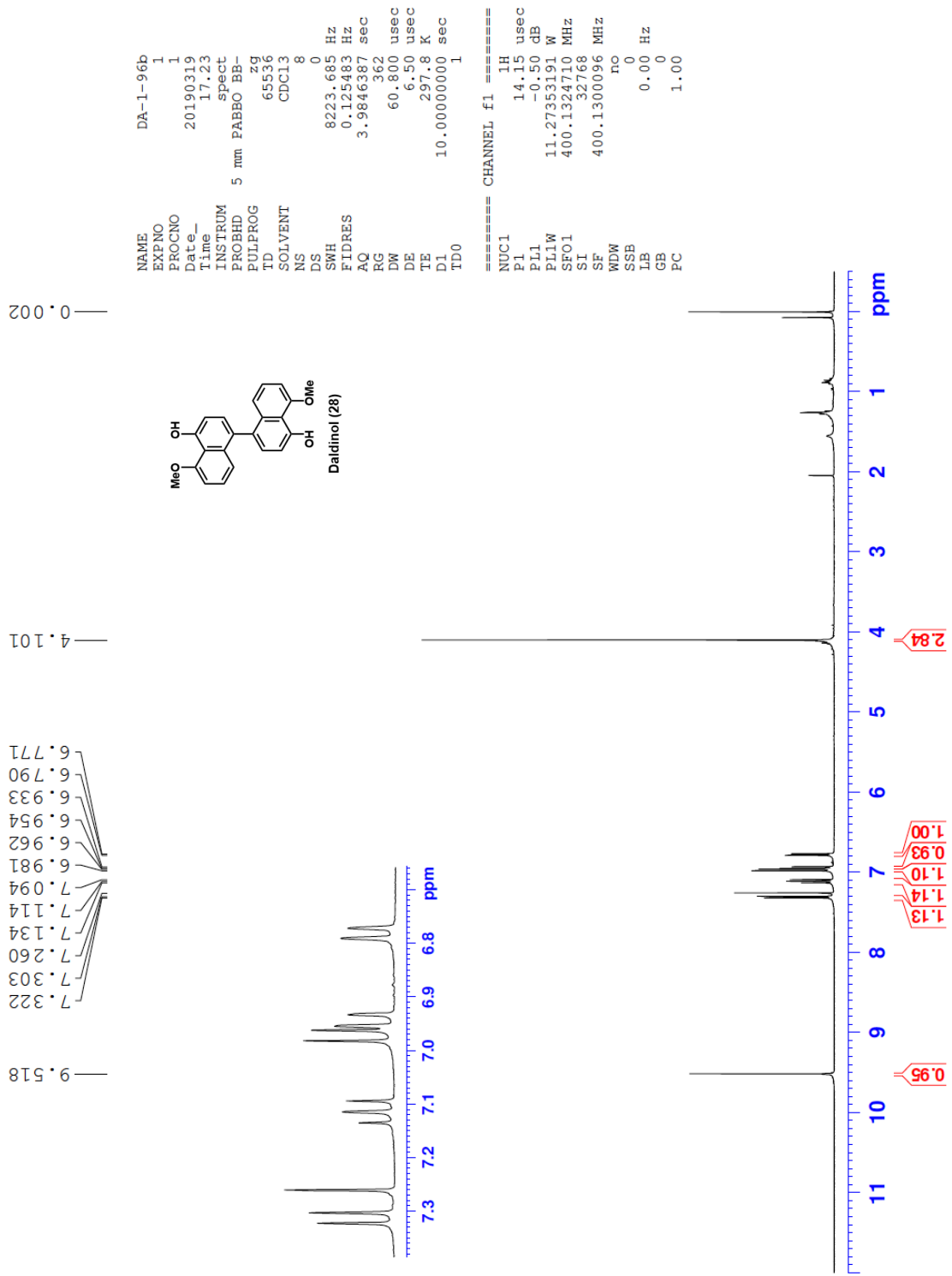


Figure 27. $^1\text{H-NMR}$ spectrum of daidinol (**28**) in CDCl_3 .

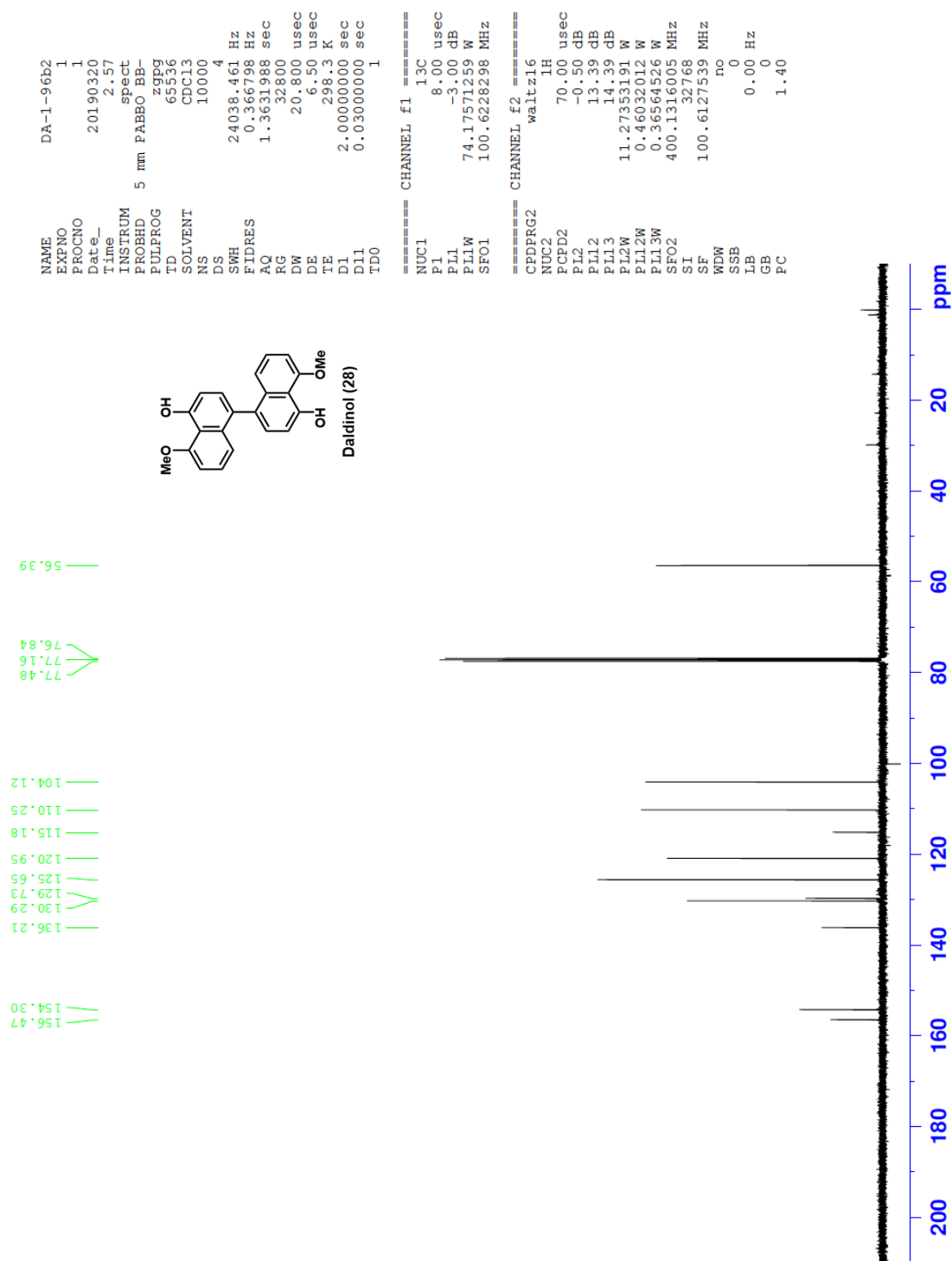


Figure 28. ^{13}C -NMR spectrum of daidinol (**28**) in CDCl_3 .

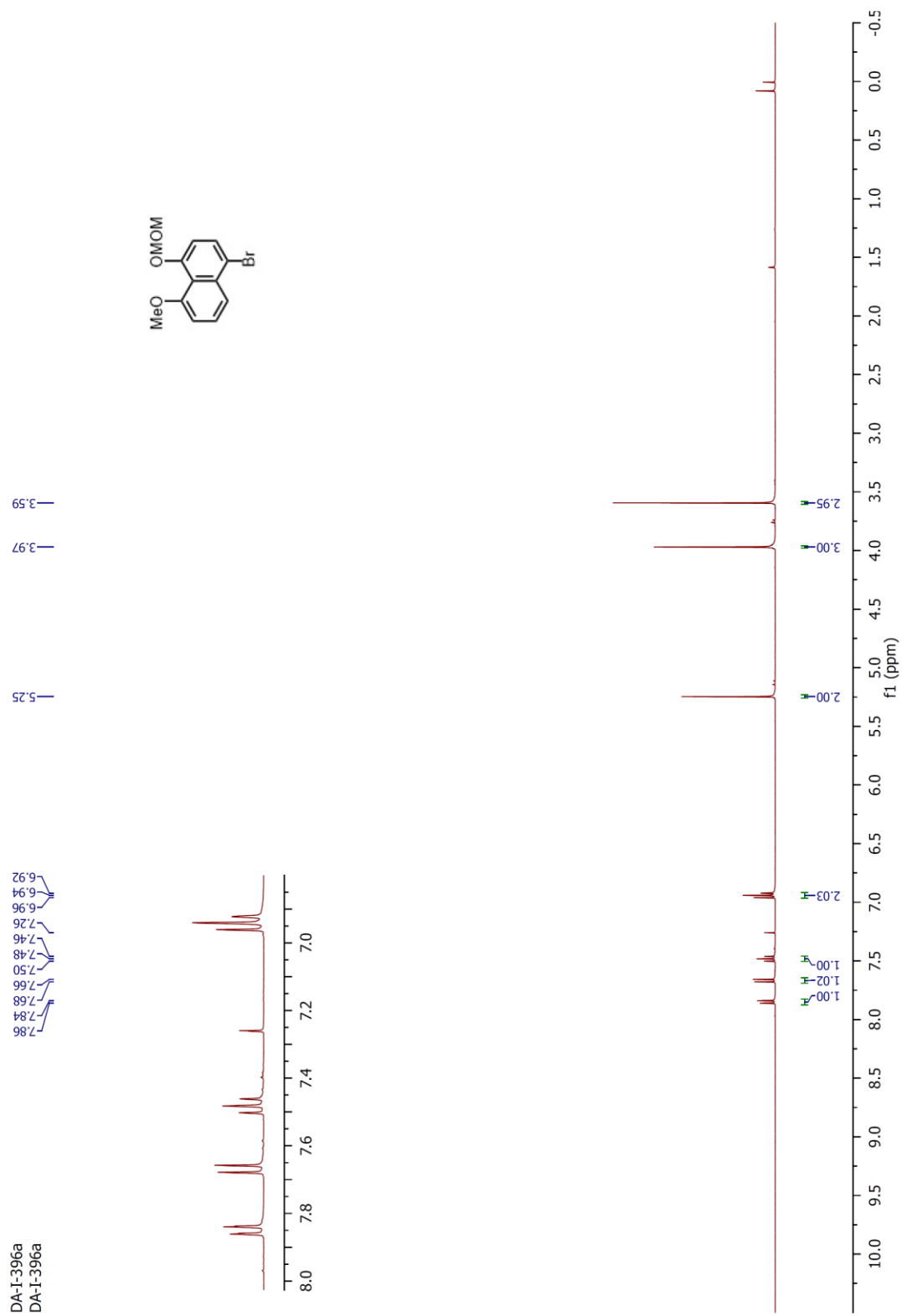


Figure 29. $^1\text{H-NMR}$ spectrum of **38** in CDCl_3 .

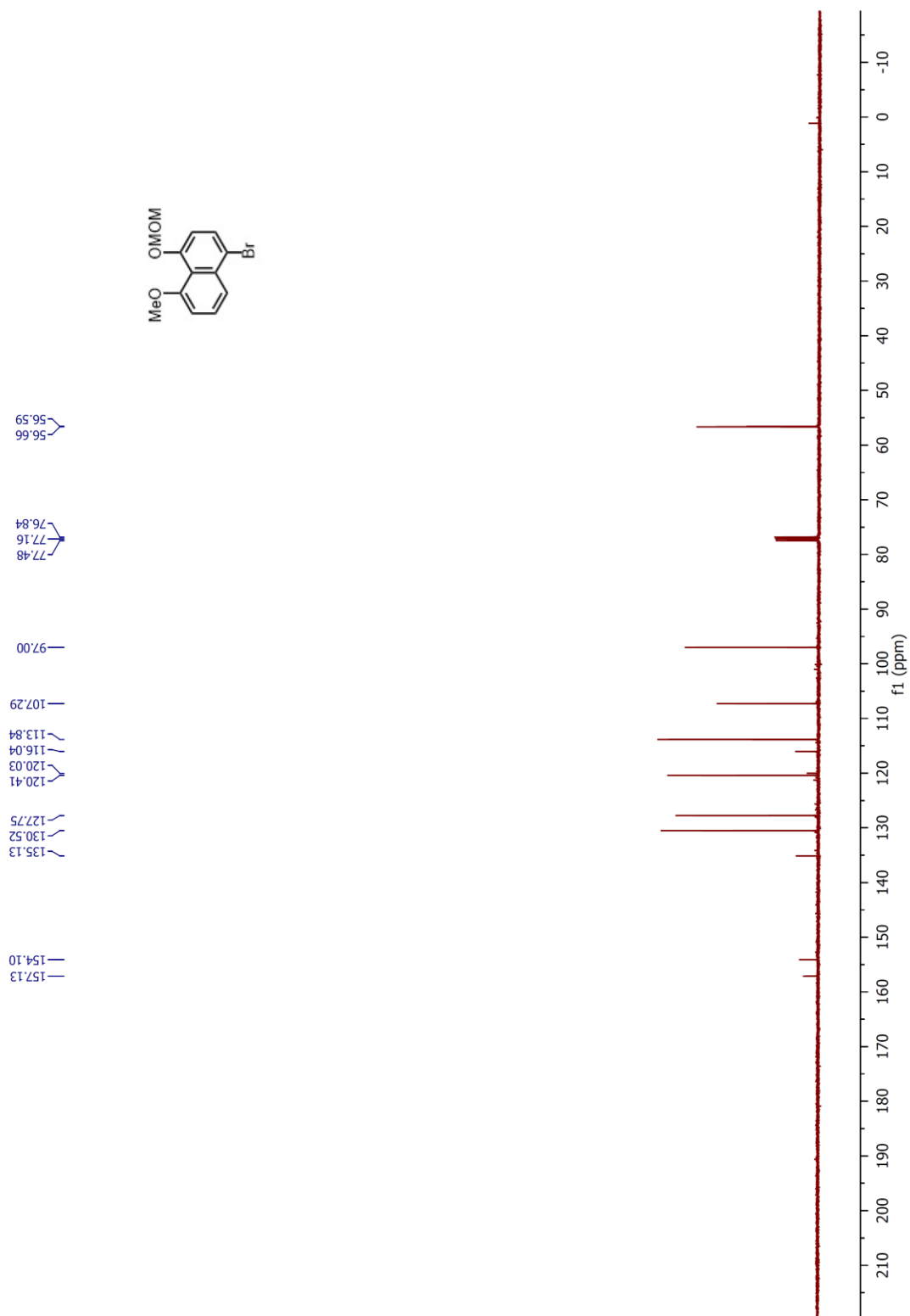


Figure 30. $^{13}\text{C-NMR}$ spectrum of **38** in CDCl_3 .

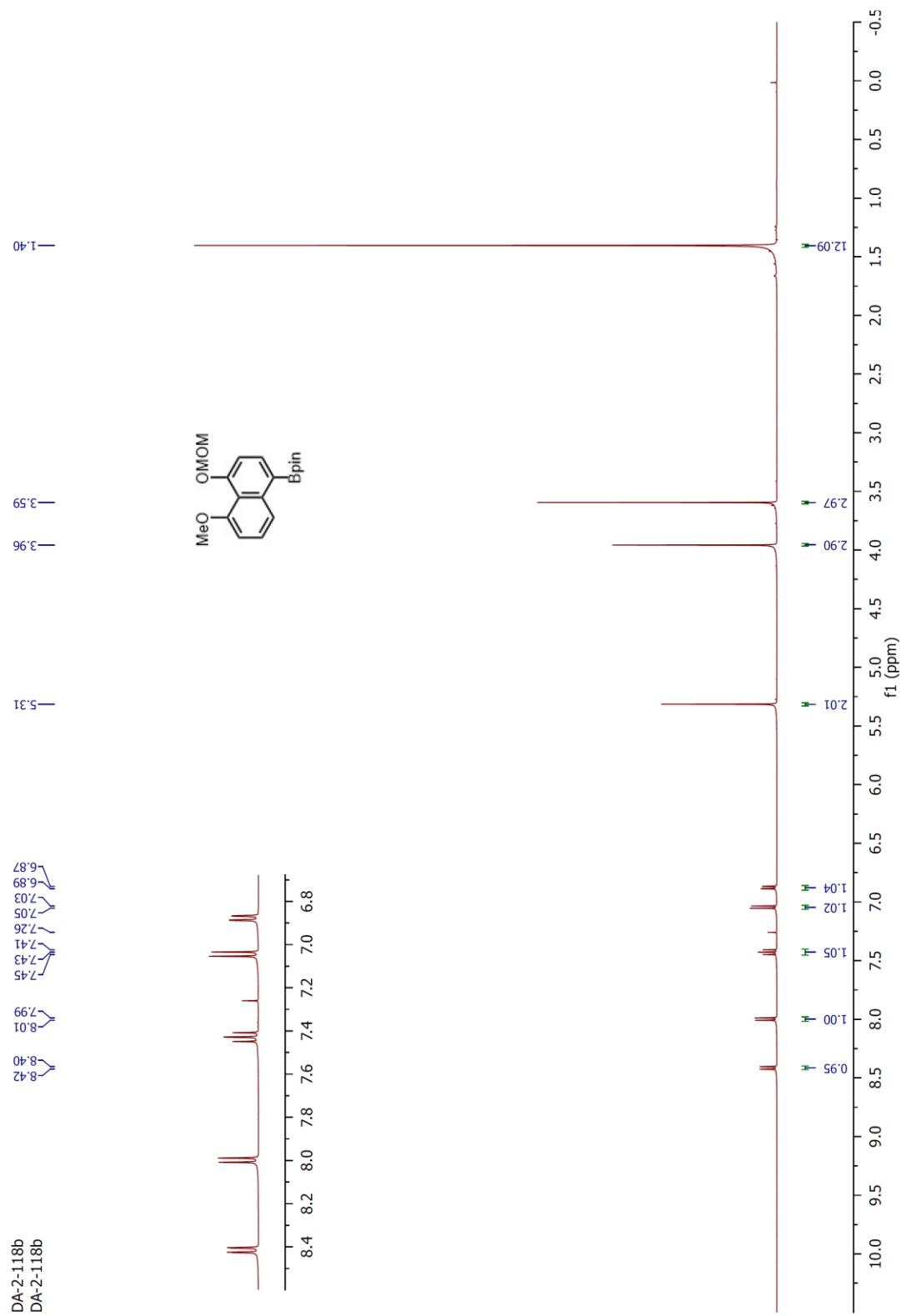


Figure 31. ¹H-NMR spectrum of **39** in CDCl₃.

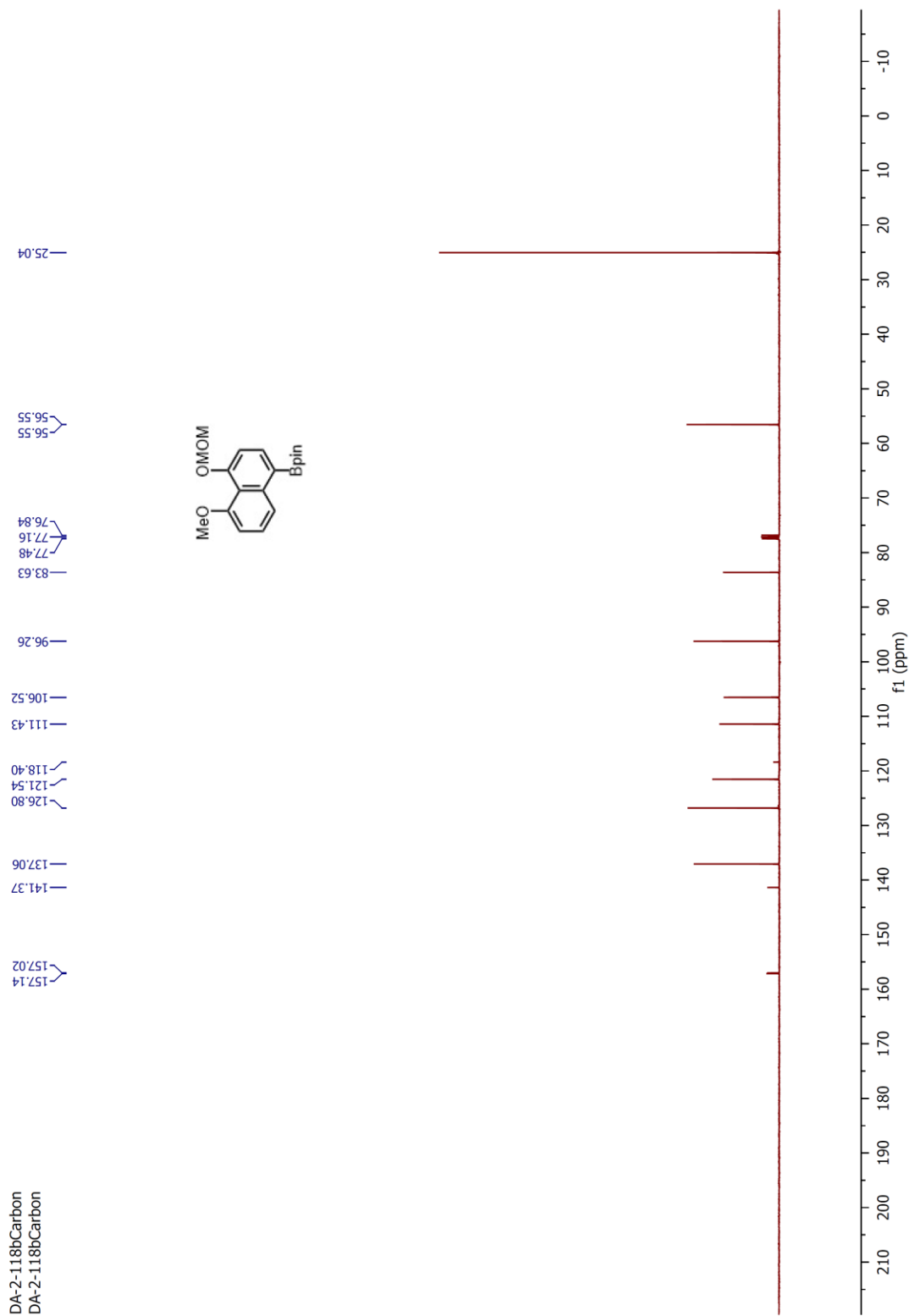


Figure 32. $^{13}\text{C-NMR}$ spectrum of **39** in CDCl_3 .

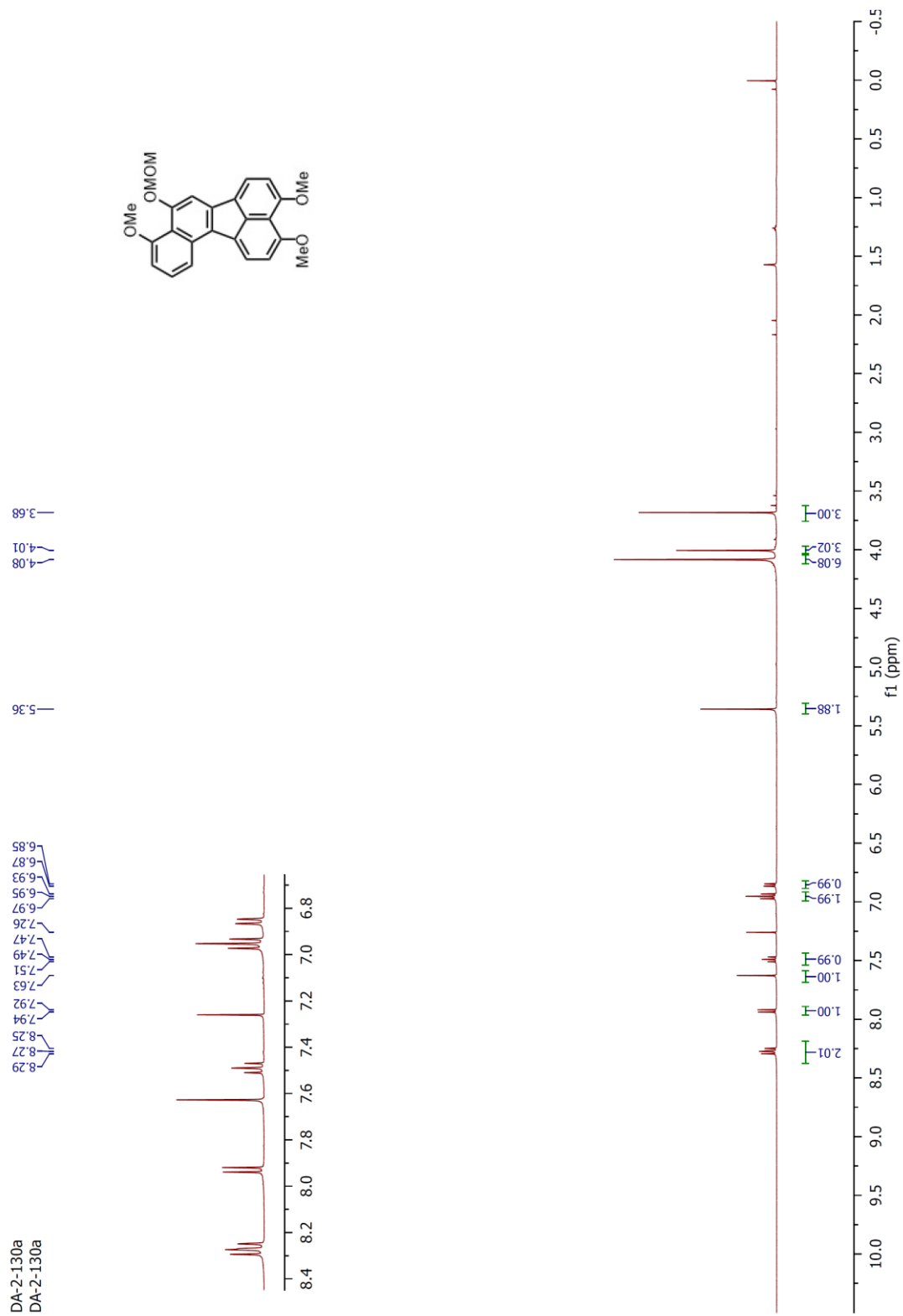


Figure 33. $^1\text{H-NMR}$ spectrum of **40** in CDCl_3 .

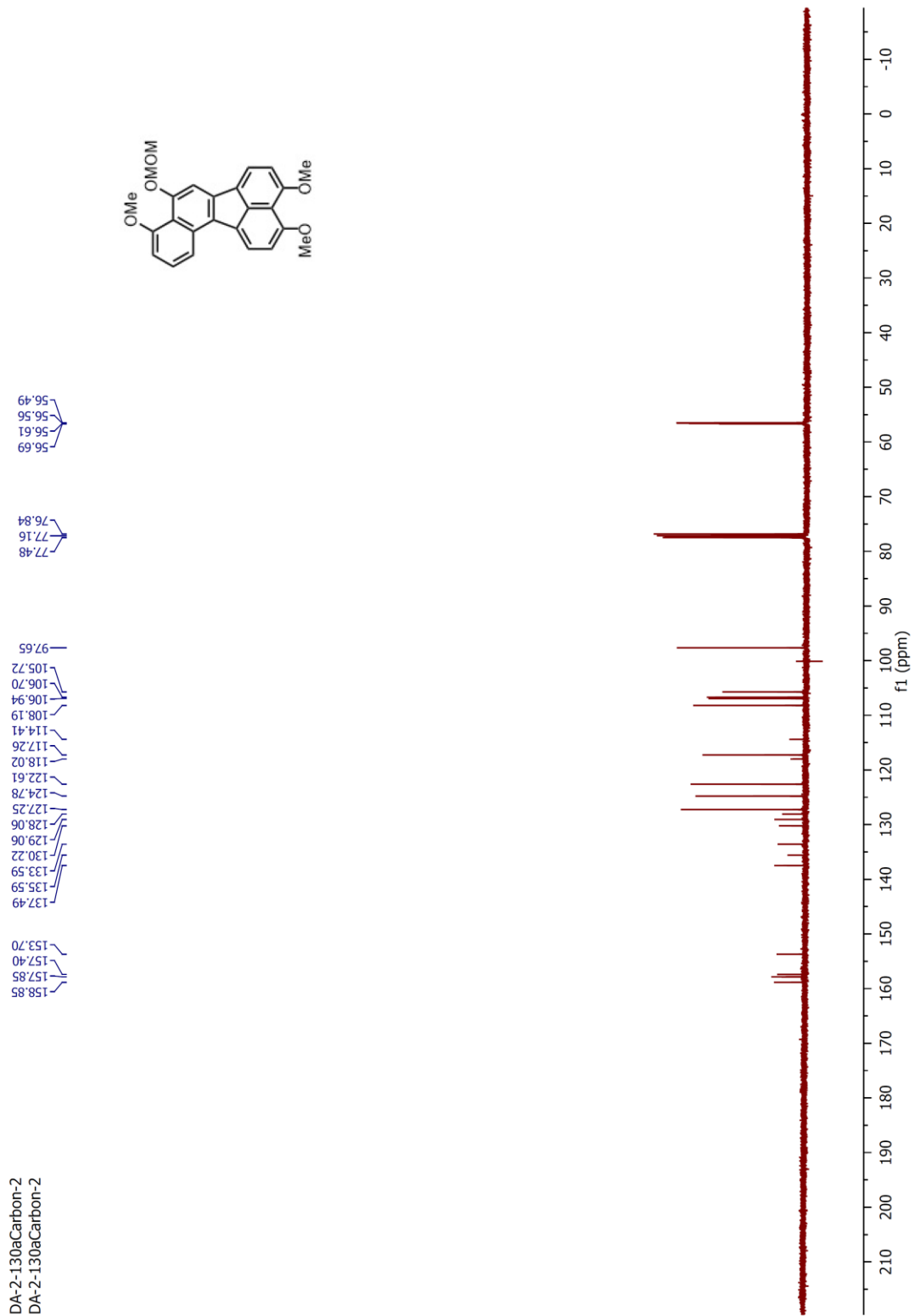


Figure 34. ^{13}C -NMR spectrum of **40** in CDCl_3 .

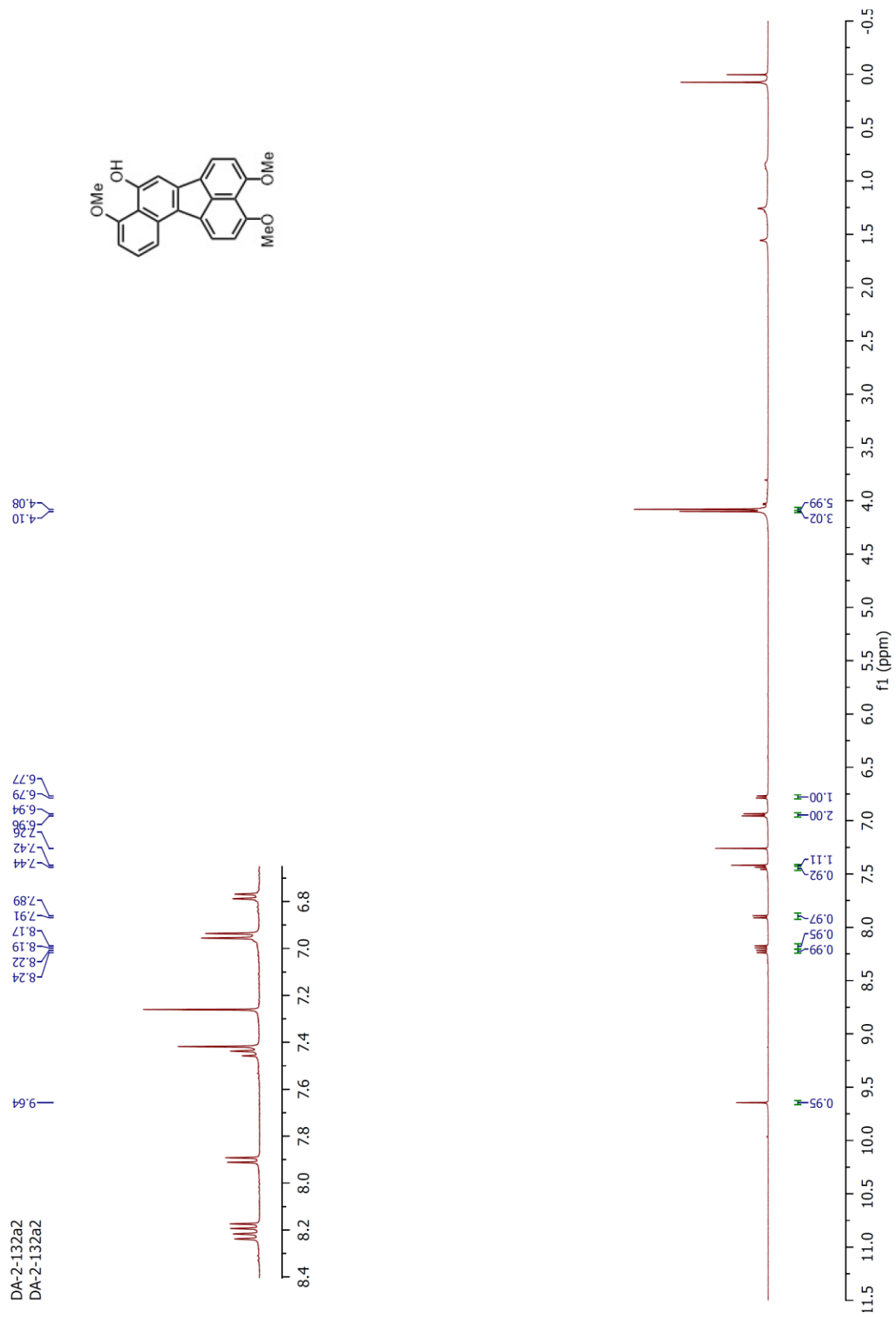


Figure 35. $^1\text{H-NMR}$ spectrum of **41** in CDCl_3 .

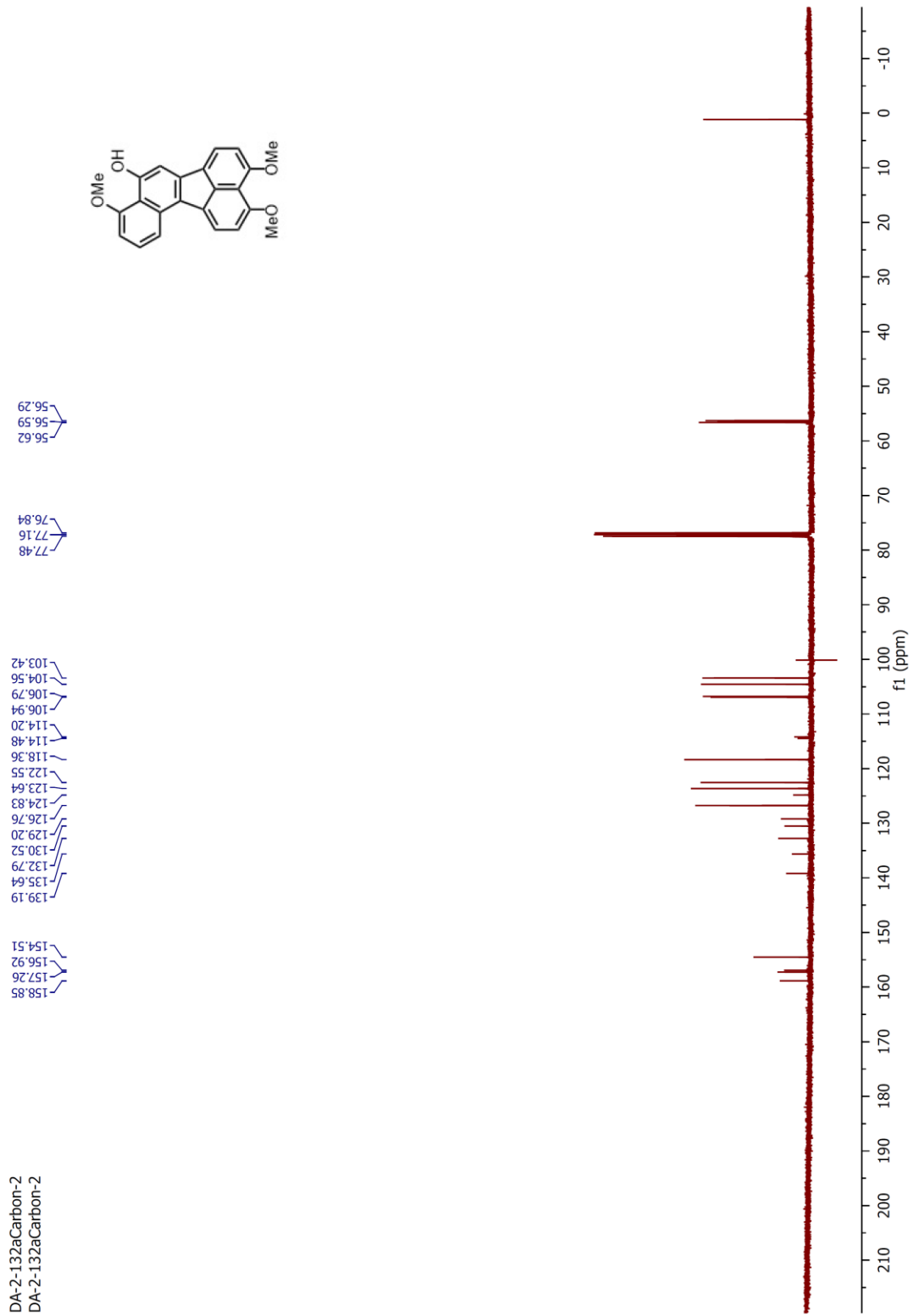


Figure 36. $^{13}\text{C-NMR}$ spectrum of **41** in CDCl_3 .

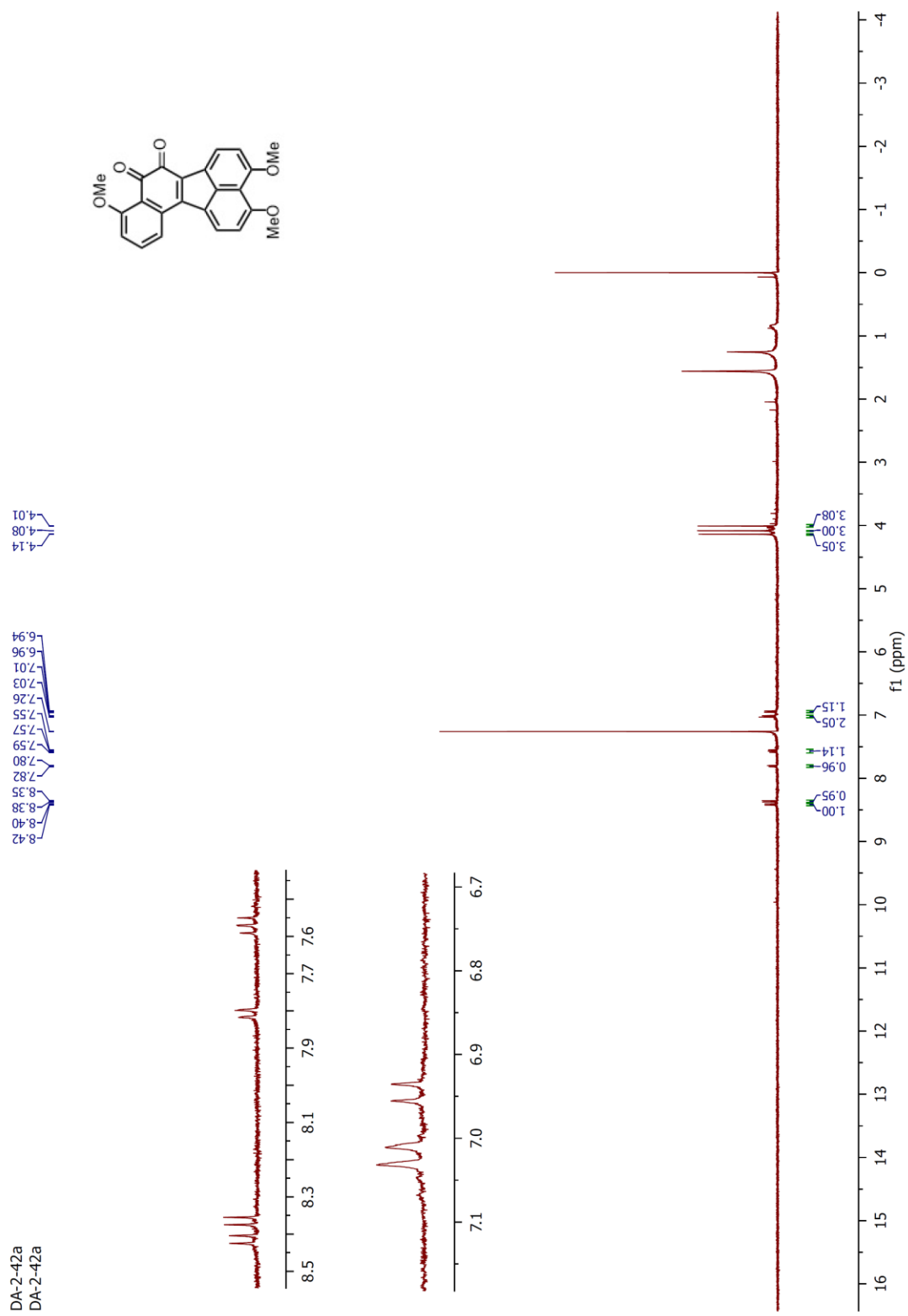


Figure 37. ¹H-NMR spectrum of **42** in CDCl₃.

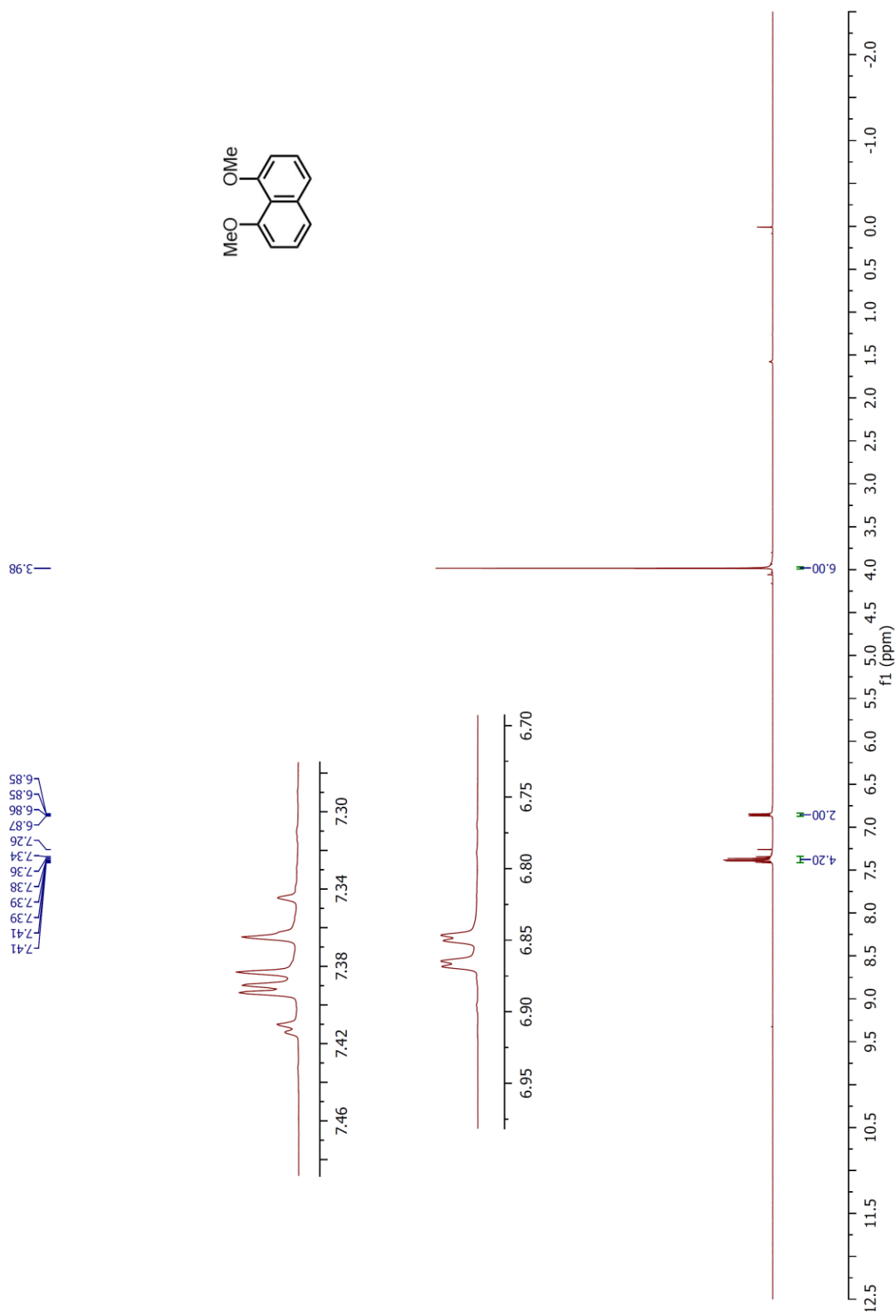


Figure 38. ¹H-NMR spectrum of **36** in CDCl₃.

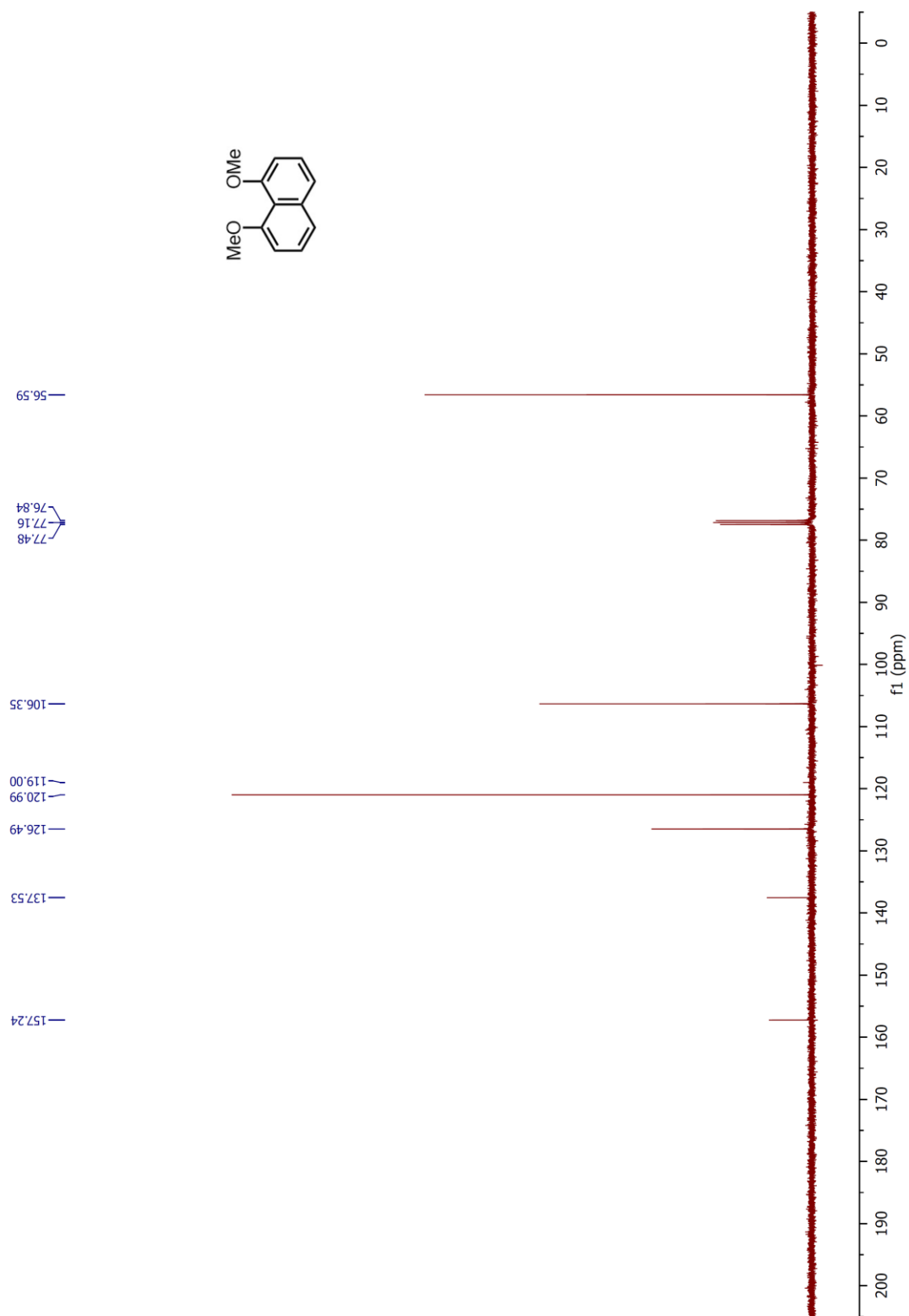


Figure 39. ^{13}C -NMR spectrum of **36** in CDCl_3 .

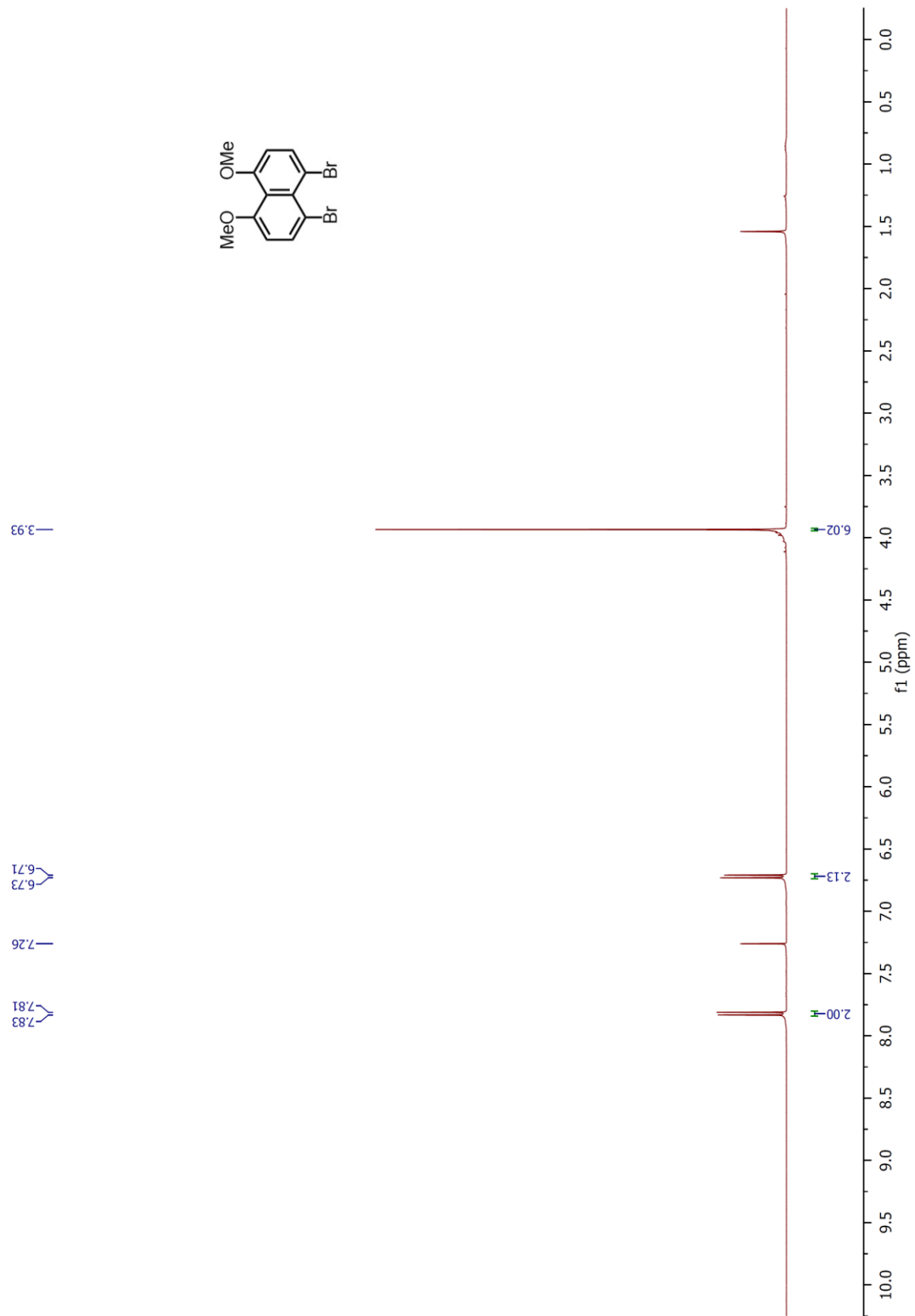


Figure 40. $^1\text{H-NMR}$ spectrum of **37** in CDCl_3 .

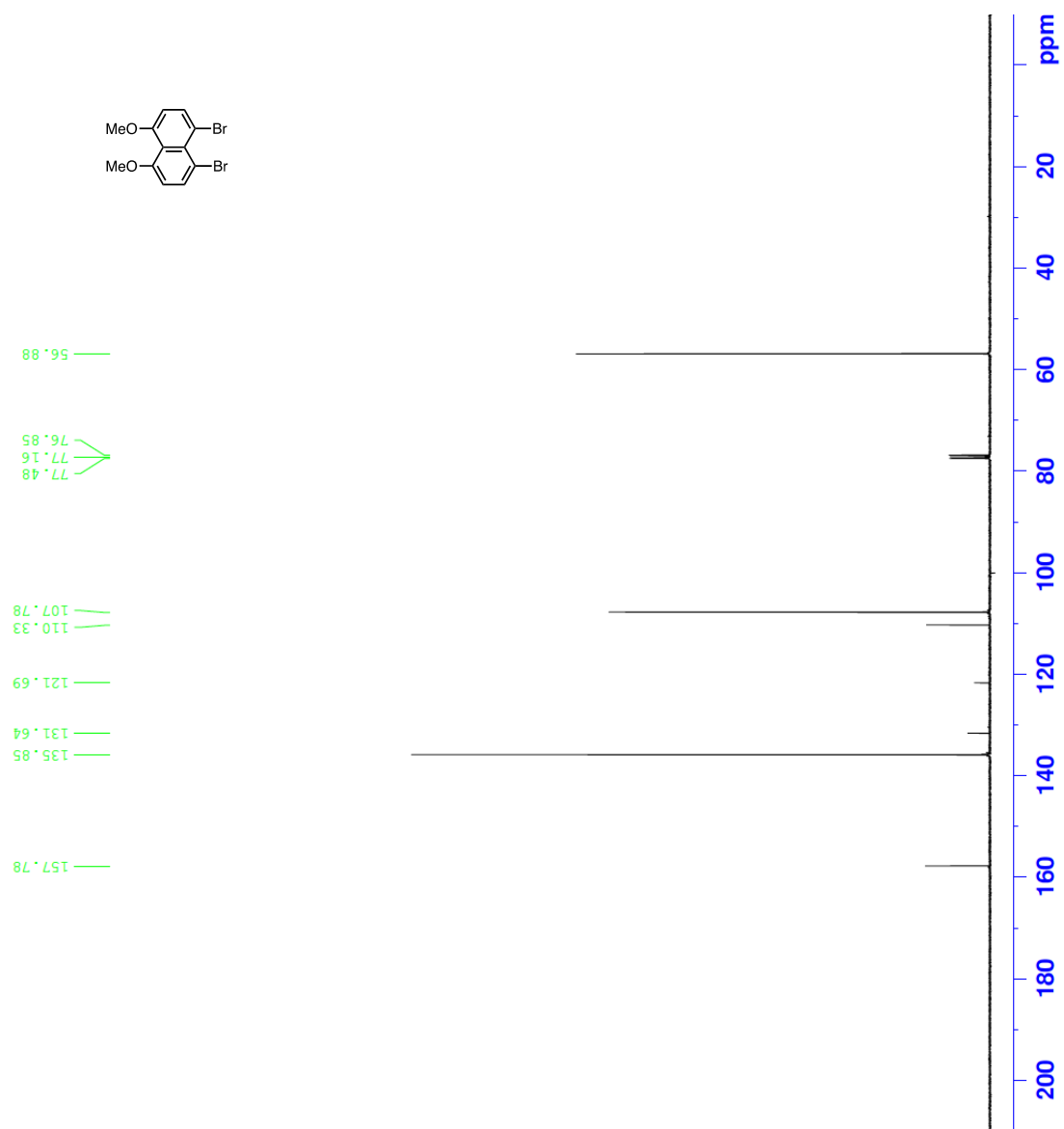


Figure 41. $^{13}\text{C-NMR}$ spectrum of **37** in CDCl_3 .

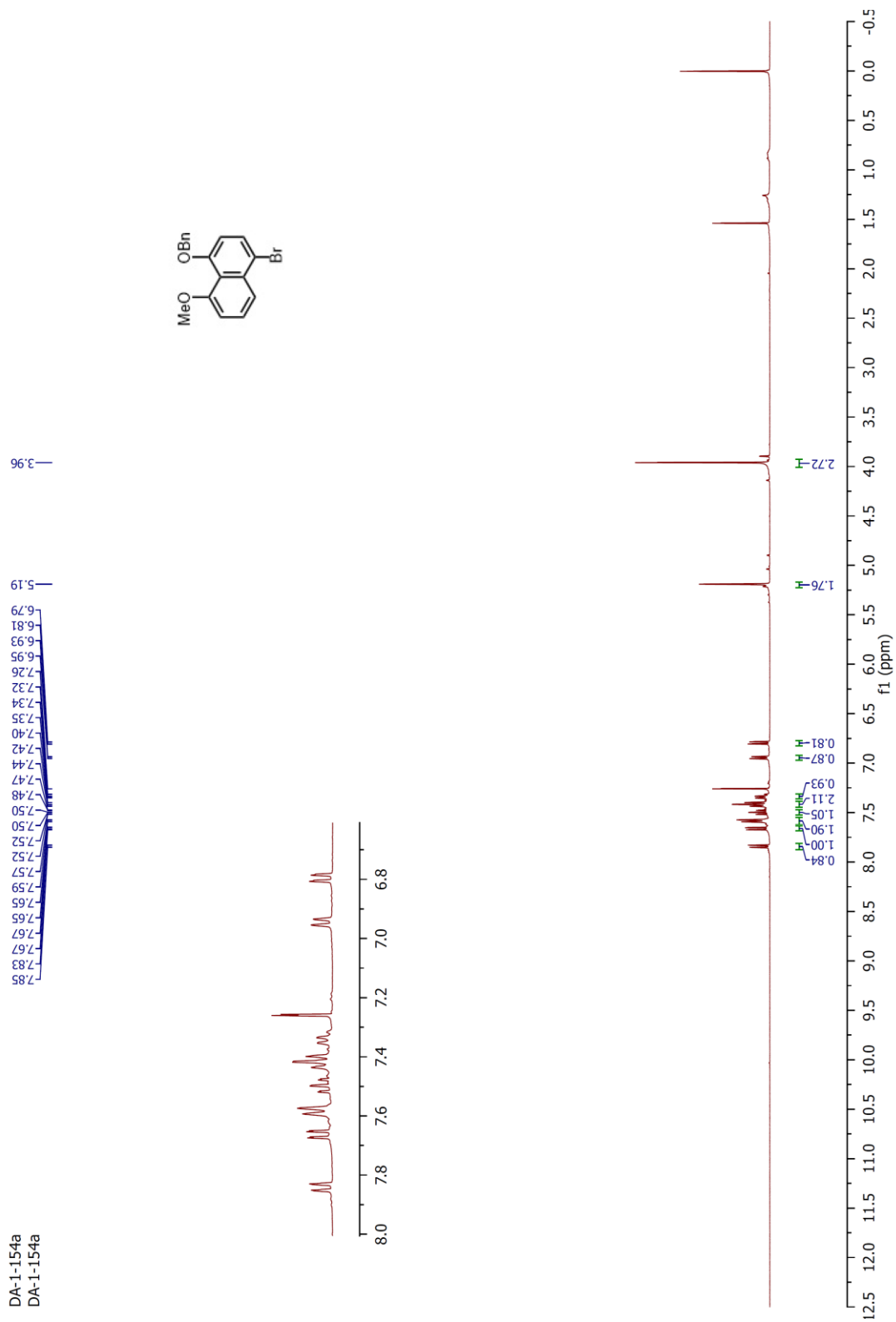


Figure 42. ¹H-NMR spectrum of **30** in CDCl₃.

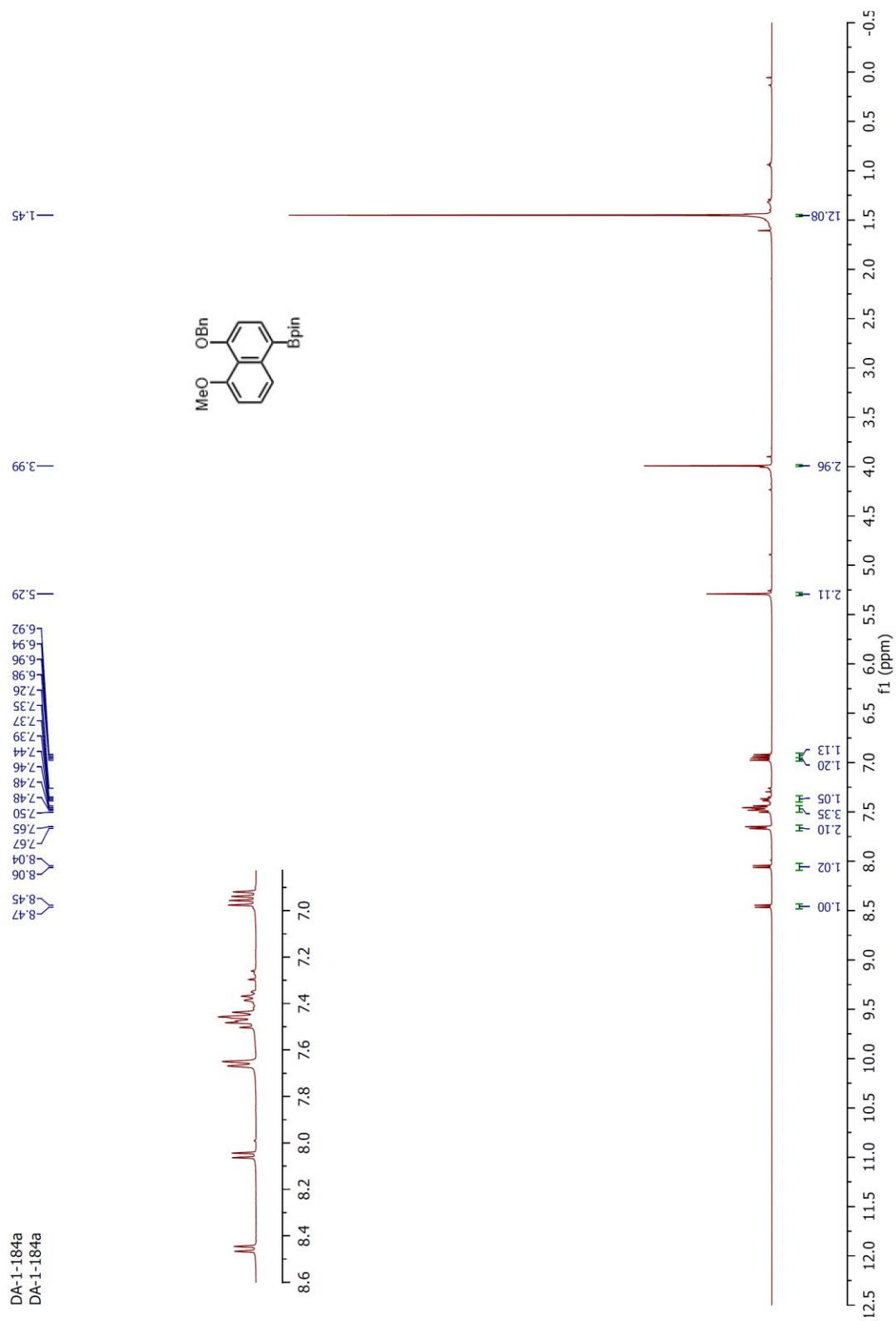


Figure 43. ¹H-NMR spectrum of **31** in CDCl₃.

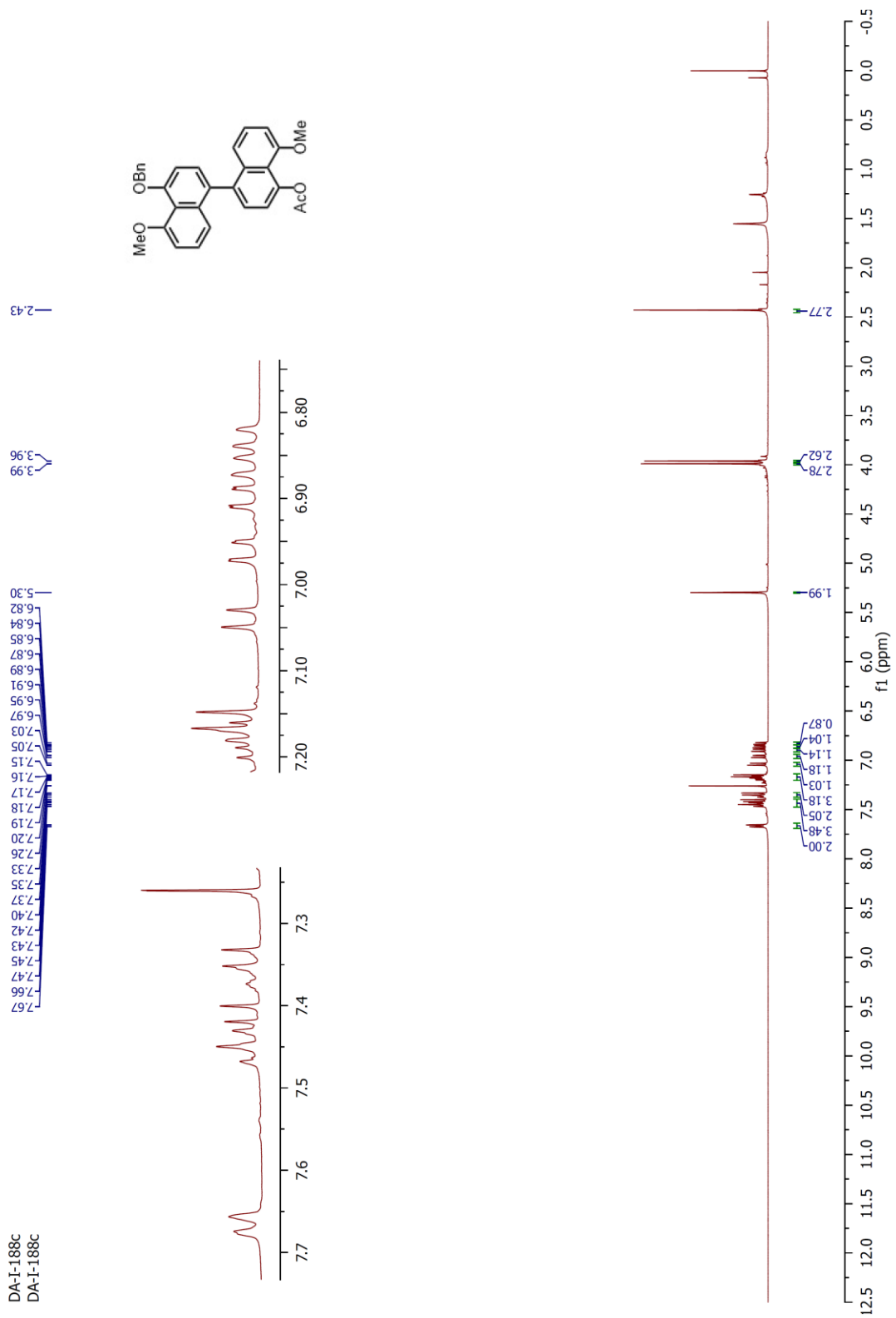


Figure 44. $^1\text{H-NMR}$ spectrum of **32** in CDCl_3 .

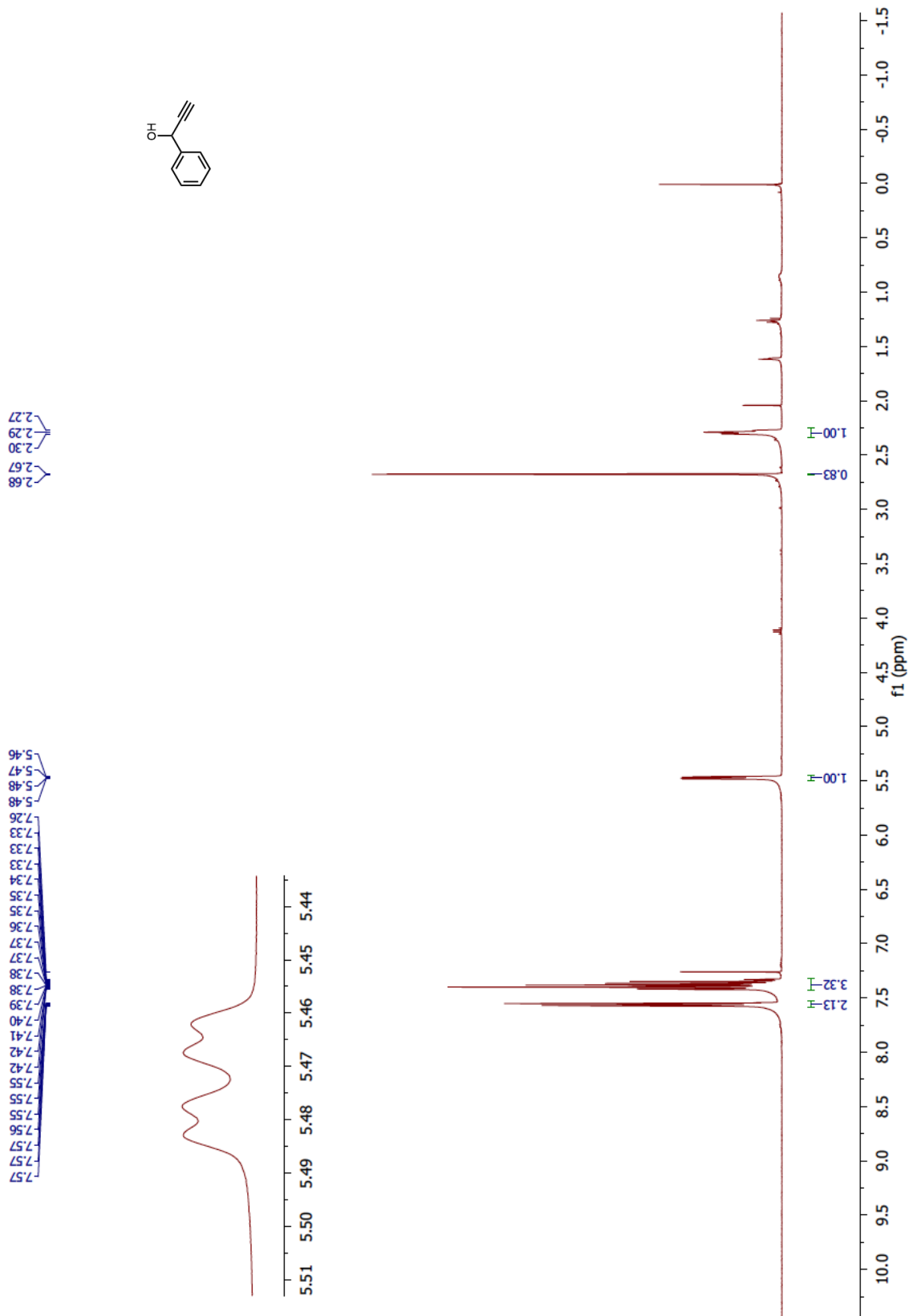


Figure 45. ¹H-NMR spectrum of **43a** in CDCl₃.

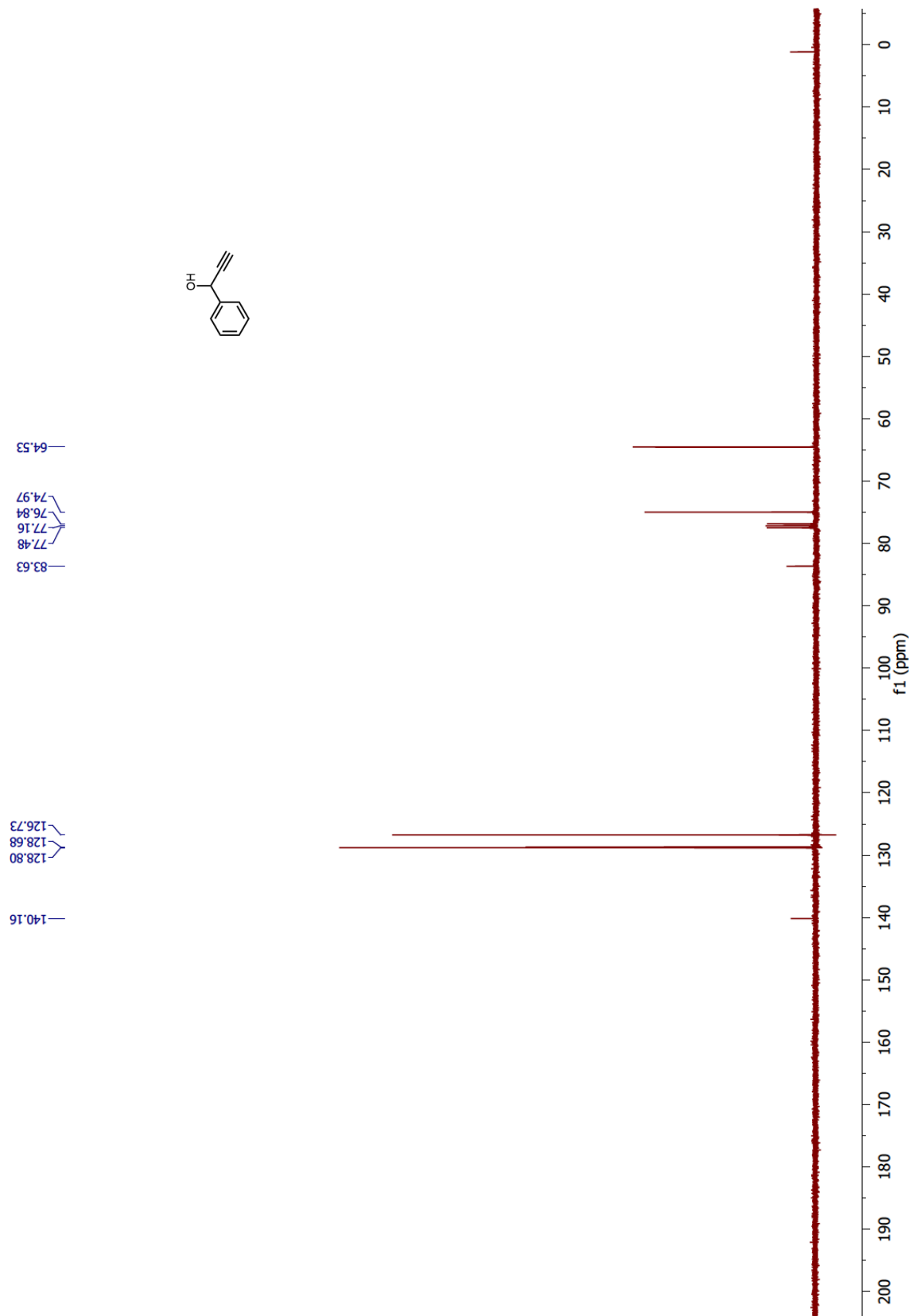


Figure 46. ¹³C-NMR spectrum of 43a in CDCl₃.

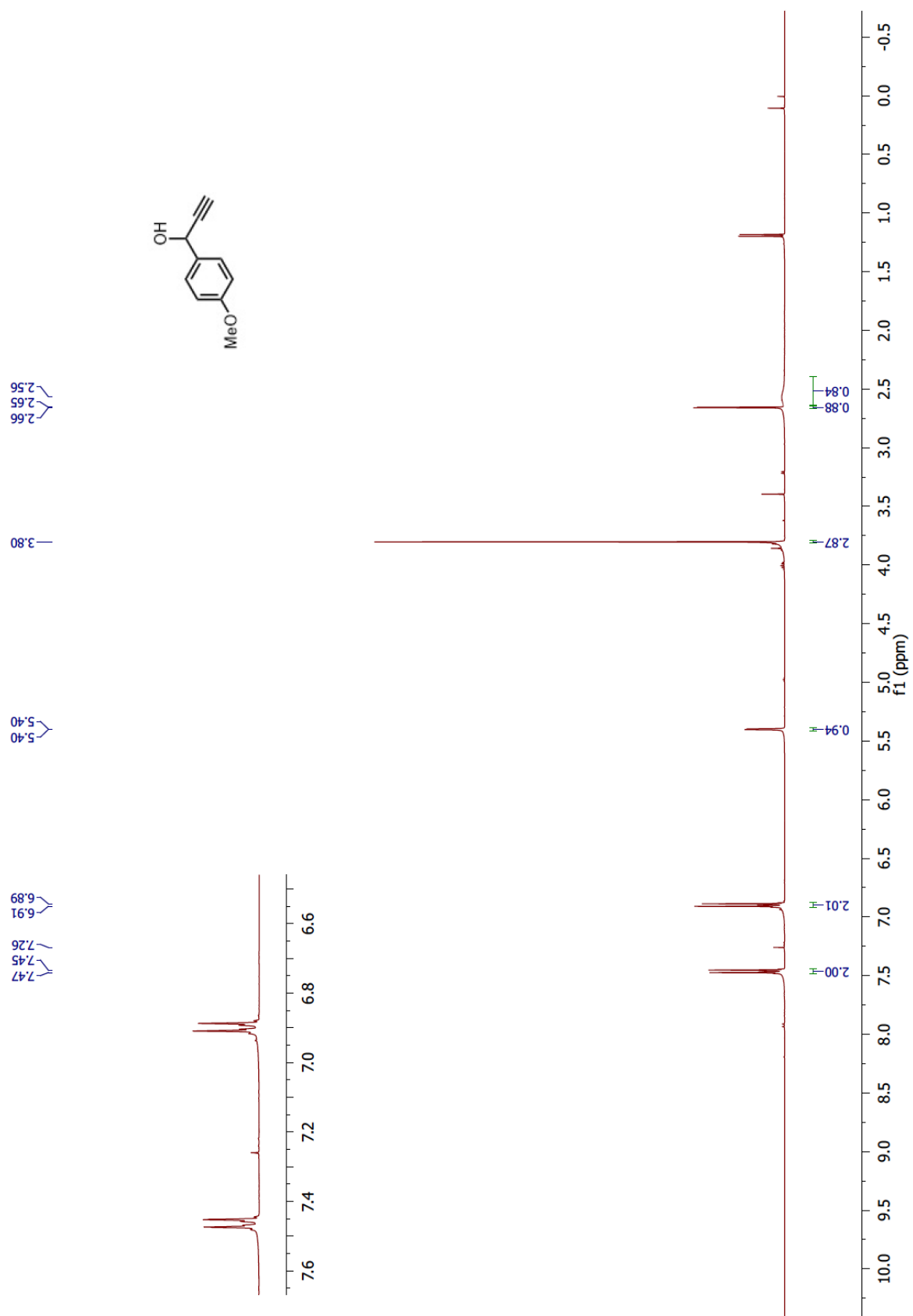


Figure 47. ¹H-NMR spectrum of **43b** in CDCl₃.

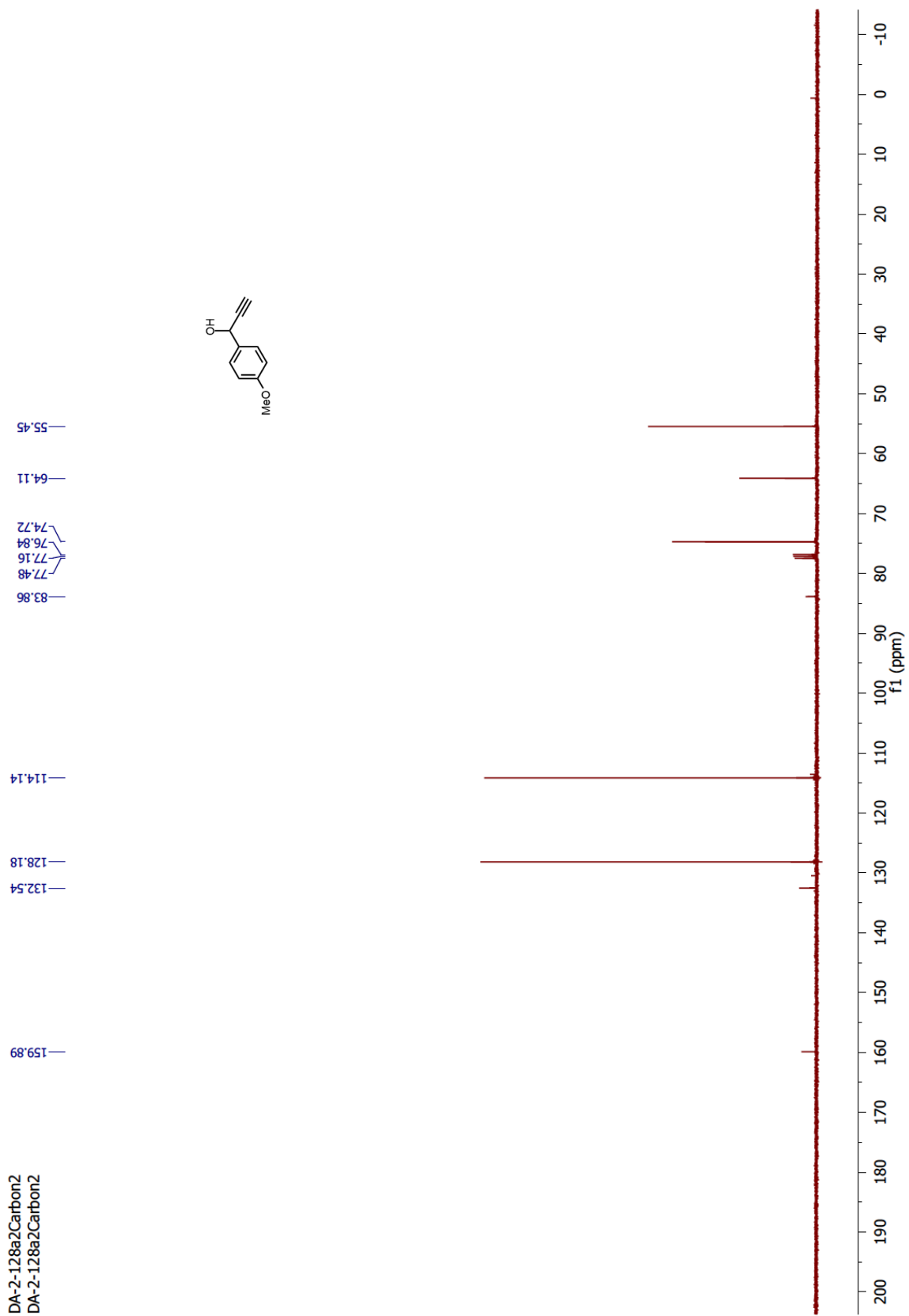


Figure 48. ¹³C-NMR spectrum of **43b** in CDCl₃.

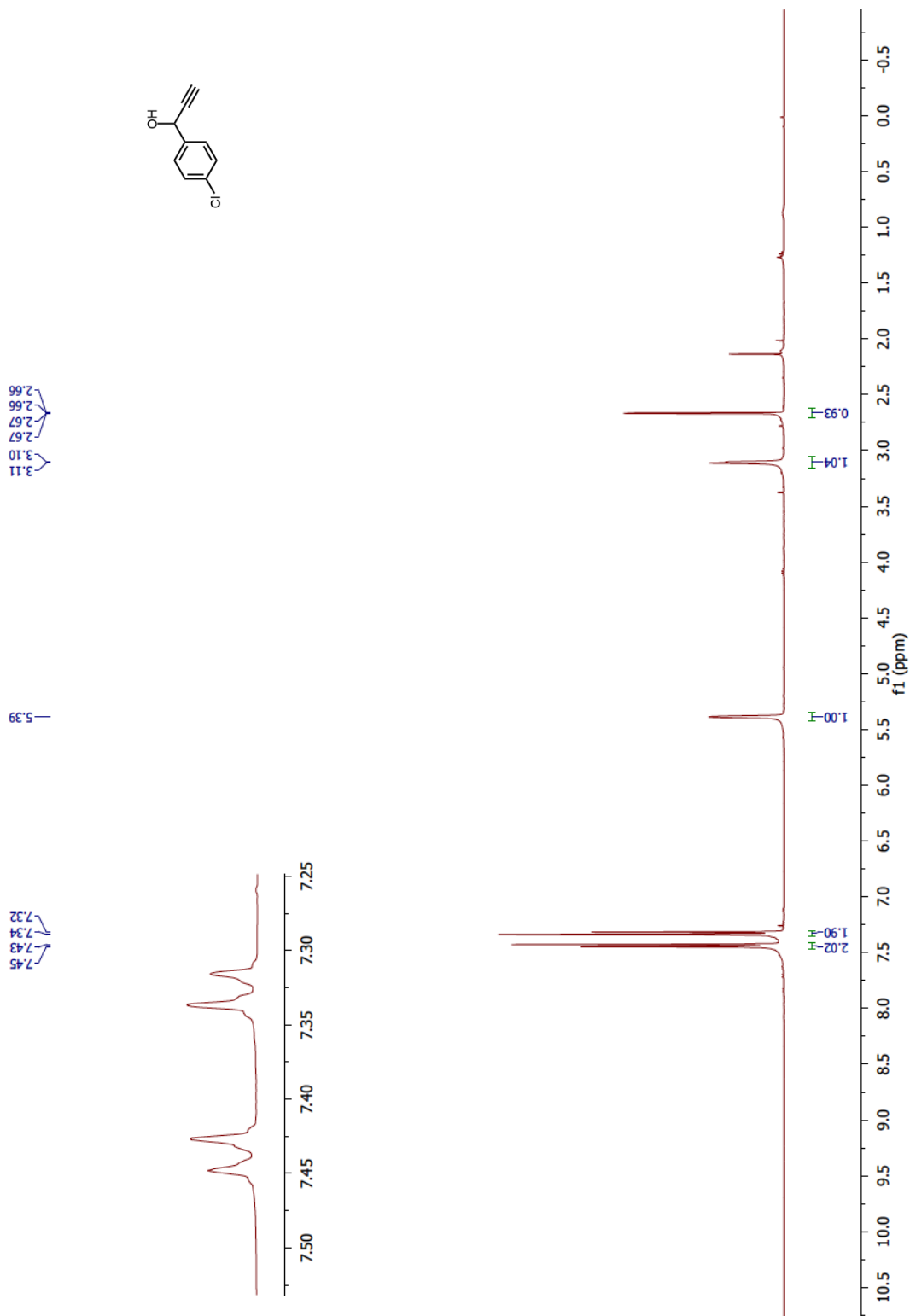


Figure 49. ¹H-NMR spectrum of **43c** in CDCl₃.

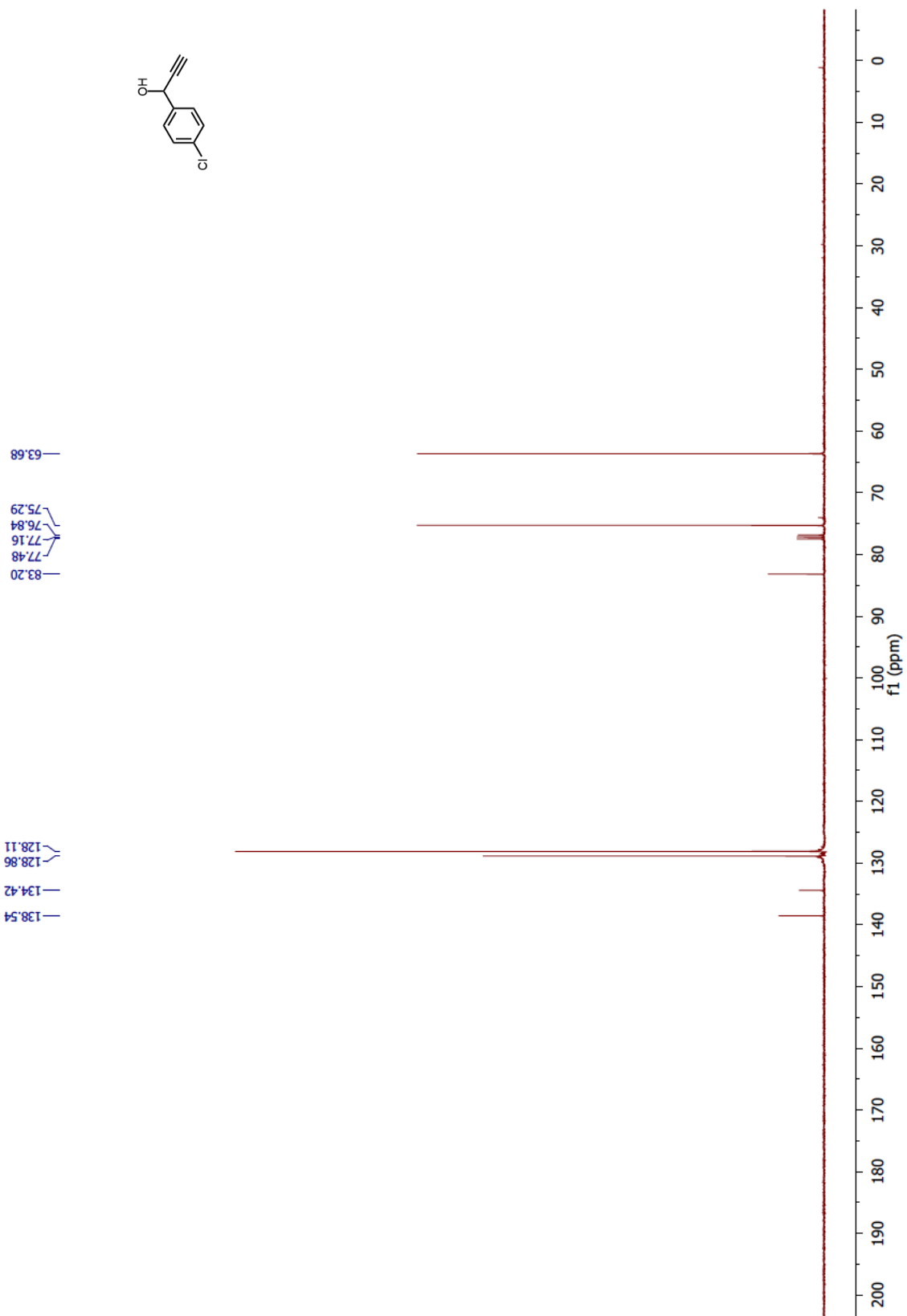


Figure 50. ¹³C-NMR spectrum of 43c in CDCl₃.

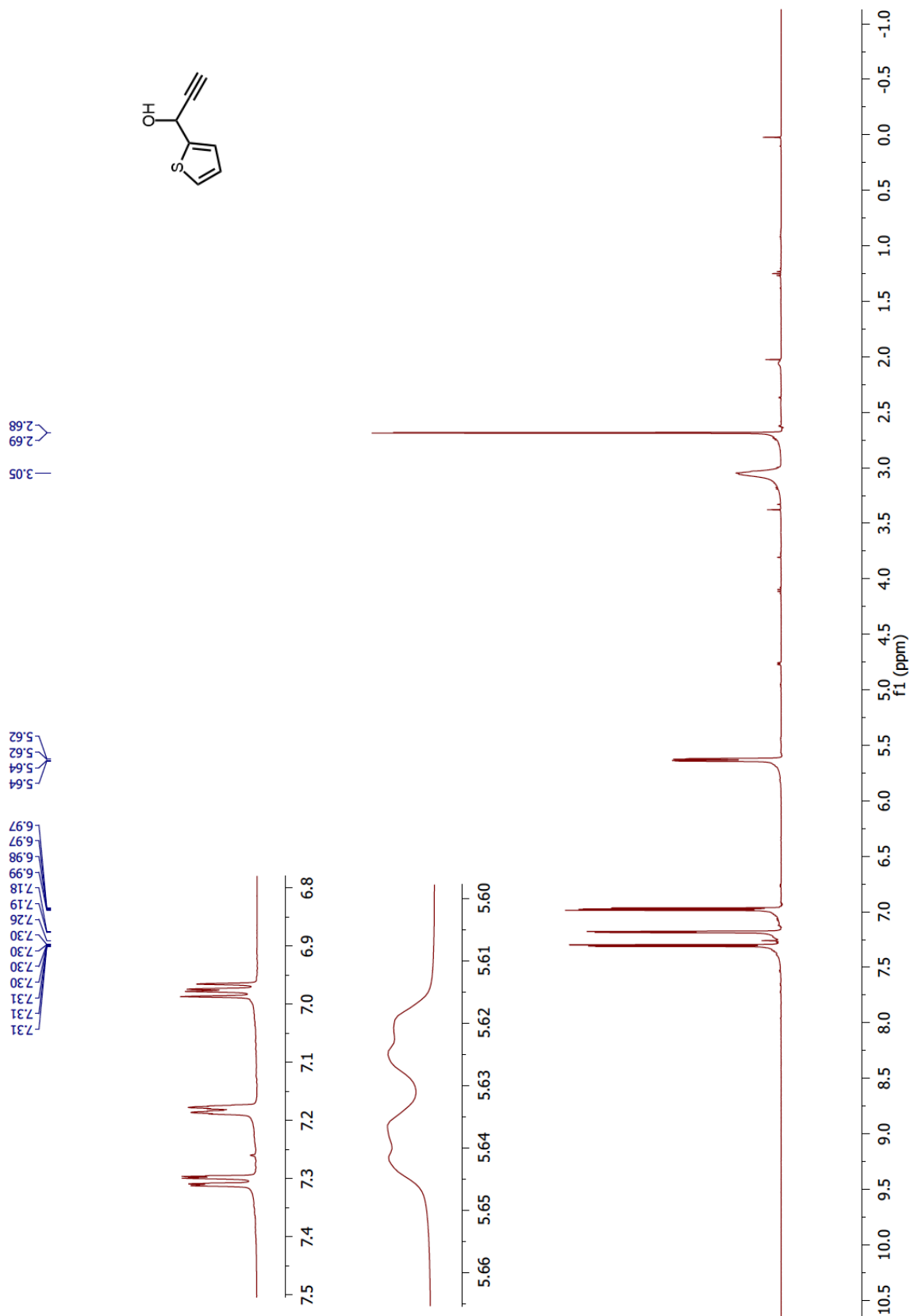


Figure 51. ¹H-NMR spectrum of 43d in CDCl₃.

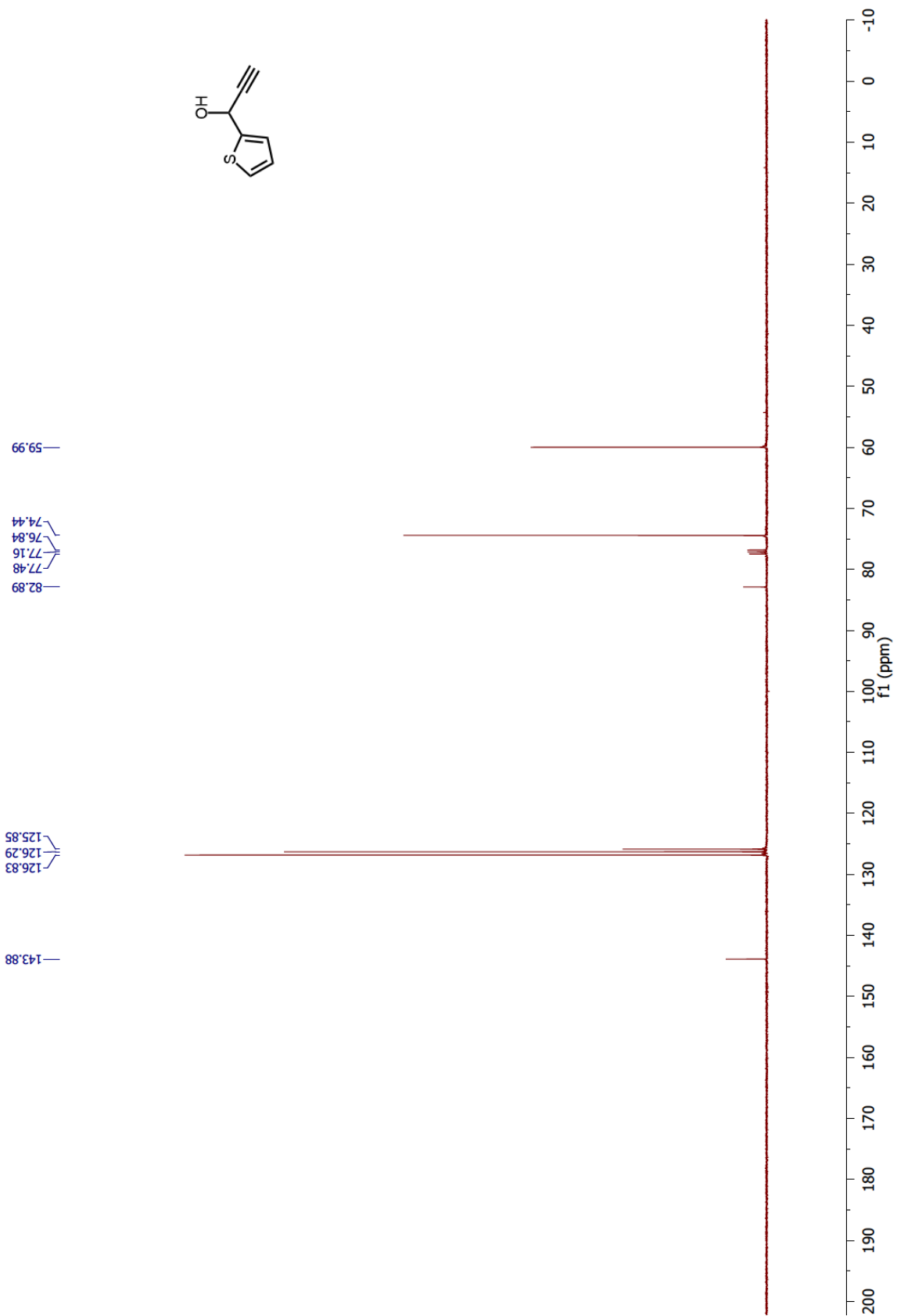


Figure 52. ¹³C-NMR spectrum of 43d in CDCl₃.

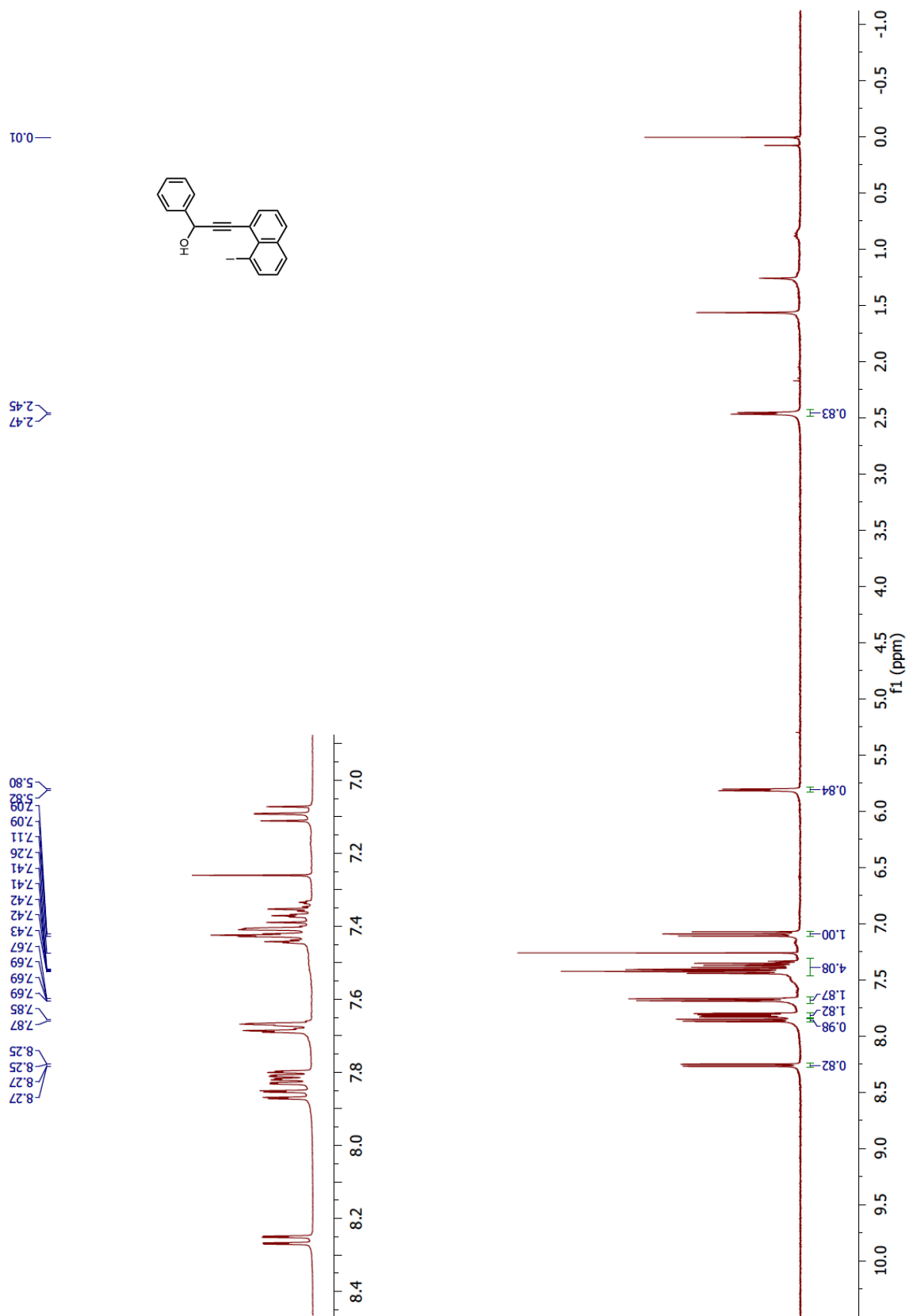


Figure 53. ¹H-NMR spectrum of **46a** in CDCl₃.

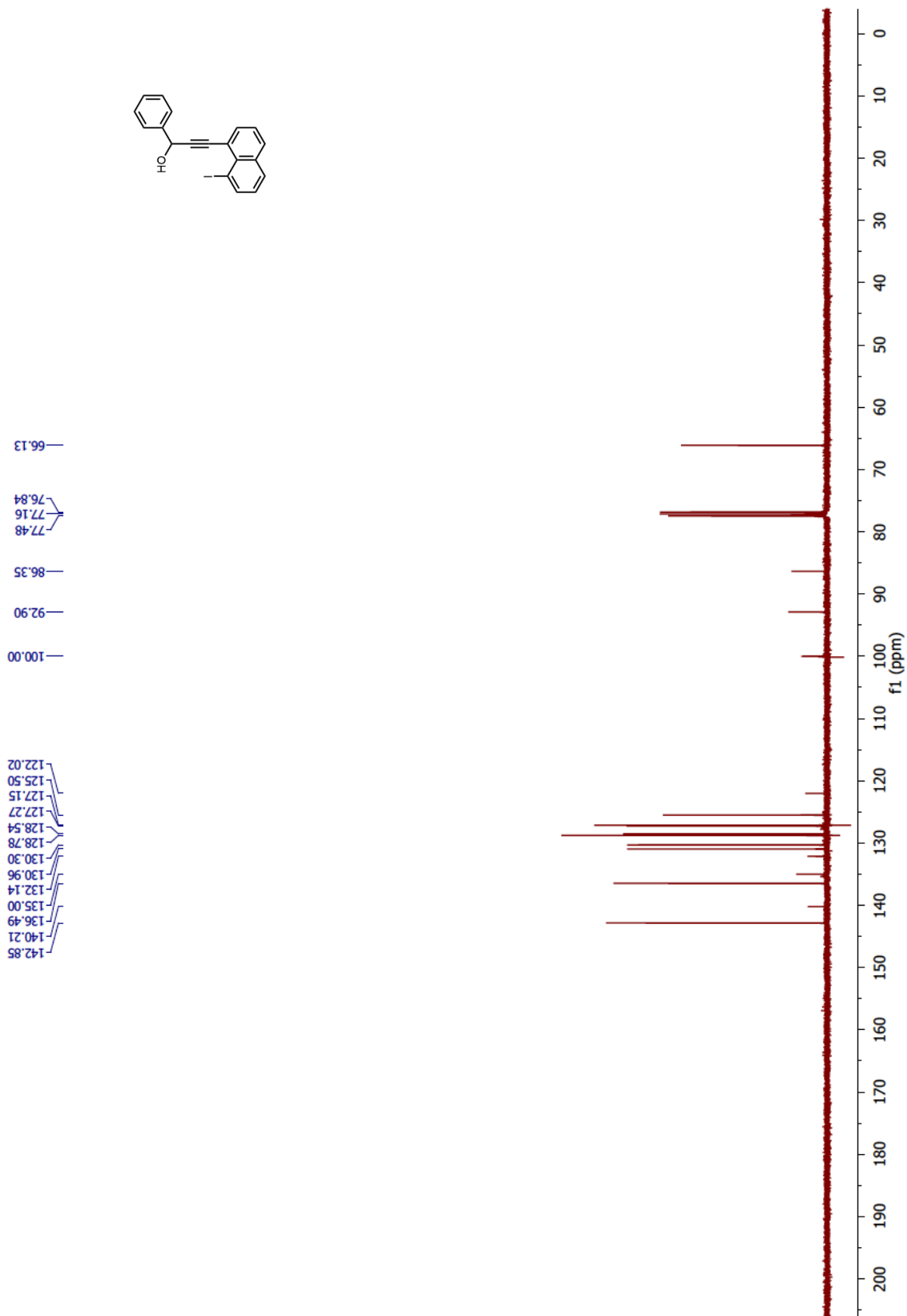
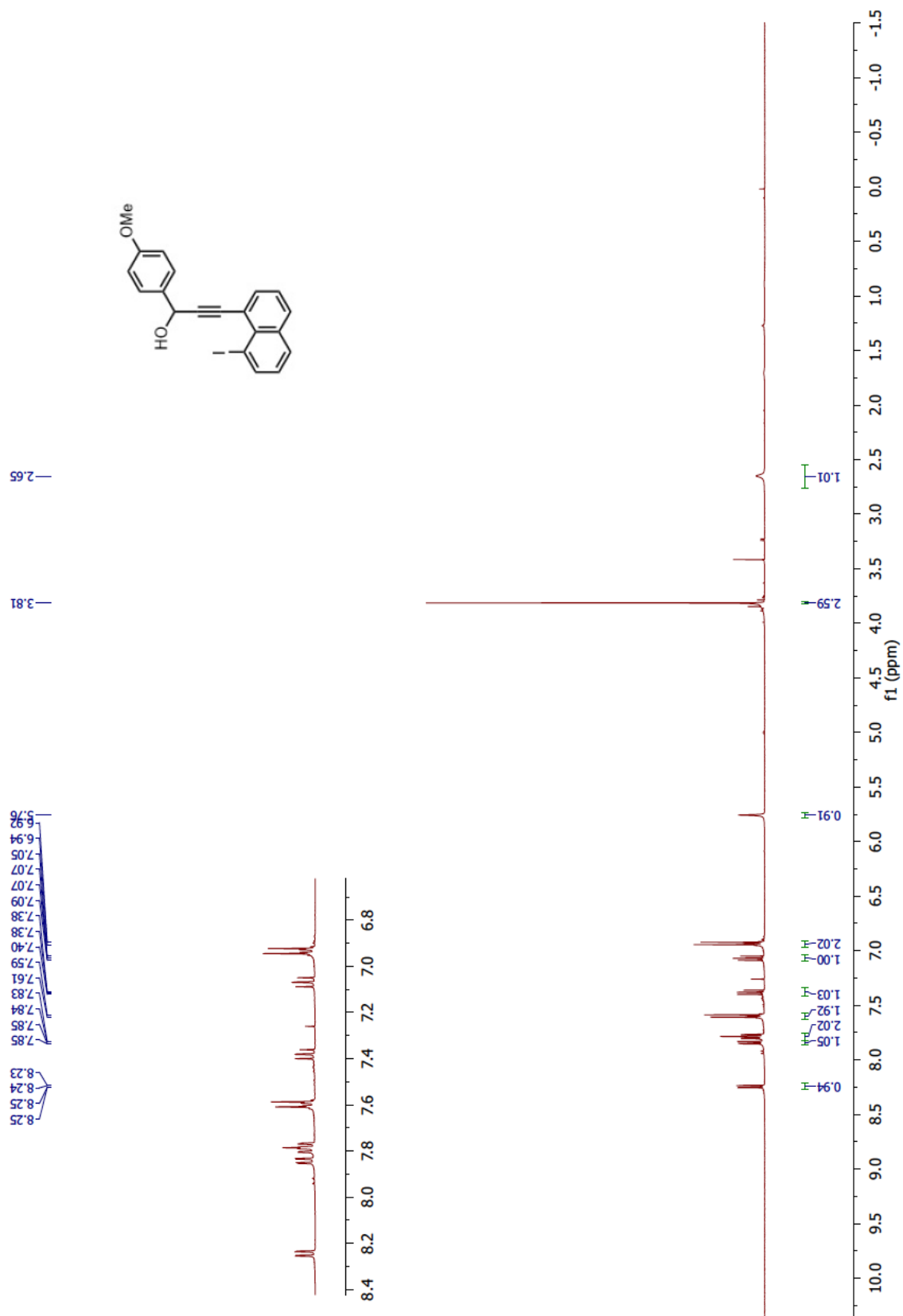


Figure 54. ¹³C-NMR spectrum of 46a in CDCl₃.



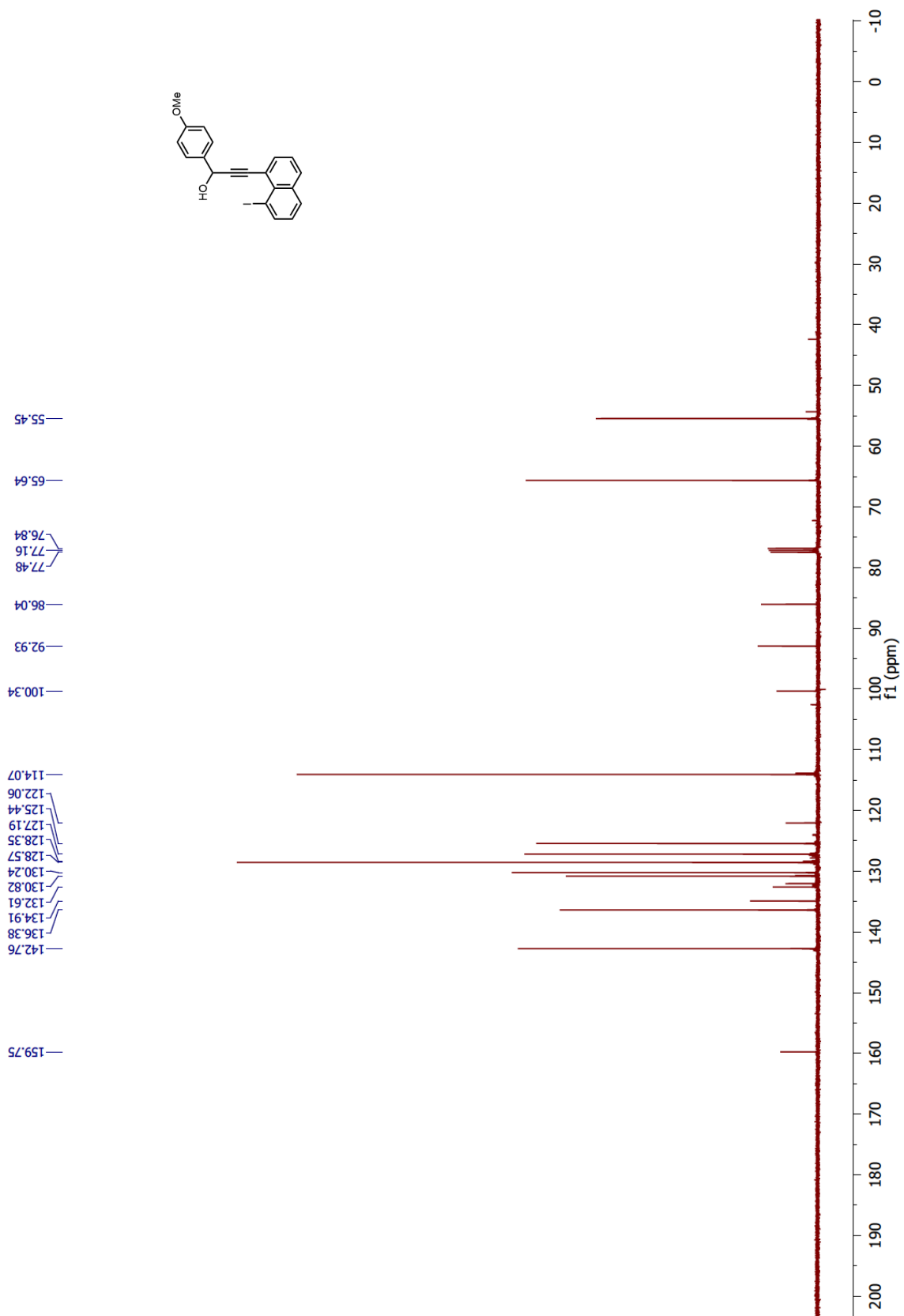


Figure 56. ^{13}C -NMR spectrum of **46b** in CDCl_3 .

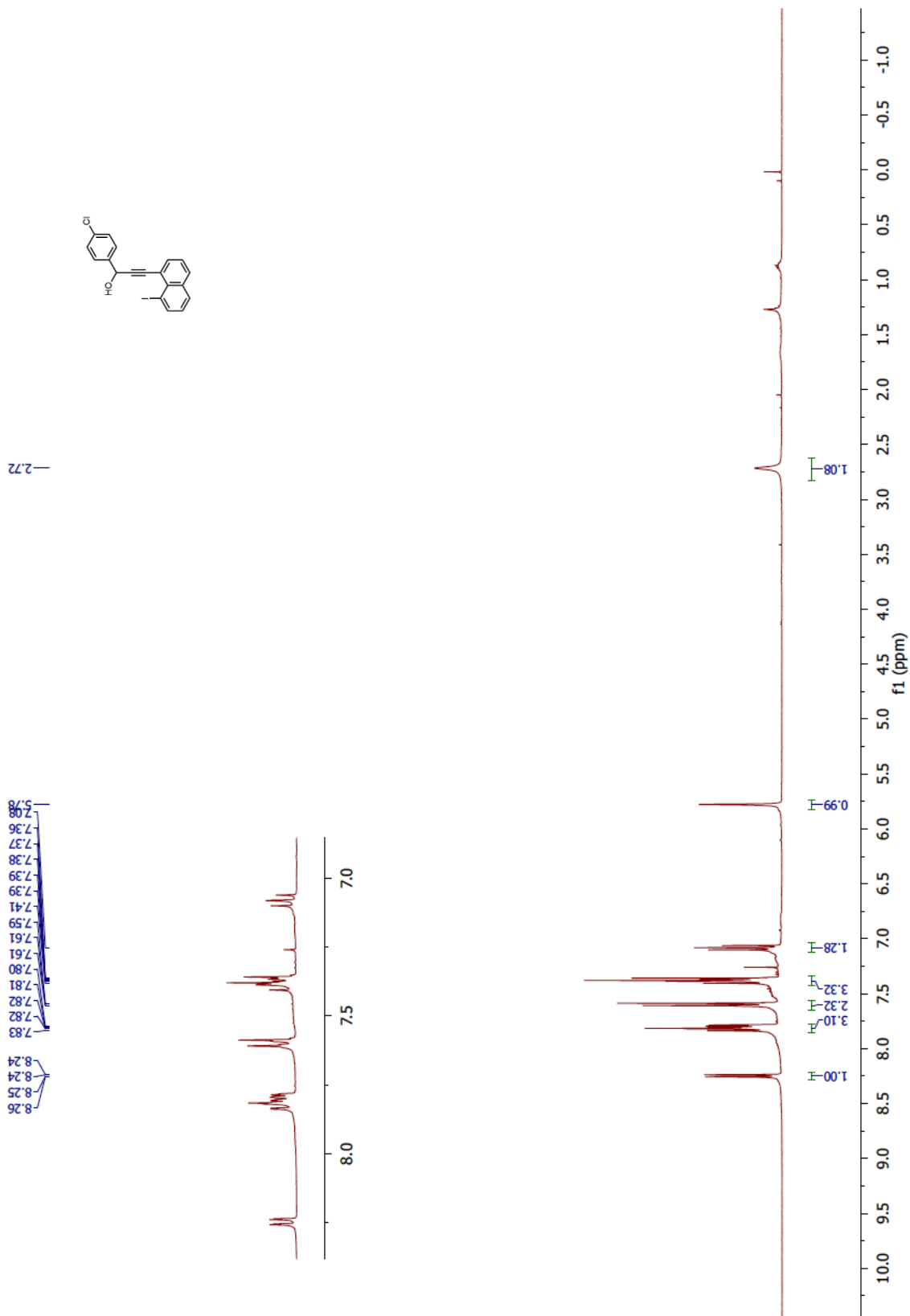


Figure 57. $^1\text{H-NMR}$ spectrum of **46c** in CDCl_3 .

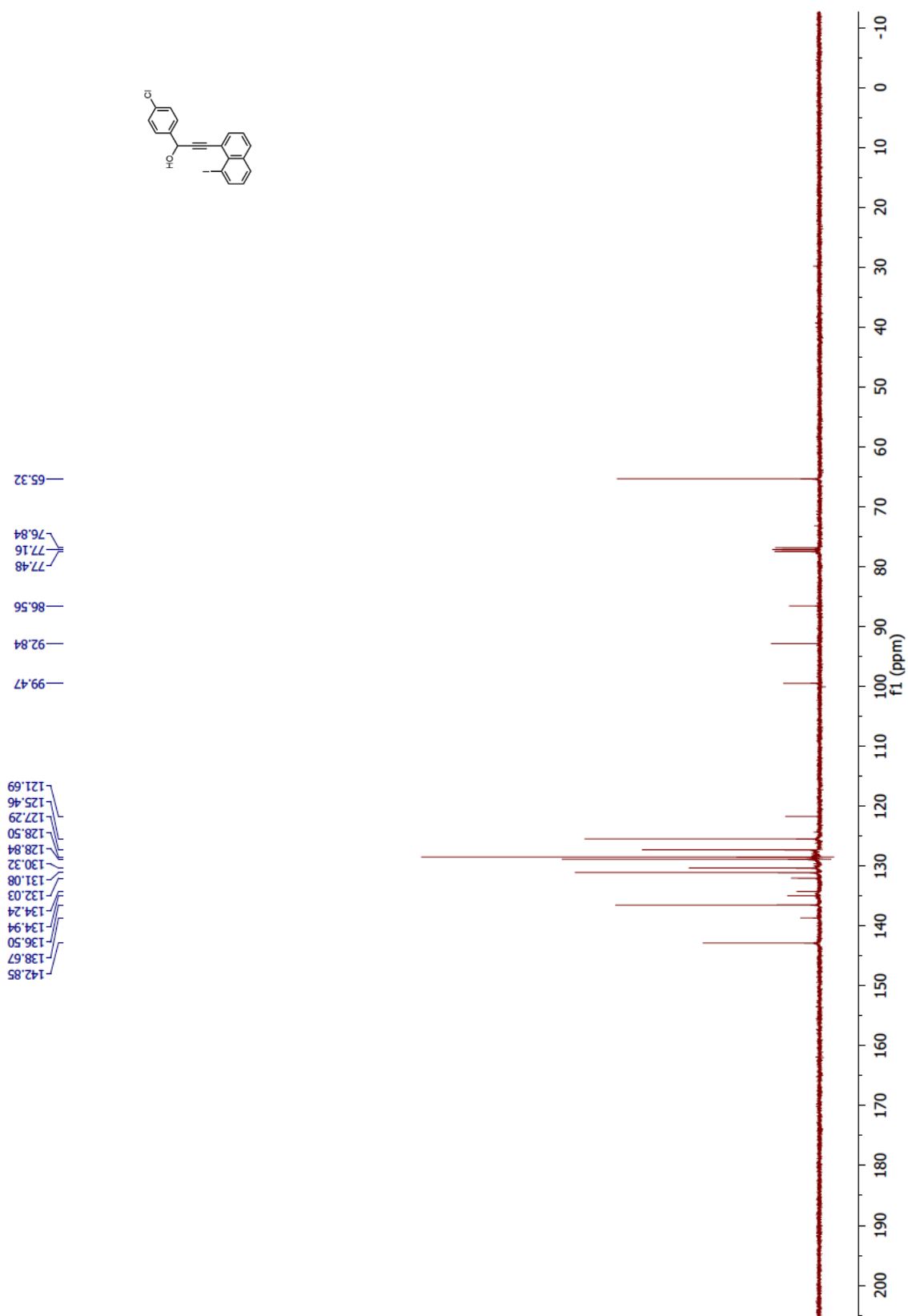


Figure 58. ^{13}C -NMR spectrum of 46c in CDCl_3 .

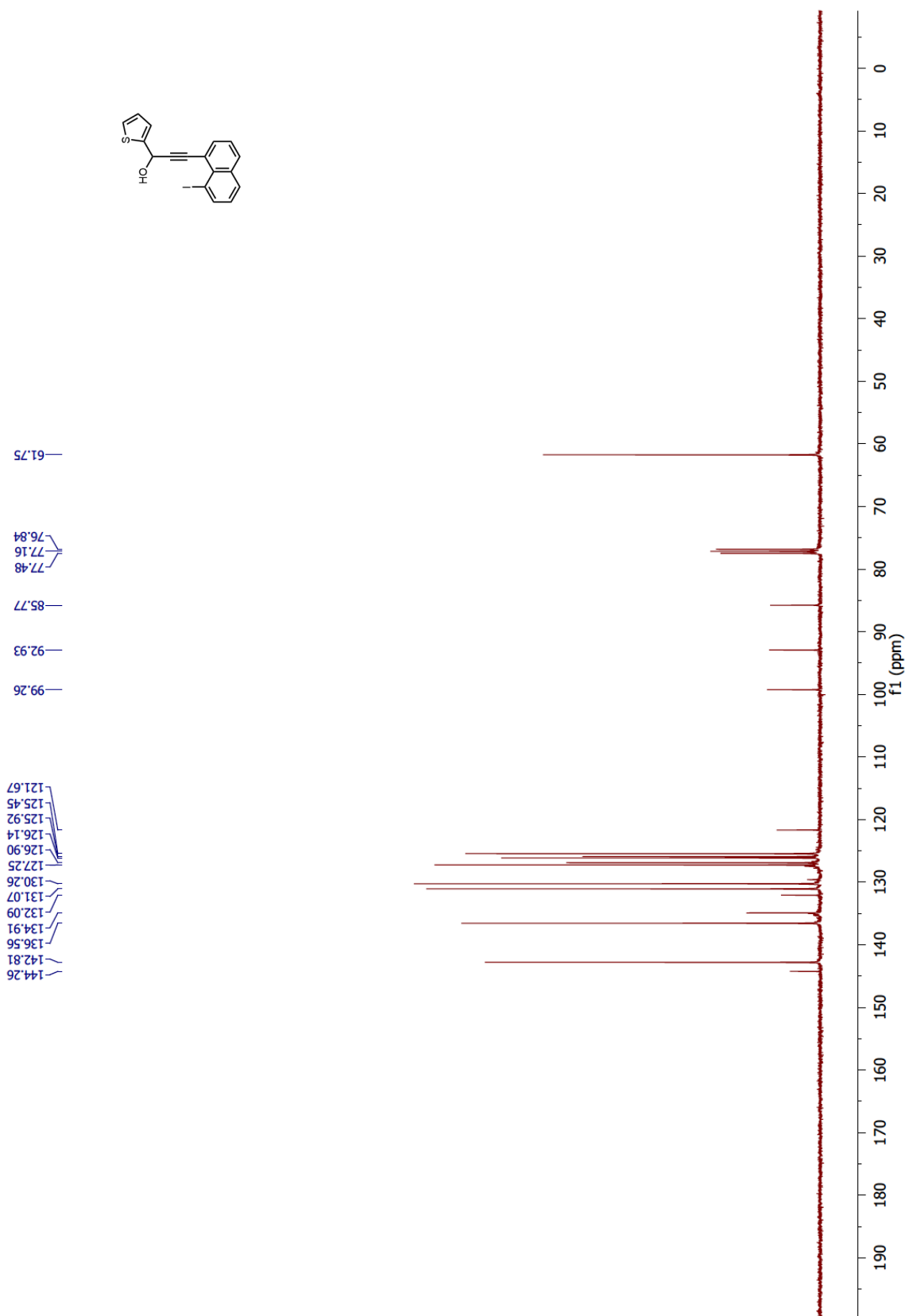


Figure 60. ^{13}C -NMR spectrum of **46d** in CDCl_3 .

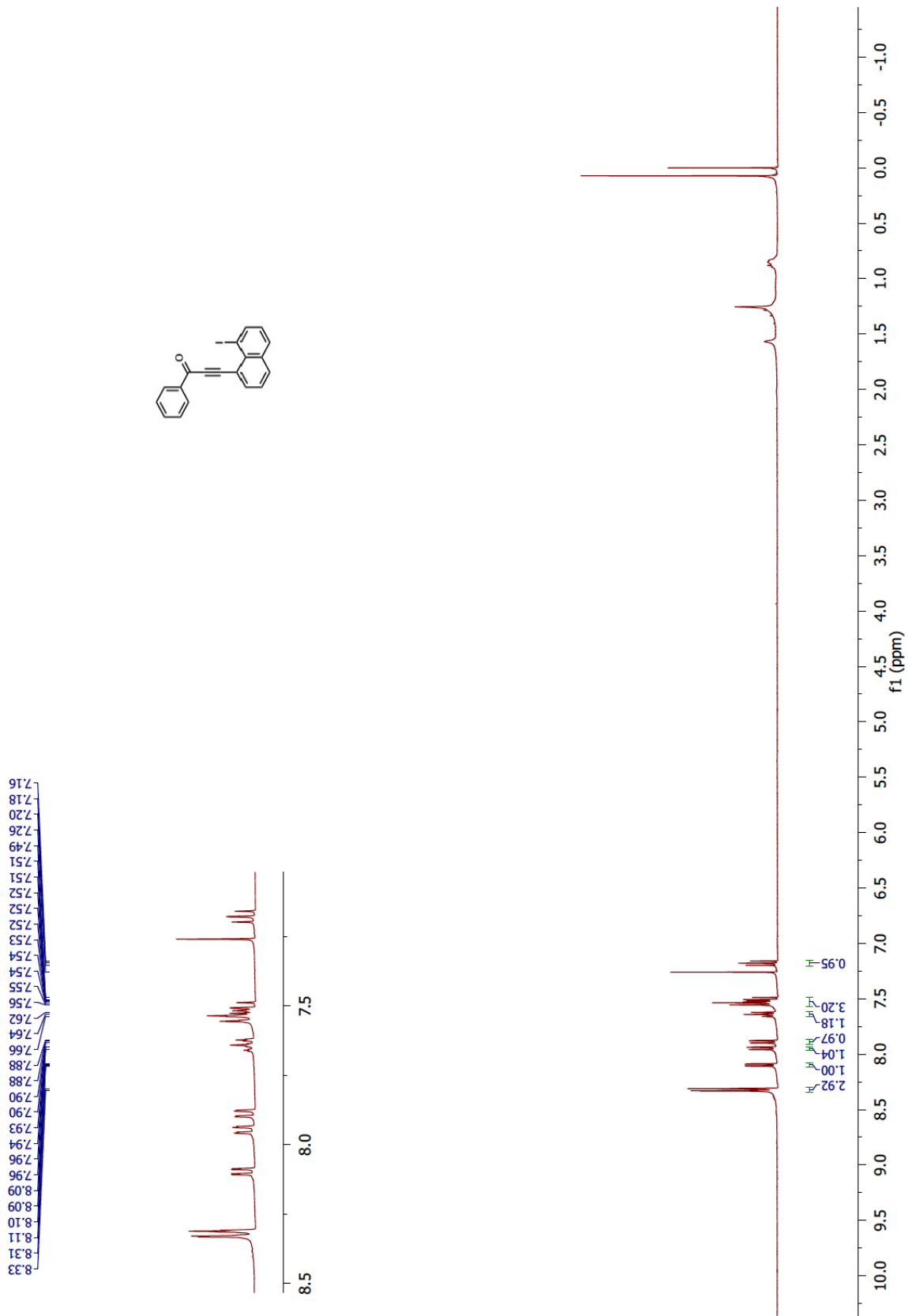


Figure 61. ¹H-NMR spectrum of **47a** in CDCl₃.

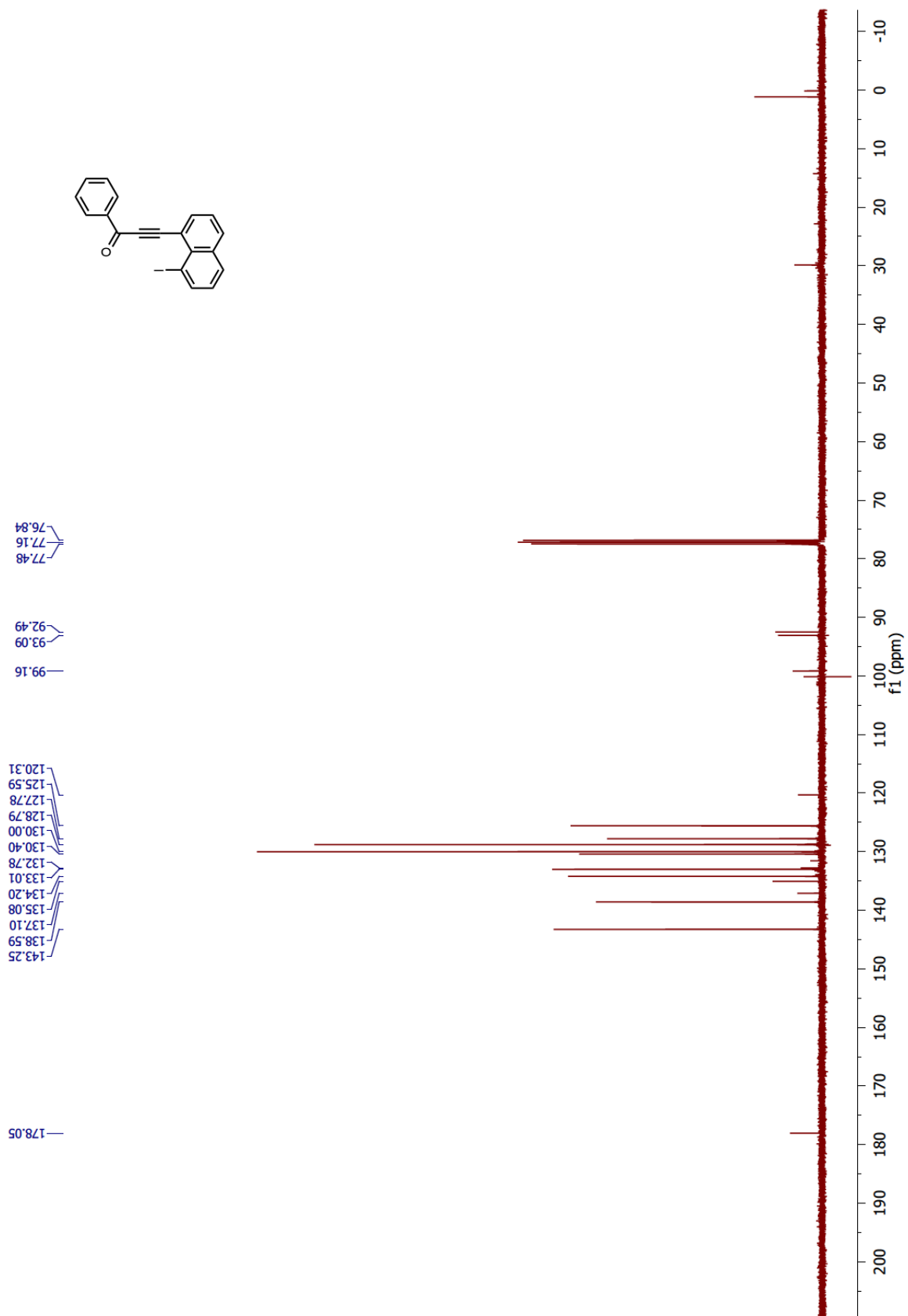


Figure 62. ^{13}C -NMR spectrum of **47a** in CDCl_3 .

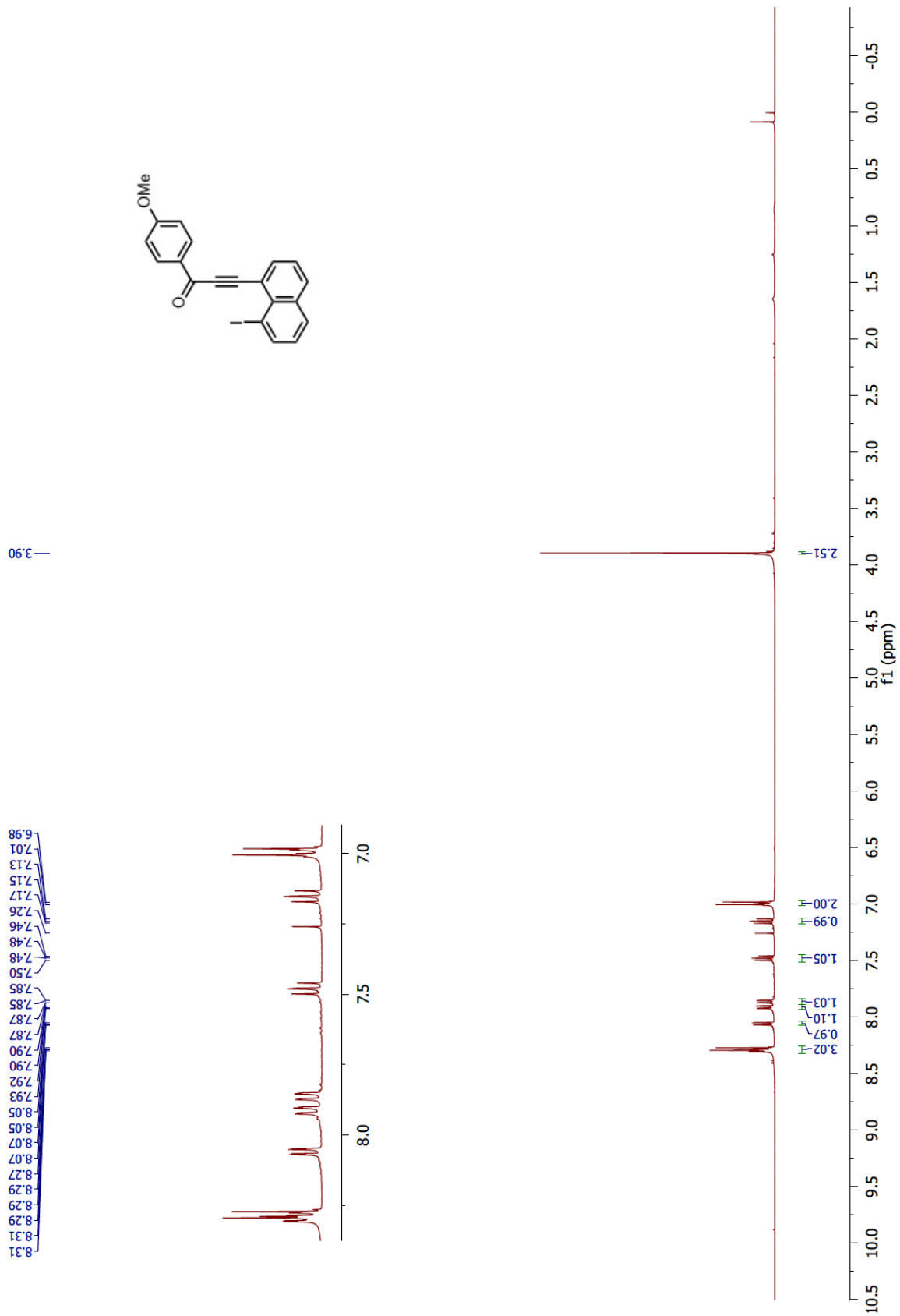


Figure 63. ¹H-NMR spectrum of **47b** in CDCl₃.

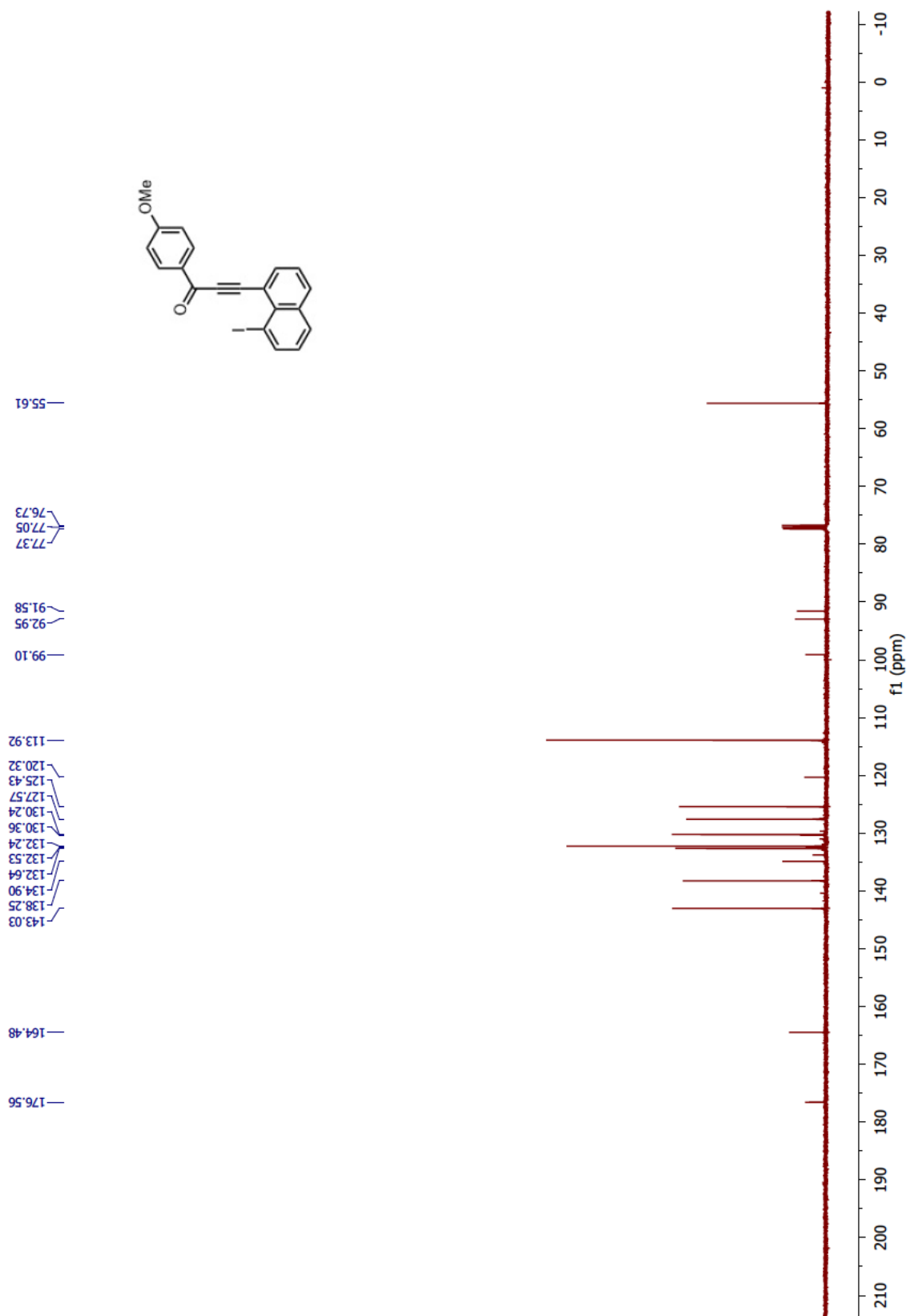


Figure 64. $^{13}\text{C-NMR}$ spectrum of 47b in CDCl_3 .

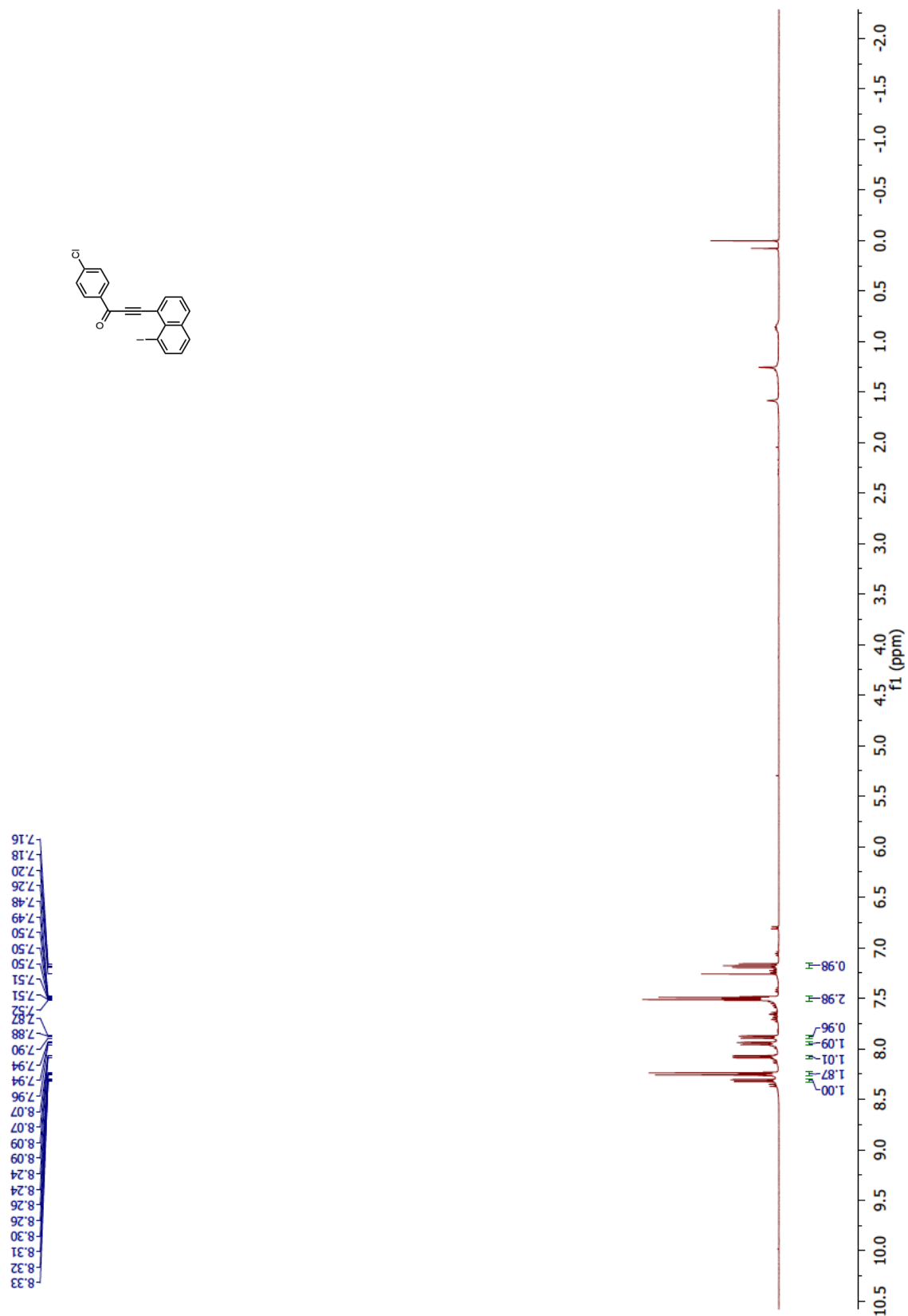


Figure 65. ¹H-NMR spectrum of 47c in CDCl₃.

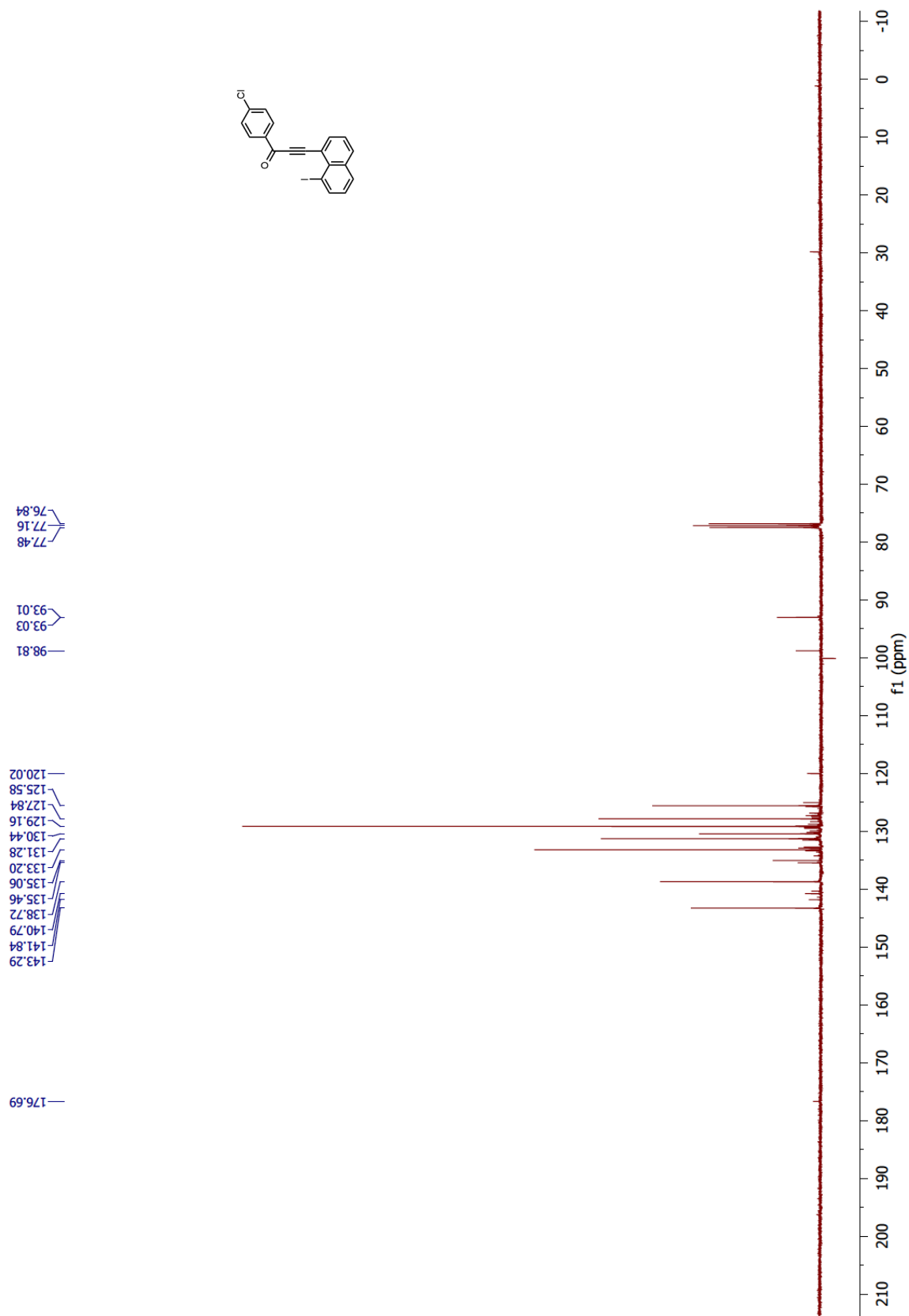


Figure 66. ¹³C-NMR spectrum of **47c** in CDCl₃.

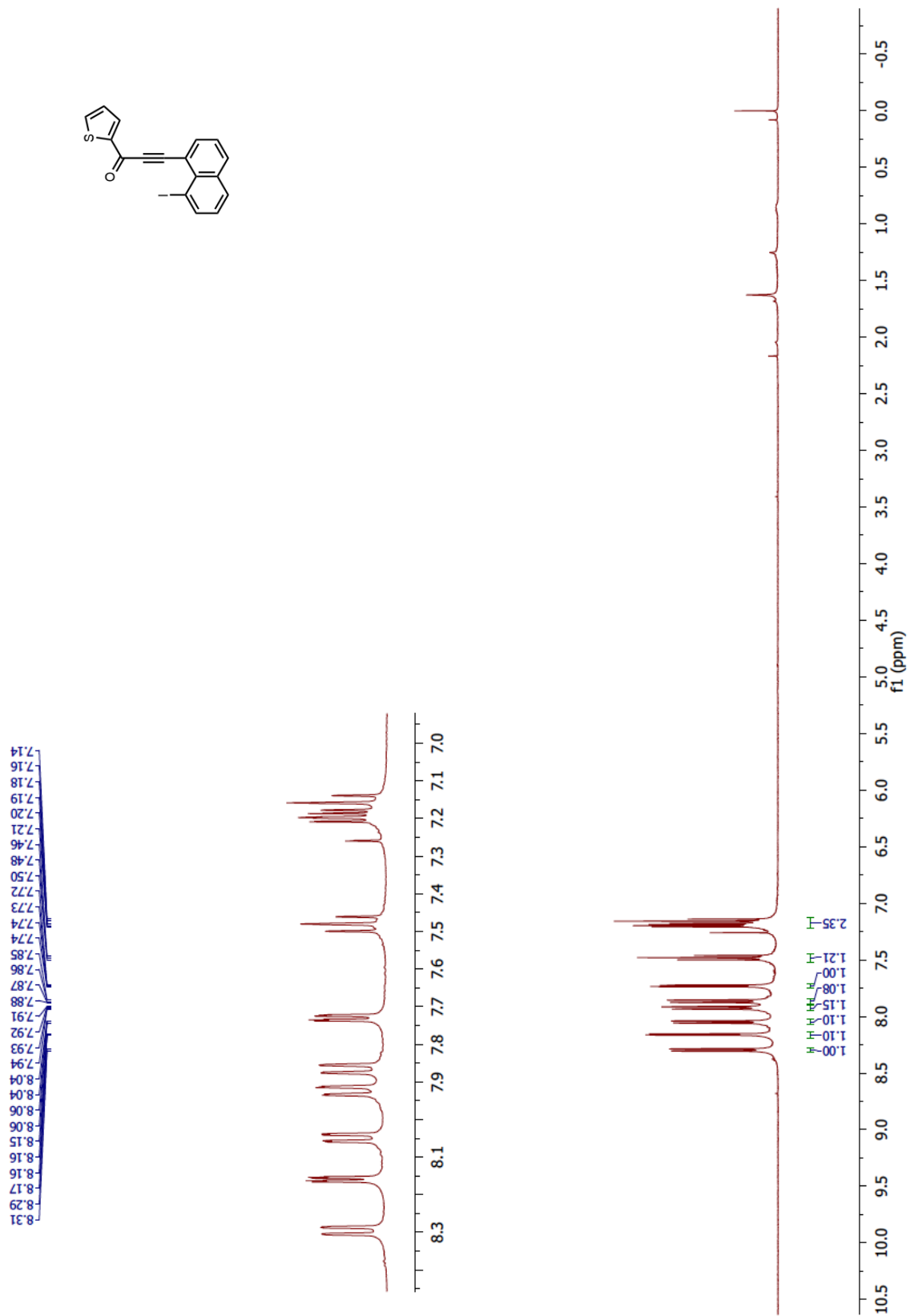


Figure 67. ¹H-NMR spectrum of **47d** in CDCl₃.

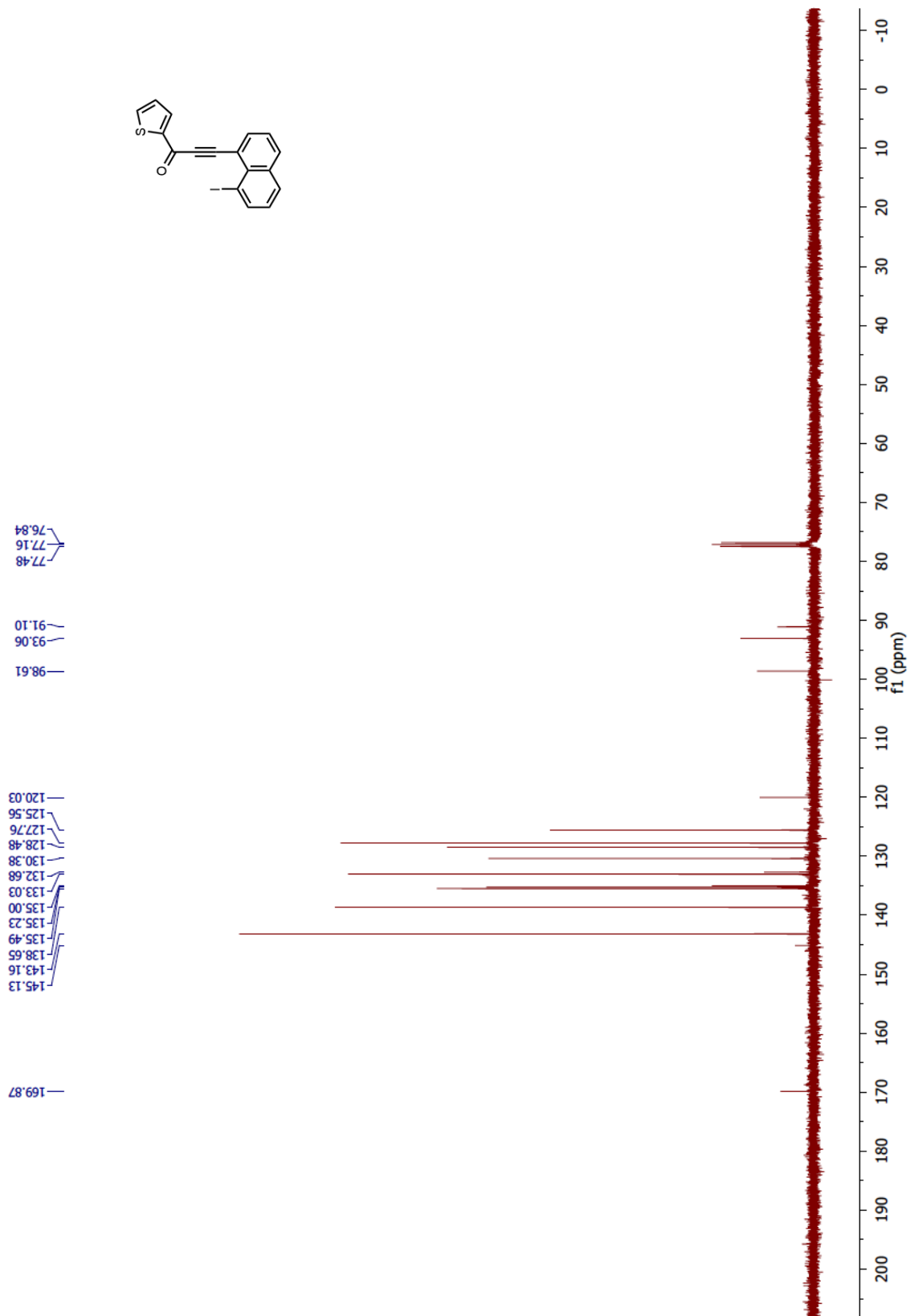


Figure 68. ^{13}C -NMR spectrum of **47d** in CDCl_3 .

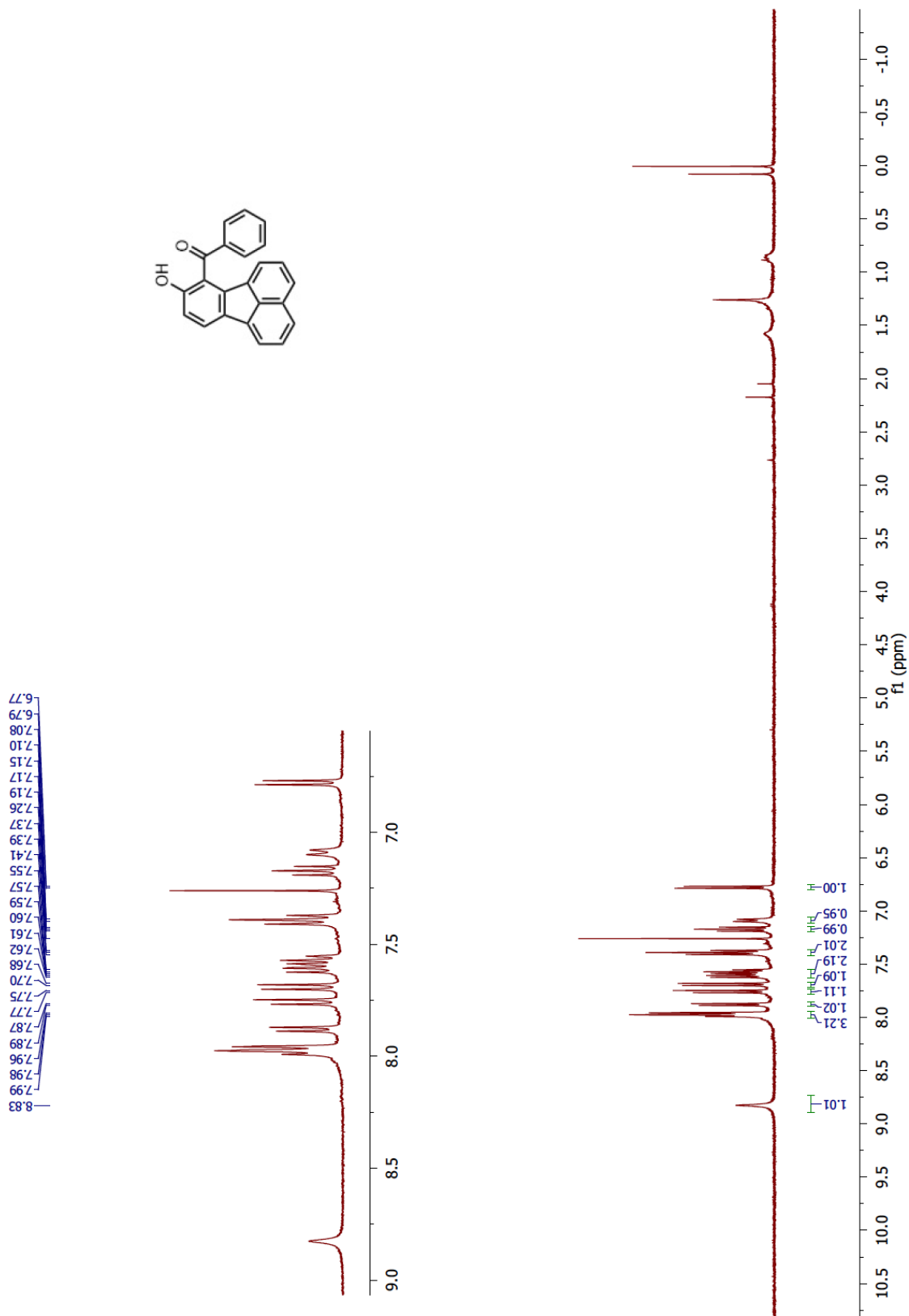


Figure 69. $^1\text{H-NMR}$ spectrum of **48a** in CDCl_3 .

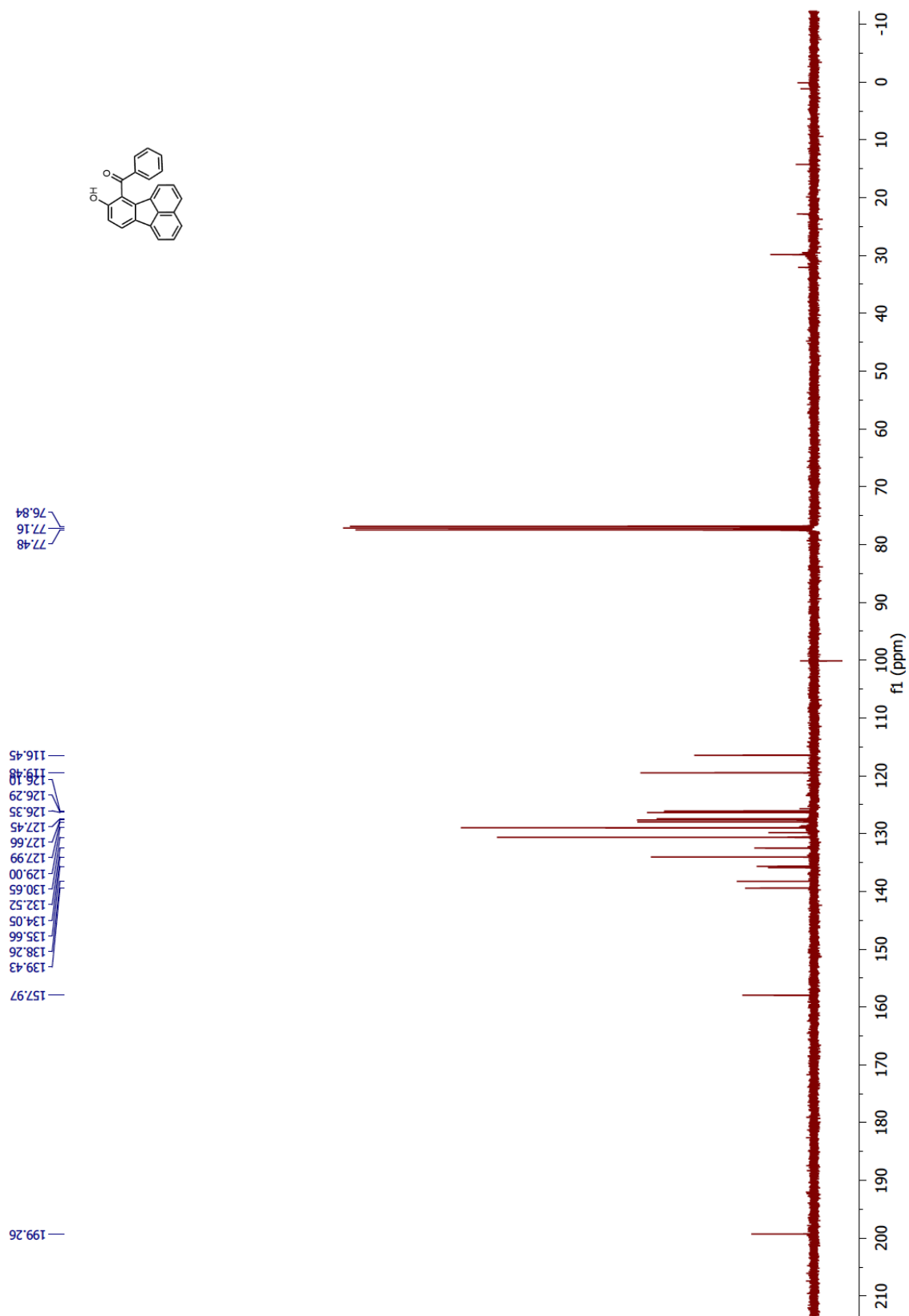


Figure 70. ¹³C-NMR spectrum of **48a** in CDCl₃.

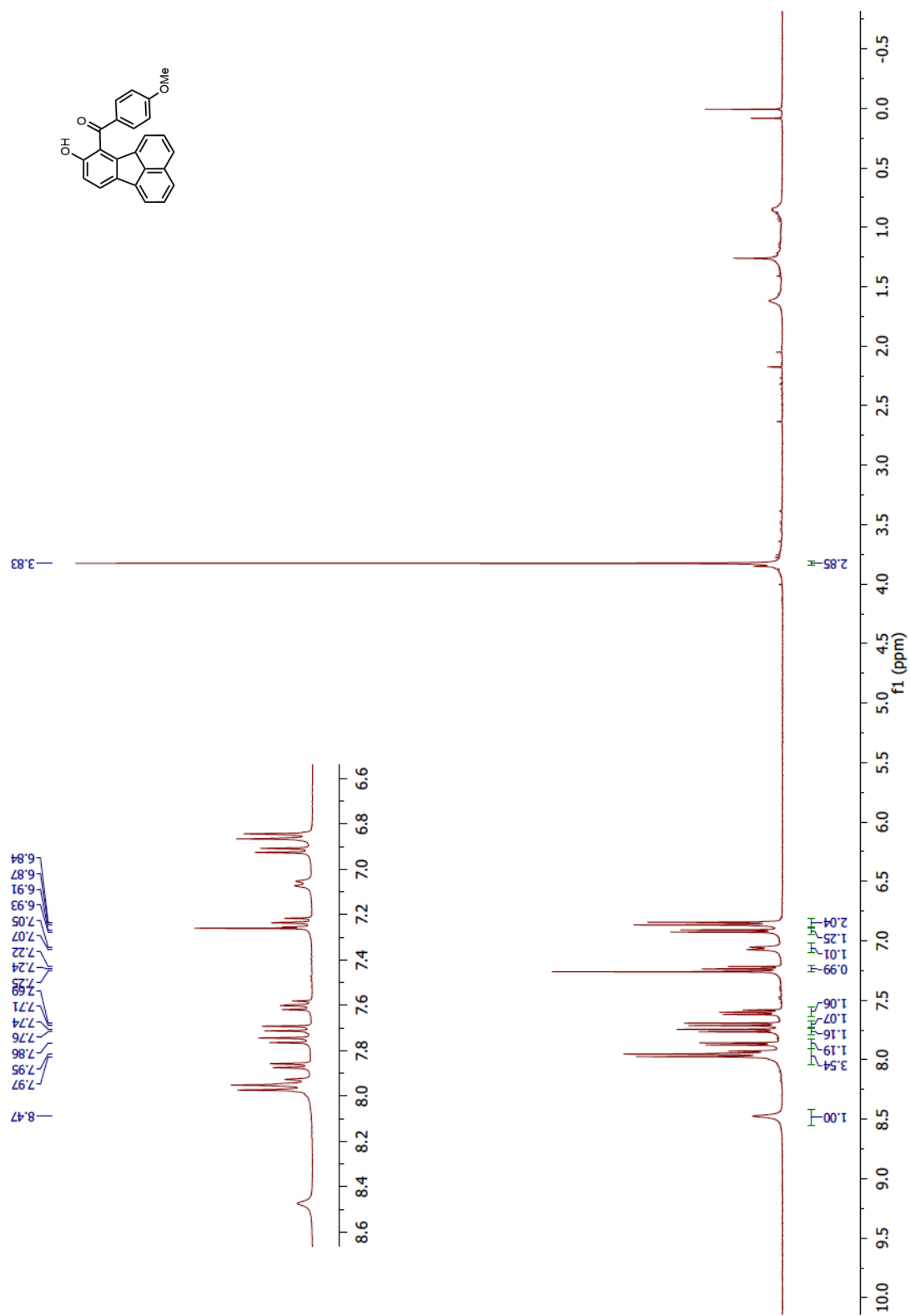


Figure 71. $^1\text{H-NMR}$ spectrum of **48b** in CDCl_3 .

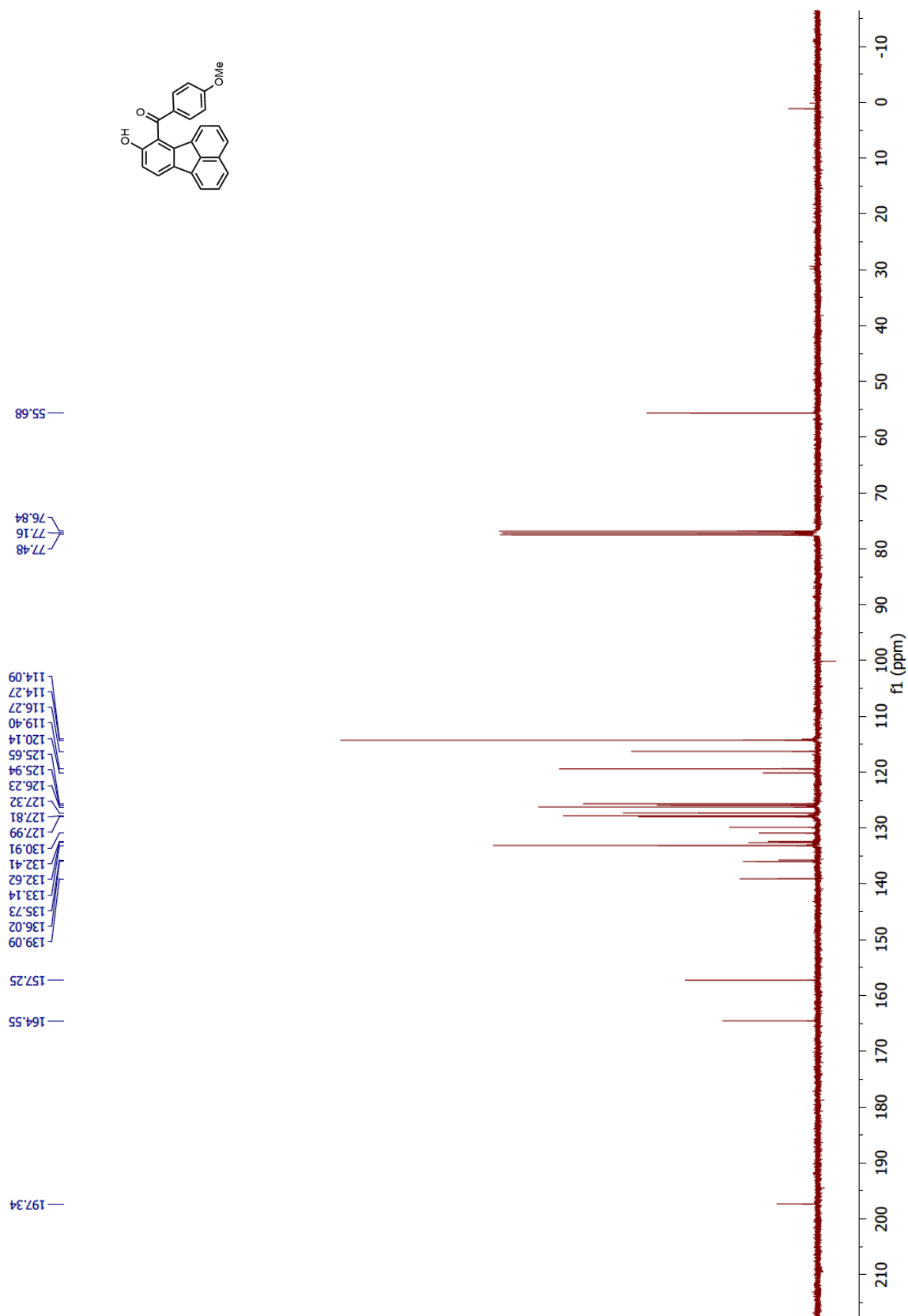


Figure 72. ¹³C-NMR spectrum of 48b in CDCl₃.

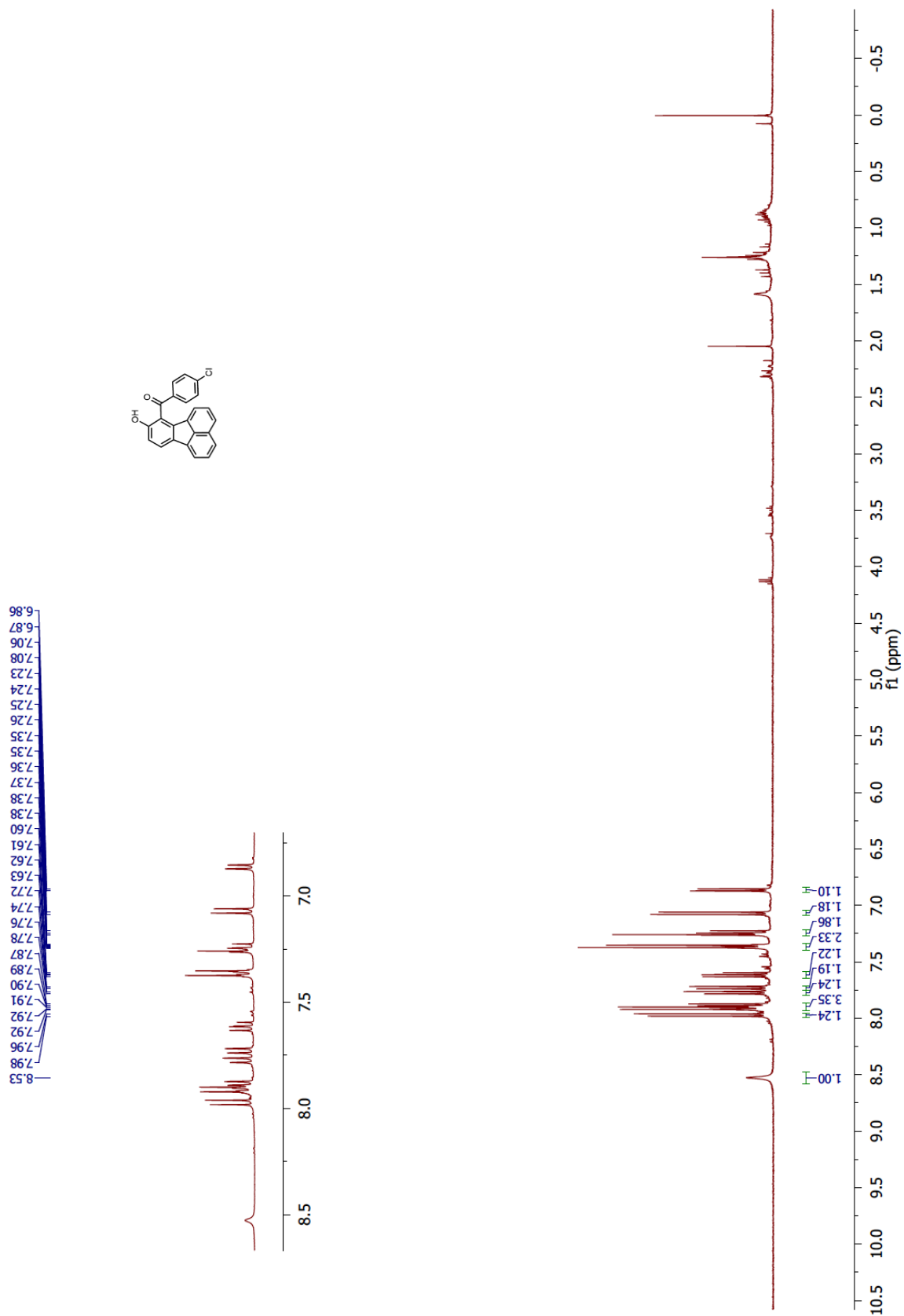


Figure 73. ¹H-NMR spectrum of 48c in CDCl₃.

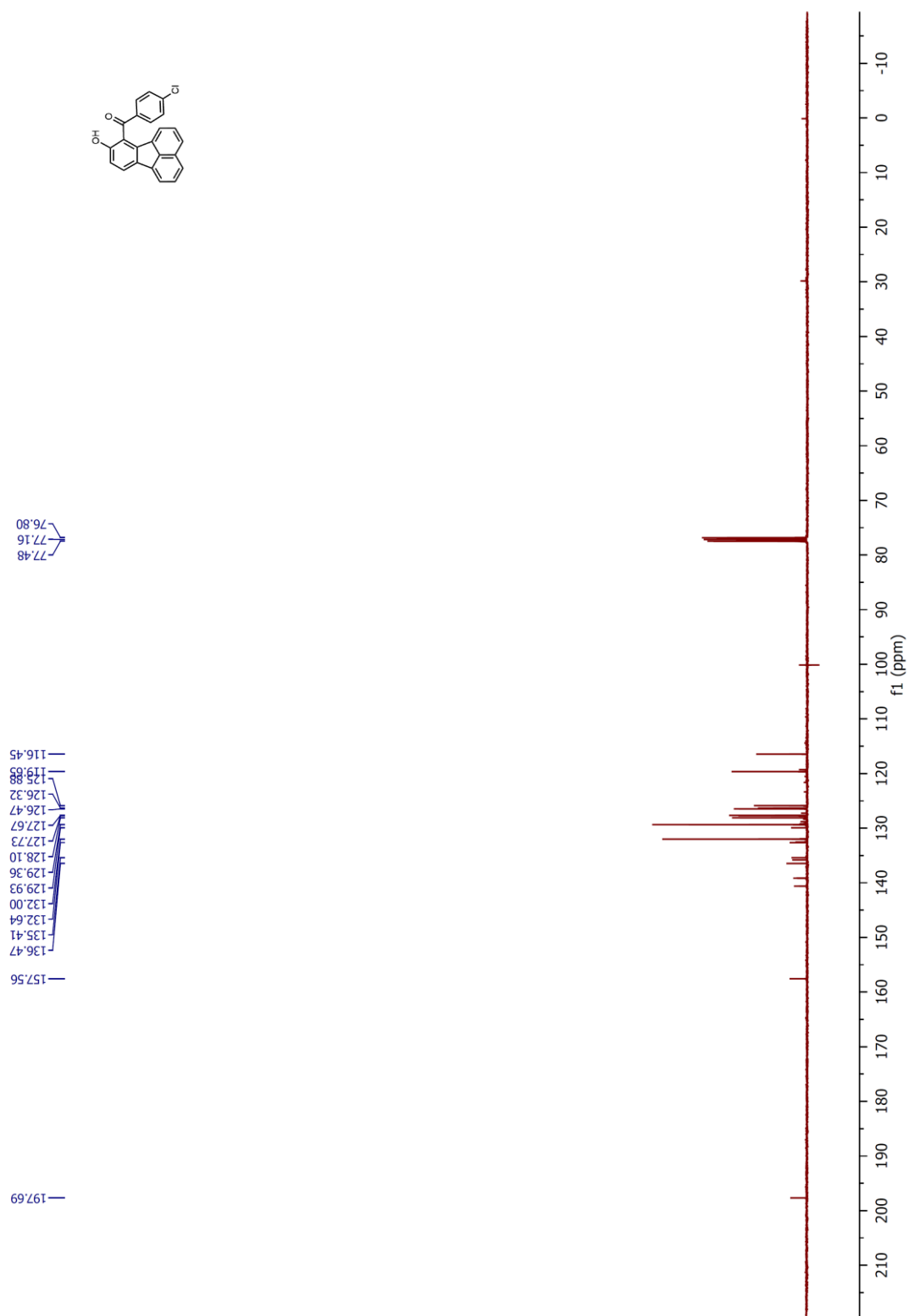


Figure 74. ¹³C-NMR spectrum of **48c** in CDCl₃.

DA-3-10a4
DA-3-10a4

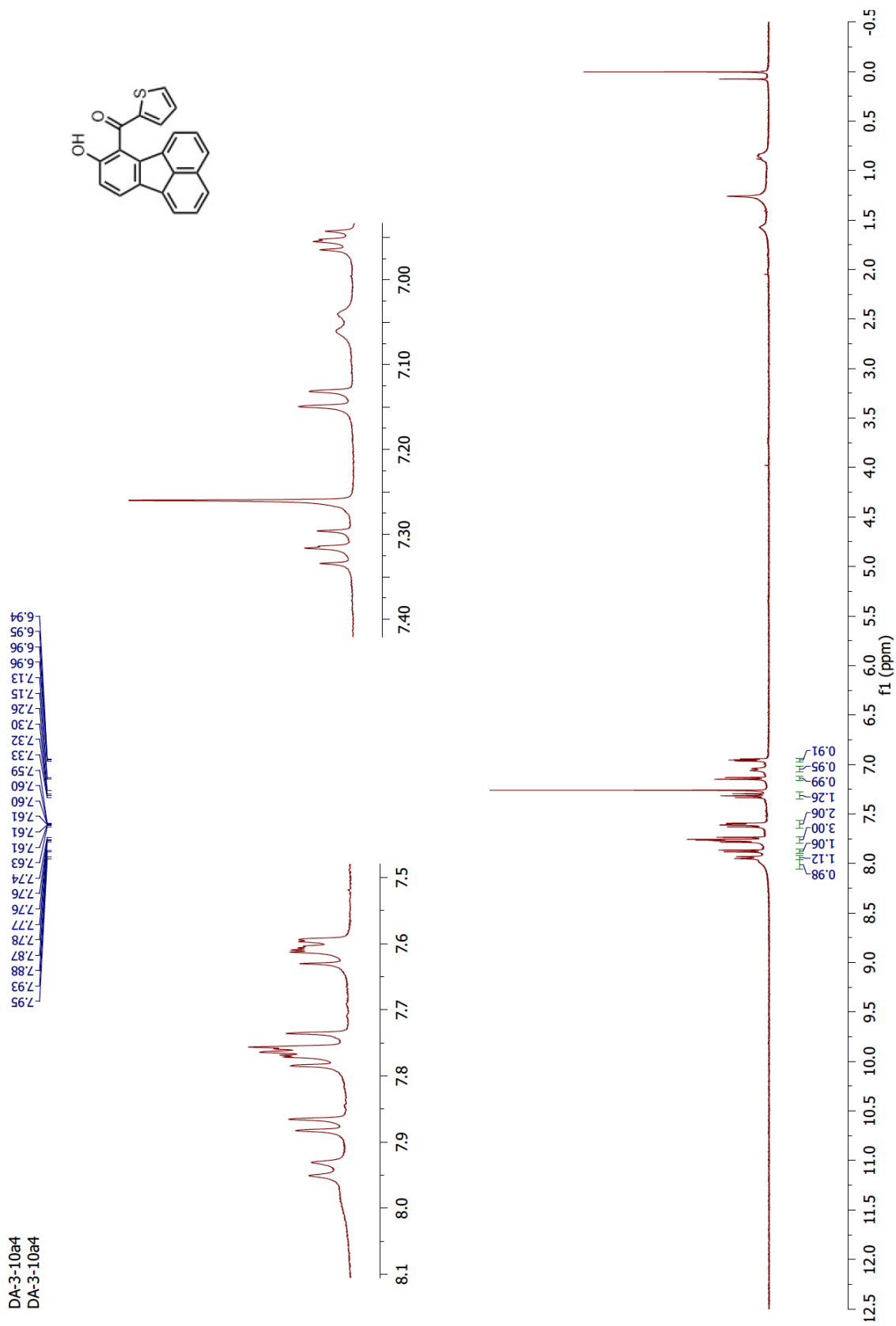


Figure 75. ¹H-NMR spectrum of **48d** in CDCl₃.

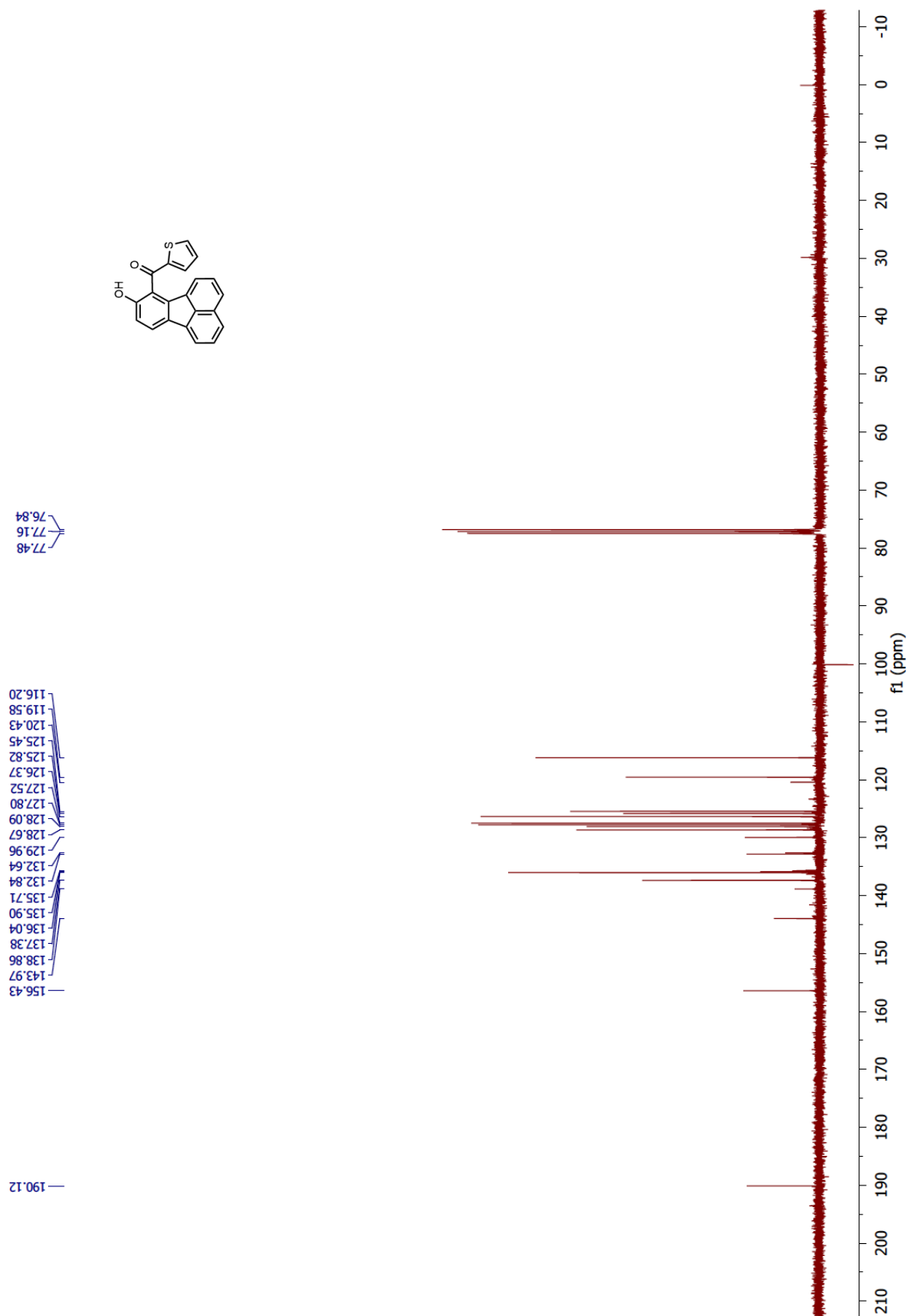


Figure 76. $^{13}\text{C-NMR}$ spectrum of 48d in CDCl_3 .

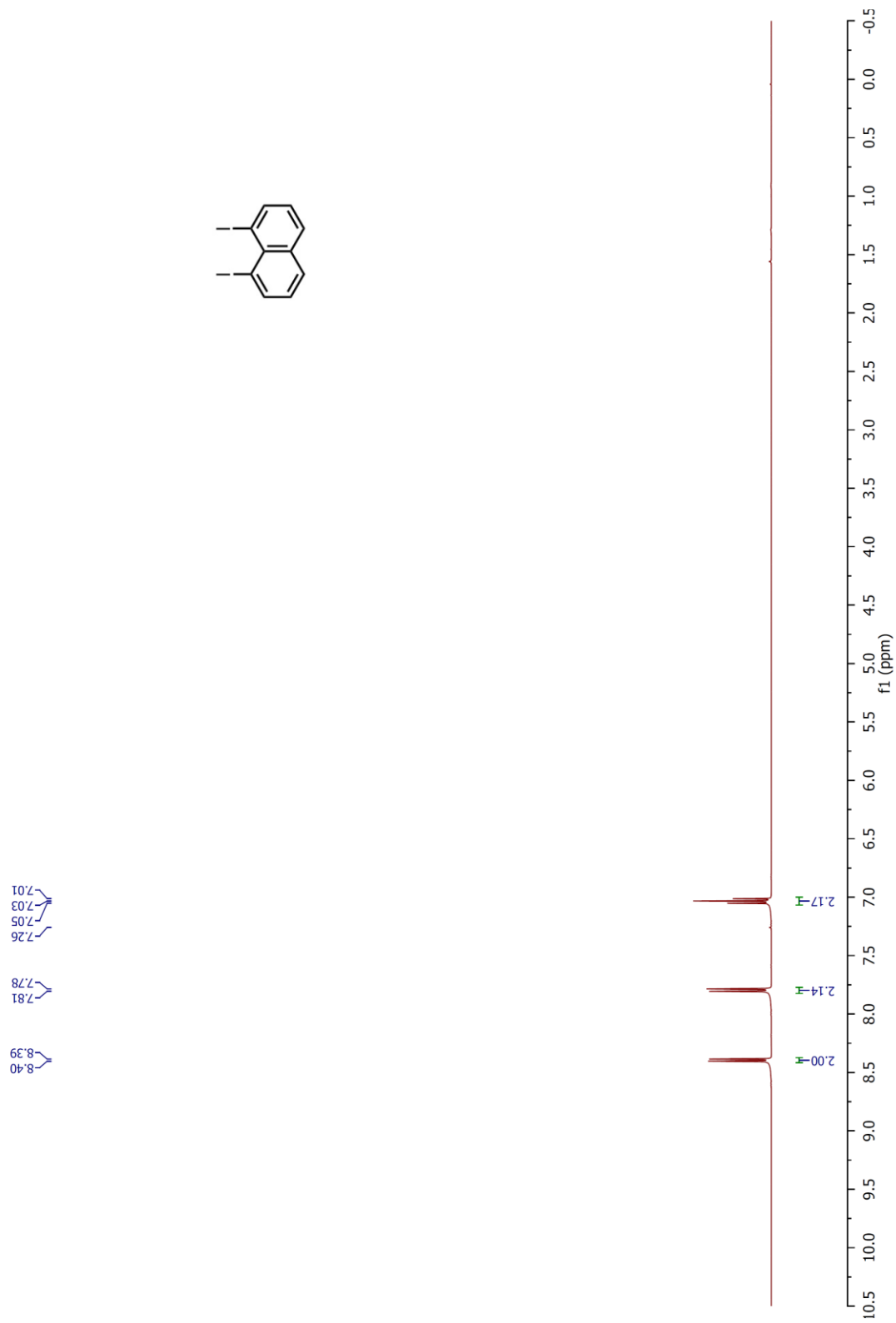


Figure 77. ¹H-NMR spectrum of **45** in CDCl₃.

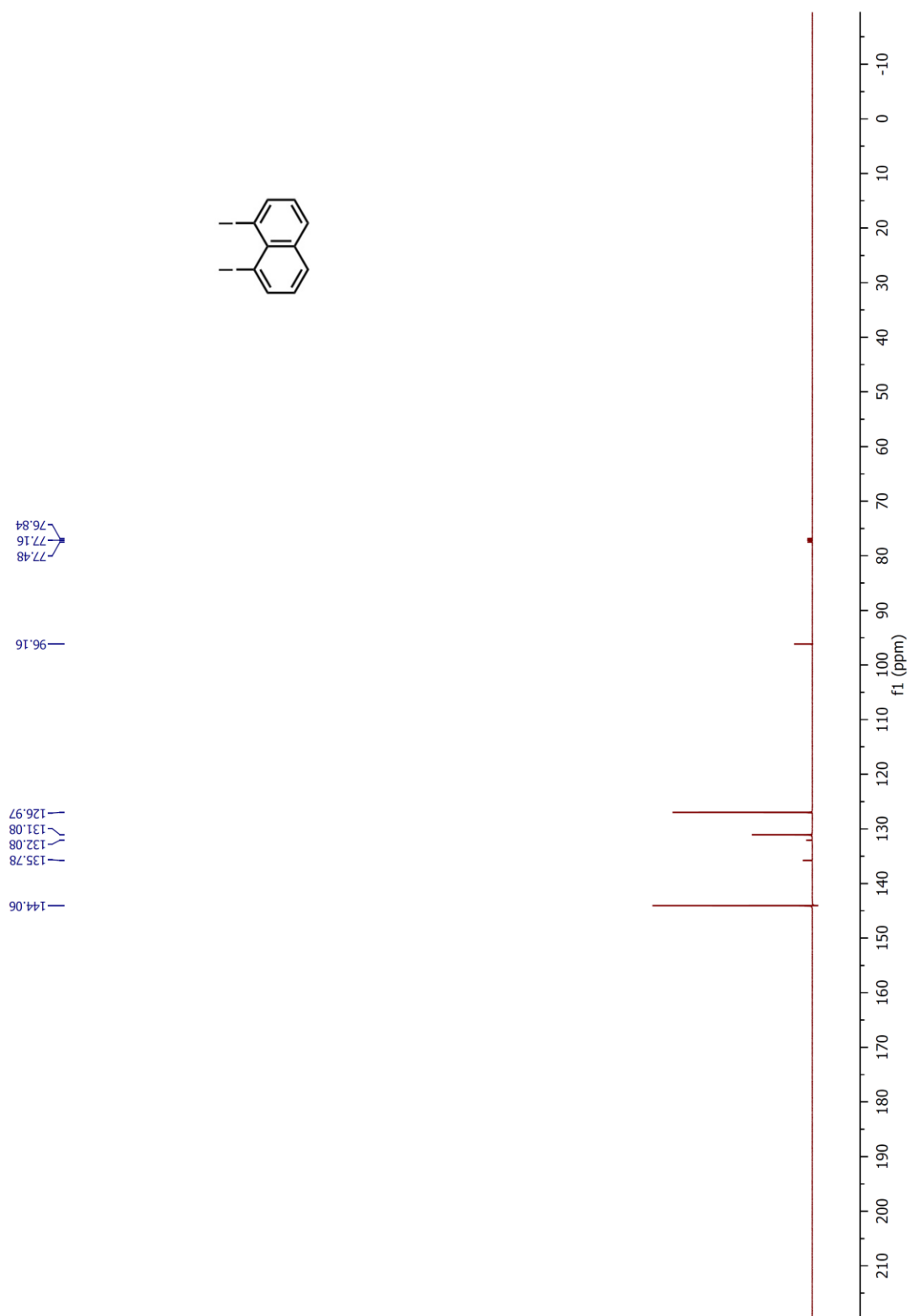


Figure 78. ¹³C-NMR spectrum of **45** in CDCl₃.

BIBLIOGRAPHY

-
- [1] Pal, S.; Metin, Ö.; Türkmen, Y. E. *ACS Omega*, **2017**, 2 (12), 8689-8696.
- [2] Sudarman, E.; Kuhnert, E.; Hyde, K. D.; Sir, E. B.; Surup, F.; Stadler, M. *Tetrahedron*, **2016**, 72 (41), 6450-6454.
- [3] Fukai, M.; Tsukada, M.; Miki, K.; Suzuki, T.; Sugita, T.; Kinoshita, K.; Takahashi, K.; Shiro, M.; Koyama, K. *J. Nat. Prod.* **2012**, 75 (1), 22-25.
- [4] Quang, D.N.; Hashimoto, T.; Tanaka, M.; Baumgartner, M.; Stadler, M. Asakawa, Y. *J. Nat. Prod.* **2002**, 65 (12), 1869-1874, b) Gu, W.; Ge, H.M.; Song, Y. C.; Ding, H.; Zhu, H. L.; Zhao, X.A.; Tan, R.X. *J. Nat. Prod.* **2007**, 70 (1), 114-117, c) Du, L.; King, J. B.; Cichewicz, R.H. *J. Nat. Prod.* **2014**, 77 (11), 2454-2458, d) Liu, Y.; Stuhldreier, F.; Kurtán, T.; Mándi, A.; Arumugam, S.; Lin, W.; Stork, B.; Wesselborg, S.; Weber, H.; Henrich, B.; Daletos, G.; Proksch, P. *RSC Adv.* **2017**, 7, 5381–5393.
- [5] Raymond L. E.; Howard J. L. *J. Chem. Soc., Perkin Trans. 1*, **1976**, 2149-2155.
- [6] (a) Yamashita, Y.; Fujii, N.; Murakata, C.; Ashizawa, T.; Okabe, M.; Nakano, H. *Biochemistry* **1992**, 31, 12069; (b) Fujii, N.; Yamashita, Y.; Saitoh, Y.; Nakano, H. *The Journal of Biological Chemistry* **1993**, 268, 13160.
- [7] Wrigley, S. K.; Ainsworth, A. M.; Kau, D. A.; Martin, S. M.; Bahl, S.; Tang, J. S.; Hardick, D. J.; Rawlins, P.; Sadheghi, R.; Moore, M. *The Journal of Antibiotic*, **2001**, 54 (6), 479-488.

-
- [8] Zhang, Y. L.; Zhang, J.; Jiang, N.; Lu, Y. H.; Wang, L.; Xu, S. H.; Wang, W.; Zhang, G. F.; Xu, Q.; Ge, H. M.; Ma, J.; Song, Y. C.; Tan, R. X. *J. Am. Chem. Soc.* **2011**, *133* (15), 5931–5940.
- [9] Lahore, S.; Narkhede, U.; Merlini, L.; Dalavalle, S. *J. Org. Chem.* **2013**, *78* (21), 10860–10866.
- [10] Tatsuta, K.; Sekine, D.; Hayama, S.; Kataoka, Y.; Hayashi, S.; Hosokawa, S. *J. Org. Chem.* **2018**, *83* (13), 7010–7018.
- [11] Pardee, A. B.; Li, Y.; Li, C. *J. Current Cancer Drug Targets*, **2002**, *2*, 227-242.
- [12] Frydman, B.; Marton, L. J.; Sun, J. S.; Neder, K.; Witiak, D. T.; Liu, A. A.; Wang, H-M.; Mao, Y.; Wu, H-Y.; Sanders, M. M.; Liu, L. F. *Cancer Research*, **1997**, 620-627.
- [13] Yang, Y.; Zhou, X.; Xu, M.; Piao, J.; Zhang, Y.; Lin, Z.; Chen, L. *Sci. Rep.* **2017**, *7* (1), 2681.
- [14] Wang, D.; Xia, MY.; Cui, Z.; Tashiro, S.; Onodera, S.; Ikejima, T. *Biol. Pharm. Bull.* **2004**, *27* (7), 1025-1030.
- [15] Thirumurugan, R. S.; Kavimani, S.; Srivastava, R. S. *Biol. Pharm. Bull.* **2000**, *23* (12) 1438-1440.
- [16] Bringmann, G.; Irmer, A.; Büttner, T.; Schaumlöffel, A.; Zhang, G.; Seupel, R.; Feineis, D.; Fester, K. *J. Nat. Prod.* **2016**, *79* (8), 2094-2103.
- [17] Kamuchi, H.; Shiraishi, Y.; Kojima, A.; Kawazoe, N.; Kinoshita, K.; Koyama, K.; *J. Nat. Prod.* **2018**, *81* (5), 1290–1294.
- [18] Fan, Y.; Feng, P.; Liu, M.; Pan, H.; Shi, Y. *Org. Lett.* **2011**, *13* (17), 4494-4497.
- [19] Türkmen, Y. E. *Turk. J. Chem.* **2018**, *42*, 1398-1407.

-
- [20] Anderson, J. R.; Edwards, R. L.; Whalley, A. J. S. *J. Chem. Soc. Perkin Trans. 1* **1983**, 2185-2192 b) Hashimoto, T.; Tahara, S.; Takaoka, S.; Tori, M.; Asakawa, Y. *Chem. Pharm. Bull.* **1994**, *42*, 1528-1530.
- [21] For a previous synthesis of daldinol (**x**), see: Andersen, N. G.; Maddaford, S. P.; Keay, B. A. *J. Org. Chem.* **1996**, *61* (26), 9556-9559.
- [22] a) Magdziak, D.; Rodriguez, A.A.; Water, R.W.V.D.; Pettus, T. R. R. *Org. Lett.* **2002**, *4* (2), 285–288, b) Wu, A.; Duan, Y.; Xu, D.; Penning, T. M.; Harvey, R. G.; *Tetrahedron*, **2010**, *66* (12), 2111-2118.
- [23] Ozanne, A.; Pouysegue, L.; Depernet, D.; François, B.; Quideau, S. *Org. Lett.* **2003**, *5* (16), 2903–2906.
- [24] Frigerio, M.; Santiagostino, M.; Spature, S. *J. Org. Chem.* **1999**, *64* (12), 4537-4538.
- [25] Snyder, S.A.; Ross, A.G.; Sherwood, T.C. *Angew. Chem. Int. Ed.* **2010**, *49*, 5146 - 5150.
- [26] Broutin, PE.; Cerna, I.; Campaniello, M.; Leroux, F.; Colobert, F. *Org. Lett.* **2004**, *24* (6), 4419-4422.
- [27] Guoqing, Z.; Guangqing, X.; Chao, Q.; Wenjun, T.; *J. Am. Chem. Soc.* **2017**, *139* (9), 3360-3363
- [28] Zhdankin, V.V. *Chem. Rev.* **2008**, *108*, 5299-5358.
- [29] Harned, A.M. *Tetrahedron Lett.* **2014**, *55* (34), 4681-4689.
- [30] Kuhakarn, C.; Kittigowittana, K.; Ghabkham, P.; Pohmakotr, M.; Reutrakul, V.; *Synt. Comm.* **2006**, *36* (19), 2887-2892.
- [31] Ghera, E.; Ben-David, Y. *J. Org. Chem.* **1985**, *50* (18), 3355-3359.

-
- [32] Golime, G.; Kim, H.Y.; Oh, K. *Org. Lett.* **2018**, *20* (4), 942-945.
- [33] Kiyotaki, K.; Kayukawa, T.; Imayoshi, A.; Tsubaki, K. *Org. Lett.* **2020**, *22* (23), 9220-9224.
- [34] Mcomie, J. F. W.; Watts, M.L.; West, D. E. *Tetrahedron*, **1968**, *24*, 2289-2292
- [35] Kumar, S.; Patil, S.; *J. Phys. Chem. C* **2015**, *119*, 19297-19304.
- [36] Kim, S-K.; Park, J-K. *Journal of Nanoscience and Nanotechnology*, **2008**, *8* (9), 4787-4792.
- [37] Yan, Q.; Zhou, Y.; Ni, B-B.; Ma, Y.; Wang, J.; Pei, J.; Cao, Y. *J. Org. Chem.* **2008**, *73* (14), 5328-5339.
- [38] Wu, W.; Li, J.; Guo, F.; Zhnag, L.; Long, Y.; Hua, J. *Renewable Energy*, **2010**, *35* (8), 1724-1728.
- [39] Wang, T.; Han, J.; Zhang, Z.; Xu, B.; Huang, J.; Su, J. *Tetrahedron*, **2012**, *68* (50), 10372-10377.
- [40] Goel, A.; Sharma, A.; Kathuria, M.; Bhattacharjee, A.; Verma, A.; Mishra, P. R.; Nazir, A.; Mitra, K. *Org. Lett.* **2014**, *16* (3), 756-759.
- [41] De La Cruz, L. K. C.; Benoit, S. L.; Pan, Z.; Yu, B.; Maier, R. J.; Ji, X.; Wang, B. *Org. Lett.* **2018**, *20* (4), 897-900.
- [42] Allen, C. F.; VanAllan, J. A. *J. Org. Chem.* **1952**, 845-854.
- [43] Chiechi, R. C.; Tseng, R. J.; Marchioni F.; Yang. Y.; Wudl, F. *Adv. Mater.* **2006**, *18*, 325-328.
- [44] Fabrizio, E.F.; Payne, A.; Westlund, N. E.; Bard, A. J.; Magnus, P.P. *J. Phys. Chem. A* **2002**, *106* (10), 1961-1968

-
- [45] Goel, A.; Kumar, V.; Chaurasia, S.; Prasad, R.; Anand, R. S. *J. Org. Chem.* **2010**, *75* (11), 3656-3662.
- [46] Campo, M. A.; Huang, Q.; Yao, T.; Tian, Q.; Larock, R. C. *J. Am. Chem. Soc.* **2003**, *125* (38), 11506-11507.
- [47] Wegner, A. H.; Scott, L. T.; Meijere, A. *J. Org. Chem.* **2003**, *68* (3), 883-887.
- [48] Quimby, M. J.; Scott, L. T. *Adv. Synth. Catal.* **2009**, *351*, 1009-1013.
- [49] Jana, R.; Chatterjee, I.; Samanta, S.; Ray, J. K. : *Org. Lett.* **2008**, *10* (21), 4795-4797.
- [50] Yamaguchi, M.; Higuchi, M.; Tazawa, K.; Manabe, K. *J. Org. Chem.* **2016**, *81* (9), 3967-3974.
- [51] Pascual, S.; Bour, C.; Mendoza, P.; Echavarren, M. *Beilstein J. Org. Chem.* **2011**, *7*, 1520-1525.
- [52] Wu, Y.; Linden, A.; Siegel, J. S. *Org. Lett.* **2005**, *7* (20), 4353-4355.
- [53] Ogawa, N.; Yamaoka, Y.; Yamada, K.; Takasu, K. *Org. Lett.* **2017**, *19* (12), 3327-3330.
- [54] For a brief discussion on arene hydroxylation reactions, see: Sang, R.; Korkis, S. E.; Su, W.; Ye, F.; Engl, P. S.; Berger, F.; Ritter, T. *Angew. Chem. Int. Ed.* **2019**, *58*, 16161-16166.
- [55] Suresh, J. R.; Whitener, G.; Theumer, G.; Bröcher, D. J.; Bauer, I.; Massa, W.; Knölker, H-J. *Chem. Eur. J.* **2019**, *25* (1), 3759-3765.
- [56] Eckert, T.; Ipaktschi, J. *Synt. Comm.* **1998**, *28* (2), 327-335.
- [57] Leadbeater, N. E.; Tominack, B. J. *Tetrahedron Lett.* **2003**, *44* (48), 8653-8656.
- [58] Parikh, J. R.; Doering, W. E.; *J. Am. Chem. Soc.* 1967, *89* (21), 5505-5507

[59] Corey, E. J.; Suggs, J. W.; *Tetrahedron Lett.* **1975**, *16* (31), 2647-2650

[60] Kawanishi, S.; Oki, S.; Kundu, D.; Akai, S. *Org. Lett.* **2019**, *21* (9), 2978-2982.